Study of acute myeloid leukaemia with known chromosomal translocations

A Thesis Submitted for the Degree of Doctor of Philosophy

By

Abdulbasit Naiel

Brunel Institute of Bioengineering

Brunel University

June 2014

ABSTRACT

Acute myeloid leukaemia ("AML") is a clonal disease characterised by increased, uncontrolled abnormal white blood cells and the accumulation of leukaemia immature cells in the bone marrow and bloodstream. Chromosomal rearrangements have been detected in almost half of AML cases. It has been proven that the chromosomal rearrangements constitute a marker for the diagnosis and prognosis of AML and have therapeutic consequences. The discovery of these rearrangements has led to a new World Health Organization ("WHO") classification system. However, small regions of cryptic chromosomal rearrangements have been identified among these cases. Such cryptic rearrangements can be explained by the identification of small regions which cannot be found by conventional chromosome banding techniques. Moreover, approximately 50% of AML cases have been found with normal karyotypes. The improvement of cytogenetic techniques, including fluorescence in situ hybridization ("FISH") and single nucleotide polymorphism ("SNP") platforms, have allowed the detection of small rearranged regions (such as copy number changes) both in normal and abnormal karyotype AML. This study identifies: (i) cryptic chromosomal translocations in leukaemia cells of AML patients; (ii) DNA copy number changes in patients with known chromosomal translocations; and (iii) the proliferating state of leukemic cells harbouring chromosomal abnormalities within a series of patients.

In the initial study, the FISH technique was performed on 7 AML patient samples to validate a novel three colour probe for the detection of t(7; 12). The results demonstrated that the new three-colour FISH approach used in this study has enabled the detection of a cryptic t(7;12) translocation as part of a complex rearrangement in one patient previously been described as having t(7;16) and ETV6-HLXB9 fusion transcript at the molecular level. To date there are only two cases of a cryptic t(7; 12) translocation reported in the literature. Additionally, the new three-colour FISH approach also enabled identification of t(7; 12) in a new seven year-old AML patient (the first case of childhood leukaemia with an onset after infancy to be found positive for t(7; 12)).

In the second study the FISH technique was used to validate three colour probe sets for the detection of 7(q22-q31) and 7(q22-q36.1) regions on several myeloid cell lines. The results indicate that the probes found chromosome 7 rearrangements in myeloid cell

lines with complex rearrangements. The three colour probe sets enabled detection of a new rearrangement in the k562 cell line, described as a duplication of 7q36 region, followed by intrachromosomal insertion of long arm material into the short arm of chromosome 7. The intrachromosomal insertion identified in k562 cell line is an uncommon form of chromosomal rearrangement in myeloid leukaemia which has not been previously reported.

In the third study, the Illumina BeadArray approach was used to assess copy number alterations ("CNAs") and copy number loss of hertrozygosity ("CN-LOH") regions in 22 AML patients samples with inv(16)(p13;q22) and t(8;21)(q22;q22) rearrangements. In order to distinguish between true CNAs and false-positive findings as well as to verify whether CNAs are present in the same clone harbouring inv (16), FISH was used on fixed chromosome and cell suspensions from the same patients. The results showed a low number of copy number losses and copy number gains in 17 (77.27%) out of 22 cases, with an average of 1.86 CNAs per case as well as copy neutral-LOH with an average of 6.7% per patient. Furthermore, interphase FISH was carried out on four cases showing a 7q36.1 deletion, 4q35.1 deletion, 16.13.11 deletion and 8q24.21-q24.3 gain identified by array. The FISH results confirmed CNAs in most cases while CNA was not confirmed in one patient. Moreover, the FISH data analysis showed that the CNAs were found in both cells without inv (16) and cells harbouring the inv (16) rearrangement.

In the final study, indirect immunofluorescence (IF) was used to determine the ki67 staining patterns in 8 stimulated and unstimulated peripheral blood samples and k562 cell lines. The results showed a high percentage of ki67 positive staining in the stimulated samples in comparison with unstimulated samples, which showed a low percentage of ki67 positive staining. In addition, a high percentage of proliferating cells were detected in the k562 cell line.

ImmunoFISH was performed on five different patient samples and leukaemia cell lines using specific probes in the regions of interest to detect the chromosomal abnormalities and using the ki67 antibody to assess the proliferation state of the cells. The results showed that the proliferation state of the cells carrying chromosomal abnormalities in two patients was higher than the proliferation state of the cells carrying abnormalities in three patients; in other words, most of the cells carrying abnormalities were proliferating in two cases and non-proliferating in three cases.

DEDICATION

This work is dedicated to my family, especially to my father who supported me each step of the way.

TABLE OF CONTENTS

LIST OF FIGURES

LIST OF TABLES

LIST OF ABBREVIATIONS

%	percentage
µl	Microliter
°C	Degree Celsius
ABL1	V-abl Abelson Murine Leukaemia Viral Oncogene Homolog 1
ACS2	Acyl CoA Synthetase 2
AF10	ALL1-fused gene from chromosome 10 protein
AF17	ALL1-fused gene from chromosome 17 protein
AF22	ALL1-fused gene from chromosome 22 protein
AF4	AF4/FMR2 family member 1
AF6	ALL1-fused gene from chromosome 6 protein
AF9	ALL1-fused gene from chromosome 9 protein alpha subunit 2; translocated to 1
AML	Acute Myeloid Leukaemia
APL	Acute Promyelocytic Leukaemia
ASXL1	Additional Sex combs Like 1 (Drosophila)
BACs	Bacterial Artificial Chromosomes
BCR	Breakpoint Cluster Region
bp	base pair
BSA	Bovine Serum Albumin
CBFA2T1	Cyclin-D related; Core-binding Factor, runt domain,
CBFB	Core-Binding Factor, Beta Subunit
CBP	CREB binding protein
CEBPA	CCAAT/Enhancer Binding Protein (C/EBP), Alpha
CGH	Comparative Genomic Hybridisation
CHIC2	Cysteine-rich Hydrophobic Domain 2
CHRAC1	Chromatin Accessibility Complex 1
O_2	Oxygen
CO_2	Carbon dioxide
CML	Chronic Myeloid Leukaemia
CNAs	Copy Number Alterations
CNLOH	Copy-neutral Loss of heterozygosity
CR	Complete Remission
Cy3	Cyanine 3
DAPI	4',6-Diamidino-2-Phenylindole
ddH_2O	Double Distilled Water
DDX10	(Asp-Glu-Ala-Asp) Box Polypeptide 10
DEK	DEK Oncogene
Del	Deletion
Der	Derivative
DLCL	Diffuse Large Cell non-Hodgkin's Lymphoma
DNA	Deoxyribonucleic acid
DNMT	DNA Methyltransferase
DNMT3A	DNA (cytosine-5-)-Methyltransferase 3 Alpha
dNTP	Deoxyribonucleotide triphosphate
EBV	Epestien-Barr Virus
EDTA	Ethylenediaminetetraacetic Acid
ELL	Eleven-nineteen Llysine-rich Leukaemia protein
EP300	E1A-binding Protein
EPS15	Epidermal growth factor receptor pathway substrate 15
ERG	V-ets erythroblastosis Virus E26 Oncogene Homolog
EtOH	Ethanol

ETV6	ETS Variant 6
EVI1	Ecotropic Virus Integration Site-1
FAB	French-American-British
FCS	Fetal Calf serum
FISH	Fluorescence in situ hybridization
FITC	Fluorescein isothiocyanate
FLT3	Fms-Related Tyrosine Kinase 3
FOXO4	Forkhead Box Protein O4
FUS	Fused In Sarcoma
HOXA9	Homeobox A9
HSC	Hematopoietic stem cell
IDH1	Isocitrate Dehydrogenase
Ins	Insertion
Inv	Inversion
ITDs	Internal Tandem Duplications
KAT6A	K (lysine) Acetyltransferase 6A
KCL	potassium chloride
KIT	Kit Oncogene
LB	Luria Bertani
LOH	Loss of heterozygosity
M	Molarity
MB	Megabase
MDS	Myelodysplastic Syndrome
Mg	Microgram
MYH11	Myosin Heavy Chain 11
MKL1	Megakaryoblastic Leukaemia (Translocation) 1
MLF1	Myeloid Leukaemia Factor 1
MLL	Myeloid/Lymphoid or Mixed-Lineage Leukaemia (Trithorax Homolog, Drosophila)
MLLT1	Myeloid/Lymphoid or Mixed-lineage Leukaemia (trithorax homolog, Drosophila); Translocated to, 1
MLLT11	Myeloid/Lymphoid or Mixed-lineage Leukaemia (trithorax homolog, Drosophila); Translocated to, 11
MLLT3	Myeloid/Lymphoid or Mixed-Lineage Leukaemia (Trithorax Homolog, Drosophila); Translocated to, 3
MPD	Myeloproliferative disorders
MTG1	Myeloid Translocation Gene on Chromosome 16
MYH11	Myosin, Heavy Chain 11
NaAc	Sodium Acetate
Nacl	Sodium Chloride
NaOH	Sodium Hydroxide
NDE1	NudE Neurodevelopment Protein 1
ng	Nanogram
NPM	Nucleophosmin
NUP	Nucleoporin
NUP214	Nucleoporin 214kDa
NUP98	Nucleoporin 98kDa
OTT	Ovary Testis Transcribed
P	petit
PACs	P1- derived artificial chromosome
PBS	Phosphate Buffer Saline
PFA	Paraformaldehyde
Ph	Philadelphia Chromosome
PHA	Phytohaemagglutinin
PML	Promyelocytic Leukaemia

PRKAG2	Protein Kinase, AMP-Activated, Gamma 2 Non-Catalytic Subunit 2
PTPN11	Protein Tyrosine Phosphatase, Non-Receptor Type 11
pUPD	partial uniparental disomy
q	qetit
RARA	Retinoic Acid Receptor, Alpha
RAS	Tyrosine Kinase Pathway
RBM15	RNA Binding Motif Protein 15
RHEB	Ras Homolog Enriched In Brain
RNase	Ribonuclease
RPMI	Roswell Park Memorial Institute
RPN1	Ribophorin I
RUNX1	Runt-related Transcription Factor1
RUNX1T1	Runt-related Transcription Factor1;Translocated to, 1 (cyclin D-related)
RWDD4	RWD Domain Containing 4
SD	Standard Deviation
SDS	Sodium Dodecyl Sulfate
SNP	Single Nucleotide Polymerase
SPI1	Spleen Focus Forming Virus (SFFV) Proviral Integration Oncogene spi1
SSC	Saline-Sodium Citrate
t	Translocation
t-AML	Therapy-related Acute Myeloid Leukaemia
TET2	Ten-Eleven-Translocation Oncogene Family Member 2
t-MDS	Therapy-related Myelodysplastic Syndrome
TOP1	Topoisomerase (DNA) I
TSG	Tumour Suppressor Gene
UPD	Uniparental disomy
V	Volume
WCP	Whole chromosome paint
WHO	World Health Organization
WT1	Wilms Tumour 1
YAC	Yeast artificial chromosome
ZBTB16	Zinc Finger and BTB domain Containing

ACKNOWLEDGEMENTS

I would like to express my special gratitude to my supervisor, Dr. Sabrina Tosi for giving me the opportunity to be her Ph.D. student, and for her endless patience and constant encouragement whenever I was in doubt during my Ph.D. research. Her invaluable guidance, critical feedback, and active involvement have made a significant contribution to the quality of my work. The experience to work with Dr. Tosi has been precious, and this experience will be the most useful and important for my future.

I also owe a special note of thank to my co-supervisors Dr. Ian kill and professor Derek Fisher for taking the time to give me, constructive comments, enthusiastic help, diverse suggestions and constructive feedback during my work.

I would like to express special thanks to Dr. Samantha knight and Dr. Daniela Moralli for fruitful research collaborations. My thanks also to Dr. Matthew Themis, Christine Newton for teaching me diverse knowledge and helping on my research capability growth.

I would also like to thank my friends Temitayo Owoka, Julie Davies, Sara Anjomani, Mehmet Bikkul, Gemma Bourne and Chetana Sharma, and other PhD students who have helped me during my PhD.

Last, but not least, I would like to thank my parents, brothers and sisters for their continuous support, inspiration, encouragement. I am especially indebted to my wife and my sons (Muhaned and Moez) for their unconditional love and support.

DECLARATION

I, Abdulbasit Gudan Ali Naiel, declare that the research work, analyses, findings and conclusions reported in my PhD thesis ***study of acute myeloid leukaemia with known chromosomal translocations*** are entirely my effort, except where otherwise acknowledged. Also, I certify that this thesis contains no material that has been submitted previously, in whole or in part, whether for the purposes of assessment, or for any other purpose such as for the award of any other academic degree or diploma.

Signature:…….

Date:…….

CHAPTER 1: INTRODUCTION

1-1 Haematopoiesis

Haematopoiesis is a normal development of different types of blood cells; the generation of blood cells initiates in the yolk sac during the early weeks of the foetal development and in the spleen and liver in the later stage. Blood cells are created throughout the bone in children, while in adults this process occurs in the central parts of the bones (Van Handel et al., 2010). All blood cell types arise from pluripotent stem cells in the bone marrow with the ability to re-new themselves. Hematopoietic stem cell (HSC) can promote the creation of more stem cells or differentiate them into two main lineages (myeloid and lymphoid) of blood cells. The myeloid lineage can be subdivided into different myeloid precursors, such as erythrocytes, megakaryocytes and myeloblast. Furthermore, the myeloblast progenitor can differentiate into various types of mature blood cells (monocytes, neutrophils, basophils and eosinophils) (see figure 1-1). The lymphoid lineage also divides into either B-cells or T-cells through the lymphocytes precursor. All mature or fully differentiated blood cells have a limited lifespan (Hoang, 2004; Warner et al., 2004).

All blood cell types such as erythrocytes, lymphocytes, monocytes and granulocytes play an important role in the human body. Erythrocytes acts as a carrier of O_2 form the lung to the organs and CO_2 from the organs to the lung. The B-lymphocytes and T-lymphocytes are involved in the immune system. Monocytes and granulocytes play a significant role in the inflammatory response that follows infection (Bellantuono, 2004). Chromosomal abnormalities or mutations in genes during the normal formation of blood cells differentiation or proliferation result in leukaemia.

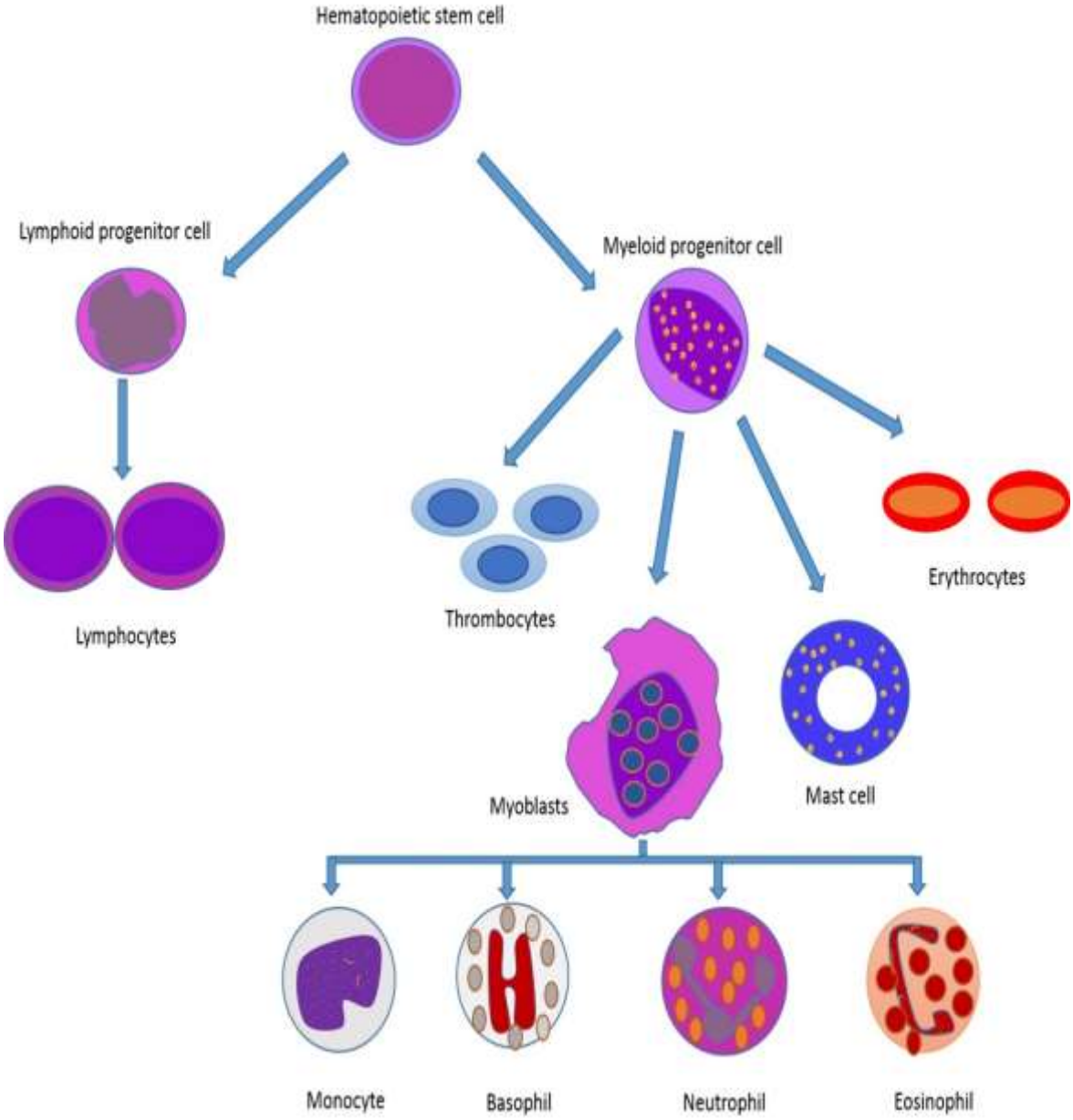

Figure 1-1: Schematic representation of normal blood cells production process

A hematopoietic stem cell gives rise to committed myeloid and lymphoid linages which differentiate all blood cell types (modified from Sanganalmath et al., 2011).

1-2 Regulation of HSC

HSC self-renewal or differentiation was argued by Till et al. (1964) to be triggered solely by stochastic factors, the event being known as the stochastic model. However, more

recent research has demonstrated that the HSC proliferative potential, and implicitly the HSC capacity for self-regeneration or differentiation, is determined by variables in the HSC environment. This is referred to as the instructive model. Currently, a consensus has been reached with regard to the fact that the regulation of the cell fate of HSC depends on the interaction between internal molecular processes and external factors of environment.

In mammals, the HSC microenvironment that underpins the maintenance and regulation of HSC self-renewal is formed by the BM, which represents the primary location where adult hematopoiesis occurs. Conducting research on mouse long bone, Lord et al. (1975) were the first to observe that the concentration of colony-forming unit-spleen (CFU-S) was greater close to the surface of bone. Furthermore, Nilsson et al. (2001) concluded that the surface of the endosteum was HSC “niche” based on direct observation of the position of fluorescently labelled donor lin-cells in the BM endosteum following syngeneic transplantation. Subsequent developments in confocal microscopy imaging enabled Zhang et al. (2003) to prove that HSC and the spindle-shaped osteoblasts covering trabecular bone physically interact with each other, as well as that the number of HSC in BM is directly proportional to the number of osteoblasts (Calvi et al., 2003; Zhang et al., 2003).

Such findings validated the key role played by osteoblasts in the BM HSC niche. The interplay between osteoblasts and HSC is supported by several adhesion molecules, such as the ICAM-1, VCAM-1 (Simmons et al., 1994), CD44, and osteopontin (OPN) (Nilsson et al., 2005; Ponta et al., 2003). It is important to note that, as a transmembrane glycoprotein, CD44 regularly undergoes splicing into different isoforms. It binds the hyaluronan present in the BM endosteum, which facilitates cell-cell interactions (Avigdor et al., 2004). Moreover, osteoblasts and osteoclasts are responsible for the production of OPN, which is a phosphorylated glycoprotein (Mazzali et al., 2002). The importance of OPN in the maintenance of HSC quiescence and effective HSC dissemination according to genetic regulations was demonstrated in transplantation experimental research with OPN-/- recipient mice.

The identification of numerous stem cell regulatory genes was aided by the abnormal expression of these genes in leukaemia (Zhu and Emerson, 2002). For instance, many researchers have reported the occurrence of upregulation of the HOX gene family in AML (Afonja et al., 2000; Drabkin et al., 2002). Thorsteinsdottir et al. (2002) particularly observed that HSC expanded due to HOXA9 overexpression, leading to a 15-fold growth in long-term repopulating cells. On the other hand, Lawrence et al. (2005) demonstrated that the long-term repopulating ability *in vivo* and multiplication *in vitro* of BM cells of HOXA9 knockout mice were considerably diminished. HOXB4 is another HOX protein that displays overexpression only in hematopoietic stem and progenitor cells, not in lineage-committed cells. The outcome of the excessive expression of HOXB4 in different tissues, such as the tissues of murine and human BM and UCB, is a growth in the HSC population, but which does not affect the mechanism of hematolymphoid differentiation (Antonchuk et al., 2001; Antonchuk et al., 2002; Buske et al., 2002; Sauvageau et al., 1995; Thorsteinsdottir et al., 1999). However, as Brun et al. (2004) found, hematopoiesis is not significantly affected by suppression of HOXB4 in mice, which means that some HOX paralogous genes are functionally redundant. Additionally, the regulation of stem-cell self-regeneration has been observed to depend on genes responsible for HOX gene regulation, such as the Polycomb group gene Bmi-1 (Iwama et al., 2004; Lessard and Sauvageau, 2003) and the trithorax group MLL genes (Ernst et al., 2004b; Ernst et al., 2004a).

1-3 The cell cycle

The cell cycle consists of a series of phases that a cell undergoes between two cell divisions. This division comprises G1, S phase, G2, and M phase, the first three phases forming the interphase. G1 is a gap where the cell division process is verified prior to the replication of the genetic material in the S phase, while G2 is another gap where the division process is verified anew prior to the cell moving into the M phase. In this latter phase, the cell begins to divide into two daughter cells through the processes of mitosis and cytokinesis (figure 1-2) (Pecorino, 2008). According to cell type, the length of time it takes for the cell cycle to complete is approximately sixteen hours, of which fifteen hours are allocated for the interphase and one hour for the mitosis. In the interphase, the chromosomes are condensed and therefore cannot be seen. Thus, a microscope has to be

used to differentiate them from other cells during the mitosis (Pecorino, 2008). Normally, cells in adults are known as quiescent because they do not undergo division, entering the G0 phase of inactivity which is excluded from the cell cycle. The mitogen inducer aids the cells to enter the cell cycle again, proceeding to the following stage, namely, the G1 restriction point. The progress of the cells through the different phases of the cell cycle is assisted by a series of proteins referred to as cyclins and which are related to cyclin-dependant kinases (cdks) present in the various cell cycle phases. Gene transcription and controlled protein decomposition are the two processes that dictate where in the cell cycle phases the various cyclins are concentrated.

1-3-1 The G1 check point

In this phase, the cyclin D-cdk4/6 is the primary cyclin-cdk complex. The Retinoblastoma (RB) protein is made by this complex to act as a molecular link for the transition between the G1 and S phases. Although it does not attach directly to the DNA, RB is involved in regulating the activity of the E2F transcription factor necessary for gene expression in the S phase.

1-3-2 The synthesis phase (S phase)

Following the G1 phase and preceding the G2 phase, the S phase of the cell cycle is concerned with genetic material replication. The role played by this phase in cell division is vital because the transmission of erroneous genetic information may result in the death of the cell or even genetic disorders.

1-3-3 The G2 check point

This phase is essential for the transition to the M phase. If a cell has not completed the S phase adequately, resulting in damage to its DNA, ATM and ATR tyrosine kinases will be activated and subsequently phosphorylate and activate Chk1 and Chk2 kinases. The target of these kinases is the Cdc25 tyrosine phosphatase which regulates cdk activity and is involved in the transition between G2 and M phases.

1-3-4 The M Phase

Mitosis takes place in the M phase of the cell cycle. The phase consists of several stages, namely, preprophase, prophase, prometaphase, metaphase, anaphase, telophase, and cytokinesis.

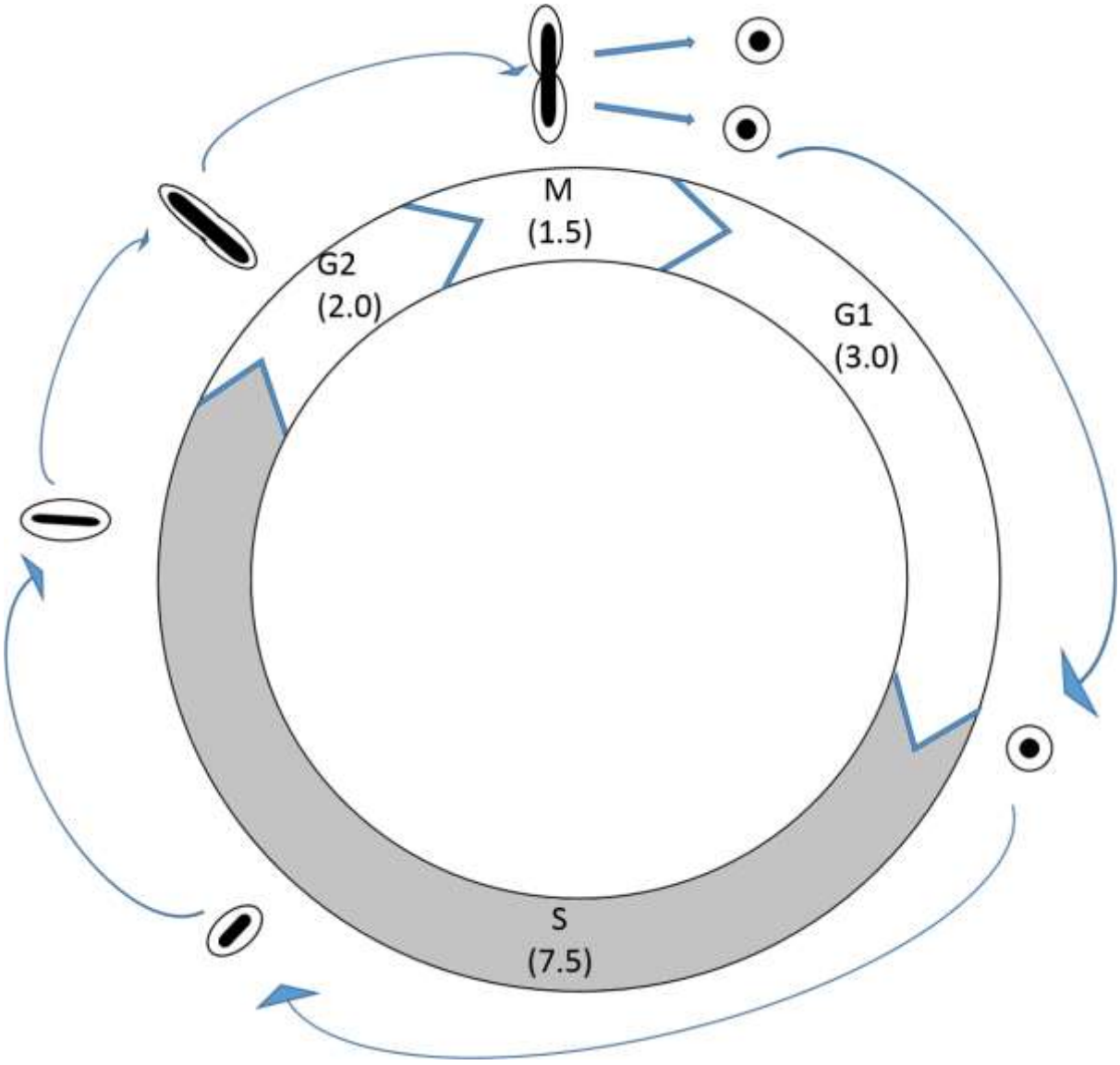

Figure 1-2: Schematic representation of cell cycle

Shows four phases of the cell cycle G1,S,G2 and M phase and the duration of each phase of the cell cycle is shown in hours. The outer circle shows cells in different phase of cell cycle. Modified from (Kuroiwa et al., 1977).

1-4 The hypothesis of Leukaemic stem cells

One major model that has been proposed as an explanation for the development of leukaemia is the stochastic model. This model argues that the capacity of stochastic multiplication or re-generation is possessed only by a limited number of cells in a homogenous population, whereas the majority of underdeveloped cells in the population lack this property. Leukaemia evolution has also been explained in terms of the hierarchy model, which holds that the few LSCs contained in a heterogeneous population determine the onset of the condition (Jamieson et al., 2004). Up to recent times, xenograft transplant research, focusing on the multiplication of rare population of human SCID leukaemia-initiating cells (SL-ICs; 1 per 1 × 106 leukemic blasts), was the only proof that leukaemia stem cells (LSCs) were responsible for the development of leukaemia (Hope et al., 2004). This was validated by Driessens et al. (2012) by lineage tracing in mice. Employing clonal analysis, the researchers discovered that tumour cells exhibiting properties similar to those of stem cells were present in an intact solid tumour. The finding lends support to the cancer stem cell (CSC) model.

1-5 Leukaemia

The term leukaemia derived from the Greek white (*leukos*) and blood (*haima*). Leukaemia is a clonal disease and does not create a tumour mass. Leukaemia can be divided into two main categorizes, myeloid and lymphoid, based on the origin of the cell type affected. Each category of leukaemia subdivides into acute and chronic, depending on how mature the cells are.

1-5-1 Definition and classification of acute myeloid leukaemia

Acute myeloid leukaemia (AML), also known as acute non-lymphoblastic leukaemia or acute myelogenous leukaemia, is a group of different malignant disorders which is characterized by rapid growth of abnormal white blood cells and accumulation of leukaemia immature cells in the bone marrow and finally in blood stream (Smith et al., 2004).

There are two most commonly used classification systems for AML, the most widely used of which is the French-American-British (FAB). However, the most recently established system is that of the World Health Organization (WHO).

1-5-1-1The French-American-British classification of AML

The FAB classification system was established by a group of French, American and British leukaemia experts in 1976. According to the FAB system, acute myeloid leukaemia can be divided into subtypes M0 through M7 based on morphological and cytochemical findings (Bennett et al., 1976). Table 1-1 shows the different subclasses of acute myeloid leukaemia according to the FAB classification system.

Table 1-1: The different subtypes of acute myeloid leukaemia according to the FAB classification

Subtype	Description	Cytogenetics
M0	Minimally differentiated acute myeloid leukaemia (AML).	
M1	Acute myeloid leukaemia without maturation.	
M2	Acute myeloid leukaemia with maturation.	t(8;21)(q22;q22), t(6;9)
M3	Promyelocytic, or acute promyelocytic leukaemia (APL)	t(15;17)
M4	Acute myelomonocytic leukaemia.	inv(16)(p13q22), del(16q)
M4 Eo	Myelomonocytic together with bone marrow eosinophilia	inv(16), t(16;16)
M5	Acute monoblastic leukaemia (M5a) or acute Monocytic leukaemia (M5b)	del (11q), t(9;11), t(11;19)
M6	Acute erythroid leukemias, including erythroleukemia (M6a) and very rare pure erythroid leukaemia (M6b)	
M7	Acute megakaryoblastic leukaemia	t(1;22)

1-5-1-2 The World Health Organization classification of AML

This classification system (WHO, 1999) was based on the immunological, cytogenetic, morphological and clinical findings (Moe et al., 2008). The revised (2008) World Health Organization classification system develops the FAB system and emphasises that the field

of heamato-oncology is changing towards a more comprehensive system. According to the WHO classification, acute myeloid leukaemias are grouped into four categories: (i) AML with recurrent genetic abnormalities; (ii) AML with multilineage dysplasia; (iii) therapy-related disorders; therapy-related AML (t-AML) and therapy-related myelodysplastic syndromes (t-MDS); and (iv) AML not otherwise categorized. The WHO classification system identified 108 new diagnostic entities in hematopathology, involving 50 new or provisional leukaemia entries (Betz and Hess et al., 2010). Table 1-2 shows the WHO classification as summarized by Vardiman et al. (2011).

Table 1-2: The WHO classification of acute myeloid leukaemia (modified from Vardiman et al., 2002)

AML with recurrent genetic abnormalities	AML with t(8;21)(q22;q22); *RUNX1-RUNX1T1* AML with inv(16)(p13.1q22) or t(16;16)(p13.1;q22); *CBFB MYH11* Acute promyelocytic leukaemia with t(15;17)(q22;q12); *PML-RARA* AML with t(9 ;11)(p22;q23); *MLLT3-MLL* AML with t(6;9)(p23;q34); *DEK-NUP214* AML with inv(3)(q21q26.2) or t(3;3)(q21;q26.2); *RPN1-EVI1* AML (megakaryoblastic) with t(1;21)(p13;q13);(*RBM15-MKL1*)
AML with multilineage dysplasia	Following MDS or MDS/MPD Without antecedent MDS or MDS/MPD, but with dysplasia in at least 50% of cells in 2 or more myeloid lineage
AML and MDS, therapy-related	Alkylating agent/radiation- related type Topoisomerase II inhibitor- related type Others
AML not otherwise specified (NOS)	AML with minimal differentiation AML without maturation AML with maturation Acute myelomonocytic leukaemia Acute monoblastic and monocytic leukaemia Acute erythroid leukaemia Acute megakaryoblastic leukaemia Acute basophilic leukaemia Acute panmyelosis with myelofibrosis

1-6 Molecular mechanisms of cancer

1-6-1 Oncogenes

Previously, the development of all human cancers was believed to be triggered by oncogenes, which were considered to represent fragments of viral DNA transferred from retroviruses. The results of the experimental work conducted by Rous (1911) revealed that tumour development could be triggered in healthy chickens through the introduction of a cell-free extract from chicken tumour cells. It was determined that the extract contained the Rous sarcoma retrovirus (RSV), which was responsible for the development of sarcomas in chickens. However, the actual virus was not the transmissible agent, but rather a nucleotide sequence that encoded the gene v-src contained in the RSV and associated with nucleotide sequences in the DNA of healthy chickens. This helped Stehelin et al. (1976) to identify the first oncogene SRC. The researchers also noted that many organisms possessed oncogenes, which are normal genes in charge of regulation of cell development and division.

The purpose of oncogenes is to encode proteins involved in the regulation of cell proliferation and/or apoptosis, and related products. The activation of oncogenes is triggered by genetic abnormalities, including translocations that give rise to new gene fusions, such as EWS-FLI1 and EWS-ERG, and the insertion of new enhancers or promoter regions to a gene region (e.g. in Burkitt's lymphoma, the juxtaposition of MYC to the human immunoglobulin heavy chain enhancer regions occurs) (Joos et al., 1992). Furthermore, gene amplification (MYCN) or activation of mutations (RAF or RAS genes) may also stimulate oncogenes (Downward, 2003). The activation of oncogenes may promote development and/or survival, resulting in the onset of cancer.

1-6-2 Tumour suppressor genes

The notion of tumour suppressor genes was first outlined by Knudson (1971) on the basis of research on the prevalence of retinoblastoma. An autosomal dominant condition, hereditary retinoblastoma usually causes bilateral tumour to develop in children's retina. Of the 60% of hereditary retinoblastoma cases, 80% affect the retina in both eyes. In addition, there are also cases of unilateral retinoblastoma occurring de novo. Knudson referred to incidence data for retinoblastoma occurring in just one eye and in both eyes

and succeeded in creating models to estimate the number of mutations leading to the onset of the condition. The researcher established that only one mutation was necessary in the case of bilateral retinoblastoma, as it already has a germline mutation, while two somatic mutations were necessary for unilateral retinoblastoma to occur. These observations formed the basis for the 'two-hit hypothesis' proposed by Knudson. Underpinning these data was the fact that, even though retinoblastoma might not occur in the children of affected parents, those individuals could nevertheless have children developing the condition. This led to the conclusion that, in order for tumorigenesis to begin, both alleles of a tumour suppressor gene have to be switched off. Friend et al. (1986) validated this conclusion when they discovered recessive mutations in both alleles of the RB gene, which was the first tumour suppressor gene that was successfully replicated.

There are various genetic methods through which tumour suppressor genes could be inactivated after the 'first-hit'. Additionally, the inactivation of these genes may also be induced by epigenetic modifications like DNA hypermethylation. The discovery of TP53 as a tumour suppressor gene was made in colorectal cancer research which employed the SV40 virus for cell malignant modification. The coding sequence of TP53 was subsequently examined. Later on, two colorectal carcinomas were observed by Baker et al. (1989) to display TP53 mutations; both carcinomas possessed deletions at 17p13 and expressed TP53 from the other allele. TP53 germline mutations are encountered in individuals suffering from the hereditary Li-Fraumeni syndrome which is associated with increased risk of breast, lung, colorectum and brain tumours. Functioning as a cellular check-point, the p53 protein not only coordinates responses throughout the cell cycle and mechanisms of DNA repair, but also harmonises cell development and apoptosis in keeping with both intrinsic and extrinsic signals (Knudson, 2001, Finlay et al., 1989). A direct correlation has been found between the occurrence of most human cancers and the inactivation of TP53 and RB or inactivation in their genetic pathways. TP53 is an integral component of a cellular system of great complexity geared towards the monitoring of DNA damage and halting the cell cycle to allow the completion of DNA repair. Apoptosis is activated in the event that damage repair fails. When TP53 is inactivated, accumulation of DNA damage is fostered by BRCA1 and other supposed "caretaker" genes, which paves the way for tumour development (Deng et al., 2003).

Mechanisms of Leukeamogenesis arising from Chromosomal Abnormalities

Leukeamogenesis arises from a series of transformational events leading to chromosomal abnormalities during proliferation and differentiation which cause apoptotic pathways (Kelly and Gilliland, 2002). These abnormalities include chromosomal deletions, amplifications and chromosomal translocations to create a rearrangement of genes.

1-7-1 Mechanisms of Leukeamogenesis arising from chromosomal deletions

With regard to haploinsufficiency, loss or inactivation of a single functional copy of the gene caused by mutation results in an insufficient production of proteins. An alternative source of chromosomal deletion which causes leukeamogenesis is the inactivation or deletion of tumour suppressor genes responsible for cell protection. Deletion of tumour suppressor genes is believed to be associated with the development of leukaemia.

1-7-2 Mechanisms of Leukeamogenesis arising from Chromosomal Translocations

The most common chromosomal abnormalities in leukaemia are Translocations. Formation or reorganisation of genes as a result of translocation can create proto-oncogenes which transform into oncogenes. Most proto-oncogenes encode transcription factors which are significant in the proliferation, differentiation and survival of the blood cells. There are several alternative mechanisms for activation of the proto-oncogenes by translocation. The most common mechanism is the formation of a fusion gene that produces abnormal proteins. For example, the BCR-ABL1 fusion gene was a result of the translocation of chromosome 9 and chromosome 22 in chronic myeloid leukaemia ("CML"). In this instance, the BCR-ABL1 fusion gene was created by the juxtaposition of the *ABL1* gene to the area of the *BCR* gene which produced the BCR-ABL1 protein which had the higher tyrosine kinase activity than the normal ABL1 protein (Melo et al., 1996). An alternative mechanism for a translocation to result in leukaemia is the activation of proto-oncogenes by the juxtaposition with constitutionally active genes. For example, in t(8;14))(q24;q11) the *C-MYC* transcription factor gene is transferred to the promoter of the *TcR* alpha gene, which causes overexpression of the *C-MYC* gene. This is important in the regulation of cell division and cell death (Knudson, 2000). A further event which is

hypothesised as being linked to the causation of leukaemia is the activation of proto-oncogenes by a positioning effect, such as the translocation of t(4;12) and t(5;12) and the involvement of the *ETV6* gene (Cools et al., 2002).

1-8 Chromosomal Abnormalities in AML

Classified as numerical or structural, chromosomal abnormalities can be defined as disturbances in the normal composition of chromosomes. Numerical abnormalities take the form of an aberrant copy number of particular chromosomes. Known as chromosomal aneuploidy, this phenomenon occurs due to the fact that chromosome missegregation takes place when the cell divides, resulting in the loss or gain of specific chromosomes (Williams and Amon, 2009). Structural abnormalities, on the other hand, take the form of chromosomes with aberrant structure and are related to misrepair of DNA double strand breaks (DSBs) in somatic cells and especially cancer cells. Both external factors, such as radiation or chemicals, and internal factors, such as reactive oxygen or delay of DNA replication forks, can cause DSBs. They are a frequent occurrence, every cell cycle having multiple DSBs (Albertson et al., 2003). In response to DSBs, complex DNA repair mechanisms have evolved to protect the integrity of the genome. It has been observed that broken chromosome ends have a tendency to merge with other broken ends, and therefore, if DSBs are not repaired, they may give rise to chromosomal rearrangements, including translocations, deletions, and duplications (Albertson et al., 2003).

1-8-1 Structural chromosomal rearrangements in AML and their prognostic significance

Most cases of acute myeloid leukaemia are associated with chromosomal rearrangements. Cytogenetic analysis indicates that 50-70% of patients with *de novo* AML have shown chromosomal rearrangements such as translocation, deletion, inversion and duplication (Smith et al., 2004). For example, the t (1; 22) (p13; q13) is associated with acute megakaryocytic leukaemia subtype (M7), which translocation results in *OTT-MLL* fusion gene (Mercher et al., 2002). In some translocations such as t (6; 9) (p23; q34) the cytogenetic aberration is very rare, constituting 0.5% to 4% in all patients with acute myeloid leukaemia, and it is associated with subtypes of AML M2 (Alsabeh et al., 1979). However, the translocation between chromosome 8 and chromosome 21 t (8; 21) has been found in 5-12% of acute myeloid leukaemia. The t (8; 21) (q22; q22) is the most frequent chromosome translocation that is associated with acute myeloid leukaemia

(M2), with well-defined and specific morphological features (Ohki et al., 1993). The t (15; 17) is always associated with acute promyelocytic leukaemia (APL also known as AML M3). The patients carrying the translocation t (15; 17) have distinct clinical and morphological features (Reiter et al., 2004). The t (15; 17) translocation is detected in approximately 95% of AML cases subtype M3. The translocation between chromosomes 15 and 17 result in the expression of the *PML-RARα* oncofusion gene (Licht et al., 2006). The t (8; 21) translocation is detected in approximately 10% of AML cases involving *AML1 (RUNX1)* and *ETO* genes (Cameron et al., 2004). The inv (3) (q21q26) or a translocation t (3; 3) (q21q26) has been found in patients with AML. These abnormalities cause an increase of the expression of the *EVI1* gene located at 3q26 (Reiter et at., 2000). The most common chromosomal rearrangement in acute myeloid leukaemia subtype M4Eo (with an incidence of 8-10%) is the inversion of chromosome 16, inv(16) (p13q22), resulting in gene fusion between *CBFB* gene located in 16q22 and the *MYH11* gene located in 16p13 (Delauney et al., 2003). Other chromosomal abnormalities of AML have been detected as a sole abnormality or in combination with other abnormalities, such as -5, -7, +4, +8, +11, +13, +19, +21, and deletions of 9q, 7q and 5q (Heim and Mitelman 2009). A complex karyotype involving three or more chromosome abnormalities has been identified in 10-12% of AML patients (Mrózek, 2008). If acute myeloid leukaemia is untreated, most patients will die over a period of days or weeks based largely on the level of blasts in the blood and bone marrow. Cytogenetics is recognized as one of the most important valuable prognostic determinators in acute myeloid leukaemia (Byrd et al., 2002; Farag et al., 2006; Grimwade et al., 2001; Mrózek et al., 2001, 2004; Schoch et al., 2003; Slovak et al., 2000). An abnormal karyotype has been found in approximately 60% of acute myeloid leukaemia both in child and adult patients (Grimwade et al., 1998). Around 25% of AML patients have favourable cytogenetics that involve t(15;17), inv (16), t(16;16) or t(8;21): these patients have a complete remission (CR) rate of over 90% and five-year survival of 65% (Grimwade et al., 1998; Grimwade et al., 2010; Moorman et al., 2001). 10% of AML patients carrying -7,-5del (5q) abnormalities of 3(q21; q26) or complex karyotype will have adverse cytogenetics. These patients can expect a CR rate of around 60% and a five-year survival rate of 10% (Grimwade et al., 2010). 40-65% of AML patients will have intermediate cytogenetics, most of them with normal karyotype. The CR rate of these patients is about 80%, with a five-year survival rate of 30-40% (Grimwade et al., 1998; Grimwade et al., 2010). Table 1-3 describes the cytogentics risk groups.

Table 1-3: Cytogentics risk groups

Risk group	Abnormalities
Favourable	**t(8;21)** **t(15;17)** **inv (16)**
Intermediate	**+8** **+21** **+22** **del(7q)** **del(9q)** **Abnormal 11q23** **All other structural/numerical abnormalities**
Adverse	**-5** **-7** **del(5q)** **Abnormal (3q)** **Complex**

1-8-2 Numerical chromosomal rearrangements in AML and their prognostic significance

Of the aneuploidies associated with AML, trisomy 8 (Patel et al., 2012), trisomy 13 (Baer and Bloomfield, 1992) and monosomy 7 (Brozek et al., 2003) are the most common. A number of transcriptional effects have been attributed to the supplementary chromosome present in AML as modifications in gene expression have been exhibited by both trisomic and diploid chromosomes (Nawata et al., 2011).

Unlike tetrasomy 8 which is associated primarily with AML, trisomy 8 occurs in numerous other haematological diseases apart from AML, either on its own or in conjunction with other abnormalities (Kim et al., 2008). Although the effect of trisomy 8 on AML prognosis has been addressed by a considerable number of researchers (Schoch et al., 2006), compared to other abnormalities, including the well-known t(8;21) translocation, trisomy 8 was not observed to be involved in leukaemogenesis. Nawata et al. (2011) confirmed this observation based on the findings of their research in which they generated trisomic H35 cells but did not find evidence of trisomy 8 participation in leukaemia development. Discussing the biological implications of the supplementary copy of chromosome 8, Wolman et al. (2002) proposed that, in spite of the reduced level of C-myc amplification indicated in some AML cases, the larger number of copies of C-myc oncogene, positioned on 8q, could be involved in leukaemogenesis. However, this abnormality is unsuitable for

targeted therapy, since augmented gene expression is the sole apparent modification caused by the trisomy. Furthermore, although trisomy 8 is prevalent in cases of AML, tetrasomy and polysomy occur as well. The presence of this rare clonal chromosomal abnormality has been observed mostly in samples of AML and myelodysplastic syndrome that were subjected to testing with chromosome 8 centromeric probe designed to determine aneuploidy (Kim et al., 2008). Based on the FAB classification, myelomonocytic and monocytic lineages of leukaemia, the main types of leukaemia in which tetrasomy presence was detected, are included in the M5 subgroup AML. Moreover, Kim et al. (2008) also reported cases of polysomy, including pentasomy and hexasomy, and consequently proposed that the poor prognosis is due to the involvement of the oncogenes MYC in 8q24, MOS in 8q22, and RUNX1T1 in this anomaly. Shin et al. (2009) obtained similar results pointing to poor prognosis based on testing carried out on a 72 years old individual with AML.

Despite occurring on a regular basis, trisomy 13 rarely takes the form of a singular karyotypic aberration (Silva et al., 2007). Moreover, Mehta et al. (1998) argued that trisomy 13, on the one hand, and the morphologic and immunophenotypic undifferentiated leukaemia AML-M0, on the other, are closely correlated. The majority of cases of trisomy 13 were associated with poor prognosis. The development of leukaemia is believed to be partially triggered by trisomy 13 which intensifies the expression of the fms-like tyrosine kinase 3 gene and causes mutations in the RUNX1 gene, while the additional copy of chromosome 13 determines the expression of the class III receptor tyrosine kinase in underdeveloped hematopoietic cells. Dicker et al. (2007) reported that, although each sample of trisomy 13 employed was RUNX1 mutated, the RUNX1 mutations in AML-M0 were not exclusively related to trisomy 13. In fact, in some cases of AML-M0, Roche-Lestienne (2006) noted that trisomy 13 occurred together with tetrasomy 13, which is considered to be the outcome of extra aberrations following transformation. Similar to RUNX1 mutations, rather than being restricted to cases of trisomy 13, tetrasomy is an irregularity of great complexity associated with a clone that displays both numerical and structural aberrations (McGrattan et al., 2002).

Based on observations of almost 40% of cases of children with poor prognosis, the chromosome 7 deletion has been identified as the most frequent irregularity in children

with AML and myelodysplastic syndrome (Hasle et al., 2007). Additionally, adults who were affected by the detonation of the atomic bomb at Hiroshima were also found to possess this irregularity Takahashi et al., 2006). This monosomy 7 often occurs in association with other abnormalities which dictate how severe the disease is.

1-8-3 Molecular rearrangement in AML and its prognostic factors

In addition to chromosomal rearrangement, many molecular abnormalities have been found in cytogenetically normal AML patients. It has been proposed that AML arises from the interaction of two classes of gene mutations. Class I mutations are responsible for the activation of genes in the kinase signalling pathways (e.g. *RTK, RAS, FLT3, KIT*, and *PTPN11*), leading to cell survival and proliferation, while Class II mutations (e.g. *PML/RARA,* CBFB*/MYH11, RUNX1/RUNX1T1, MLL/PTD, CEBPA, and SPI1*) inactivate the transcription factors (Gaidzik et al., 2008; Gilliland et al., 2001). The mutation in nucleophosmin (*NPM1*) has been reported in approximately 40-50% of de novo AML patients with normal karyotype, and is predictive of a better prognosis (Meani et al., 2009; Schnittger, 2005). The mutations of fms-like tyrosine kinase 3(*FLT3)* gene are the second most common mutations in de novo AML and seem to be activated in one-third of AML cases. Internal tandem duplications (ITDs) in the juxtamembrane domain of *FLT3* have been described in 25% of AML cases. Patients with *FLT3* -ITD have a tendency to have a poor prognosis (Abu-Duhier et l., 2001; Beran et al., 2004; Thiede et al., 2002; Gilliland et al., 2002; Kainz et al., 2002; Kottaridis et al., 2001; Schnittger et al., 2002; Thiede et al., 2002). Additional genetic changes in acute myeloid leukaemia involving dominant-negative mutation of the tumour suppressor gene *CEBPA* have been reported in 16% of AML M2 patients. AML patients with *CEBPA* gene mutation are associated with better prognosis (Fröhling et al., 2004; Pabst et al., 1999; Preudhomme et al., 2002). Recent studies have demonstrated prevalent mutations, such as DNA methyltransferase (*DNMT*3A) mutations and mutations in the ten-eleven-translocation oncogene family member 2 (*TET2*) (Bacher et al., 2010; Delhommeau et al., 2009; Ley et al., 2010; Takahashi et al., 2011;), as well as mutations in the isocitrate dehydrogenase (*IDH*1) gene (Green et al., 2010; Mardis et al., 2009). Moreover, the presence of *c-KIT* has been showed in AML patients (Paschka et al., 2006). Furthermore, *ASXL1* mutations have been identified in 40 AML patient samples, and the *ASXL1* gene

encodes protein involved in the regulation of chromatin remodelling (Gelsi-Boyer et al., 2009). Despite the mutations of *WT1* gene first being detected in haematological malignancies more than a decade ago, the specific roles of *WT1* in normal and malignant haematopoiesis remain unknown. The *WT1* gene has been linked to the regulation of differentiation, proliferation and cell survival (Owen et al., 2010). Recently, 470 patients with *de novo* non-M3 AML were examined and 63 *RUNX1* mutations were identified in 62 patients. *RUNX1* is required for eventual haematopoiesis, and its functional dysregulation results in leukaemia (Tang et al., 2009). The genetic changes that are responsible for a poor outcome in most patients with AML are unknown (Ley et al., 2010). Ley et al. (2010) found that 62 out of 281 patients had mutations in *DNMT3A* gene that were proven to affect translation, and also 18 different mutations were identified in 37 patients that were proven to affect amino acid R882. Furthermore, six frameshift, six nonsense and three splice-site mutations and a 1.5-Mbp deletion encompassing *DNMT3A* were identified. In 56 out of 166 patients, mutations were extremely strengthened in the group of patients with an intermediate-risk cytogenetic profile, but were absent among 79 patients with a favourable-risk cytogenetic profile. Table 1-4 shows the examples of chromosomal abnormalities in acute myeloid leukaemia that have been characterized at the molecular level.

Table 1-4: Chromosomal abnormalities in AML characterized at molecular level (Mrozek et al., 2000)

Abnormalities	Gene
Affecting the *EVI1* gene at 3q26	
inv(3)(q21q26)	***EVT1***
t(3;3)(q21;q26)	***EVT1***
Involving the *NPM* gene at 5q34	
t(3;5)(q25;q34)	***MLF1-NPM***
Involving the *MOZ* gene at 8p11	
inv(8)(p11q13)	***MOZ-TIF2***
t(8;16)(p11;p13)	***MOZ-CBP***
t(8;22)(p11;q13)	***MOZ-EP300***
Involving the nucleoporin genes *CAN* at 9q34 or *NUP98* at 11p15	
t(6;9)(p23;q34)	***DEK-CAN***
t(7;11)(p15;p15)	***HOXA9-NUP98***
inv(11)(p15q22)	***NUP98-DDX10***
t(11;20)(p15;q11)	***NUP98-TOP1***
Involving the *ABL* gene at 9q34	
t(9;22)(q34;q11)	***ABL-BCR***

Abnormalities	Gene
Involving the *CLTH* gene at 11q14	
t(10;11)(p11-15;q13-23)	***AF10-CLTH***
Involving the *ETV6* gene at 12p13	
t(3;12)(q26;p13)	***ETV6***
t(4;12)(q11-12;p13)	***BTL-ETV6***
t(5;12)(q31;p13)	***ACS2-ETV6***
t(7;12)(p15;p13)	***ETV6***
t(7;12)(q36;p13)	***ETV6***
t(12;13)(p13;q12)	***ETV6***
t(12;22)(p12-13;q11-13)	***ETV6-MN***
Involving the *MLL* gene at 11q23	
t(1;11)(p32;q23)	***AF1P-MLL***
t(1;11)(q21;q23)	***AF1Q-MLL***
t(2;11)(p21;q23)	***MLL***
t(4;11)(q21;q23)	***AF4-MLL***
t(6;11)(q21;q23)	***AF6q21-MLL***
t(6;11)(q27;q23)	***AF6-MLL***
t(9;11)(p22;q23)	***AF9-MLL***
t(9;11)(q21-22;q23)	***MLL***
ins(10;11)(p11;q23q13-24)	***MLL***
t(10;11)(p11-13;q13-23)	***AF10-MLL***
t(10;11)(q22;q23)	***MLL***
+11	***MLL***
t(11;11)(q13;q23)	***MLL***
t(11;15)(q23;q14-15)	***MLL***
t(11;16)(q23;p13)	***MLL-CBP***
t(11;17)(q23;q12-21)	***MLL-AF17***
t(11;17)(q23;q23)	***MLL***
t(11;17)(q23;q25)	***MLL-AF17q25***
t(11;19)(q23;p13.1)	***MLL-ELL***
t(11;19)(q23;p13.3)	***MLL-ENL***
t(11;22)(q23;q11)	***MLL-AF22***
t(11;22)(q23;q13)	***MLL-EP300***
t(X;11)(q13;q23)	***AFX1-MLL***
t(X;11)(q22-24;q23)	***MLL***
Involving the core binding factor genes *CBF* bat 16q22 or *CBFA2* at 21q22	
inv(16)(p13q22)	***MYH11-CBF b***
t(16;16)(p13;q22)	***MYH11-CBF b***
t(3;21)(q26;q22)	***EAP, MDS1,EVI1,CBFA2***
t(8;21)(q22;q22)	***CBFA2T1-CBFA2***
t(16;21)(q24;q22)	***MTG16-CBFA2***
t(17;21)(q11.2;q22)	***CBFA2***
Involving the *RAR* agene at 17q12-21	
t(5;17)(q35;q12-21)	***NPM-RAR a***
t(11;17)(q23;q12-21)	***PLZF-RAR a***
t(15;17)(q22;q12-21)	***PML-RAR a***

Abnormalities	Gene
Involving the *ERG* gene at 21q22 t(16;21)(p11;q22)	***FUS-ERG***

1-9 The two-hit model of leukaemogenesis

As previously mentioned, the multiplication, hematopoietic differentiation and death of AML stem cells are aberrant due to genomic damage. In keeping with the two-hit model of leukaemogenesis, it is possible to categorise these oncogenic events into two categories (Kelly and Gilliland, 2002) (Figure 1-4). The underlying concept of this model is that gene rearrangements and mutations that are beneficial from the viewpoint of proliferation and/or survival and those that disrupt hematopoietic differentiation are involved in a cooperative relationship (Kelly and Gilliland, 2002; Fröhling et al., 2005). In spite of the simplified form of this model, the proliferation and/or survival of hematopoietic progenitors are favoured by class I mutations (e.g. activation of mutations of cell-surface receptors like RAS or tyrosine kinases like FLT3), fostering their clonal expansion (Fröhling et al., 2005; Kosmider and Moreau-Gachelin, 2006; Moreau-Gachelin, 2006). Hematopoietic differentiation is disrupted by another type of genomic damage, namely, class II mutations, such as core-binding-factor gene rearrangements caused by t(8;21), inv(16), or t(16;16), or by the PML–RARA and *MLL* gene rearrangements (Fröhling et al., 2005; Kosmider and Moreau-Gachelin, 2006).

Both *in vitro* simulations of leukaemogenesis and AML molecular screening events can benefit from the two-hit model of leukaemogenesis, as it integrates an activating lesion of tyrosine kinase pathways and an event that suppresses myeloid differentiation. This model can provide reasonable explanations for the occurrence of t(8;21) and inv(16) AML, both of which are frequently associated with KIT mutations (Dash and Gilliland, 2001; Care et al., 2003; Park et al., 2011), as well as the occurrence of t(15;17) AML which is related with FLT3 aberrations (Schnittger, 2002; Thiede, 2002; Schnittger et al., 2011).

The two-hit model gained acknowledgement after research on mice revealed that class I

and class II mutations alone do not induce AML, but only give rise to a myeloproliferative disorder (Renneville et al., 2008). The development of AML requires the presence of both classes of mutations, which are said to be cooperating. Another argument in favour of the two-hit model is that the frequency of class I and II mutations occurring together is greater than the frequency of occurrence of two class I mutations or two class II mutations (Dash and Gilliland, 2001; Care et al., 2003;; Schnittger et al., 2006; Renneville et al., 2008; Park et al., 2011). Nevertheless, as Egger et al. (2004) noted, this model is unable to provide a satisfactory explanation of the -5/-7 AML, although it is flexible enough to allow changes in order to explain the function of epigenetic factors. In AML, a range of supposed tumour suppressor genes undergo hypermethylation and therefore are inhibited; from a functional perspective, this hypermethylation is akin to a genetic mutation since, once it has occurred, it does not go away (Schoofs, Berdel and Müller-Tidow, 2013). It is not unfeasible for new drug production to focus on those gene mutations that have been determined to influence proliferation or differentiation pathways. Inhibiting detection of RAS to the plasma membrane, FLT3-specific inhibitors or farnesyltransferase inhibitors can be used to target class I mutations at molecular level. Moreover, compounds promoting normal hematopoietic differentiation, such as all-trans-retinoic acid (ATRA) used to treat acute promyelocytic leukaemia related to the PML-RARA fusion, and even histone deacetylase (HDAC) inhibitors could be employed to target class II mutations (Renneville et al., 2008).

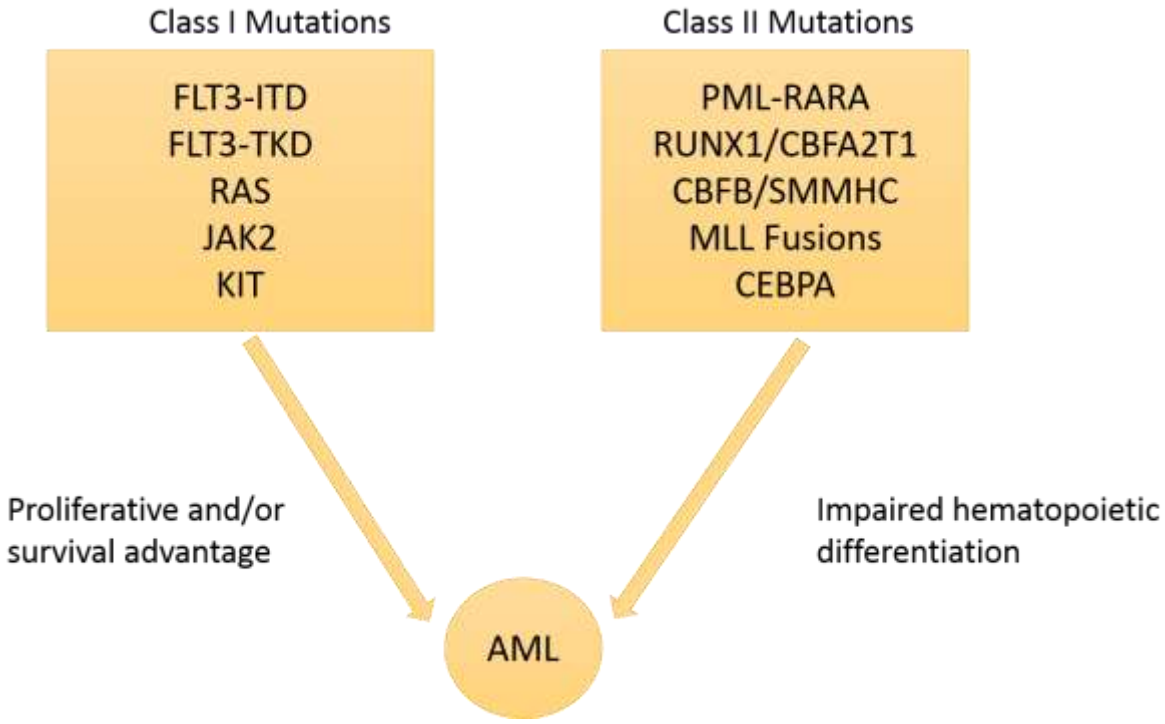

Figure 1-3: Schematic representation of model for collaboration between two groups of mutations

Groups confer a proliferative and/or survival advantage and impair hematopoietic differentiation (modified from Gaidzik et al., 2008).

1-10 Copy number changes in AML

Copy number changes in AML can be either a copy number variation (CNV) which is defined as a loss or a gain of genetic material greater than 1kb in length (Feuk et al., 2006; Freeman et al., 2006) or copy number alteration (CAN) which can be either loss of genetic materials or gain of genetic materials that result in one or more extra copies of a genomic region (e.g. trisomy in the case of gain of an entire chromosome or duplication in the case of the presence of one additional copy of a DNA segment). CNAs can be detected by cytogenetic techniques (e.g. fluorescent in situ hybridization [FISH], comparative genomic hybridization, array comparative genomic hybridization, and by single nucleotide polymorphisms [SNP] arrays).. CNAs have been identified in AML patients with normal and abnormal karyotypes. Walter et al. (2009) identified 201 acquired CNAs among 86 AML patients (in 86 AML genomes) using SNP arrays. The deletions were more common than amplifications. Of 201 alterations, 198 included known genes and 154 loci included at least one gene that was previously implicated with AML or MDS. Copy-neutral loss of heterozygosity was identified in only 7 out of 86 AML genomes. Moreover, Kawankar et al. (2011) examined 86 Indian patients with AML. Of these, 40 AML patients showed an

abnormal karyotype and 46 patients showed no chromosome abnormalities. Of the 46 patients without chromosomal abnormalities, 24 showed DNA CNAs, including losses and gains. The DNA copy number changes included chromosomes 1, 3, 6, 12, 15, 16, 17 (gains) and 1, 4, 2, 3, 5, 7, 8, 9, 10, 11, 13, 15, 18, 20, 21 (losses) (Kawankar et al., 2011). CNAs and UPDs have also been identified in cytogenetically normal AML or AML with uncompleted karyotype (Ballabio et al., 2011); 15 large CNAs were detected in seven out of 23 AML samples. CN gains were found in six samples while CN losses were identified in three out of seven cases.

1-10-1 Loss of heterozygosity

Loss of heterozygosity (LOH) in cancer cells originates from a chromosomal deletion. However, it can also be present in a tumour without loss of DNA, and this is the case of copy-neutral loss of heterozygosity (CNLOH). CNLOH can include a whole chromosome (uniparental disomy, or UPD) when one of the homologous parental chromosomes is deleted and the other is duplicated, or only a part of a chromosome (partial UPD, or pUPD) (Heinrichs et al., 2010).

1-10-2 Mechanisms of formation of copy number changes

The presence of copy number changes is not restricted to specific regions of the genome, but rearrangements are more likely to happen in some regions than in others. Copy number changes can be recurrent or non-recurrent, depending on their breakpoints and formation methods. Recurrent copy number changes are characterised by restriction of breakpoints aggregation and junction to the area of low copy repeats (LCRs). Also known as segmental duplications (SDs), LCRs represent segments of DNA which appear over two times in the haploid genome, are at least 1 Kb in size but may extend to more than 300 Kb, and their paralogous copies exhibit over 95% sequence identity (Edelmann et al., 1999; Bailey et al., 2001). In the case of recurrent rearrangements occurring during meiosis as well as during mitosis at reduced frequency, LCRs support the unfolding of the non-allelic homologous recombination (NAHR) process which gives rise to copy number chages of identical size and closely similar boundaries in carriers. A connection has been found between a number of these recurrent copy number changes and human diseases (Reiter et al., 1998; Stankiewicz and Lupski, 2002). By contrast, non-recurrent copy number changes possess dispersed breakpoints and the nucleotide homology shared by

the boundaries is restricted or absent altogether. Moreover, non-recurrent copy number changes vary in size and their formation is induced by non-homologous end-joining (NHEJ) and replication-based processes, which are defined by models such as the fork stalling and template switching and microhomology-mediated break-induced replication models. As concluded by several researchers, it is these non-recurrent copy number changes typically developing from replication-based processes that mostly cause disease in humans (van Binsbergen, 2011; Hastings et al., 2009). Additionally, apart from LCRs, it has been acknowledged that genomic features are also involved in the development on non-recurrent copy number changes.

1-11 Methods used to diagnose AML

1-11-1 Conventional cytogenetics

Chromosome banding methods have been used for the diagnosis of leukaemia since the 1970s. The most commonly used chromosome banding stain is Giemsa or G-banding, which allows the discrimination of metaphasic chromosomes based largely on their specific banding patterns. While chromosome banding analysis remains a very important routine method at diagnostic laboratories to give an overview of chromosomal abnormalities in leukaemic cells, this method has several drawbacks. In some types of leukaemia, the leukaemic cells often fail to proliferate in the culture, resulting in an insufficient number of metaphase chromosomes for detailed analysis. It is also possible that the chromosome banding method cannot reach the resolution power to detect translocation between chromosome ends, such as t(7;12), and/or to identify chromosomal deletions where the size of the deleted region is smaller than 5-10 MB (Baldwin et al., 2008). It has been shown that chromosomal abnormalities can also occur in non-dividing or interphase cells, but not in metaphase cells, which cannot be detected by conventional cytogenetic method (Ballabio et al., 2011). Other weaknesses of chromosome banding include that it is time-consuming, and its aberrations can often be difficult to interpret. In recent years, the resolution of cytogenetic techniques has been increased to compensate the limitation of traditional cytogenetic methods.

1-11-2 Molecular cytogenetic methods

Molecular cytogenetics concern the study of DNA or genes at the chromosome level, in which a labelled probe consisting of a specific DNA sequence binds to a specific region of metaphase chromosome or interphase DNA.

1-11-2-1 Fluorescent in situ hybridization (FISH)

FISH is an important molecular cytogenetic method widely used in clinical laboratory to detect chromosomal abnormalities in solid tumours and in haematological malignancies (Hu et al., 2014). FISH detection relies on the use of specific probes to detect specific regions of interest within the chromosome, or whole chromosome paint (WCP) to detect structural and numerical chromosomal rearrangements and/or multi-colour probes to identify the cytogenetic changes in the whole of the genome. Labelled probes can be visualized directly if the probe is labelled with flourochorm or detected by affinity, such as avidin or streptavidin, or antibodies if the probe is labelled with biotin or digoxigenin systems (Bridger and Volpi, 2010; Morris, 2011) . FISH has the ability to identify cryptic translocations such as the t(12;21) in ALL (Romana et al., 1994) and cryptic deletions such as the 4q12 deletion that results in a PDGFRA–FIP1L1 fusion gene (Gotlib et al., 2004). It can also analyse both metaphase and large number of non-dividing interphase cells. The resolution of cytogenetic techniques has been further improved by applying genome-wide microarrays, such as comparative genomic hybridization (CGH), CGH array and single nucleotide polymorphism (SNP) arrays.

1-11-2-2 Comparative genomic hybridization (CGH)

CGH modifies the FISH technique to allow the identification of gains or losses in the whole genome. This technique is based on the use of labelling DNA extracted from the patient with green and a normal control DNA with red. The mixture of patient DNA and normal DNA is hybridized into a slide containing normal metaphases preparation. The advantage of the CGH is that there is no need to prepare metaphase from the patient sample, but a significant weaknesses is the limitation of resolution, which only allows the identification of large gains or losses regions, and it is unable to find balanced translocations and inversions. The resolution of CGH application has been improved by replacing the

metaphase chromosome with bacterial artificial chromosomes (BACs) or oligonucleotides placed as spots on slides or chips. (Campbell, 2011; Le Scouarnec and Gribble, 2012).

1-11-2-3 Array Comparative genomic hybridization

At present, bacterial artificial chromosomes (BACs) and oligonucleotide arrays are the two main categories of array targets that are employed. Whereas at first BACs were given priority (Pinkel et al., 1998), in more recent times, the oligonucleotide arrays have attracted increased attention as they provide a wider genome coverage. The existence of a comprehensive human genome map and sequence enabled the formation of both types of arrays. As explained by Ylstra et al. (2006), the BACs may incorporate DNA extracted from insert clones of size ranging from 150 to 200 Kb, may be spotted straight on the array, or else may use the spotting of PCR products that have been subjected to amplification from the BAC clones. The use of this technique is based on the use of two different labelled DNA, one extracted from a patient labelled in red and the other extracted from a normal control DNA labelled in green. The two different labelled DNA (patient and control) are hybridized onto a glass slide containing DNA fragments (Bejjani et al., 2006) (see figure 1-4). The arrays are characterised by a high level of sensitivity and validation of results can be undertaken with FISH, the BAC DNA serving as a probe. However, Ishkanian et al. (2004) cautioned that producing BAC DNA is effort-consuming and a resolution higher than 100 Kb cannot be achieved, even on an entire genome tiling path array. By contrast, oligonucleotide arrays exhibit greater format flexibility which allows for higher resolution and customisation. Currently, oligonucleotide arrays are compatible with a range of platforms, either derived from genome-wide oligonucleotide markers based on SNP or developed from a virtual probe library covering the genome which affords a resolution of very high quality (Shaikh et al., 2007). The application of both BACs and oligonucleotide arrays in the determination of copy number modifications in individuals suffering from intellectual deficit (ID), multiple congenital anomalies (MCA) and autism has met with success. Diagnosis has been undertaken on the basis of several distinct methods of array design. A targeted array can be defined as consisting of particular genome areas, like the subtelomeres and areas in charge of recognised microdeletion/microduplication syndromes, but which lacks probes covering the entire genome (Bejjani et al., 2006; Shaffer et al., 2006). Originally employed in postnatal

clinical applications, this array type has also been applied in prenatal cases to address irregular ultrasounds or to conduct general screening (Le Caignec et al., 2005; Sahoo et al., 2006). Complete genome coverage is provided by an entire genome or tiling path array, the resolution being influenced by the manner in which the probes are spaced. For instance, the resolution used in clinical testing is associated with probe spacing ranging from 50 Kb to 1 Mb, with extra coverage being frequently provided in the subtelomeric areas (Toruner et al., 2007). Furthermore, in comparison to a targeted array, the increased coverage offered by entire genome arrays enables the detection of 5% more irregularities (Baldwin et al., 2008). As far as research is concerned, oligonucleotide entire genome arrays possessing extremely high density and custom arrays targeting particular areas have been invaluable tools in the identification of new syndromes, determination of target gene deletions and description of breakpoint areas (Seltzer et al., 2005; Urban et al., 2006; Wong et al., 2008).

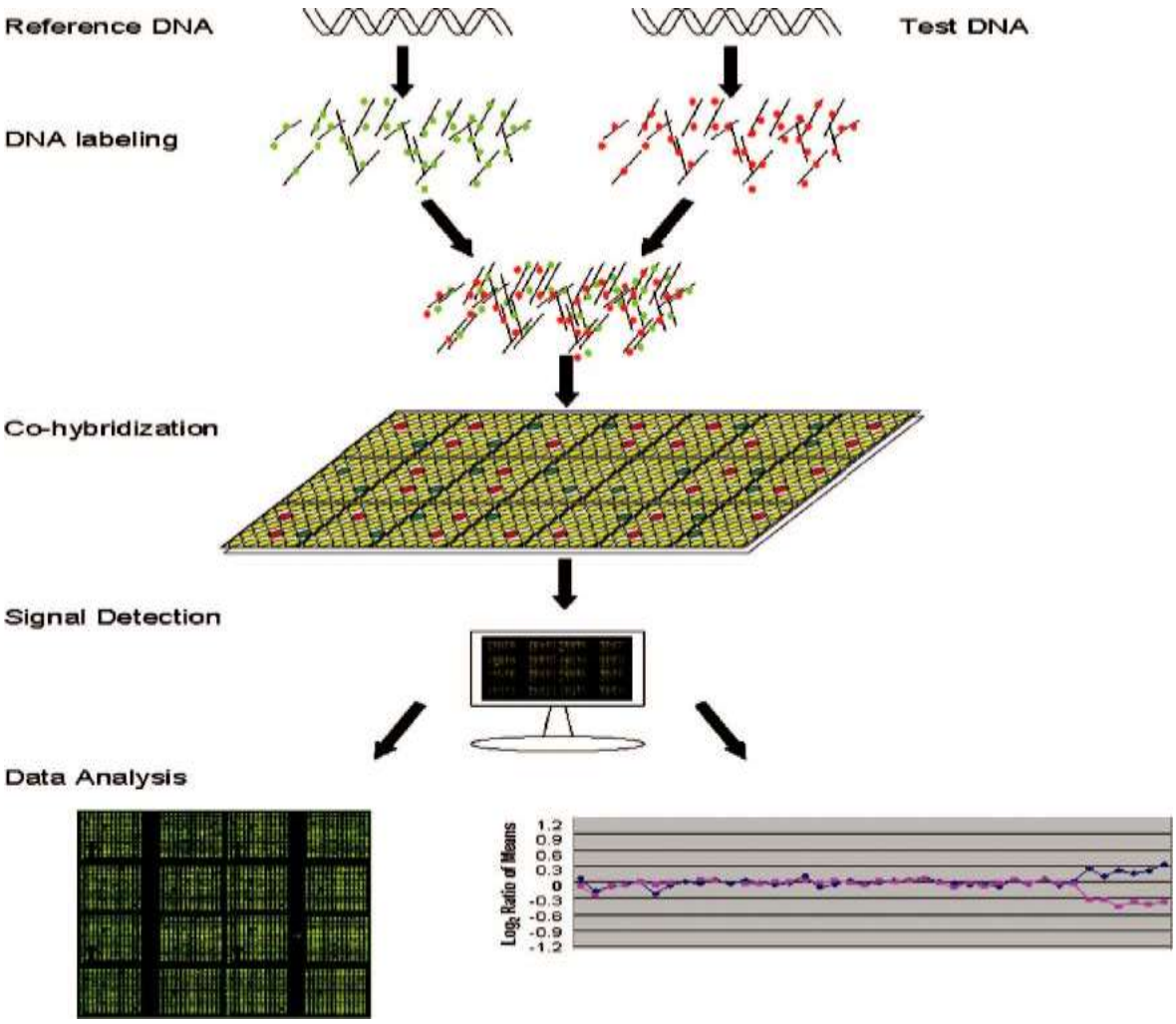

Figure 1-4: Schematic representation of microarray-based comparative hybridization technology

Whole DNA from a normal control labelled in green (left) and whole DNA from a patient labelled in red (right). The normal and patient DNA are co-hybridized onto a solid surface in which oligonucleotides or BACs have been located (middle). Imaging programs evaluate the fluorescence level for each DNA target and data analysis software are used to visualize the variations (lower). (Adopted from Bejjani and Shaffer, 2006).

1-11-2-4 Illumina bead-based microarrays

BeadArrays are self-assembling arrays consisting of minuscule beads to which probes are affixed. The separate production of every array involves exposure of a random array surface to an extensive accumulation of pre-prepared beads. As a result, the beads are selected at random and put together into wells on the array surface (Fan et al., 2006). Every bead array is allocated a particular DNA sequence, which is copied on approximately 30 beads on an array. The same probe sequence is present in a large number of copies in every bead with a diameter of 3 microns. As specified by Kuhn et al. (2004), for the same type of bead, the number and the location of the copies on an array are random. Moreover, every bead has an additional sequence for decoding, known as illumiCode, which is identical for same type beads. Every IllumiCode undergoes hybridisation in a foreseeable manner, giving rise to a number of specifically developed dye-labelled sequences. According to the level of hybridisation, every bead is allocated to a red or green state. In this way, a binary sequence for every bead is obtained from several hybridisations. A unique correlation must exist between this binary sequence and the anticipated IllumiCode response. By conducting such decoding hybridisations, Illumina ensures that the arrays provided contain bead types with more than five copies. The Illumina technology is also useful in high-throughput experiments as it can process BeadArrays in parallel. A sentrix BeadChip represents a slide made of glass which supports a large amount of observations of this chip; the number of samples that can be processed at the same time ranges from 1 to 16, and for each sample an extremely high number of genes can be profiled. Each of the 96 arrays included in the sentrix Array Matrix constitutes a hexagonal fibre optic bundle consisting of about 50,000 beads and 1,500 different types of beads. This means that just one sentrix array matrix can support the processing of 96 samples at the same time (figure 1-5).

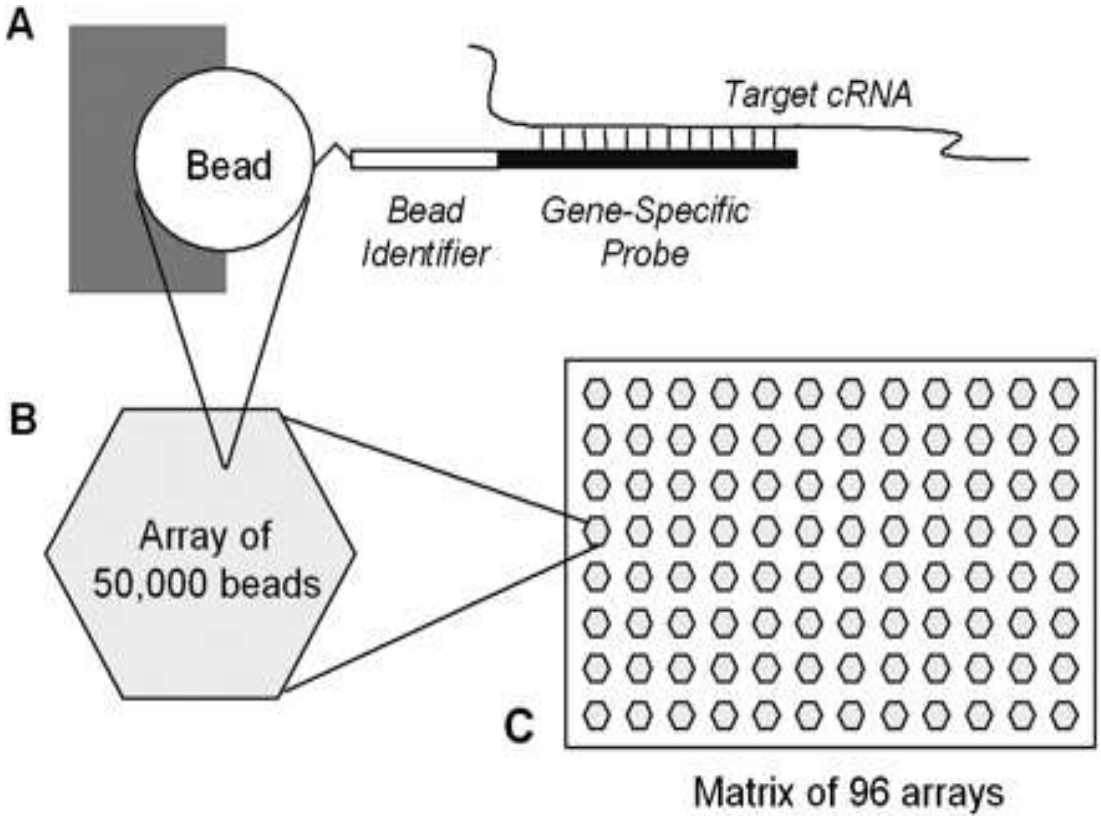

Figure 1-5: Schematic representation of a randomly assembled gene-specific array.

(A) An individual bead affixed in a well, a chimeric oligonucleotide is attached to the well by its 5' end.

(B) Array of 50,000 beads with a diameter of ~ 14 mm and each bead is affixed in a well at the end of an individual fibre bundle.

(C) 96 array matrix are arranged in the bundle. (Adopted from Kuhn et al., 2004).

1-11-2-5 Affymetrix GeneChips microarray

The high-density oligonucleotide-based arrays that contain small DNA oligonucleotides called probes are known as Affymetrix GeneChips. The chemical synthesis of these DNA probes takes place in particular areas on a coated quartz surface. A feature is defined as the precise location of a probe and the features present on just one array can number in the millions (Peeters and Van der Spek, 2005). In a feature, the synthesis of DNA probes occurs on wafers made of silicon through the process of photolithography. The DNA probes on the array are 11-µm in size and 25 nucleotides in length, 22 probes divided into 11 pairs constituting a probe set. The present U133-2plus GeneChip microarray consists of 54,000 distinct probe sets which account for around 30,000 identified genes and EST sequences. Detection of the presence of the RNA or DNA

complementary sequence in the sample is the purpose of each probe on an Affymetrix GeneChip. To accurately determine the presence of the complementary molecule in a given sample, the probe has to be sufficiently precise to differentiate a sequence from other similar ones at molecular level. Since one array can contain countless features, every sequence expressed is associated with multiple probes which generate highly sensitive and reproducible results. Furthermore, a high degree of specificity is afforded by the 25-mer long oligonucleotide probe, as a result of which signal and background noise can be differentiated. The standardised biotin labelling protocol underpinning the Affymetrix gene expression arrays employs an Oligo(dT)-primed linear amplification method based on *in vitro* transcription. In accordance with this, the standard Affymetrix fluidics and scanning station follow tight protocols. GeneChip technologies present several attributes that make them advantageous, such as the multiple probes targeting a single gene which ensures that experiments are specific and reproducible, as well as computerised monitoring of the experimental procedure from hybridisation to quantification (Han et al., 2004).

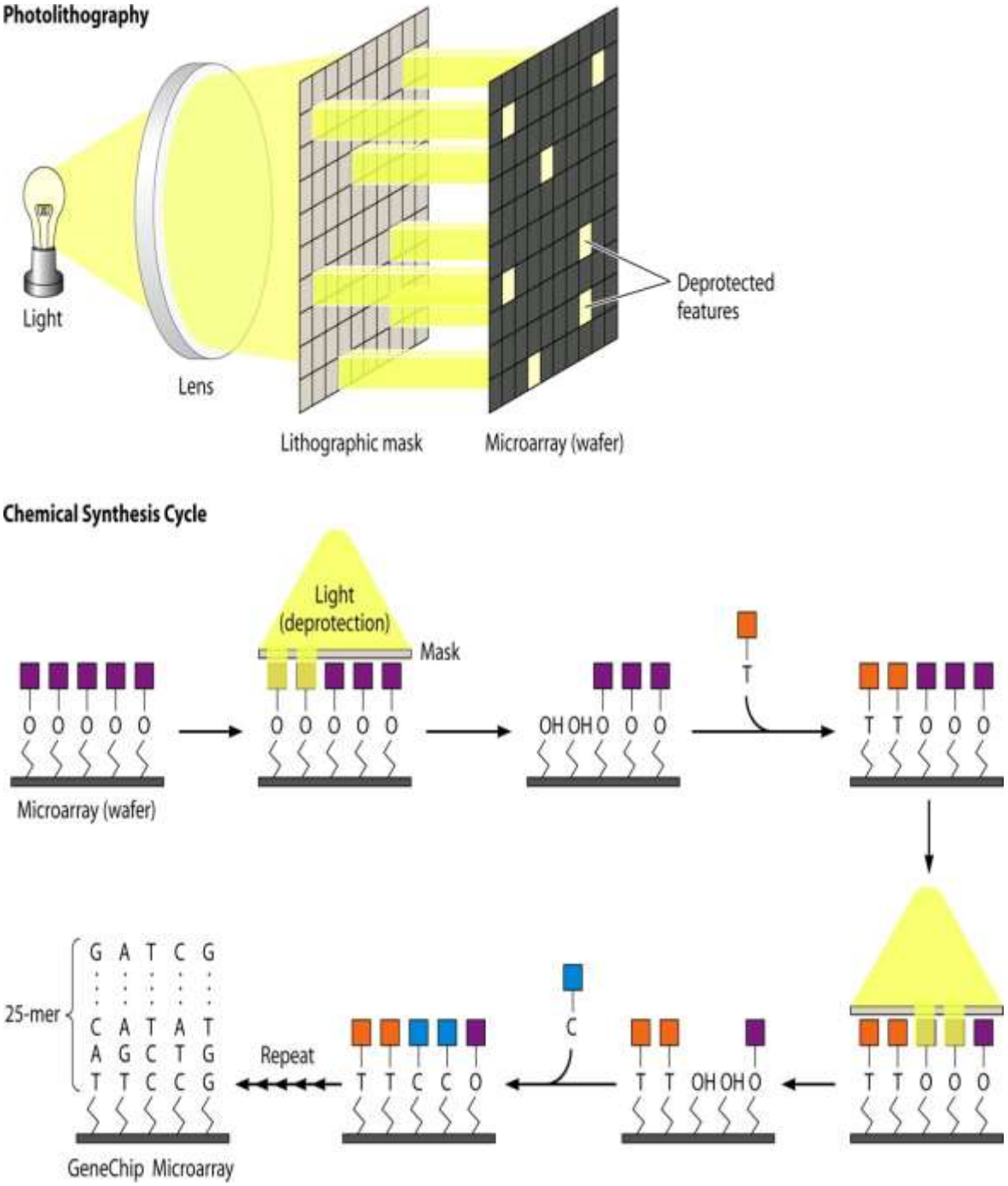

Figure 1-6: Schematic representation of Affymetrix GeneChip oligonucleotide micorarray.

A synthesis of DNA probes occurs on wafers made of silicon through the process of photolithography (Top). Ultraviolet light is shined through a lithographic mask that performance as a filter to either transfer or block the light from the microarray surface (wafer). The consecutive application of specific lithographic masks regulates the order of sequence synthesis on the surface. The chemical synthesis of these standers takes place in particular areas on a coated quartz surface (Bottom). The Ultraviolet light removes the protective groups (orange squares) from the standers (T). The nucleotides are washed over the microarray. The process of passing light through a lithographic mask, deprotection of standers and adding new

nucleotides are repeated many times.(Adapted from Miller and Tang, 2009).

1-4 Aim of study

The general aim of this research is to study leukaemia with recurrent chromosomal abnormalities in order to provide better insight into genetic events underlying leukemogenesis. The project focuses on different types of acute myeloid leukaemia and will cover the following aspects:

1. Acute myeloid leukaemias characterized by the presence of the t(7;12) rearrangement. Question: Can the rearrangement be accurately identified using a novel three-colour fluorescence in situ hybridization approach?
2. Acute myeloid leukaemia characterized by the presence of deletion 7(q). Question: Can the deletion 7(q) be detected using a new three colour probe sets?
3. Acute myeloid leukaemias characterized by the presence of inv(16). Questions: (a) Can CNAs be identified in these leukaemias? (b) If yes, are CNAs present in the same leukaemic clone harbouring the inv(16)? If not, are the CNAs present in the non-dividing population of cells? Do CNAs have an impact on the prognosis of this group of patients?
4. Acute myeloid leukaemia characterized by the presence of specific chromosomal abnormalities. Question: what is the proportion of leukaemic cells in proliferative versus non-proliferative state?

These questions are answered by pursuing the following objectives:

1. To test a new probe set specifically designed by MetaSystems GmbH to target the t(7;12) in a three-colour fashion on a series of AML patients.
2. To validate a new probe set for the detection of del 7(q) in a series of leukaemia cell lines.
3. To analyse the data generated via an Illumina array approach on a series of inv(16) patients and validate the presence of CNAs by FISH.
4. To investigate the proliferative status of leukemic cells in several patients and normal blood samples by immunoFISH using probes to target the specific chromosomal abnormality and an antibody against the proliferation marker Ki67.

CHAPTER 2: MATERIALS AND METHODS

2-1 Patient samples

Patient samples used in this study were provided as archival methanol-acetic acid fixed chromosome suspensions by several cytogenetics laboratories:

(i) Chromosome Laboratory, University Children's Hospital, University of Giessen and Marburg, Germany;
(ii) Paediatric Haematology, San Gerardo Hospital, Monza, Milan, Italy;
(iii) St Anna Children's Hospital, Vienna, Austria.

2-2 Peripheral blood samples

Stimulated and unstimulated peripheral blood cells used in this study were provided either as archival methanol-acetic acid fixed or a cryopreserved human peripheral blood lymphocytes (PBL) (Caltag Medsystems, UK).

2-3 Leukaemia and lymphoma cell lines

Five different cell lines were used in this study:

Farage (CRL-2630) cell line was derived from patient who had diffuse large cell non-Hodgkin's lymphoma (DLCL). According to Ben-Bassat et al. (1992), cytogenetic analysis showed trisomy of chromosome 11 in this cell line. Farage cells are positive for Epestien-Barr Virus (EBV) and do not express cytoplasmic immunoglobulin. This cell line was purchased from the ATCC-LGC standard partnership.

K562 cell line was derived from an elderly female patient with cryonic myeloid leukaemia. The cytogentic analysis of this cell line showed Philadelphia chromosome (Ph) and aneuploidy (lozzio et al., 1975). This cell line was provided by collaborators in Oxford.

Pfeiffer (CRL-2632) cell line was established from patient with leukaemic phase of diffused large cell lymphoma with cleaved and non-cleaved nuclei in 1992. Pfeiffer cells are negative for Epestien-Barr Virus (EBV). Several chromosomal abnormalities are

present including the typical t(14;18)(q32;q21) translocation of follicular lymphomas. This cell line was purchased from the ATCC-LGC standard partnership.

GDM1 cell line was derived from peripheral blood of 66-67 years old female patient with acute myelomonoblastic leukaemia. The chromosome banding analysis of this cell line showed various chromosomal abnormalities that involved a deletion of chromosome 6, trisomy 8, del (6q), add (+7q), and a deletion of short arm of chromosome 12 (Ben-Bassat et al., 1982). This cell line was obtained from the National Institute for Cancer Research, Genova, Italy.

GF-D8 cell line was established from peripheral blood of an 82 year-old man with AML subtype M1. The G-banding analysis of this cell line showed monosomy 5, deletion of 7q22, inv(7) and additional abnormalities such as add(8q), add(11q), del(12p),monosomy 15 and monosomy 17 (Rambaldi et al., 1993).

2-4 Probes

The following probes were either provided by or purchased from MetaSystems GmbH, Altlussheim, Germany:

1. A break-apart probe with an spectrumorange labelled hybridizing centromeric to ETV6 gene in 12p13, a FITC labelled probe hybridizing telomeric to ETV6;
2. A revised version for 12p13 with an spectrumorange labelled part hybridizes proximal to the *ETV6* gene at 12p13 and a FITC labelled probe hybridizes to the distal region of ETV6;
3. A locus-specific probe which hybridizes to flanking region of the HLXB9 gene labelled in blue (aqua);
4. A dual fusion probe for inv16 with an spectrumorange labelled probe spans the breakpoint at 16q22 and includes the CBFB region and a FITC labelled probe spans the breakpoint at 16p13 and includes the MYH11 region;
5. Three-colour FISH probe for the detection of del(7q22-q31) with an spectrumorange labelled probe hybridizes to 7q22, a FITC labelled probe hybridizes specifically to 7q31 and a blue (aqua) labelled probe which spans the centromere of chromosome 7;

6. Three-colour probe for the detection of del(7q22-q36.1) with an spectrumorange labelled probe detects deletions at 7q22 band, a FITC labelled probe hybridizes to 7q36 region and a blue (aqua) labelled probe which spans the centromere of chromosome 7;
7. Whole chromosome 7 paint directly labelled with spectrumorange;
8. Partial chromosome 7 paint, with a green paint (FITC) hybridizing to the short arm of chromosome 7 and an spectrumorange paint spanning the long arm of chromosome 7.

In addition, the following probes were used in this study:

9. Whole chromosome paint probes for chromosome 12 labelled with biotin and chromosome 16 labelled with FITC (obtained from Cambio, Cambrdge, UK);
10. Bacterial artificial Chromosomes (BACs) for 7q36.1 (RP11-504N9), 4q35.1 (RP11-184A23), and 8q24.3 (RP11-195E4) regions (obtained from BACPAC Resources Center, Oakland, USA);
11. D8Z2 probe for chromosome 8.

2-5 Cell culture

Cell lines (Farage, K562, Pfeiffer and peripheral blood lymphocytes) were recovered from liquid nitrogen and maintained in RPMI media supplemented with 15% of foetal calf serum (FCS) (Gibco, Glasgow, UK). 1% of penicillin and streptomycin (Gibco, Glasgow, UK) were also added. Cell cultures were grown at 37°C with 5% CO_2. Cells were blocked in mitosis by treatment with colcemid (0.05mg/ml) 30 minutes before harvesting.

2-5-1 Stimulation of peripheral blood lymphocytes

Peripheral blood lymphocytes cells were stimulated using PHA at concentration of 0.5ul/ml or were left untreated for controls. The cells were maintained in RPMI media supplemented with 15% of FCS (Gibco, Glasgow, UK) and 1% of penicillin and streptomycin (Gibco, Glasgow, UK). The cells then were incubated for 72 hours at 37°C with 5% CO_2.

2-5-2 Harvesting of cultures

Cells were centrifuged for five minutes at 1200 rpm (MSE, Centaur2E Centrifuge, UK). The supernatants were then discarded. The pellets were re-suspended in 10 ml of hypotonic solution (0.075 M potassium chloride - KCL) at room temperature. The samples were incubated for ten minutes at 37˚C. Ten drops of fixation solution (3 parts methanol: 1 part acetic acid) were added. Cells were centrifuged again at 1000 rpm for five minutes and supernatants were then discarded and the pellet re-suspended in 1 ml fixation solution by vortexing. Fixation solution (9 ml) was added slowly to the samples. After an incubation of fifteen minutes at room temperature, the samples were centrifuged for five minutes at 1000 rpm. The supernatants were discarded, and washes with fixation solution were repeated several times.

2-5-3 Preparation of slides

The methanol/acetic acid fixed chromosomes and cells of both patient samples and cell lines were centrifuged for three minutes at 3000 rpm. Each sample was re-suspended in 200 µl of fresh fixative solution. Chromosome suspension (8 µl) was dropped onto the centre of clean slides. Slides were labelled with the patient reference number or the cell line names and were then air dried. The cells suspension cytospin slide centrifuge was used to spin cells cultured in suspension onto slides, 300 µl of the culture was added to the chamber and was centrifuged at 700 rpm for five minutes. The quality of the slides was checked using light microscope.

2-6 Preparation of the DNA probe

2-6-1 Bacterial Artificial Chromosome

Using information from the University of California, Santa Cruz Genome Browser on Human Feb. 2009 (GRCh37/hg19) Assembly database, BAC clones were selected for the long arms of chromosome 4q35.1 (RP11-184A23 and RP11-51B8), chromosome 7q36.1 (RP11-504N9 and RP11-104H2) and chromosome 8q24.3 (RP11-195E4) from the BACPAC Resources Centre (BPRC). The clones were obtained as bacterial LB agar stabs culture. A loopful of each culture was then streaked onto an agar plates containing luria Bertani LB medium (1% (w/v) NacI, 1% (w/v)) bactotryptone, 0.5% (w/v) yeast extract (Fisher

Scientific UK), 1.5% (w/v) agar technical (Oxoid, UK) and 12.5 µg/ml chloramphenicol. Plates were then incubated at 37˚C overnight. One loopful from each plate was re-suspended in 10 ml of LB broth, and 12.5 µg/ml chloramphenicol and incubated at 37˚C overnight on shaker. Five hundred µl of 80% glycerol in medium was added to 500 µl of each bacterial suspension and then stored at -80˚C. For the DNA isolation and/or DNA extraction from clones, BACs DNA was isolated from 10 ml of each bacterial suspension using 300 µl of buffer 1 (P1) solution (15 mM Tris (pH8) (Fisher Scientific), 10 mM EDTA (Fisher Scientific) and 100 µg/ml RNase A (sigma-Aldrich). 300 µl of buffer 2 (P2) solution (0.2 M NaOH and 1% SDS) was added to the mixture gently and incubated for five minutes at room temperature, followed by the addition of 300 µl buffer 3 solution (3M potassium acetate) drop by drop with gentle mix. The suspensions were then incubated on ice for ten minutes.

The mixtures were centrifuged at 10000 rpm for ten minutes at 4˚C and supernatants (containing DNA) were transferred to 2 ml tubes containing 800 µl of ice-cold isopropanol and mixed (by inverting the tube several times). The mixtures were incubated overnight at -20˚C in order to allow DNA precipitation. After overnight incubation the tubes were centrifuged at 10000 rpm for fifteen minutes at 4˚C. The supernatant was removed and 500 µl of ice-cold 70% ethanol was added to each tube. The pellets were washed by inverting the tube several times. The tubes were centrifuged in microcentrifuge at 10000 rpm for ten minutes at 4˚C. The supernatants were removed and the pellets were allowed to dry at room temperature for two hours prior to re-suspension in 40 µl of ddH2O by gently occasional tapping of the bottom of the tubs.

2-6-2 Agarose gel electrophoresis

To validate the DNA size, the extracted BACs DNA was added to water with 1 µl of DNA size III marker (PeQlab, Erlangen, Germany) and 1µl of DNA dye to achieve a final volume of 6µl. The mixture was loaded onto 1% agarose gel stained with ethidium bromide (0.5µg/ml). The gel was run in TBE buffer (0.089 M Tris, 0.089 boric acid and 2Mm EDTA, Ph8.0) at 80 volts for one hour.

2-6-3 Measurement of DNA concentration

DNA concentration was measured using Nanodrop (Nanodrop 200oC, Thermo Scientific, UK). 1 µl of each DNA sample was taken and placed in the sample chamber of the Nanodrop. The reading obtained was the concentration of DNA samples in ng/µl. For the DNA samples, the DNA concentration was over 1000ng/ µl.

2-6-4 Labelling of DNA probes

Probes were labelled using nick translation (BioNick™ DNA Labelling System, Invitrogen, UK), which is a technique for DNA labelling of FISH probes used in this study (table 2-1).

Table 2-1: Probes labelled by nick translation

Patient no.	Chromosome band	BACs
26	7q36.1	RP11-504N9 and RP11-104H2
27	4q35.1	RP11-184A23 and RP11-51B8
30	8q24.3	RP11-195E4
L020944	Cen 8	D8Z2
H010340	Cen8	D8Z2
0132108	Cen8	D8Z2

1 µg of each of these probes was mixed with 5 µl of 10xdNTP mix (0.2 mM each dCTP, dGTP, dTTP, and 0.1mM dATP and biotin-14-dATP), 5 µl of 10x enzyme mix (DNA polymerase I and DNase I) and ddH2O to make up the final volume of 50 µl. the mixtures were mixed and incubated for two hours at 16˚C.

2-6-5 Agarose gel electrophoresis

To check the presence of labelled DNA, the DNA was diluted in water, 1 µl of DNA size XIII marker (PeQlab, Erlangen, Germany) and 1µl of DNA dye to achieve a final volume of 6µl. The mixture was loaded onto 2% agarose gel stained with ethidium bromide (0.5µg/ml). The gel was run in TBE buffer (0.089 M Tris, 0.089 boric acid and 2Mm EDTA, Ph8.0) at 80 volts for one hour.

2-6-6 Purification of labelled probes

Illustra microspin G-50 column (GE Healthcare, UK) was used to remove the unincorporated nucleotides, labelled probe was added to the top of the column and then centrifuged at 6000 rpm for one minute; 5 µl of salmon sperm DNA (11.0 mg/ml), 10 µl 3 M NaAC and 2.25 V 100% ice-cold EtOH were added to the purified samples. The DNA was then precipitated overnight at -20˚C and centrifuged at 13000 rpm for 30 minutes at 4˚C. The pellet was washed with 200 µl of ice-cold EtOH 70% and centrifuged at 13000 rpm for 1five minutes at 4˚C. The DNA pellet was then dried and resuspended in 20 µl of ddH2O. The purified samples were then stored at -20˚C until use.

2-7 Fluorescence in situ hybridization (FISH)

2-7-1 Denaturation of the target DNA

The slides were washed in 2XSSC (pH7.0) with shaking for five minutes. The slides were then dehydrated through an alcohol series (70%, 90% and 100%) followed by air-drying for five minutes. The slides were placed in 70% formamide solution containing 20XSSC and water at 70˚C for five minutes. After the denaturation, the slides were washed with ice-cold 2XSSC for five minutes and then dehydrated again through an alcohol series (70%, 90% and 100%) and air-dried at room temperature.

2-7-2 Probe denaturation

Commerical probe sets and biotin labelled probes were prepared. COT 1 DNA was added to the latter to block the repetitive sequences of the genomic DNA (Roche Diagnostics GmbH, Germany). The mixture was centrifuged using speed vacuum centrifuge. All probes were conducted in a dark atmosphere to protect them from light. Before adding the probes to the slides, they were denatured at 65˚C for ten minutes in a water bath and then placed in a water bath for ten minutes at 37˚C.

2-7-3 Hybridisation

The slides were labelled with their probe names, then the denatured probes were added onto the slides, and the slides were covered with 22x22 mm coverslip, then the coverslips were sealed to the slides using bicycle glue. The slides were left to dry for a few minutes

and then put back into a moist chamber in a water bath at 37˚C overnight to allow the probes to hybridise to the target chromosomes.

2-7-4 Post-hybridization washes and detection of labelled probe

The slides were collected from the water bath, and the bicycle glue was carefully removed. The slides were washed in 2xSSC with five minutes shaking to remove the coverslip, then they were placed in a coplin jar containing 0.4xSSC for five minutes. The jar was placed in 72˚C, and after five minutes of washing the slides were washed again with 2xSSC for five minutes.

For the biotin labelled probe, 3% bovine serum albumin (w/v) (BSA in 4XSSC, 0.05%Tween20) (Sigma, UK) blocking solution was added to the slides and covered with parafilm, placed in a moist chamber and then into a 37˚C water bath for an hour (blocking solution is used to stop unspecific binding). After that the parafilms were removed gently, and diluted Streptavidin-Cy3 and/or Streptavidin -Cy5 solutions were added to the slides and covered with parafilm, then the slides were incubated for twenty minutes at 37˚C in water bath, then washed three times in 4xSSC/Tween20 for five minutes each in the dark. In order to amplify the probe hybirdisation signals the diluted biotin (anti-avidin conjugated) was added to the slides and they were incubated for twenty minutes at 37˚C in water bath. The slides then washed three times in 4xSSC/Tween20 for five minutes each in dark. The Streptavidin-Cy3 and/or Streptavidin-Cy5 solutions were added to the slides and covered with parafilm, then the slides were incubated for twenty minutes at 37˚C in water bath, then washed three times in 4xSSC/Tween20. Finally, the slides were washed in 1% phosphate buffer saline (PBS)(Sigma, UK) for another five minutes in the dark, and a DAPI solution (Vectashield, Vector Laboratories, UK) was added to the slides, then they were covered with 22x40 coverslip and sealed with bicycle glue.

2-8 Fixation methods

Stimulated and unstimulated samples (AH, AN, GO, JS, 2,5, LU and PB) were fixed in 3:1 methanol/acetic acid while the stimulated and unstimulated cells from (PB) were fixed in ice cold 4% paraformaldehyde for ten minutes and permeabilised with 0.2% Triton X-100 (Sigma-Aldrich) for ten minutes at 4˚C. The k562 cell line was fixed in 1:1

methanol/acetone for ten minutes and also in ice cold 4% paraformaldehyde for ten minutes and permeabilised with 0.2% Triton X-100 (Sigma-Aldrich) for ten minutes at 4˚C.

2-9 ImmunoFISH

Methanol-acetic acid fixed chromosome suspensions were prepared for the immuno-FISH experiment. The inv(16) probe was directly labelled with spectrumorange and FITC used for direct detection. BACs biotin labelled probes were indirectly visualized with streptavidin Cy3 and streptavidin Cy5. These probes were used according to the manufacturer's instructions with slight modifications. Slides were denatured with 70% formamide at 70°C for five minutes. Probe mixture was denatured at 65°C for ten minutes, incubated at 37°C for ten minutes, and subsequently applied to the slides. Slides were incubated for overnight at 37°C. After overnight incubations, slides were washed with 2x SSC for five minutes followed by another wash in 0.4x SSC for five minutes at 72°C. Blocking solution (3% BSA+ 4x SSC/Tween20) was added to the slides. Biotin labelled probes were detected using streptavidin Cy3 streptavidin Cy5. The slides were then mounted in Vectashield (Vector Laboratories Ltd., Peterborough, UK) containing 49, 6-Diamidine-29-phenylindole dihydrochloride (DAPI). The slides were washed three times with 1X PBS for five minutes each. Cells were then blocked with 1% NCS (Newborn Calf serum) in 1X PBS for one hour. 75 ul of monoclonal mouse anti-Human Ki-67 anti-body (mAbs) (Dako, Denmark) at the desired concentration (1: 75 in 1% NCS) was added to the cells. The cells were incubated in the oven for an hour. After the incubation time, the slides were washed three times in 1XPBS. 75 ul of the fluorescein anti-mouse secondary antibody (Vector Lab), diluted 1:75 in 1% NCS, was then added to the slides and incubated for an hour in the oven. The cells were washed again with 1X PBS three times for five minutes each and then were mounted using vectashield mounting medium with 4,6-diamidino-2-phenylindole (DAPI)(Vector Laboratories,UK) to produce blue fluorescence.

2-10 Indirect immunofluoresence (IIF)

Cells fixed with methanol/acetone, paraformaldehyde and methanol-acetic were prepared for the immunofluoresence staining. The slides were washed three times with 1X PBS for five minutes each. Cells fixed in methanol/acetic acid and methanol/acetone were blocked with 1% NCS (newborn calf serum) in 1X PBS for one hour, while cells fixed

in 4% paraformaldehyde were blocked with 1% BSA in 1X PBS and 0.2% tween twenty for one hour. The monoclonal mouse anti-human Ki-67 primary antibody (mAbs) (Dako, Denmark) was diluted in (1:75) of 1% NCS or 1% BSA blocking solution to block the non-specific binding. The cells were covered with the diluted primary antibody and then incubated in the oven for an hour. After the incubation time, the slides were washed three times in 1XPBS. The fluoresencein anti-mouse secondary antibody (Vector Lab) was diluted (1:75) of 1% PBS or 1% BSA and then was added to the slides and incubated for an hour in the oven. The cells were washed again with 1X PBS 3 times for five minutes each and then were mounted using vectashield mounting medium with 4,6-diamidino-2-phenylindole (DAPI)(Vector Laboratories,UK) to produce blue fluorescence.

2-11 Microscope analysis and imaging

The slides were viewed under Olympus BX41 Fluorescence Microscope (Zeiss axioplan epifluorescence microscope, Carl Zeiss,) and Olympus BX-51 microscope to check the chromosomal abnormalities. All slides were examined under 100X immersion oil objective. Metaphases and interphase cells were captured with a camera (Scion FW Camera, Merge image processor, Version 1.0) and were previewed on MAC computer using SmartCapture3 sofware and with a CCD camera (739 3 575, pixel size 11 3 11 mm) with metasystems Isis v. 5.3 software and with a JAI CVM4+ progressive-scan 24 fps B&W fluorescence CCD camera and Leica Cytovision Genus v7.1 software.

2-12 Statistical analysis

To determine the cut off level of different hybridization signals of each probe, the hybridization signal pattern of each probe in at least 200 hundred nuclei from three different normal controls and patient samples was counted and analysed independently by three trained observers. The average of number of hybridization signals of each probe from three different normal controls was also calculated by each observer. From this, the mean average of number of hybridization signals of each probe between the three observed was then calculated. Following this, statistical analysis was performed using mean ± 3 × SD formula. All statistical analysis was done using Microsoft excel.

CHAPTER 3: A NOVEL THREE-COLOUR FLUORESCENCE *IN SITU* HYBRIDIZATION APPROACH FOR THE DETECTION OF T(7;12) IN ACUTE MYELOID LEUKAEMIA REVEALS A NEW CRYPTIC THREE-WAY TRANSLOCATION T(7;12;16)[1]

3-1 Introduction

A large number of chromosomal abnormalities have been identified in AML, one of which is a translocation between chromosome 7 and chromosome 12 t(7;12)(q36;p13). This translocation involves the *ETV6* gene located on the short arm of chromosome 12. The *ETV6* gene has been found to be involved in translocations with more than 40 partner genes in various types of leukaemia (De Braekeleer et al., 2012). The t(7;12) is a recurrent chromosome abnormality in infant leukaemia with an estimated incidence of 20-30% (Tosi et al., 2003; Von Bergh et al., 2006). The t(7;12)(q36;p13) is not associated with any specific AML subtype and to date has been associated with poor prognosis (Tosi et al., 2003; Von Bergh et al., 2006). This translocation has been found as the only abnormality in two out of 44 cases reported in the literature (table 3-1 summarizes the total number of published t(7;12) cases in the literature).

Additional cytogenetic features are described in almost all cases, with the presence of an extra chromosome 19 in 33 out of 44 cases and/or an extra chromosome 8 in twelve out of 44 cases. An extra chromosome 13 has been also found in two out of 44 cases. Despite the genomic breakpoint of 7q36 being heterogeneous, the HLXB9/ETV6 fusion transcript has been detected at the molecular level in some cases of t(7;12) where the exon 1 of *HLXB9* fused with the exon 3 of *ETV6* (Beverloo et al., 2001; Simmons et al., 2002; Tosi et al., 2003). The ectopic expression of *HLXB9* has been detected at the transcript level in all t(7;12) cases investigated (Ballabio et al., 2009; Park et al., 2009, Von Bergh et al., 2006).

[1] The contents of this chapter have been published as a scientific article: Naiel, A., Vetter, M., Plekhanova, O., Fleischman, E., Sokova, O., Tsaur, G., Harbott, J., and Tosi, S. (2013). A Novel Three-Colour Fluorescence in Situ Hybridization Approach for the Detection of t(7;12)(q36;p13) in Acute Myeloid Leukaemia Reveals New Cryptic Three Way Translocation t(7;12;16). *Cancers*, 5(1):281-295.

These data suggest that the presence of such ectopic expression of the *HLXB9* gene might promote leukaemogenesis in t(7;12) cases. Several studies have shown that an overexpression of *HLXB9* gene is present in other types of cancer, such as hepatocellular carcinoma and colorectal cancer (Hollington et al., 2004; Wilkens et al., 2011).

3-2 Aim of this study

The aim of this study is to validate a new three colour fluorescence in situ hybridization (FISH) approach which enables the detection of the t(7;12)(q36;p13) rearrangement. In order to achieve the above aim, the following objectives will be pursued:

1. To carry out FISH experiments using the commercially available probes set to:
    i. (i) a number of samples derived from patients known to carry the t(7;12) rearrangement;
    ii. (ii) a number of samples derived from patients in which the presence of t(7;12) has not been confirmed before.

2. To analyse the FISH data using microscopy and specialised software.

3-3 Materials and methods

3-3-1 Patient samples

Seven patient samples were used in this study, of which six have previously been studied and one is new. Archival methanol: acetic acid-fixed cell suspensions were obtained from the following laboratories:

i. Chromosome Laboratory, University Children's Hospital, University of Giessen and Marburg, Germany;
ii. Paediatric Haematology, San Gerardo Hospital, Monza, Milan, Italy;
iii. St Anna Children's Hospital, Vienna, Austria.

The clinical and cytogenetic characteristics of the patients are summarized in Table 3-2. Patient samples were selected according to the presence of t(7;12) (cases nos. 1-4) and the presence of *HLXB9- ETV6* fusion transcript (case no. 7).

Table 3-1: Total number of reported t(7;12) cases

AML, acute myeloid leukaemia; NOS, not otherwise specified, MDS, myelodysplastic syndrome; ALL, acute lymphoid leukaemia; ABL, acute bilineage or biphenotypic leukaemia; AMKL, acute megakaryoblastic leukaemia; Pt no. in the second column from right refers to the patient no. as indicated in the original report.

No.	Disease	Karyotype	Pt no.	Reference
1	T-ALL	48,XX,t(7;12)(q36;p13),+8,+19	116	Andreasson et al., 2000
2	AML-M0	47,XX,t(7;12)(q36;p13),+19	1	Ballabio et al., 2009
3	AML	48,XX,t(7;12)(q36;p13),+8,+19	2	Ballabio et al., 2009
4	AML	46,XY,t(7;12)(q36;p13)/47,idem,+8	13	Hagemeijer et al., 1979
5	AML-M4	47,XY,t(7;12)(q36;p13),+8	46	Hagemeijer et al., 1981
6	AML-M2	47,XX,t(7;12)(q36;p13),+19	1	Hauer et al., 2008
7	AML-M5a	49,XY,t(5;7;12)(q31;q36;p13),+8,+19,+del(22)(q13)	1	Park et al., 2009
8	ABL	48,XY,t(7;12)(q36;p13),+19,+22	2	Park et al., 2009
9	AML-M0	48,XY,t(1;7;12)(q25;q36;p13),+8,+19	3	Park et al., 2009
10	AML-M2	47,XX,t(7;12)(q36;p13),+19/49,idem,+X,+8	63	Raimondi et al., 1999
11	ANL-M2	47,XX,t(7;12)(q36;p13.1),+19	64	Raimondi et al., 1999
12	AML-M6	46,XY,der(7)t(7;12)(q32;p13)del(12)(p13)/ 47,idem,+19/47,idem,+8	26	Satake et al., 1999
13	AML-M2	48,XX,t(7;12)(q32;p13),+13,+19	27	Satake et al., 1999
14	AML	47,XY,t(7;12)(q36;p13),+19	1	Simmons et al., 2002
15	AML	48,XY,ins(12;7)(p13;q36;q11.1),+13,+19	2	Simmons et al., 2002
16	AML	46,XY,t(7;12)(q36;p13)	1	Slater et al., 2001
17	AML	47,XY,der(7)t(7;12)(q36;p13)del(12)(p13p13),der(12)t(7;12)(q36;p13),+19	2	Slater et al., 2001
18	AML	47,XY,t(7;12)(q36;p13),+19	3	Slater et al., 2001
19	AML	47,XX,t(7;12)(q36;p13),+19/48,idem,+19	4	Slater et al., 2001
20	AML	47,XX,t(7;12)(q36;p13),+19	6	Slater et al., 2001
21	AML	46,XX,t(7;12)(q36;p13)	9	Slater et al., 2001

No.	Disease	Karyotype	Pt no.	Reference
22	AML	46,XX,t(7;12)(q32;p13) 47,idem,+19	10	Slater et al., 2001
23	AMKL	46,XX,add(7)(q22),del(12)(p12;p13)	1	Taketani et al., 2008
24	MDS	46,XX,der(7)t(7;12)(q22;p13)del(7)(q22q36)	1	Tosi et al., 1998
25	AML-M5	47,XY,del(7)(q32q35-36),t(7;12)(q36:p13),+19	2	Tosi et al., 1998
26	AML-M1	47,XX,t(7;12)(q36;p13),+19	3	Tosi et al., 2000
27	T-ALL	50,XX,+6,del(12)(p13),+18,+19,+22	4	Tosi et al., 2000
28	AML-M0	47,XY,t(7;12)(q36,p13),+der(19)	5	Tosi et al., 2000
29	AML-M4	48,XY,t(7;12)(q36;p13),+8,+19.	6	Tosi et al., 2000
30	ALL-L2	47,XY,t(7;12)(q36;p13),+19 .	7	Tosi et al., 2000
31	AML	47,XX,t(7;12)(q36;p13),+8/48,idem,+19/ 50,idem,+X,+19,+19/51,idem,+X,+8,+19,+19	17	Tosi et al., 2000
32	AML-M0	47,XY,t(7;12)(q36;p13),+19.	6	Tosi et al., 2003
33	AML	48,XY,t(7;12)(q36;p13),+8,+19.	7	Tosi et al., 2003
34	AML-M0	46,XX,t(7;12)(q32;p13)/47,idem,+19	1	Von Bergh et al., 2006
35	AML-M2	47,XX,t(7;12)(q36p13),+19	4	Von Bergh et al., 2006
36	ALL	47,XX,del(7)(q31),del(12(p13)	5	Von Bergh et al., 2006
37	AML-M0	47,XX,+19	6	Von Bergh et al., 2006
38	AML-M5	47,XX,t(7;12)(q36p13),+19	7	Von Bergh et al., 2006
39	AML	48,XY,t(7;12)(q36;p13),+8,+19	2	Wildenhain et al., 2010
40	AML-M2	47,XX,t(7;12)(q36;p13),+ 19	3	Wildenhain et al., 2010
41	AML-M0	47,XX,t(7;12)(q36;p13),+ 19	4	Wildenhain et al., 2010
42	AML-M0	47,XX,del(7)(q11.2~21),del(12)(p13),+mar 5	5	Wildenhain et al., 2010
43	AML-M2	47,XX,del(12)(q12),+19	6	Wildenhain et al., 2010
44	AML-NOS	46XY,inv(2)(p11;p13),t(7;12)(q36;p13),der(16)t(1;16)(q22;p13),add(21)(q22).	5	Wlodarska et al., 1998

Table 3-2: Clinical and cytogenetic date of the patients

pt	Age/ sex	Disease	Karyotype	Reference
1	7 mo/F	AML	46,XX,der(7)t(7;12)(q22;p13)del(7)(q22q36)	Tosi et al. (1998, 2003)
2	3 mo/ M	AML-M0	47,XY,t(7;12)(q36;p13), +der(19)	Tosi et al. (2003)
3	5 mo/F	AML-M1	47,XX,t(7;12)(q36;p13),+19	Tosi et al. (2003)
4	8 mo/F	AML	47,XX,t(7;12)+19	Hauer et al. (2007)
5	7 y/F	AML-M0	48,XX,t(7;12)+19	Present study
6		AML	53,XY,del(2)(q31),+5,+6,+9,add(11)	Wildenhain et al. (2010)
7	4 mo/F	AML-M2	47,XX,t(7;16)(q36;q12),+mar	Wildenhain et al. (2010)

Pt, patient; AML, acute myeloid leukaemia; mo, months; y, years; M, male; F female.

3-3-2 Probes

The following probes were designed and provided by MetaSystems GmbH, Germany:

i. A break-apart probe set with an spectrumorange labelled probe hybridizing to the centromeric region of *ETV6* gene in 12p13 and a FITC labelled probe hybridizing to the telomeric region of *ETV6*

ii. A probe combination made of two loci that hybridize to flanking regions of the *HLXB9* gene labelled in blue (Aqua)(see figure 3-1);

iii. Revised version of (i) with an spectrumorange labelled probe that hybridizes to a region proximal to the *ETV6* gene at 12p13 and a FITC labelled probe that hybridizes to the distal region of ETV6 (see figure 3-9).

In addition, the following probes were obtained from Cambio (Cambridge, UK):

iv. Whole chromosome 16 paint (wcp16) direct labelled with FITC;

v. Whole Chromosome 12 paint biotin labelled (Cambio, Cambridge, UK).

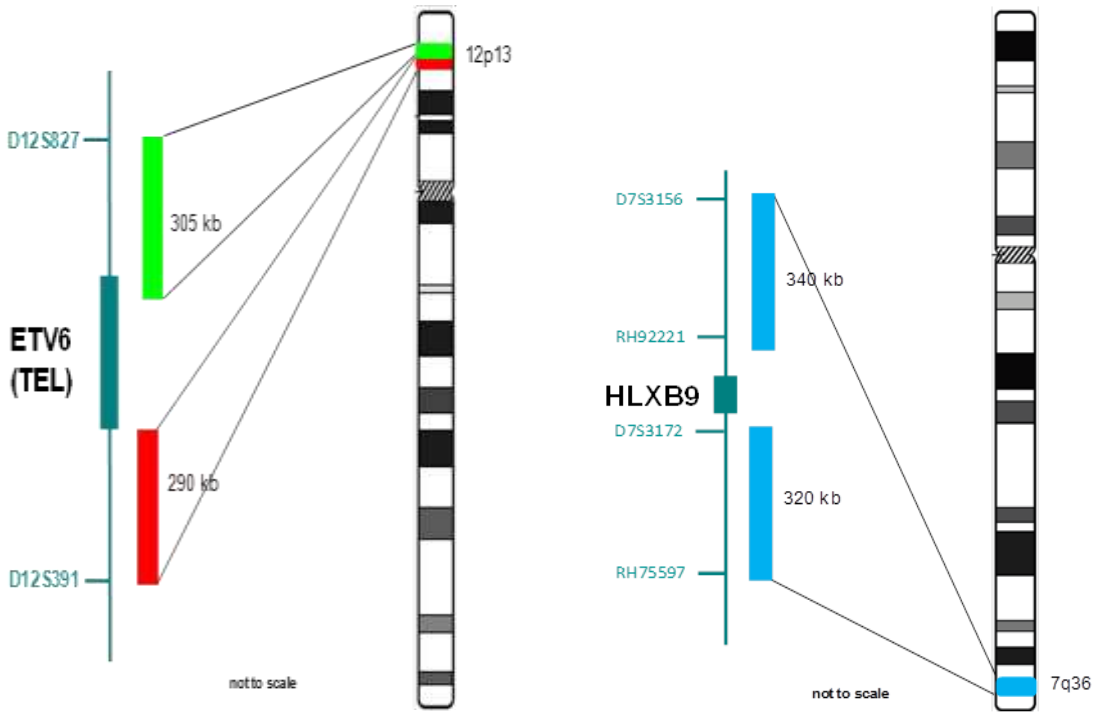

Figure 3-1: Ideograms of chromosomes 12 and 7 with details of the localization of the probes used for FISH

On the right of each chromosome ideogram, the chromosomal bands of the 12p13 and 7q36 are indicated. On the left of the ideograms, the probes used and their position along the genomic sequence are indicated.

3-3-3 FISH

FISH analysis was performed on bone marrow metaphases from archival methanol: acetic acid fixed cell suspensions stored at -20°C. The three-colour custom designed probe set (MetaSystems GmbH, Germany) and whole chromosome 16 paint (wcp16) (Cambio, Cambridge, UK) directly labelled with FITC were used for direct detections. Whereas, the whole Chromosome 12 paint biotin labelled (Cambio, Cambridge, UK) was indirectly visualized with streptavidinCy3. These probes were used according to the manufacturer's instructions. Slides were denatured with 70% formamide at 70°C for five minutes. Probe mix was denatured at 65°C for ten minutes, incubated at 37°C for ten minutes, and subsequently applied to the slides under a 22/22 mm cover-slip. After overnight of hybridization, slides were washed with 2x SSC (pH 8.0) for five minutes on shaker, followed by another wash in 4xSSC/tween 20 for five minutes on shaker and then one more wash in 1x PBS for five minutes on shaker. The slides then were mounted with Vectashield (Vector Laboratories, UK) containing 49, 6-Diamidine-29-phenylindole dihydrochloride (DAPI). FISH images were captured using a Zeiss axioplan epifluorescence

microscope (Carl Zeiss,) equipped with a CCD camera (739 3 575, pixel size 11 3 11 mm) and MetaSystems Isis v. 5.3 software.

3-4 Results

A total of seven patient samples were analysed in this study, of which six patients had previously been reported. Patients no. 1-4 had already been studied for the presence of the t(7;12) (Hauer et al., 2008; Tosi et al., 1998, 2003), whereas patients no. 6-7 failed to show a t(7;12) in previous reports (Wildenhain et al., 2010). Patient no. 5 was newly diagnosed. Clinical and cytogenetic characteristics of the patients are summarized in table 3-1. FISH studies were carried out using a new three-colour probe set on all patients. Furthermore, patient no. 7 was investigated using whole chromosome 16 paint (wcp16) and whole chromosome 12 paint (wcp12). FISH confirmed t(7; 12)(q36; p13) in six patients out of seven. Four patients out of seven (no. 1-4) previously reported as having t(7;12) translocation were confirmed as t(7;12) positive (see figure 3-2 and 3-3). One case (no. 6) was t(7;12) negative (see figure 3-4). Moreover, the t(7;12) translocation was detected in one patient (no. 5) aged 7 years old (see figure 3-5 and 3-6) and a cryptic chromosome translocation t(7;12;16) was identified as part of complex rearrangement that involved an insertion of chromosome 12 on the der(7) and a translocation of chromosome 16 onto the der(7) in patient no. 7 (see figures 3-7 and 3-8). The breakpoints at 12p13 (in five cases: patients no. 1-5) were within the *ETV6* gene between the spectrumorange labelled probe and the FITC labelled probe and proximal to the *HLXB9* probe targeted by the blue (aqua) probe. In patient no. 7 the breakpoints at 12p13 occurred also within *ETV6*: one is in a region distal to the one reported in the other patients, while one is proximal to the spectrumorange labelled probe. This resulted in a different pattern of FISH signals, with green (FITC) signals on the der (12) whereas the der (7) showed blue (aqua), green (FITC) and red (spectrumorange) signals (see figure 3-7). In addition, the breakpoints at long arm of chromosome 7 were proximal to the *HLXB9* region in four cases and distal to the *HLXB9* region in two cases. The breakpoints localization at 12p13 in patient no. 7 were reconsidered using revised probe for ETV6 region. The breakpoint at 12p13 include one within *ETV6* gene between the green (FITC) and red (spectrumorange) labelled probes (but not involved in the FITC labelled probe as shown in the previous probe), and one is proximal to the red (spectrumorange) labelled

probe, which resulted in der (7) carrying only red (spectrumorange) signal and der (12) only green (FITC) signals (figure 3-9).

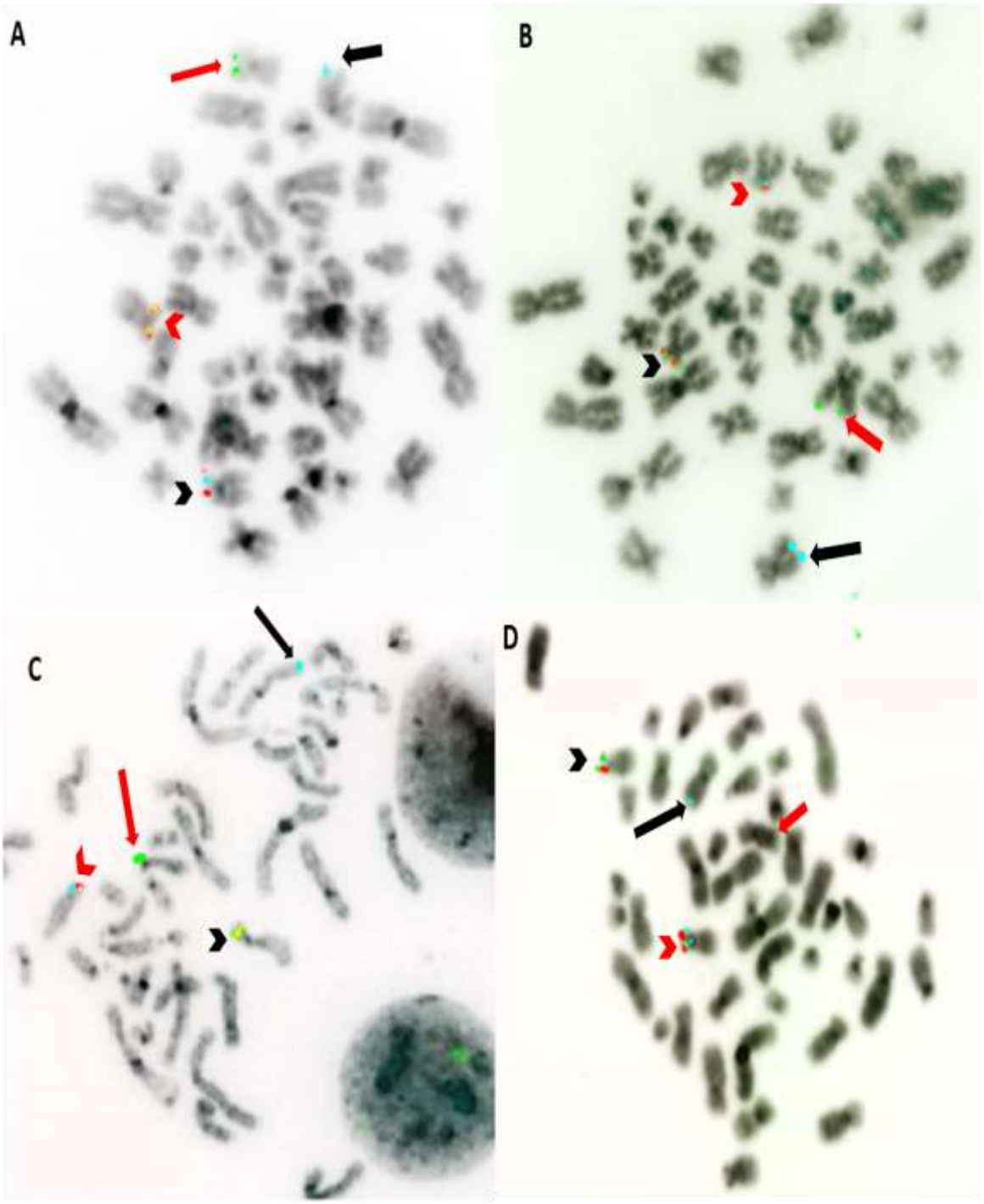

Figure 3-2: Examples of FISH performed on bone marrow metaphases from patients 1-4

Three-colour FISH using a break-apart probe specific for ETV6 gene on chromosome 12 in green (FITC) and red (spectrumorange) and specific probe for HLXB9 gene on chromosome 7 in blue (aqua) shows the translocation of chromosome 12 material onto the der(7) and translocation of chromosome 7 segment onto der 12 as well. The chr(7) and chr(12) are indicated by black arrows and black arrowheads. The

der(7) and der(12) are shown by red arrows and red arrowheads. The DAPI counterstaining has been converted into grey scale. Patients no. 1-4 are shown in panels A-D respectively.

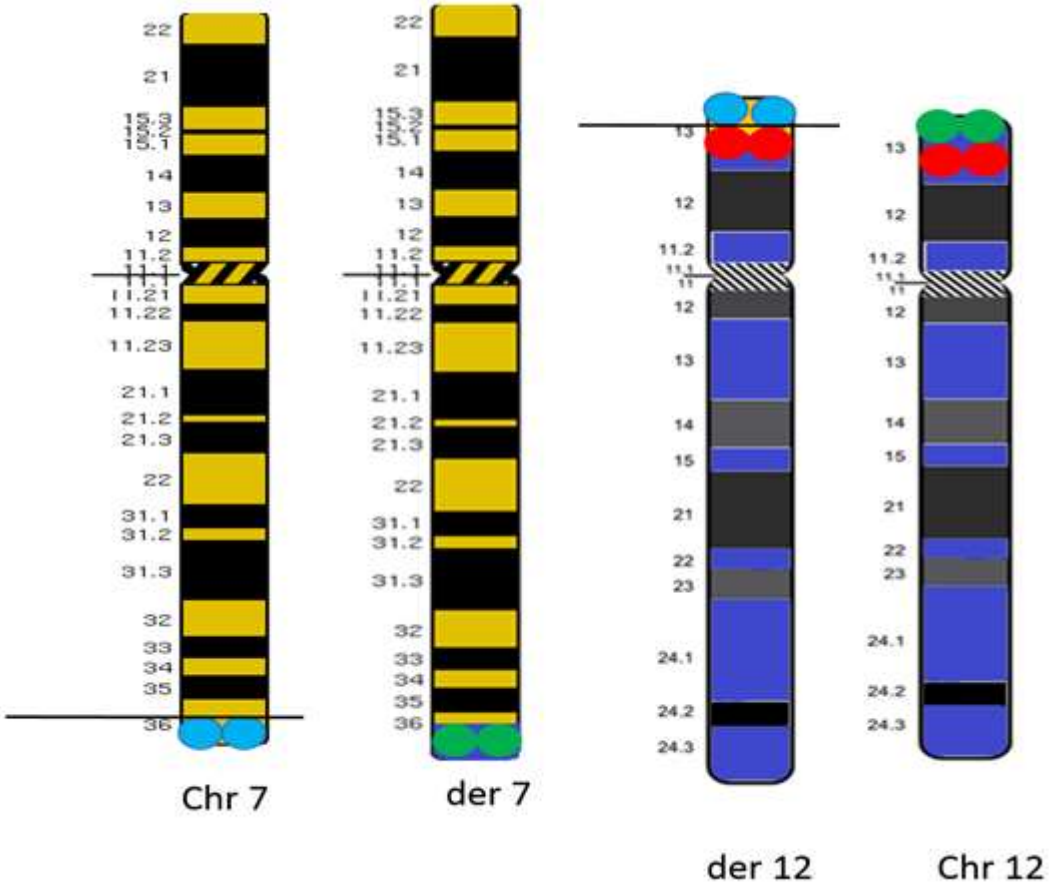

Figure 3-3: Ideogram of the t(7;12) rearrangement occurring in patients 1- 4

The schematic representation shows the translocation breakpoint on chromosome 7 and 12 with hybridization signals specific for both *ETV6* gene in green (FITC) and red (spectrumorange) and *HLXB9* (in blue).

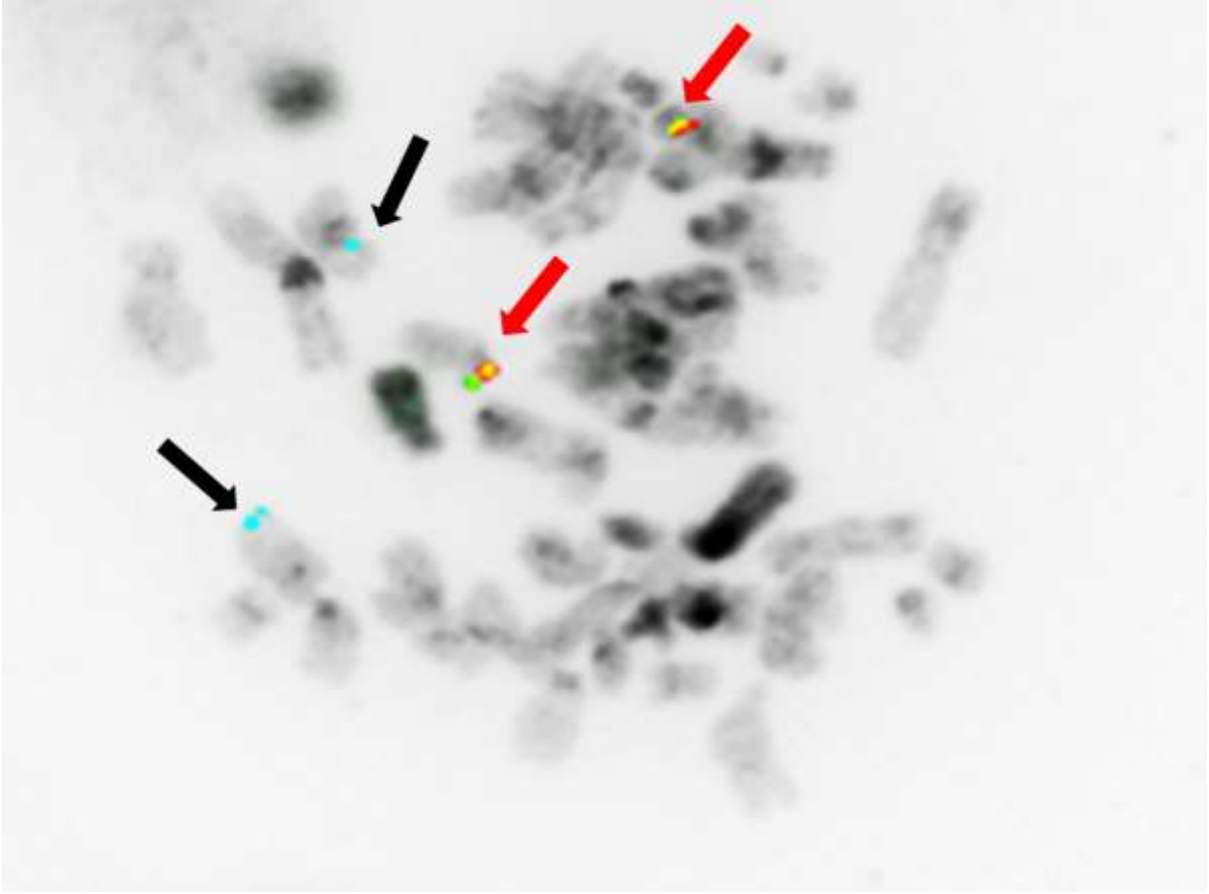

Figure 3-4: Example of FISH performed on metaphase chromosomes from patient 6 negative for t(7;12)(q36;p13)

ETV6 probe (FITC and spectrumorange) hybridized to both normal chromosomes 12. The HLXB9 probe (aqua) hybridized to both the normal homologue of chromosome 7. The black arrows indicated HLXB9 on chromosome 7q36. The ETV6 on chromosome 12p14 is indicated by the red arrows. The DAPI counterstaining has been converted into grey scale.

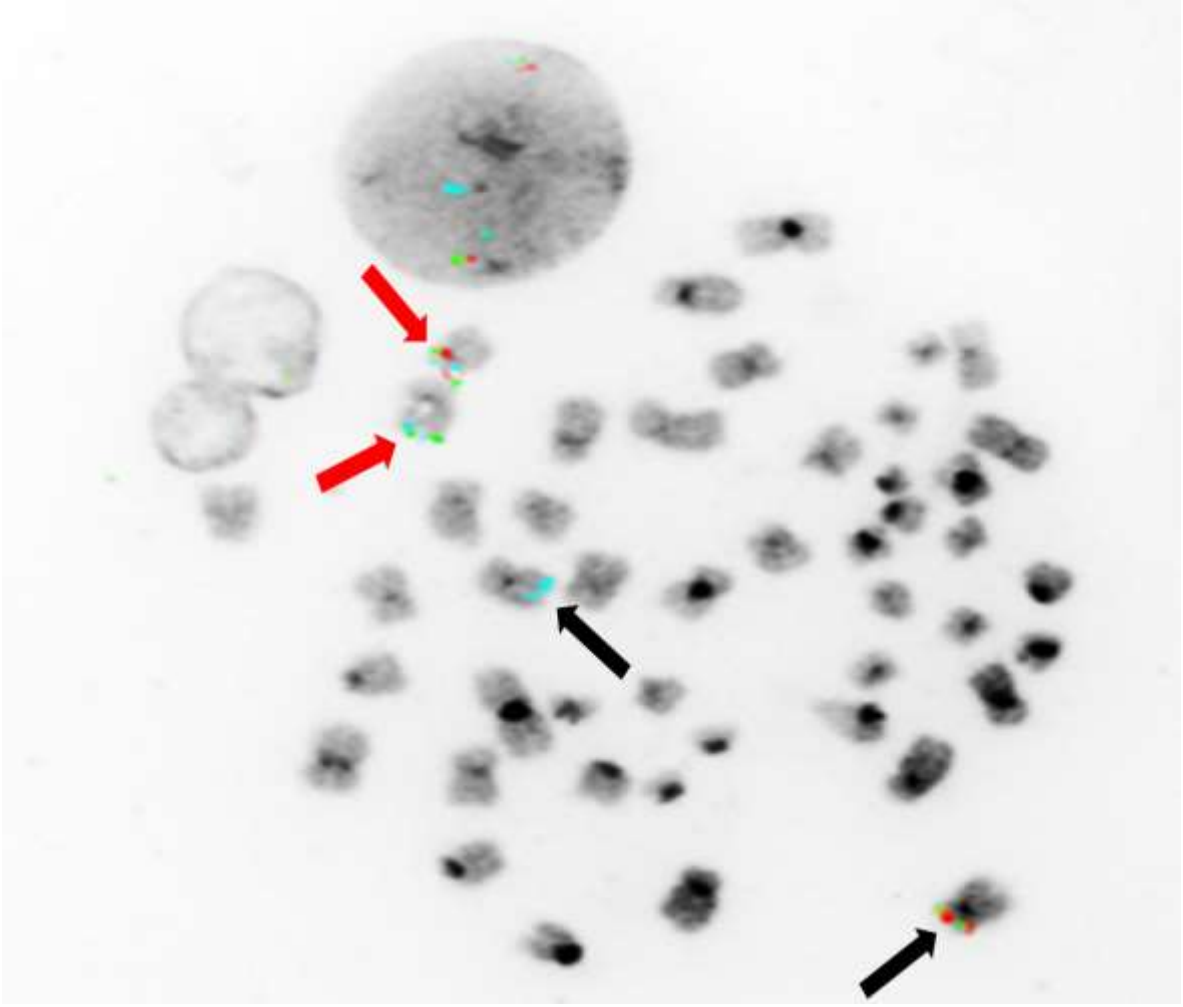

Figure 3-5: Example of FISH performed on metaphase chromosomes from patient no. 5

A normal chromosome 12 is detected by green and red signals and a normal chromosome 7 is detected by blue signal. The green and blue signals are seen on the derivative 7. The green, red and blue signals are seen on the derivative 12. Red arrows indicate derivatives 12 and 7, while black arrows indicate the normal chromosome 12 and 7. The DAPI counterstaining has been converted into grey scale.

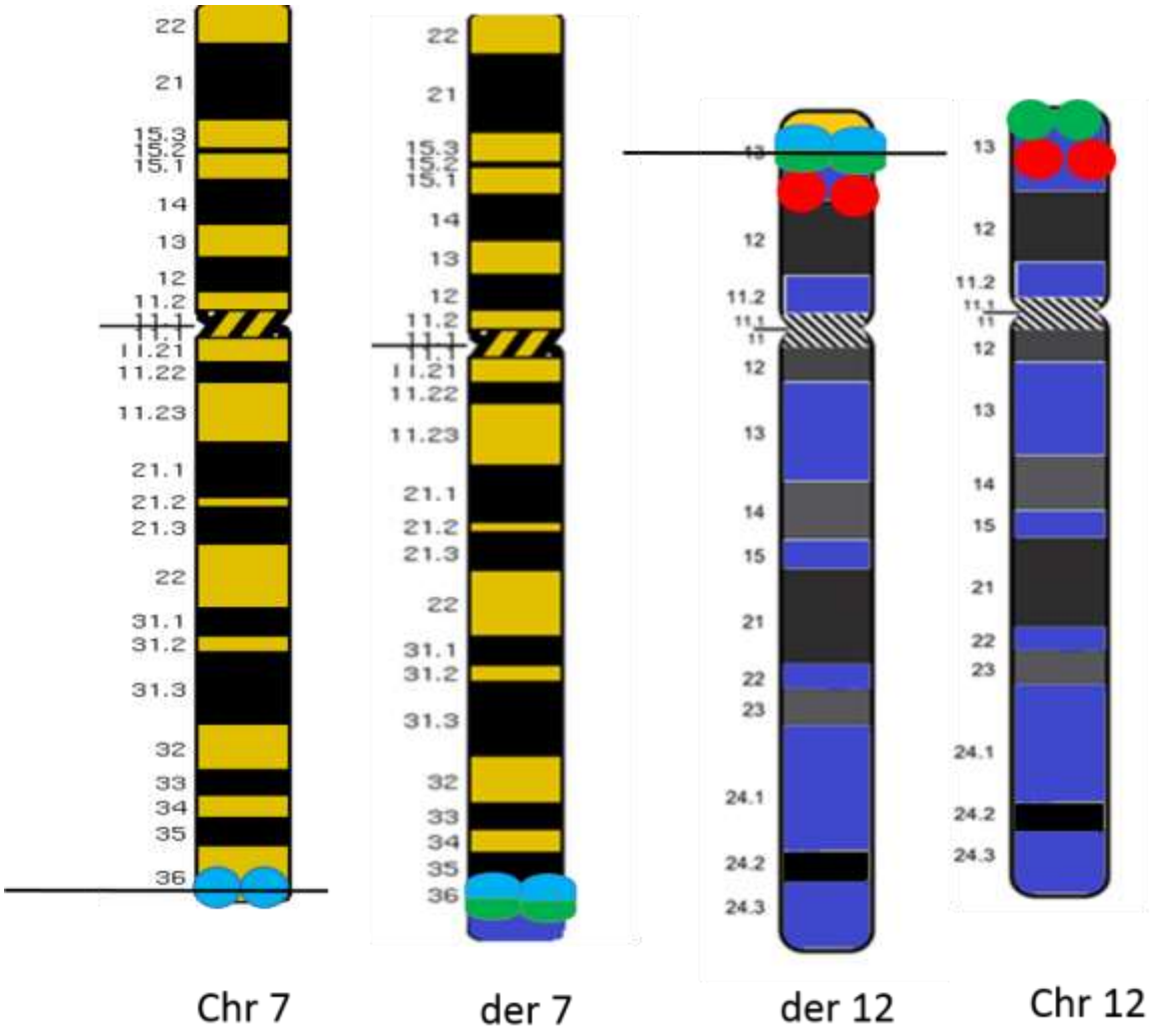

Figure 3-6: Ideogram of the t(7;12) rearrangement occurring in patient no. 5

The schematic representation shows that the translocation breakpoint on chromosome 7 and 12 with hybridization signals specific for both *ETV6* gene in green (FITC) and red(spectrumorange) and *HLXB9* (in blue).

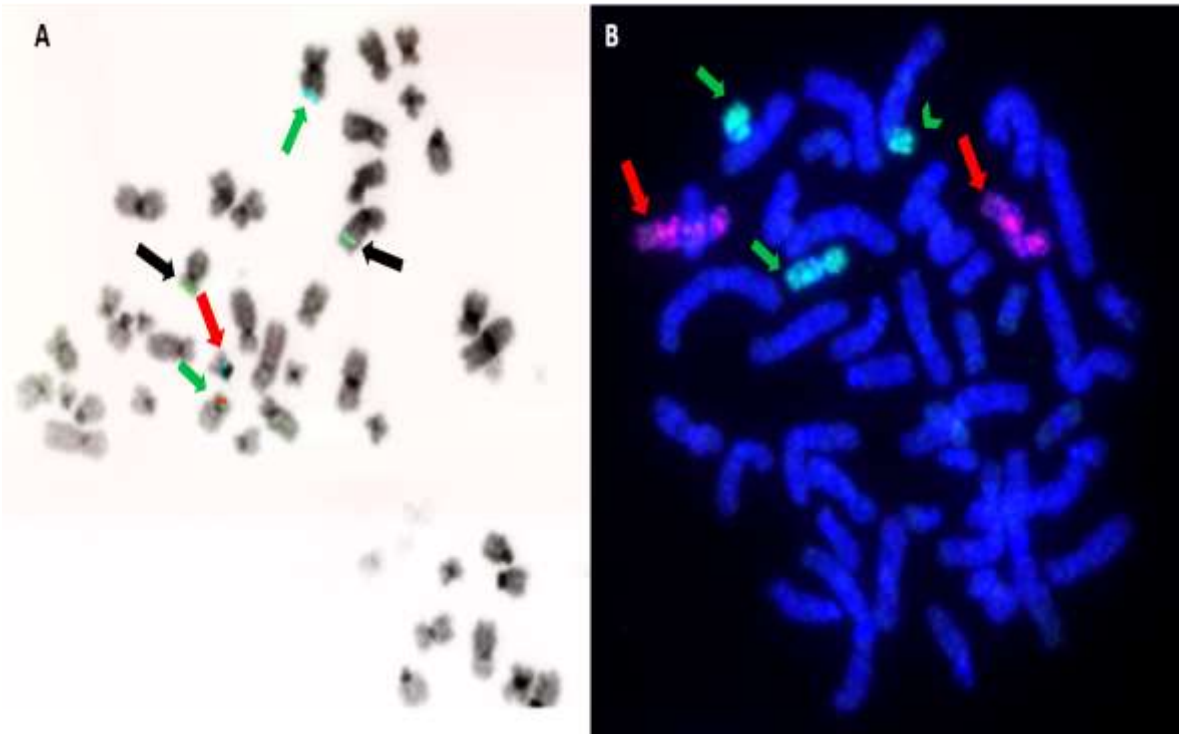

Figure 3-7: Example of FISH performed on metaphase chromosomes from patient no. 7

(A) FISH analysis of a metaphase from patient no. 7 reveals complex translocation that involves an insertion of chromosome 12 as shown by green and red signals on the der(7). Green arrows indicate the normal chromosomes 7 and 12, the black arrows show: (i) the der(7) (carrying green and red signals for *ETV6*); and (ii) the der(12) showing only green signals for a portion of *ETV6*. The red arrow indicates the der(16) carrying blue signals close to the centromere.

(B) FISH analysis of patient no. 7 with a translocation t(7;16) the green paint denotes the wcp 16 probe labelled with FITC, and the red (spectrumorange) paint indicates wcp 12 probe labelled with cy3. Green arrows show fully painted chromosomes 16, of which one is visibly shorter than the other, the green arrowhead shows chromosome 16 material translocated on the der(7). The red arrow shows chromosome 12.

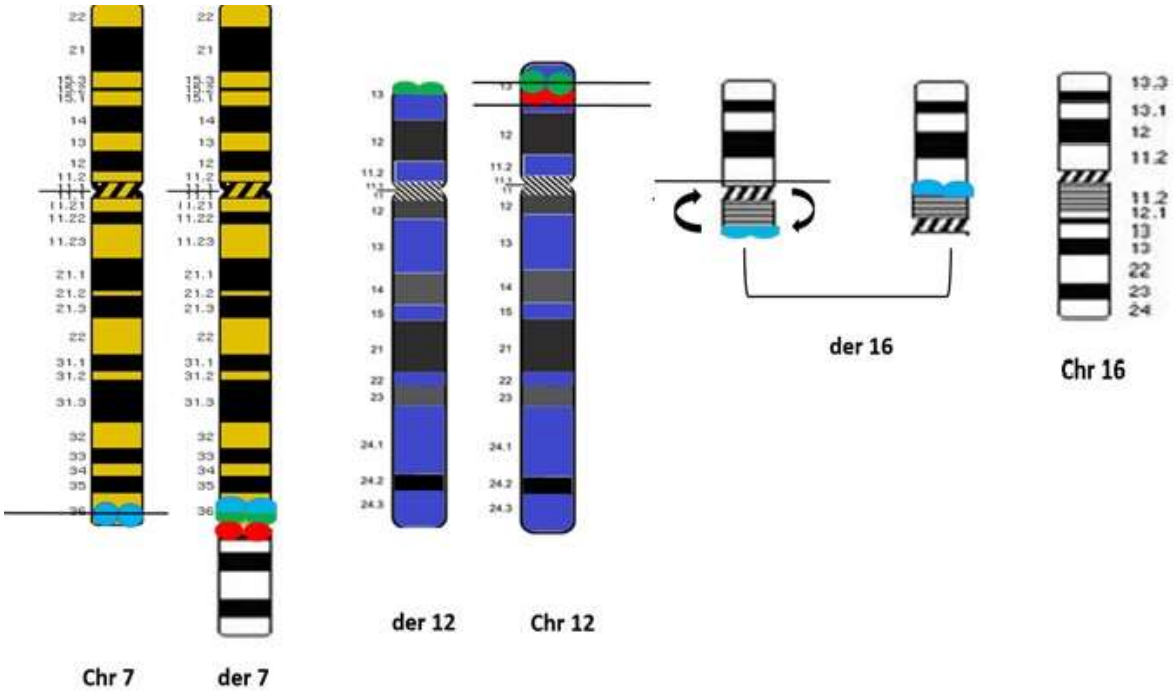

Figure 3-8: Schematic representation of the complex rearrangements in patient no. 7

Chromosomes 7, 12 and 16 are shown on the left side of their corresponding derivatives. The der(7) includes an insertion of chr 12 material with breakpoints at 7q36 within the blue (aqua) probe. This results in the visualization of the three differently labelled probes very close to each other. The der(7) terminates with chromosome 16 material. The der(12) shows an interstitial deletion of the ETV6 region (due to translocation onto the der(7)) resulting in the presence only of the green (FITC) probe. The breakpoints that generated the der(12) occurred in two regions, one proximal to the red signal and one in the middle of the green signal. The region comprised within these breakpoints is inserted into the der(7). The blue signals on the der(16) are caused by a translocation of 7q36 with breakpoint within the blue (aqua) probe onto the der(16). The location of blue signals in a region close to the centromere of the der(16) indicates that an inversion has also occurred.

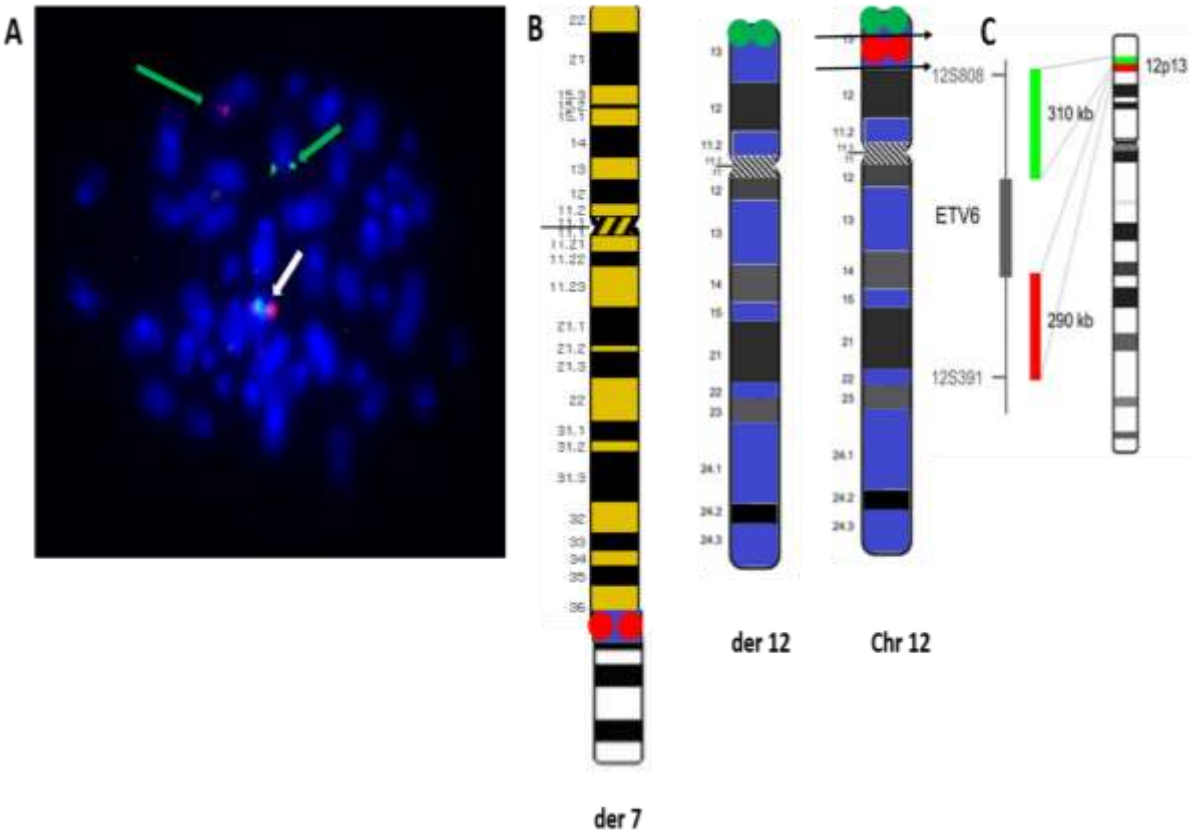

Figure 3-9: FISH analysis of a metaphase from patient no. 7 using redesigned ETV6 probe

(A) FISH image reveals a cryptic translocation that involves an insertion of chromosome 12 as shown by red signals on the der(7). Green arrows indicate the der(7) carrying red hybridisation signals and the der(12) carrying green hybridisation signals; the white arrow shows the normal chromosome 12 (carrying green and red signals for *ETV6*).

(B) Chromosome ideograms of the cryptic t(7;12) rearrangement, the breakpoints at chromosome 12 are proximal to green (FITC) probe and also proximal to the red (spectrumorange) probe. This results in a der (7) carrying red signals and der (12) with green signals.

(C) Schematic representation showing the revised *ETV6* probe with a green (FITC) probe more distal to the *ETV6* gene than the previous *ETV6* probe.

3-5 Discussion

The t(7; 12) is a recurrent chromosomal abnormality in infant patients with AML who are younger than 18 months of age. The t(7;12) translocation is not associated with any specific AML subtype (Von Bergh et al., 2006). Trisomy 8 and/or trisomy 19 are described in almost all cases (Simmons et al., 2002; Slater et al., 2001; Tosi et al., 2000; Von Bergh et al., 2006). PAC and YAC clones such as PAC H_DJ1121A15 and CEPH YAC 965c12 mapping

to 7q36 have been used for the detection of t(7;12) translocations in previous studies (Beverloo et al., 2001; Slater et al., 2001; Tosi et al., 2003). A new three-colour FISH approach was used in this study. This enabled us to confirm that the genomic breakpoints at 7q36 are heterogeneous (Beverloo et al., 2001; Simmons et al., 2002; Tosi et al., 2003). In this study the breakpoints in four patients (1-4) were proximal to *HLXB9*, and were distal to *HLXB9* in two different patients (5-7). These data are in agreement with previous research (Hauer et al., 2007; Tosi et al., 1998, 2003).

The application of this new probe set also enabled the detection of a cryptic t(7;12) translocation as a part of a complex rearrangements in one patient previously described as having t(7;16) and ETV6-HLXB9 fusion transcript at the molecular level (Wildenhain et al., 2010). Only two cases of a cryptic t(7;12) translocation have been reported in the literature (Park et al., 2009). The reported cryptic t(7;12) translocations involved chromosomes 5 and 1, but not chromosome 16. The possible mechanism for the formation of the t(7;12;16) complex rearrangement involves an insertion of chromosome 12 material into chromosome 7, a translocation between chromosome 7 and chromosome 16 and a subsequent inversion of chromosome 16. Furthermore, the new three-colour FISH approach has also enabled us to identify the t(7;12) in a new seven year-old patient with AML. This patient is the first case of childhood leukaemia with an onset after infancy positive for t(7;12). We were also able to confirm t(7;12) in four patients that had been previously reported as having t(7;12) translocation. Although the t(7;12) is considered a poor prognostic factor, it needs to be investigated whether this is still the case in the higher age group (seven years old and above) and the cryptic t(7;12) translocations. The prognosis in children aged 20 months or younger is very poor. This could be related to the infants, because they cannot tolerate high doses of cytotoxic chemotherapy in treatment regimens. The finding of a cryptic t(7;12) and the t(7;12) rearrangement in the seven year-old AML patient indicated that the incidence of t(7;12) rearrangement in AML might be higher than reported previously.

CHAPTER 4: THREE-COLOUR PROBE SETS FOR THE DETECTION OF CHROMOSME 7 ABNORMALITIES IN MYELOID MALIGNANCIES

4-1 Introduction

Chromosome rearrangements have been observed in hematological malignancies including leukaemia. The presence of these abnormalities can be used as a marker for diagnosis and as a prognositic factor for the outcome of the disease. Several chromosomal rearrangements are associated with favourable prognosis, such as t(15;17)(q22;q12), t(8;21)(q22;q22), inv(16) and t(16;16)(p13q22), intermediate risk group including t(9;11)(p22;q23),del(7q), del(9q), del(11q), del(20q), +8,+11,+13,+21 and normal karyotypes and unfavourable prognosis; for example, inv(3)(q21;q26), t(3;3)(q21;q26), t(9;22)(q34;q11), t(8;16)(p11;p13),del(5q), -5 and -7 (Grimwade et al., 1998; Marchesi et al., 2011; Von Neuhoff et al., 2010). Some of the commonly found chromosomal abnormalities in leukaemia are chromosome 7 alterations (Ling et al., 2005). Brozek et al. (2003) observed chromosome 7 rearrangements in 18% of AML cases and in 30% of ALL cases (Brozek et al., 2003). In other studies, -7 and del(7q) were identified in 7.8% (Byrd et al., 2002), 8% (Mauritzon et al., 1999) and 12% (Perkins et al., 1997) of AML cases. FISH technique can help to identify and map hidden chromosome rearrangements. Several studies investigated chromosome 7 aberrations in human myeloid leukaemia cell lines. The GDM1 cell line was derived from peripheral blood of a 66-67 year-old female patient with acute myelomonoblastic leukaemia. Cytogenetic analysis of this cell line using G-banded chromosomes showed a complex karyotype: 48,XX,der(2)t(2;11)(q36;q13),t(6;7)(q23;q36),+8,del(12)(p11.2p12.2),+13,del(16)(q23) (Ben Bassat et al., 1982). FISH studies on the GDM1 cell line have shown a translocation between chromosome 6 and chromosome 7, with breakpoints at 6q23 and 7q36 regions, resulting in an overexpression of HLXB9 (Nagel et al., 2005).

The GF-D8 cell line was established from the peripheral blood of an 82 year-old man with AML subtype M1. The G-banding analysis of this cell line showed monosomy 5, deletion of 7q22, inv(7) and additional abnormalities such as add(8q), add(11q), del(12p), monosomy 15 and monosomy 17 (Rambaldi et al., 1993). The cell line GF-D8 was later

characterized by Tosi et al. (1999) using molecular cytogenetic techniques such as multiplex FISH, FISH with subtelomeric probes and comparative genomic hybridization. Abnormalities of chromosome 7 were described as deletion of 7q accompanied with translocation between chromosome 7 and chromosome 15, and between chromosome 7 and chromosome 12. The deletion breakpoints on long arm of chromosome 7 were at 7q22 and 7q33 regions followed by a translocation of the terminal region of 7q on chromosome 12 and an insersion of chromosome 7 material into chromosome 15 (Tosi et al., 1999).

FISH analysis of GF-D8 cell line identified two rearranged chromosome 7 containing a del(7q) and an inv(7q). The inv(7q) had proximal breakpoint localized between 7q31.1-q31.3 and distal breakpoint at 7q35-q36 (Tosi et al., 1999). The K562 cell line was derived from an elderly female patient with cryonic myeloid leukaemia. The cytogentic analysis of this cell line showed the presence of Philadelphia chromosome (Ph) and aneuploidy (lozzio et al., 1975). The K562 cell line has been investigated by various cytogenetic and molecular cytogenetic techniques. Gribble et al. (2000) studied the chromosomal abnormalities in k562 cells by G-banding, M-FISH and CGH techniques. The chromsome banding analysis of k562 cell showed +i(7)(q10),del(7)(q31.2:q36),del(7)(q21q36). The M-FISH analysis revealed an intrachromosomal rearrangement of chromosome 7, whereas the CGH analysis showed normal structure of chromosome 7. In another study, M-FISH analysis presented four copies of chromosome 7 with one normal copy and three markers (M4, M5 and M6), while G-banding analysis showd M4 inv(7), M5 del(7)(p15) and M6 der(7)rea del(7) (Naumann et al., 2001).

4-2 Aim of this study

The aim of this study is to validate three-colour probe sets for the detection of 7(q22-q31) and 7(q22-q36.1) on several myeloid cell lines. In order to achieve the above aim, the following objectives will be pursued:

1. To carry out FISH experiments using the commercially available probes set to a number of samples derived from leukaemia cell lines.
2. To analyse the FISH data using microscopy and specialised software.

4-3 Materials and methods

4-3-1 Cell lines

Human cell lines used in this study included:

i. Farage (CRL-2630) cell line derived from a patient with diffuse large cell non-Hodgkin's lymphoma (DLCL). This cell line was used as a control;
ii. GD-F8 cell line derived from a patient with acute myeloid leukaemia subtype M1;
iii. GDM1 cell line was also derived from patient with acute myeloid leukaemia;
iv. k562 cell line was derived from a patient with chronic myeloid leukaemia.

4-3-2 Probes

Probes used were:

i. Three colour probes with an spectrumorange labelled probe hybridizing to the q22 region of chromosome 7, a FITC labelled probe spans the q31 region of chromosome 7 and aqua labelled probe hybridizing to the centromere of chromosome 7;
ii. Three colour probes with an spectrumorange labelled probe hybridizing to the q22 region of chromosome 7, a FITC labelled probe spans the q36.1 region of chromosome 7 and a aqua labelled probe hybridizing to the centromere of chromosome 7;
iii. Locus -specific probe made of two loci that hybridize to flanking regions of the *HLXB9* gene labelled in aqua;
iv. Whole chromosome 7 paint directly labelled with spectrumorange;
v. Partial chromosome 7 paint with a green paint (FITC) hybridizing to short arm of chromosome 7 and an spectrumorange paint spans the long arm of chromosome 7.

All probes were used to detect chromosome 7 abnormalities and were commercially obtained from Metasystems GmbH, Germany.

4-3-3 FISH

The FISH experiments were performed on methanol: acetic acid fixed suspenstion cells of four different human cell lines. All probes in these experiments were used for direct detection of chromosome 7 abnormalities. These probes were used according to the to the manufacturer's instructions. The slides were washed in saline-sodium citrate (2XSSC pH=7.0) while shaking for five minutes (SSC buffer in 20Xconcentration, Sigma, UK). They were then dehydrated through an alcohol series (70%, 90% and 100% ethanol) followed by air-drying for five minutes. The slides were denatured in 70% formamide denaturing solution containing 2XSSC at 70o C for five minutes. Following the denaturation, the slides were washed again with 2XSSC for five minutes, then dehydrated again through an alcohol series (70%, 90% and 100% ethanol) and air dried at room temperature. All probes were denatured at 80°C for 2 minutes and incubated at 37°C for ten minutes to allow re-annealing of repetitive sequences. The denatured probes were added to the denatured cells on the slides and incubated at 37°C overnight. After the incubation time, the slides were washed in 2XSSC for five minutes. They were then washed in phosphate-buffered saline (PBS) for five minutes. The slides then were mounted in Vectashield (Vector Laboratories) containing 49, 6-Diamidine-29-phenylindole dihydrochloride (DAPI). Fluorescent images were captured with a Zeiss axioplan epifluorescence microscope (Carl Zeiss,) equipped with a CCD camera (739 3 575, pixel size 11 3 11 mm) and MetaSystems Isis v. 5.3 software.

4-4 Results

FISH was performed on four different human cell lines to detect chromosome 7 abnormalities using different probes for region of interest.

4.4.1 Verification and validation of 7(q22-q31) and 7(q22-q36.1) probes on Farage cell line

This human lymphoma cell line was used as a normal control in this study. The FISH analysis of 7q22-7q31 probe shows both normal chromosomes 7 harbour signals on 7q22 in red (spectrumorange) colour, 7q31 in green (FITC) and on centromere in light blue (aqua) (see figure 4-1). Our FISH results of 7q22-q36.1 also show normal pattern of FISH signals on 7q22 in red (spectrumorange), 7q36.1 in green (FITC) and on centromere 7 in

light blue colour (see figure 4-2). Results from both 7(q22-q31) and 7(q22-q36.1) probes show the expected signals on chromosome 7.

4.4.2 Verification of 7 q22-q31 and 7q22-q36.1 probes in GF-D8 cell line

FISH was conducted using 7q22-q31 and 7q22-q36.1 probes. Our FISH results of 7q22-q31 probe set show three copies of chromosome 7. Normal chromosome 7 with red signals on q22 region, green signals on q31 region and light blue signals on the centromere. The second copy has a paracentric inversion of a fragment of chromosome 7 with potiental breakpoints distal to q22 region and distal to q31 region result in change in the postion of q31 region which located more distally close to the chromosome's telomere. There is a deletion of segment of a long arm in the third copy of chromosome 7, and two potiental breakpoints within the long arm; one is proximal to q22 region and one is distal to the q31 region, making it an interstitial deletion (see figure 4-3). Our FISH results of 7q22-q36.1 also show three copies of chromosome 7. Normal chromosome 7 with red signals on q22, green signals on q36.1 and blue signals on centromere. The FISH signals on the second copy of chromosome 7 show normal position of q22 (red signals) and q36.1 (green signals) regions confirming that the breakpoints of inv(7) occurred distal to q22 and q31 regions. The chromosome carrying 7q36 region in green signals is the der(12) as this cell line had a translocation between chromosome 7 and 12 (see figure 4-4).

4.4.3 Verification of 7 q22-q31 and 7q22-q36.1 regions in GDM1 cell line

FISH was also performed on this cell line to validate the 7q22-q31 and 7q22-q36.1 probes. The FISH results of the two probes show normal copies of chromosome 7 in this cell line as well as normal localisation of signals on q22 (in red), q31 (in green FITC) and q36.1 (also in green FITC) regions on the long arm of chromsome 7 (see figure 4-6).

4.4.4 Verification of 7q22-q31 and 7q22-q36.1 regions in k562 cell line

FISH using 7q22-q31 and 7q22-q36.1 probes identified four copies of chromosome 7 in the K562 cell lines. Images of multi-colour FISH performed on the same cell line were provided for analysis and comparison (see figure 4-7). These also showed the presence of four copies of chromosome 7. The localisation of FISH singals of 7q22-q31 probe were normal, with red signals on q22 band, green signals on q31 band and light blue signals on

centromeric 7 (see figure 4-8); however, the distribution of FISH signals of 7q22-q36.1 probe were different. The FISH result shows that three copies of chromosome 7 have normal patterns of FISH signals (red signals at 7q22 band, blue signals at the centromeric region and green signals at the q36.1 region), whereas the fourth copy has green signals on both arms of the chromosome 7, suggesting that there is a duplication of the q36.1 region followed by an intrachromosomal translocation involving both ends of chromosome 7 (see figure 4-9).

In order to understand the intrachromosomal rearrangements of chromosome 7, FISH analysis was carried out using WCP7 and locus-specific probe flanking the HLXB9 gene at q36 region of chromosome 7. FISH results confirmed that from four copies of chromosome 7, one had four blue FISH signals on both arms (see figure 4-10). Chromosome 7 was also investigated to confirm the duplication and the intrachromosomal translocation using partial chromosome 7 paint. Our FISH analysis confirmed the duplication of q36.1 region and either an insertion of long arm material into short arm of chromosome 7, or an intrachromosomal translocation between two ends of chromosome 7 (see figure 4-11).

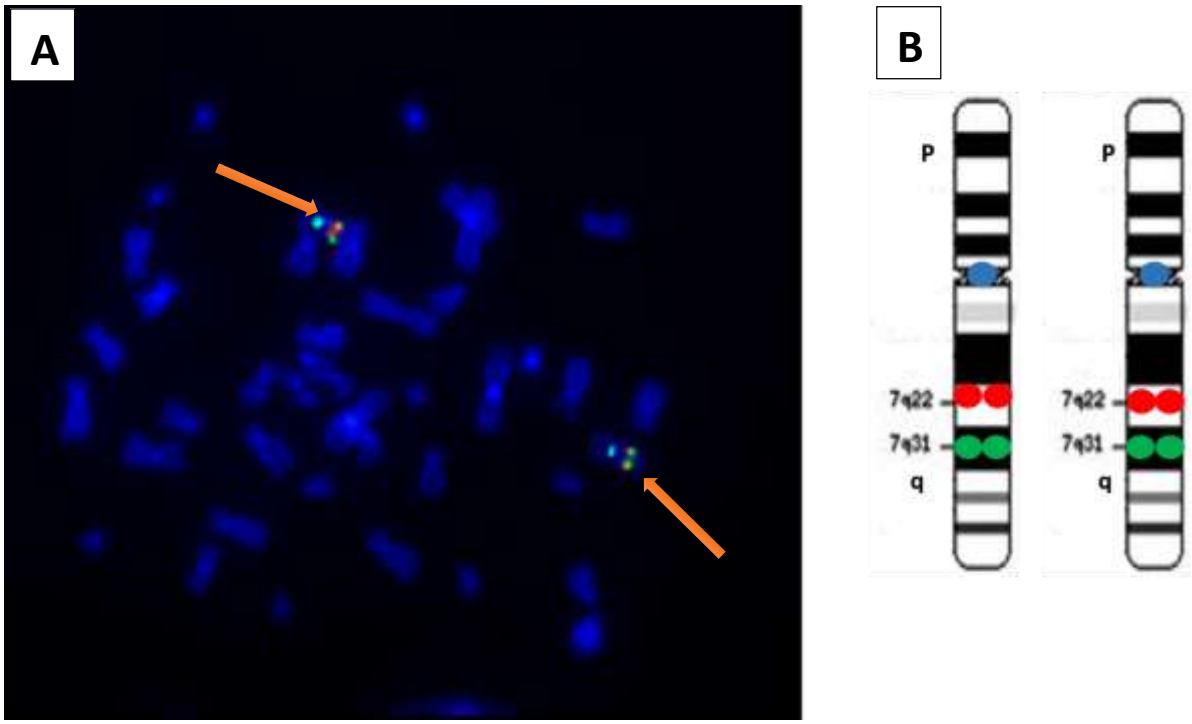

Figure 4-1: Example of FISH using probe 7(q22-q31) in Farage cell line

(A) metaphase chromosome obtained from Farage cell line showing the FISH signals using a specific locus probe target long arm of normal chromosome 7 at band 2 sub band 2 (q22) in red (spectrumorange), specific locus probe spans the q31 region on normal chromosome 7 in green (FITC) and specific locus probe hybridize the chromosome 7 centromere in light blue (aqua). Chromosomes are counterstained in DAPI (blue colour).

(B) Ideograms of chromosome 7 showing the hybridization patterns of del 7 (q22, q31) probe on normal chromosome 7.

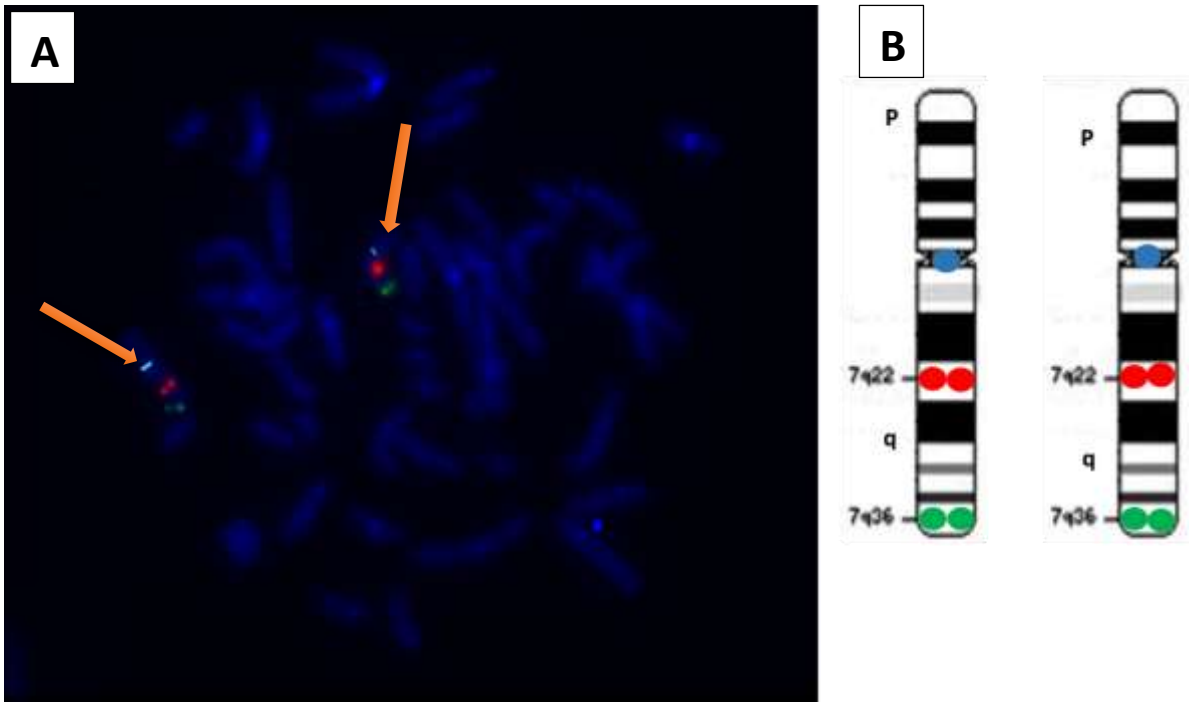

Figure 4-2: Example of FISH using probe 7(q22-q36.1) in Farage cell line

(A) metaphase chromosome obtained from Farage cell line showing the FISH signals using a specific locus probe target long arm of normal chromosome 7 at band 2 sub band 2 (q22) in red (spectrumorange), specific locus probe spans the q36.1 region on normal chromosome 7 in green (FITC) and specific locus probe hybridize the chromosome 7 centromere in light blue (aqua). Chromosomes are counterstained in DAPI (blue colour).

(B) Ideograms of chromosome 7 showing the hybridization patterns of del 7 (q22, q36.1) probe on normal chromosome 7.

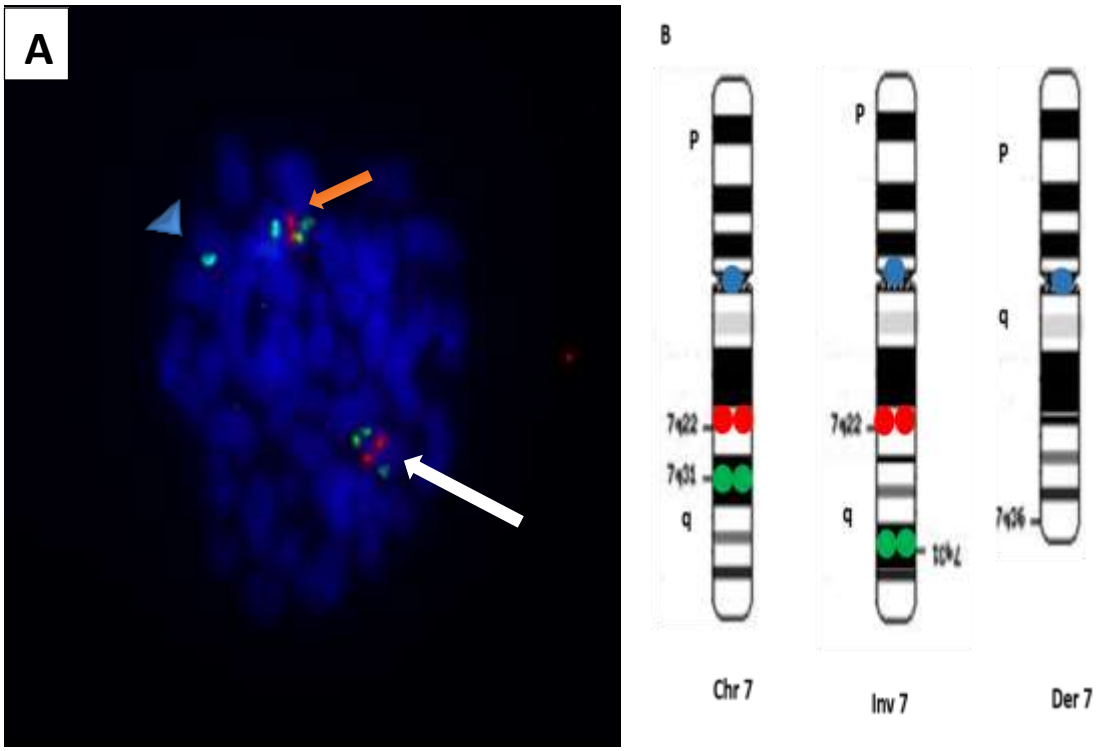

Figure 4-3**: Example of FISH using probe 7(q22-q31) in GF-D8 cell line**

(A) Metaphase chromosome image obtained from GF-D8 cell line shows (i) three FISH signals (light blue, red and green) on normal chromosome 7 (orange arrow), (ii) three FISH signals (light blue, red and green) on inverted chromosome 7 (white arrow) and (iii) blue signal on derivative chromosome 7 (arrowhead). Chromosomes are counterstained in DAPI (blue colour).

(B) Ideograms of chromosome 7 showing the hybridization patterns of del 7 (q22, q31) probe on (i) normal chromosome 7 on the left side, (ii) inverted chromosome 7 in the middle and (iii) derivative chromosome 7 in the right side.

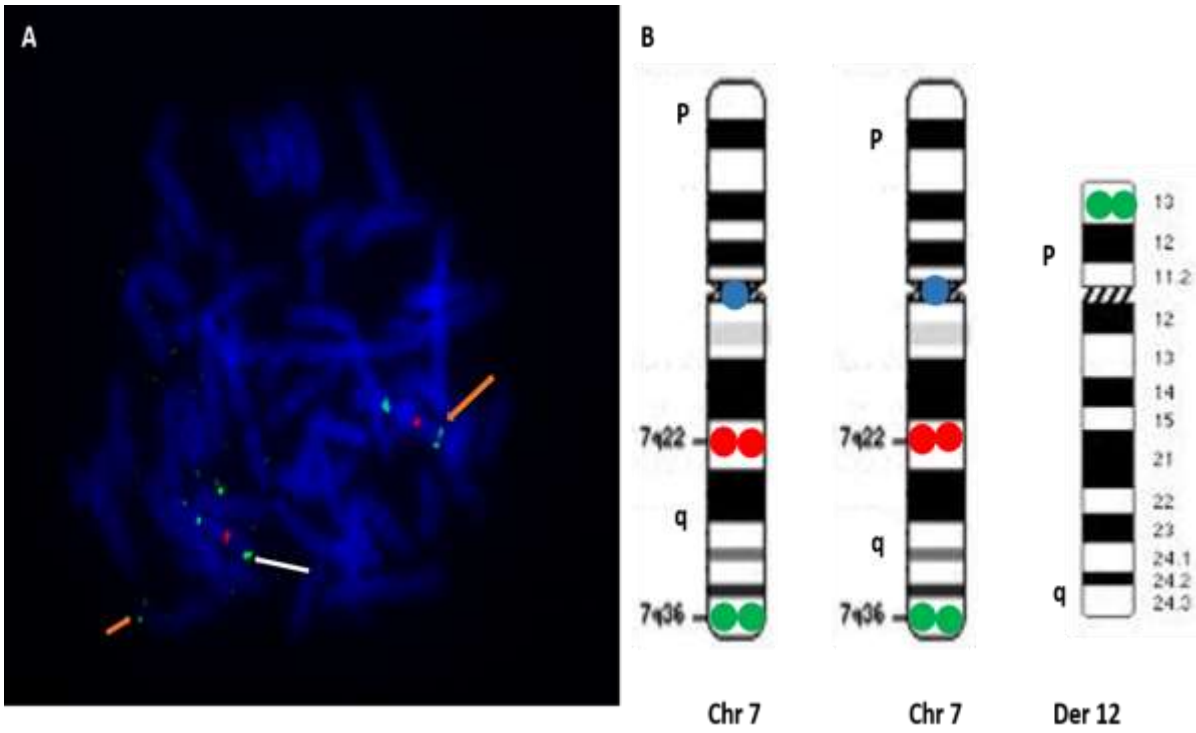

Figure 4-4: Example of FISH using probe 7(q22-q36.1) in GF-D8 cell line

(A) Metaphase chromosome image obtained from GF-D8 cell line shows (i) three FISH signals (light blue, red and green) on normal chromosome 7 (Orange arrow), (ii) three FISH signals (light blue, red and green) on inverted chromosome 7 (white arrow) and (iii) green signal on derivative chromosome 12 (white arrow). Chromosomes are counterstained in DAPI (blue colour).

(B) Ideograms of chromosome 7 showing the hybridization patterns of del 7 (q22, q36.1) probe on (i) normal chromosome 7 on the left side, (ii) inverted chromosome 7 in the middle and (iii) derivative chromosome 12 in the right side.

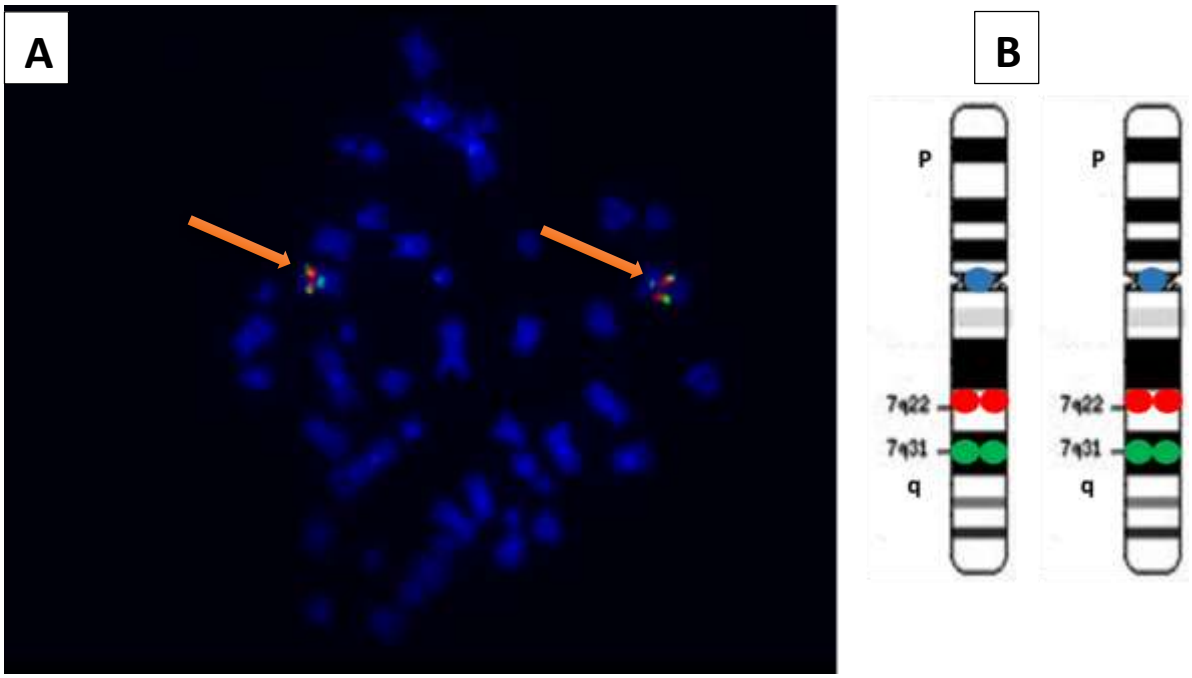

Figure 4-5: Example of FISH using probe 7(q22-q31) in GDM1 cell line

(A) Metaphase chromosome obtained from GDM1 cell line showing the FISH signals using a specific locus probe target long arm of normal chromosome 7 at band 2 sub band 2 (q22) in red (spectrumorange), specific locus probe spans the q31 region on normal chromosome 7 in green (FITC) and specific locus probe hybridize the chromosome 7 centromere in light blue (aqua). Chromosomes are counterstained in DAPI (blue colour).

(B) Ideograms of chromosome 7 showing the hybridization patterns of del 7 (q22, q31) probe on normal chromosome 7.

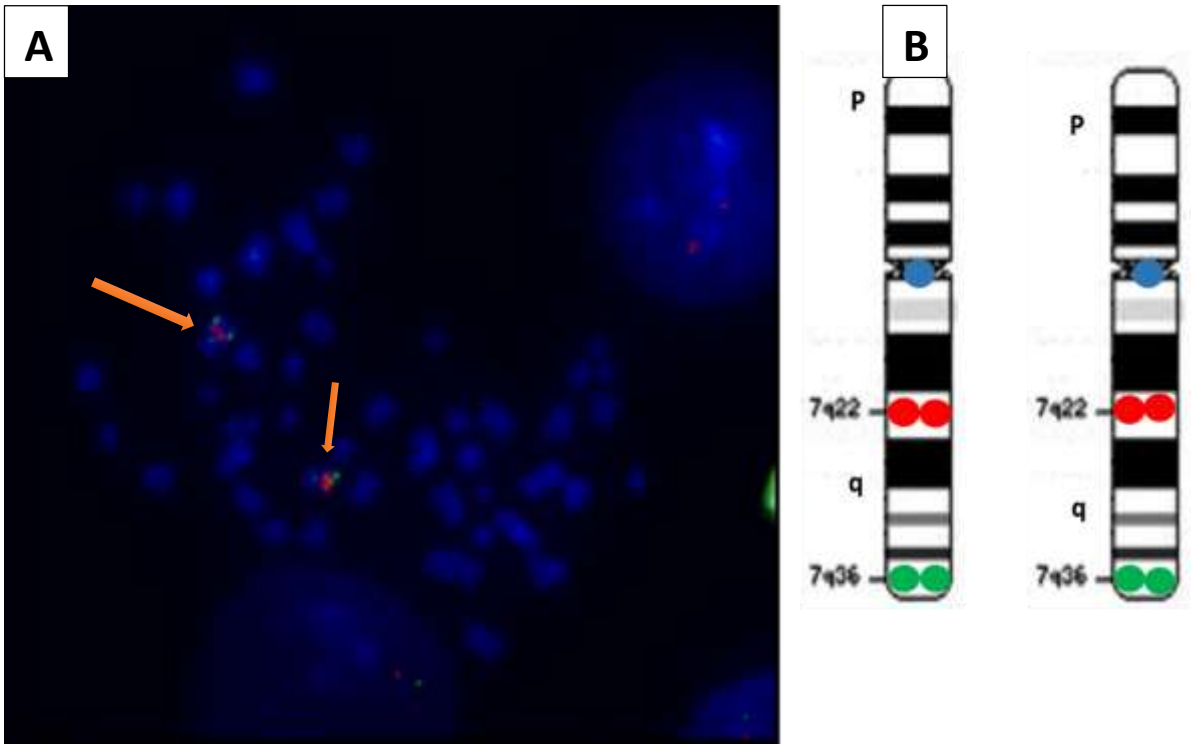

Figure 4-6: Example of FISH using probe 7(q22-q36.1) in GDM1 cell line

(A) metaphase chromosome obtained from GDM1 cell line showing the FISH signals using a specific locus probe target long arm of normal chromosome 7 at band 2 sub band 2 (q22) in red (spectrumorange), specific locus probe spans the q36.1 region on normal chromosome 7 in green (FITC) and specific locus probe hybridize the chromosome 7 centromere in light blue (aqua). Chromosomes are counterstained in DAPI (blue colour).

(B) Ideograms of chromosome 7 showing the hybridization patterns of del 7 (q22, q36.1) probe on normal chromosome 7.

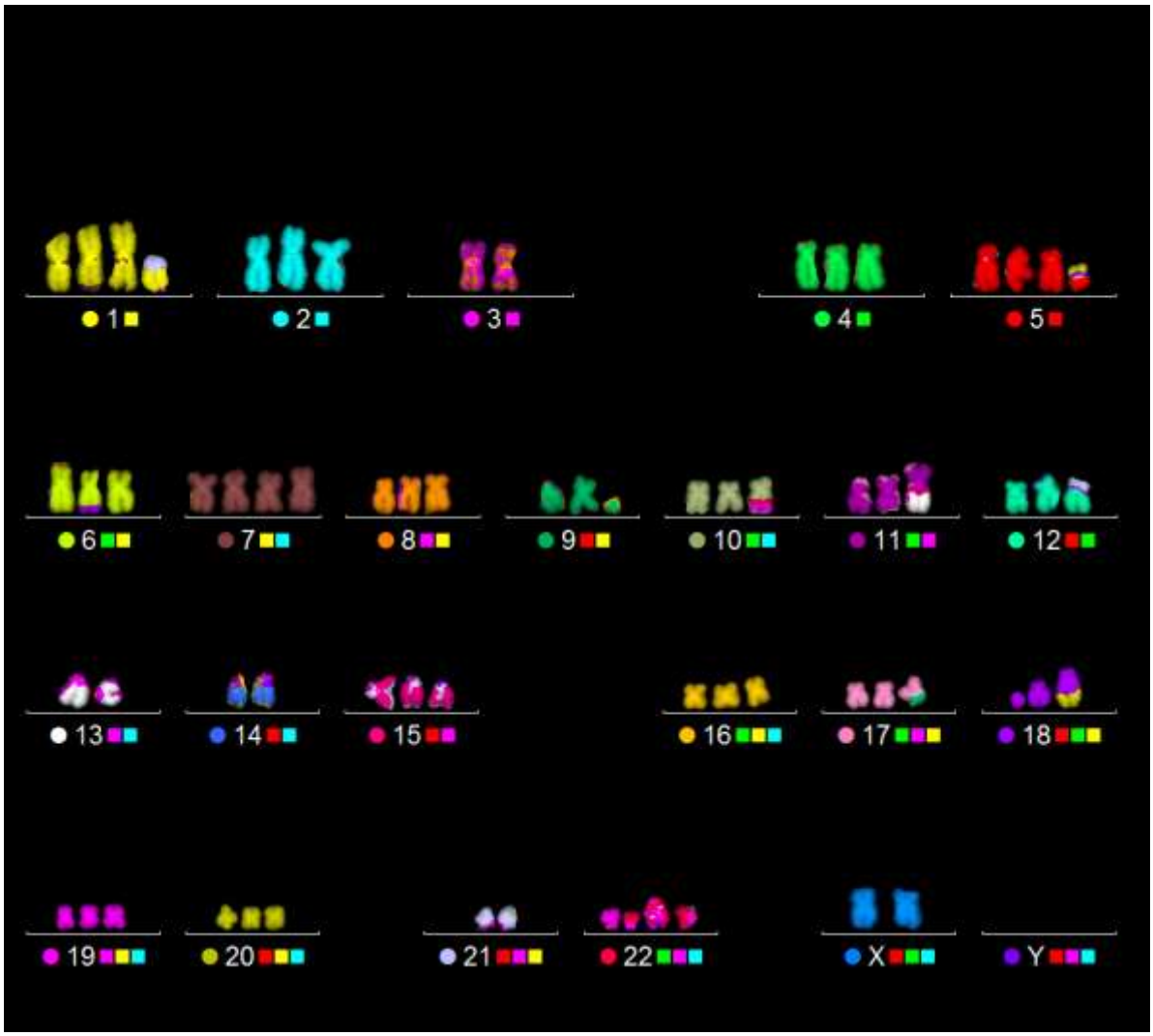

Figure 4-7: Example of M-FISH karyotype of k562 cell line

M-FISH revealed complex rearrangments of chromosomes involved numerical and structural chromosomal abnormalities such as trisomies of chromosomes 2, 4, 6, 8, 9, 10, 11, 12, 15, 16, 17, 18, 19 and 20. Four copies of chromosomes 1, 5, 7 and 15 were observed. One copy of chromosome 7 is longer in comparison with the other three copies of chromosome 7 in brown colour (Figure generated by others in the Tosi's laboratory and provided to me by my supervisor).

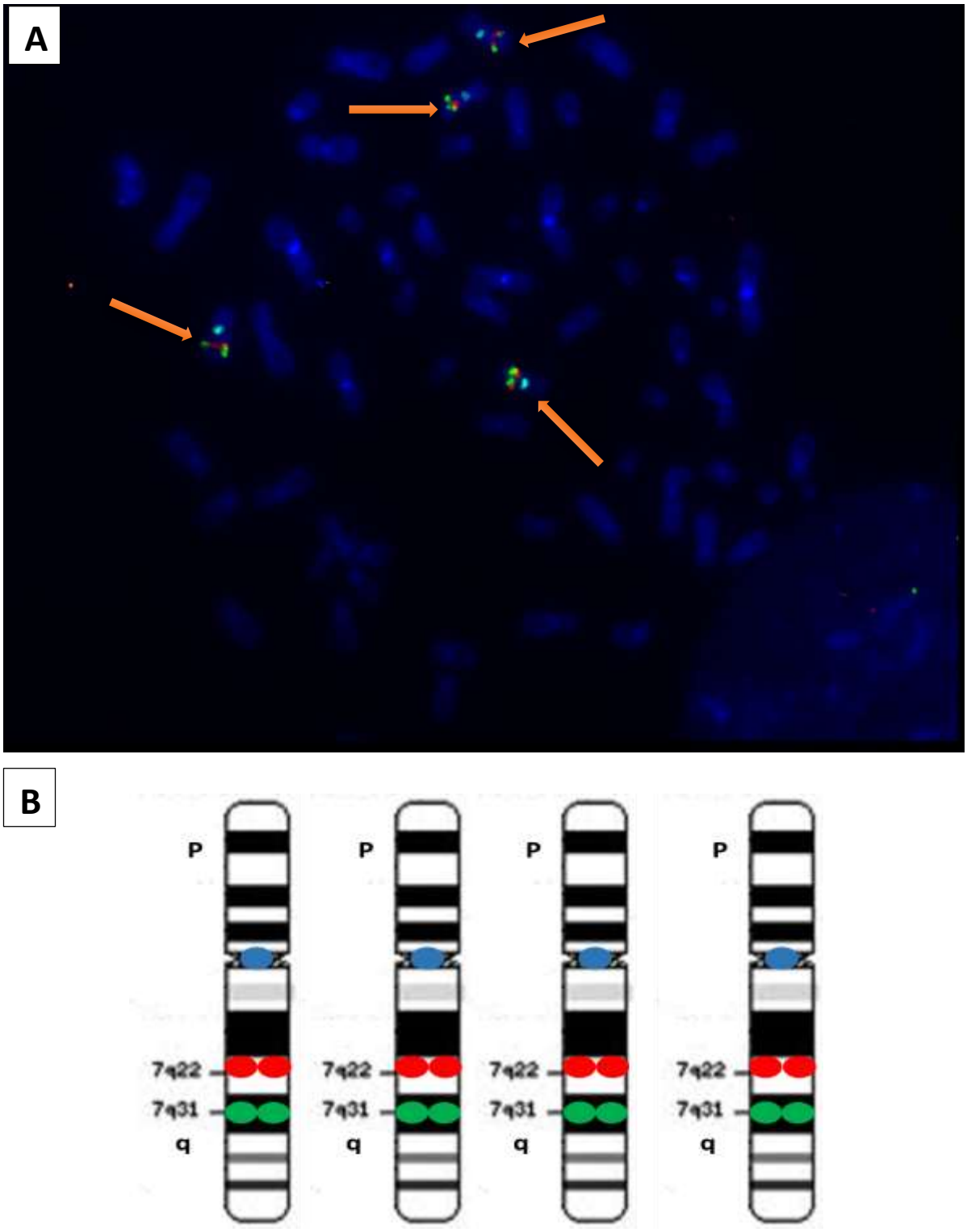

Figure 4-8: Example of FISH using probe 7(q22-q31) in k562 cell line

(A) metaphase chromosome obtained from k562 cell line showing FISH signals on four copies of chromosome 7 using a specific locus probe target long arm of normal chromosome 7 at band 2 sub band 2 (q22) in red (spectrumorange), specific locus probe spans the q31 region on normal chromosome 7 in green (FITC) and specific locus probe hybridize the chromosome 7 centromere in light blue (aqua) (orange arrow). Chromosomes are counterstained in DAPI (blue colour).

(B) Ideograms of chromosome 7 showing the hybridization patterns of del 7 (q22, q31) probe on normal chromosome 7.

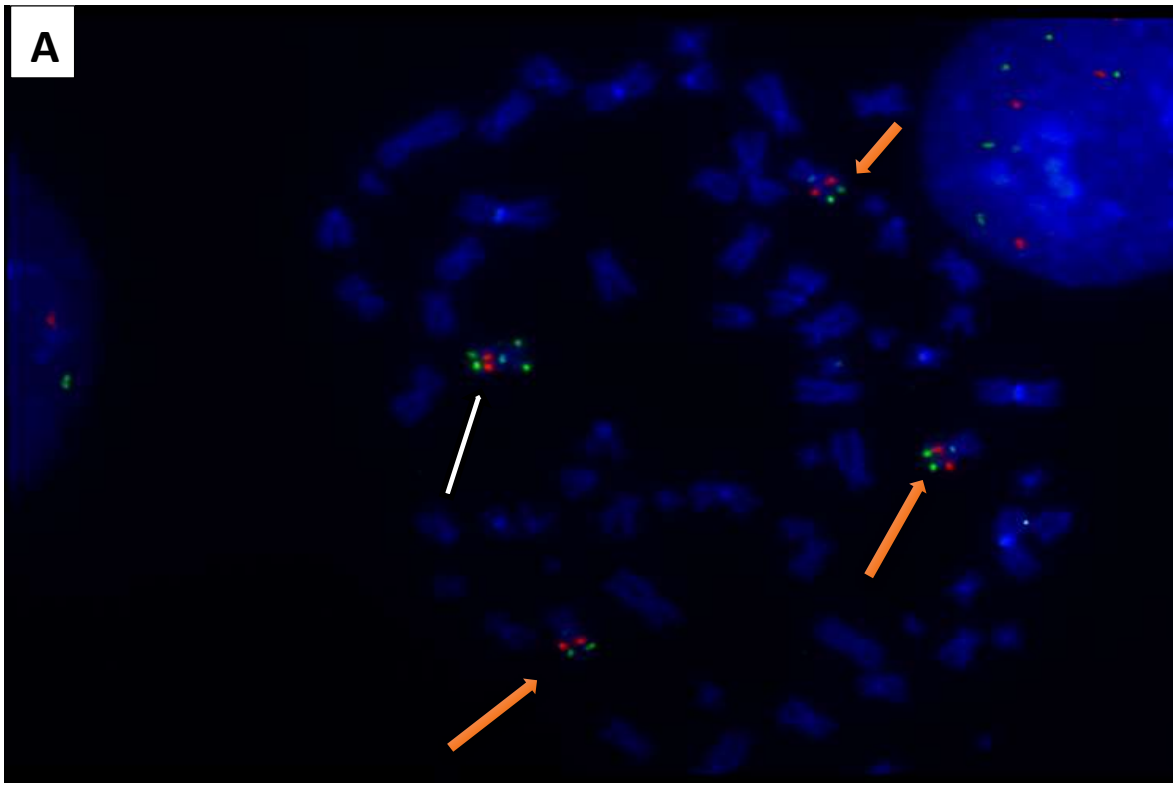

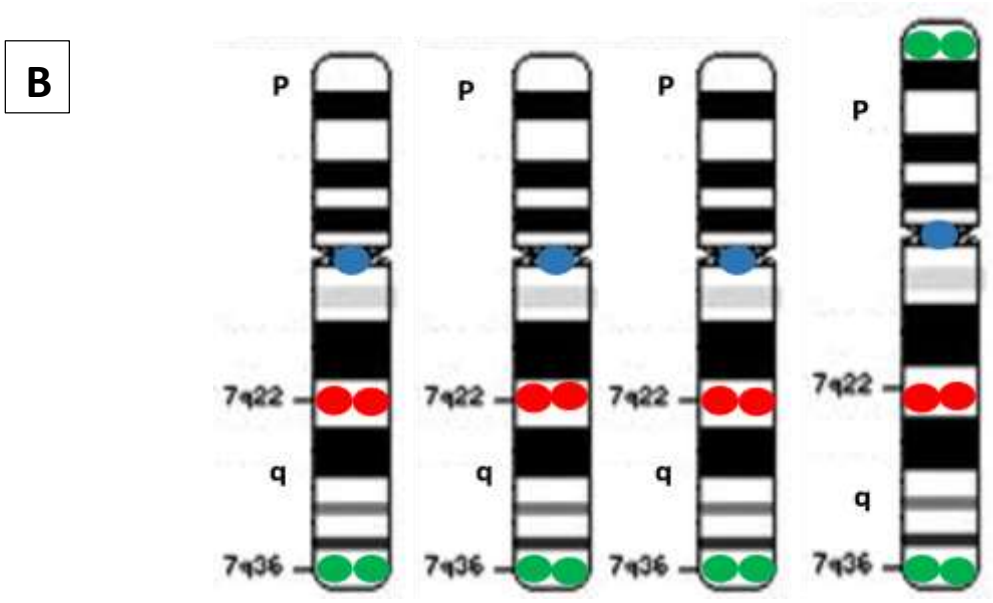

Figure 4-9: Example of FISH using probe 7(q22-q36.1) in k562 cell line

(A) metaphase chromosome obtained from k562 cell line showing a specific locus probe target long arm of chromosome 7 at band 2 sub band 2 (q22) in red (spectrumorange), specific locus probe spans the q36.1 region on chromosome 7 in green (FITC) and specific locus probe hybridize the chromosome 7 centromere in light blue (aqua). The orange arrows show the normal patterns of 7(q22, q36.1) probe on three copies of chromosome 7 and the white arrow shows the fourth copy of chromosome

with green signals on both arms of the chromosome. Chromosomes are counterstained in DAPI (blue colour).

(B) Ideograms of chromosome 7 showing the hybridization patterns of del 7 (q22, q36.1) probe on four copies of chromosome 7.

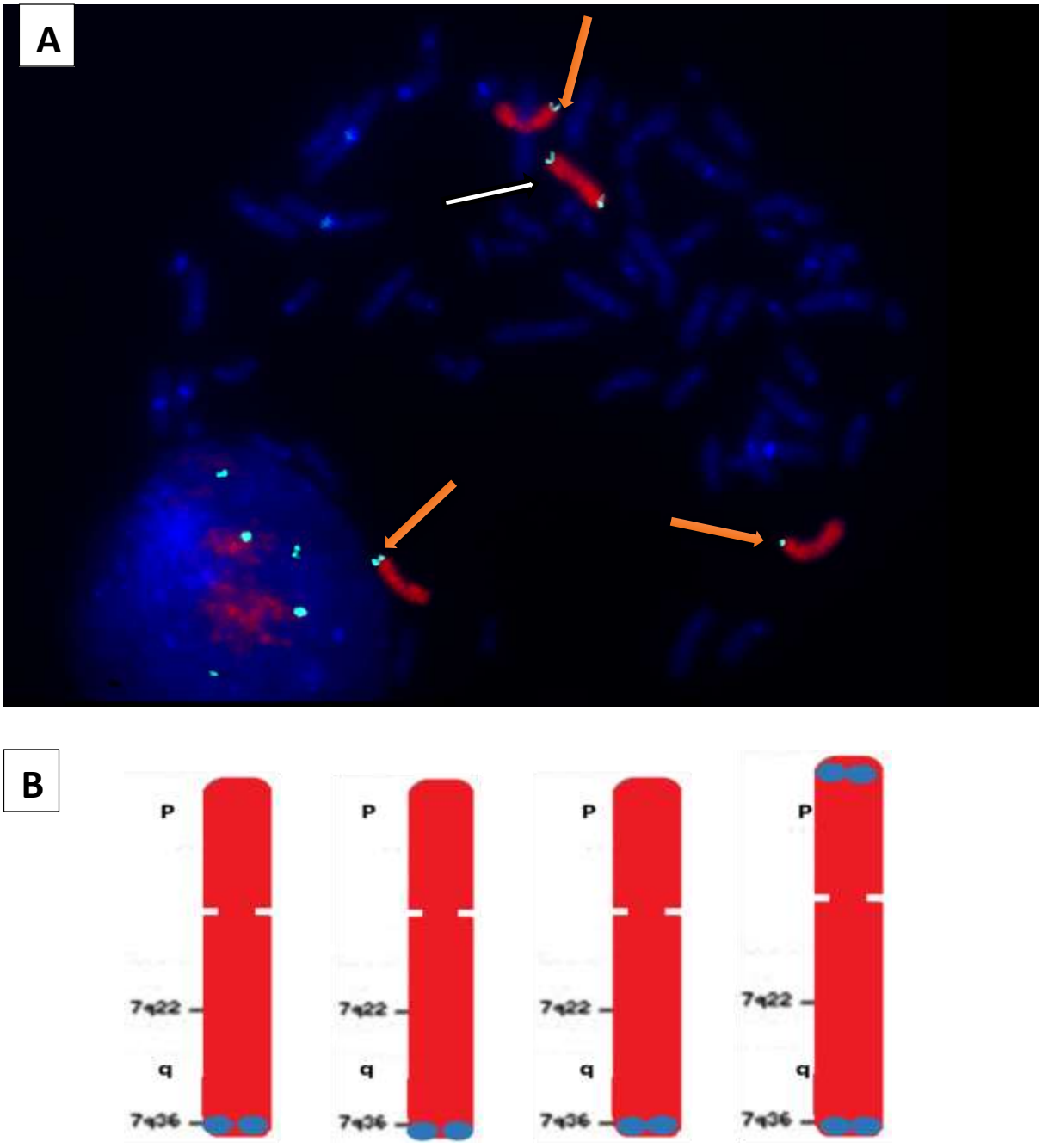

Figure 4-10: Example of dual colour FISH on K562 metaphase

(A) FISH experiment was performed using WCP 7 in red (spectrumorange) and a specific locus probe flanking the HLXB9 gene at q36.3 in light blue (aqua). The orange arrows indicate three copies of chromosome 7 with one blue signal each and while the white arrow shows the fourth copy of chromosome 7 with blue signals on both arm of the chromosome. Chromosomes are counterstained in DAPI (blue colour).

(B) Ideograms of chromosome 7 showing the hybridization patterns of HLXB9 and WCP 7 probes on four copies of chromosome 7.

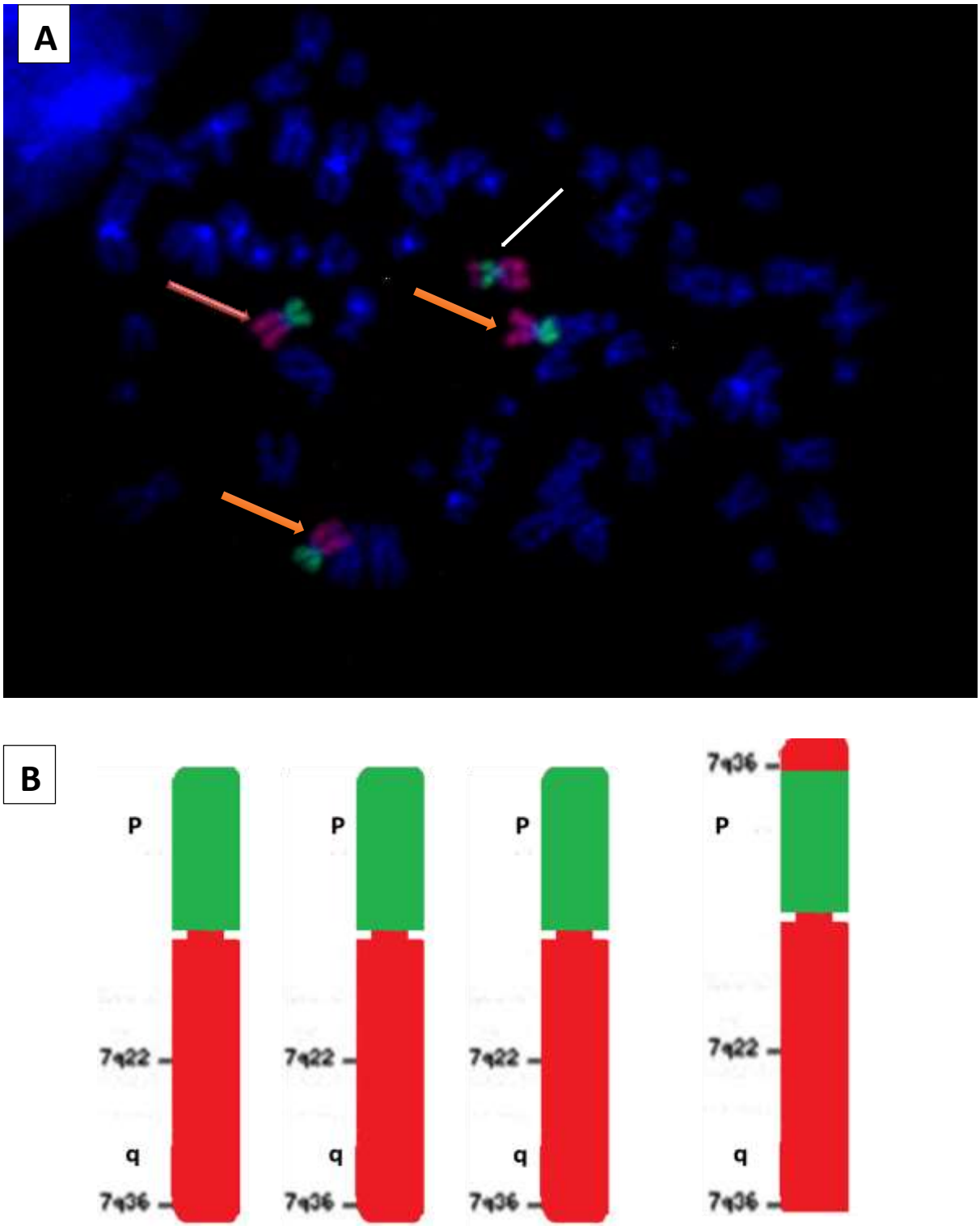

Figure 4-11: Example of dual colour paint FISH on K562 metaphase

(A) FISH was performed using partial chromosome 7 paint (short arm in green and long arm in red (spectrumorange)). The orange arrows indicate three copies of chromosome 7 with green paint (FITC) on short arm and red (spectrumorange) paint on long arm. The white arrow shows the

fourth copy of chromosome 7 with both green (FITC) and red paint on short arm and red (spectrumorange) paint on long arm of the chromosome. Metaphase is counterstained in DAPI (blue colour).

(B) Ideograms of chromosome 7 showing the hybridization patterns of partial chromosome 7 paint on four copies of chromosome 7.

4-5 Discussion

The detection of chromosomal abnormalities in leukaemia is very important in the diagnostic setting, as information on cytogenetics enables clinicians to make informed decisions on the type of therapy to be given to a patient. Abnormalities of chromosome 7 are generally considered indicators of poor prognosis (Von Neuhoff et al., 2010). It is therefore important to be able to detect those abnormalities during diagnosis to allow appropriate treatment. In the 1990s, many studies focused on the identification of critical regions in del(7q), hoping to map a potential tumor suppressor gene (Dohner et al., 1998; Fischer et al., 1997; Johnson et al., 1996; Liang et al., 1998; Tosi et al., 1999). It was concluded that different regions on chromosome 7 were prone to breakage giving rise to deletions of different size and location (Curtiss et al., 2005; Dohner et al., 1998; Liang et al., 2005; Nagel et al., 2005; Tosi et al., 1999). Several commercial probes have been designed to cover the most commonly reported deleted regions on chromosome 7 to enable diagnostic labs to detect chromosome 7 abnormalities accurately and in a timely fashion (Andersen et al., 2004; Bajaj et al., 2011).

In the present study, FISH localization of (i) 7q22 and 7q31, (ii) 7q22 and 7q36.1 and (iii) 7q36 regions have been investigated in several human leukaemia cell lines using appropriate three-colour probe sets for the detection of del(7)(q22-q31) and del(7)(q22-q36.1) and locus-specific probe for *HLXB9* gene. Whole and partial chromosome 7 paint have also been used to verify the intrachromosomal rearrangements of chromosome 7. The three-colour probe sets for del(7q22-q31) and del(7q22-q36) were validated on Farage cell line which is known to have no chromosomal rearrangements, thus it was used as a normal control. The FISH results show normal pattern of FISH signals of 7(q22-q31) and 7(q22-q36). Our investigation of chromosome 7 rearrangements in GDM1 cell line also shows normal loclization of 7(q22-q31) and 7(q22-q36) regions. The GDM1 cell line known to have a t(6;7) (q23; q36) translocation with breakpoint proximal to HLXB9 gene at 7q36.3 (Nagel et al., 2005). The three-colour probe set for 7(q22-q31) hybridised

to metaphase chromosome of GF-D8 cell line has enabled us to confirm trisomy 7, deletion of 7(q22-q31) with breakpoints within q22 and distal to q31 regions and an inv(7), corroborating the findings of Tosi et al. (1999a, 1999b) (figure 4-12).

However, the inv(7) breakpoints (distal to q22 and distal to q31) of GF-D8 observed in this study differed from those of Tosi et al. (1999a), who repored the proximal breakpoint of the inv(7) between 7q31.1 and 7q31.3 and the dstial breakpoint between 7q35-q36 and 7q36. Nevertheless, the observation of the proximal breakpoint of inv(7) (distal to 7q22) is very much in agreement with Johnson et al. (1996), who found a constitutional inversion of 7q in two patients, one with MDS and one with BM hypoplasia; the proximal breakpoint was mapped at 7q22.1. Moreover, the inv(7) breakpoints in GF-D8 cell lines were further confirmed by 7(q22-q36) probe, which showed normal position of 7q22 and 7q36. The 7q22-q36 probe also confirmed the the deletion of 7q22-7q33 region and translocation or insertion of chromosme 7 q36 material onto short arm of chromosome 12, as previously described by Tosi et al. (1999a). The 7(q22-q31) deletion was previously identified in MDS and AML cases (Dohner et al., 1998; Fischer et al., 1997). These studies suggested that this region might contain specific genes (e.g. tumor suppressor gene, TSG), which contribute to MDS or AML development. Recently, McNerney et al. (2013) performed transcriptome sequencing and SNP array analysis on de novo and therapy-related myeloid neoplasms with either -7 or del(7q). They detected a deletion of the 7q22.1 regions containing the *CUX1* gene, and further examined the TSC activety of *CUX1* gene using in vivo models. They concluded that the CUX1/cut is a conserved, haploinsufficient TSG that plays a critical role in the regulation of haematopoiesis.

The structure of chromosome 7 in k562 cell line was previously investigated using M-FISH, CGH, Locus-Specific FISH (Gribble et al., 2000; Naumann et al., 2001); the rearrangements of chromosome 7 in both studies were described as tetrasomy 7, del 7q, inv(7)(p11-q). Our FISH results of K562 cell line showed normal localization of 7(q22-q31) regions on four copies of chromosome 7, but the distribution of FISH signals of 7(q22-q36) probe were different. The FISH results showed three copies of chromosome 7 have normal patterns of FISH signals.

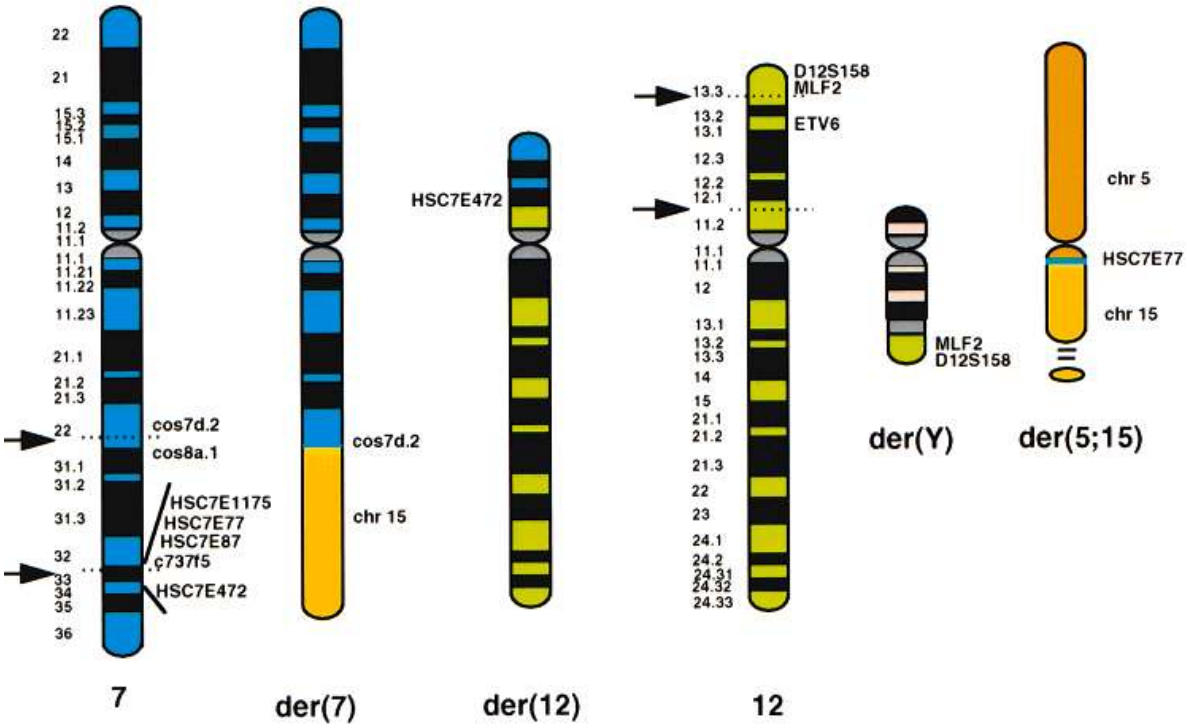

Figure 4-12: Schematic representation of the abnormalities involving chromosomes 7, 12, Y, and the der(5;15)

The arrows indicate to the deletion breakpoints at 7q and 12p and also the translocation between chromosome 7, 12 and 15 (Tosi et al., 1999 b).

Interestinglly, the three colour probes enable the detection of a new rearrangement in k562 cell line, which is described as a duplication of 7q36 region followed by either an intrachromosomal insertion of long arm material into short arm of chromosome 7, or an intrachromosomal translocation between two ends of chromosome 7. This finding was further investigated using *HLXB9* probe in combination with WCP 7. The results showed four copies of chromosome 7 were fully painted, and four signals of HLXB9 probe on both arms of one copy of chromosome 7. Furthermore, the partial chromosome 7p and 7q paint was used to understand whether the four signals of 7q36 region were observed on both arms of one copy of the chromosome as a result of an inversion or due to hidden rearrangements. The result of the partial paint showed a 7q paint on 7p arm which confirmed the duplication of 7q36 region followed by an intrachromosomal insertion of 7q36 material into short arm of chromosome 7.

Moreover, this result showed that no pericentric inversion 7 was detected in this cell line as previously described. It has been reported that the cytogenetic discrimination of the intrachromosomal insertion and peicentric inversion abnormalitis can be difficult (Madan,

1995). Consequently, these results suggest that the intrachromosomal 7 insertion that identified in this cell line might be misdiagnosed as a pericentric inversion 7. The intrachromosomal insertion identified in k562 cell line is uncommon forms of chromosomal rearrangement; only 41 cases have been reported in the literature, none of which had myeloid malignancy (Ardalan et al., 2005; Farrell and Chow, 1992; Kim et al., 2011; Lybaek et al., 2009; Madan and Menko, 1992). The other observation is the detection of a duplication of 7q36 region, known as a common deleted region in myeloid malignancy. To the best of our knowledge, this is the first case found with 7q36 duplication in myeloid malignancy.

CHAPTER 5: STUDY OF DNA COPY NUMBER CHANGES IN INV(16) LEUKAEMIA

5-1 Introduction

As mentioned in chapter 1, various chromosomal rearrangements have been found in AML, including translocations, duplications, inversions, insertions and deletions. These rearrangements are well known to contribute to leukaemia. Genetic aberrations are widely used as markers for diagnosis and prognosis. One of the most frequent chromosomal rearrangement in AML is the inversion of chromosome 16, inv(16)(p13;q22) which is detected in approximately 8% of patients diagnosed with AML subtype M4eo (Byrd et al., 2002; Grimwade et al., 2010). This translocation fuses the myosin heavy chain11 gene (MYH11) at 16p13 to the core-binding factor beta subunit gene (CBFB) at 16q22, resulting in fusion gene (Berger et al., 1985; Betts et al., 1992). However, several mouse model studies have shown that the CBFB-MYH11 fusion causes a block in myeloid differentiation and is insufficient to initiate leukaemia, suggesting that additional genetic mutations are required for leukaemic transformation (Castilla et al., 1996; Kogan et al., 1998; Kundu et al., 2002). Gilliland (2001) proposed that at least two classes of mutations are required to form leukaemia: class I mutations, which increase cell proliferation affecting genes such as RAS, c-KIT or FLT3; and class II mutations, which cause a block in haematopoiesis differentiation and involve genes such as CBF fusion genes. The association of AML with the inv(16) rearrangement has a favourable prognosis (Arthur et al., 1983, 1989; Bloomfield et al., 1987; Holmes et al., 1985; Le Beau et al., 1983). Nevertheless, It has been reported that the inv(16) patients with KIT exon 8 mutations are associated with an increased relapse rate (Care et al., 2003; Kim et al., 2013; Mrozek et al., 2008; Schwind et al., 2013). Paschka et al. (2013) showed that trisomy 8, KIT mutations and FLT3 mutations have an impact on the outcome of AML patients with inv(16) and therefore these alterations can be used as a prognostic marker to allow the identification of patients at high risk of relapse. They also showed that trisomy 22 has no impact on patient outcomes.

The assessment of karyotypic abnormalities remains a valuable tool for prediction of outcome of patients with AML. Chromosome banding is routinely used to detect

chromosomal rearrangements, including balanced chromosomal abnormalities (translocations and inversions) and unbalanced chromosomal abnormalities (trisomies, duplications and deletions). However, it has limited resolution power, amounting to less than <10 Mb (Grimwade et la., 2009). The use of molecular cytogenetic methods such as FISH or higher resolution approaches such as single-nucleotide-polymorphism (SNP) platforms have improved the detection of DNA CNAs in AML (Maciejewsk et al., 2008). Recently, a few studies have reported CNAs in AML cases with abnormal karyotype. Kuhn et al. (2012) found low CNAs in 300 diagnostic and 41 relapse acute myeloid leukaemia cases, with t(8;21)(q22;q22) and inv(16) (p13;q22) or t(16;16)(p13;q22) using Affymetrix 6.0 SNP microarrays; the mean of CNAs per case was 1.28 at diagnosis and 3.17 at relapse. Kuhn et al. (2012) also detected recurrent minimally deleted regions at 7q36.1, 9q21.32, 11p13, and 17q11.2 and focal gain at 8q24.21 and 11q25. CN-LOH was detected in 7% of cases. A study of 111 paediatric de novo AML cases using single-nucleotide-polymorphism microarrays showed a low number of CNAs in the leukaemia cells of these cases with an average of 2.38 per patient. In additional, the rare recurrence of CNAs was observed in these cases (Radtke et al., 2009).

Cosat et al. (2013) studied 15 confirmed inv(16) and t(8;21) cases using a single-nucleotide polymorphism-array. Of these, four cases showed trisomy 22, 9p13 duplication, trisomy 9 and terminal deletion of 9q22 by G-banding. They found that trisomy 22 was not detected by array, whereas 9p13 duplication interpreted by G-banding was defined as 1q25.2 gain by array, and trisomy 9 detected by G-banding was in fact trisomy 8 revealed by array, while terminal 9q22 deletion identified by G-banding was found as interstitial 9q22 deletion by array. Moreover, they identified recurrent submicroscopic regions at 4q28, 9p11, 16q22.1 and 16p23 and CN-LOH regions in these patients. In a different study, CNAs were found in a case of an isolated del(20q) abnormality using whole-genome single nucleotide polymorphism array (SNP-A)-based karyotyping. The additional genomic alterations detected were described as copy neutral loss of hetrozygosity (CN –LOH) of 11q13, 1-q25 and copy number gain of 20q. The gain of 20q was also confirmed by FISH analysis. It was suggested that the presence of CNAs in this type of abnormality might be associated with poor prognosis (Hahm et al., 2012).

Mullighan et al. (2009) described the presence of copy number loss of the *IKZF1* gene in acute lymphoblastic leukaemia with t(9;22) translocation. This cytogenetic group is

associated with poor outcomes, suggesting that deletion of the *IKZF1* gene might be used as a prognostic marker to identify patients with high risk of relapse. In addition to AML with rearrangements, several published studies have reported CNAs in karyotypically normal AML cases. Barresi et al. (2010) investigated 19 normal karyotype AML cases using high resolution SNP array. A low number of CNAs per patient was observed, with an average of one CNA per patient, and also few recurrent CNAs were identified. Other studies also detected CNAs in normal karyotype AML. Akagi et al. (2009) identified CNAs in nine out of 38 normal karyotype samples, while Ballabio et al. (2011) found CNAs in AML patients with normal and incomplete karyotype using whole genome array comparative genome hybridization (aCGH). Among these CNAs, loss and gain of large chromosome regions were detected by array and confirmed by FISH; these CNAs were found in interphase rather than metaphase. Moreover, it was found that cells carrying these CNAs involving large chromosomal regions were cells in a non-proliferative status.

Walter et al. (2009) found CNAs in both normal karyotype AML and AML with abnormal karyotype cases using SNP array. They stated that CNAs were more common in AML patients associated with poor prognosis in contrast to normal karyotype AML, which is associated with intermediate risk of relapse. The identification of CNAs has led to the improvement of treatment and clinical outcomes of some cases of AML patients with normal and abnormal karyotypes (Fenaux et al., 1993). Therefore, it is important to understand more about the genetic basis of leukaemia and its implications for clinical practice so that evidence-based practice (e.g. treatment strategies) can be developed.

5-2 Aim of this study

In this study, Illumina beadarray approach was used to assess CNAs and CN-LOH regions in 22 AML patients samples with inv(16)(p13;q22) and t(8;21)(q22;q22). In order to distinguish between true CNAs and false-positive findings and to verify whether CNAs are present in the same clone harbouring inv(16), FISH was used on fixed chromosome and cell suspensions from the same patients. We further investigated whether the cells carrying the abnormalities were proliferating or non-proliferating/quiescent using indirect immunofluorescence method with an antibody specific to the proliferation marker (Ki-67). The proliferation studies mentioned here are described in detail in chapter 6.

5-3 Materials and methods

5-3-1 Patient samples

Genomic DNA samples from 22 AML patients with confirmed inv(16) and t(8;21) were provided to us by collaborators at the Children's Hospital, University of Giessen and Marburg, Germany, and at the Paediatric Haematology Clinic, Ospedale San Gerardo, Monza, Italy. Four inv(16) patient samples out of 22 were selected for FISH study on the basis of: (i) presence of CNAs as proven by array data; and (ii) availability of material in the form of fixed chromosomes and cell suspensions. Inv (16) was the only abnormality in two patients (no. 29 and 30), while two cases had additional chromosomal rearrangement, including trisomy 22 in case no. 26, and t(X;1) in case no.27. Median age was five years (range 1-17 years), and the sample comprised four females and one male. Clinical and cytogenetics details of the patients are given in table 5-1

Table 5-1: Clinical and cytogenetic data of the patients reported in this study

Pt	Age	Disease	Reported Karyotype
26	5y 4mo	AML-M4	47~48,XX,inv(16)(p13q22),+?20,+22[10]
27	17y 4mo	AML	46,XX,inv(16)(p13q22)[8]/46,idem, der(1)?t(X;1)(p?11;q21),?der(X)?t(X;1)(p?11;q21
29	4y 8mo	AML-M4eo	46,XX,inv(16)(p13q22)
30	11y 4mo	AML-M4	46,XY,inv(16)(p13q22)

Y: years, mo: months. All patient samples in the table were provided by Professor J. Harbott, Children's Hospital, University of Giessen and Marburg, Germany.

5-3-2 Cell line

Three different commercially available cell lines were used as a normal control to test the specificity and efficiency of BACs biotin labelled probes used for FISH:

1. Farage (CRL-2630) cell line was derived from patient who had diffused large cell non-Hodgkin's lymphoma (DLCL).
2. GM17878B Lymphoblastoid cell line derived from normal peripheral blood of healthy individual cell line.
3. GM17208B Lymphoblastoid cell line derived from normal peripheral blood of healthy individual.

The cell lines were purchased from Coriell Institute for Medical Research.

5-3-3 Probes

FISH analyses were performed using probes for the inv(16)(p13;q22) (MetaSystems GmbH, Altlussheim, Germany). The same probe was used to detect the deletion of 16p13.11 region in one of the patients. In addition, the following BACs were used to confirm other CNAs detected by Illumina array analysis: RP11-504N9 (7q36.1; 151,254,565 to 151,424,079); BAC RP11-184A23 (4q35.1; 184,483,495 to 184,649,497); BAC RP11-195E4 (8q24.3; 141,431,223 to 141,608,396) (BACPAC Resources Center, Oakland, USA).

5-3-4 Fluorescence in situ hybridization

Methanol-acetic acid fixed chromosome suspensions were prepared for the FISH experiment. Importantly, the cell preparations used for FISH were derived from samples obtained at the same time as those used for karyotyping and DNA extraction for Illumina array experiment. The inv(16) probe directly labelled with spectrumorange and FITC was used for direct detection of the inversion in all samples. These probes were used according to the manufacturer's instructions with slight modifications. BACs biotin labelled probes were indirectly visualized with streptavidin Cy5. Slides were denatured with 70% formamide at 70°C for five minutes. Probe mixture was denatured at 65°C for ten minutes, incubated at 37°C for ten minutes, and subsequently applied to the slides. Slides were incubated overnight at 37°C. After overnight incubations, slides were washed with 2x SSC for five minutes followed by another wash in 0.4x SSC for five minutes at 72°C. Blocking solution (3% BSA+ 4x SSC/Tween20) was added to the slides. Biotin labelled probes were detected using streptavidin Cy5. The slides were then mounted in Vectashield (Vector Laboratories Ltd., Peterborough, UK) containing 4, 6-Diamidine-29-phenylindole dihydrochloride (DAPI).

5-3-5 Microscope analysis

Hybridized chromosomes and nuclei were viewed and images were captured using: (i) a Zeiss axioplan epifluorescence microscope (Carl Zeiss, Cambridge, UK) equipped with a CCD camera and MetaSystems Isis v. 5.3 software; and (ii) an Olympus BX41 Fluorescence

microscope (Zeiss) equipped with a charge-coupled device (CCD) camera (Scion FW camera, Merge image processor, Version 1.0) and SmartCapture3 sofware; and (iii) an Olympus BX-51 microscope equipped with a JAI CVM4+ progressive-scan 24 fps B&W fluorescence CCD camera and Leica Cytovision Genus v7.1 software.

5-3-6 Statistical analysis

Cut off levels were calcuated using the mean ± 3 × SD formula in order to establish the normal reference ranges against abnormal cut off percentage (Ballabio et al., 2011). Calculation of cut off value was done using Microsoft Excel.

5-4 Results

5-4-1 Illumina array analysis

Illumina array data for 22 patient samples with inv(16) were generated in collaboration with Dr. Samantha Knight at the Wellcome Trust Centre of Human Genetics, Oxford. CNAs were identified in 17 out of 22 cases (77.27%). In total, 41 losses and gains events with an average of 1.86 CNAs per patient were identified. Losses were more common than gains, with 27 regions of loss (size range: 303.696-58356.271 kbp) and 14 regions of gain (size range: 469.961- 63262.461 kbp) detected. Most of them were submicroscopic alterations. Among the detected CNAs, two recurrent affected regions were observed having losses at 7q36.1 (3.42 Mb) in two cases and at 9q13-q33.1 in two cases. Moreover, Copy Neutral Loss of Heterozigosity (CN-LOH) was detected in 19 cases out of 22 (86.4%), with an average of 6.7% per patient. The detected size of CN-LOH ranged from 19.427 to 6758.432 kbp. Recurrent CN-LOH regions were also found, including the following chromosome regions: 2p16.1, 2p21, 2q13, 6p12.3, 7q11.21, 7q11.22, 8q21.3, 8q23.3, 9q13, 12q24.11-q24.13 and 20q11.21. Some of these altered regions contain genes known to be associated with AML such as *MYC*, *MLL, IDH1, ASXL1* and *RUNX1* genes. Four regions were selected to be confirmed by FISH including three regions of loss in 7q36.1 (3.42 Mb), 16p13.11 (491.204 kbp), 4q25.1 (907.338) and one gain of 8q24.21-q24.3 (18.629476 Mb). No class I gene mutations (*c-KIT, FLT3* and *RAS*) were observed in these cases.

5-4-2 Comparison of Illumina array data and chromosome banding data

Karyotypes were assessed according to chromosome banding analysis was available in only four cases (no. 26, 27, 29 and 30). As proof of concept, additional gain of chromosome 22 materials (n=26) as reported in the karyotype was also observed by Illumina array. However, the translocation between chromosome X and 1 (patient no.27) reported in the karyotype, was not confirmed by Illumina array. This was expected because this type of array identifies loss or gain of material and not balanced rearrangements. In two cases (no.26 and no.31) a deletion of 7q36.1 was detected by Illumina array in two cases and was not seen by chromosome banding analysis. This is due to the size of the deleted regions being in both cases less than 5 Mb. However, in case no. 30 Illumina array identified a large amplified region > 18 Mb at 8q24.21-q24.3, which was missed by cytogenetics. Furthermore, in three cases small deletions ranging from 0.9 to 4.76 Mb on 13q21.33, 7q33-q34, 4q35.1, 16p13.11 and 16q22.1 were observed by Illumina array but invisible by cytogenetics.

5-4-3 Confirmation of Illumina array data by FISH

Five different BAC clones were chosen for regions of 7q36.1 (RP11-504N9 and RP11-104H2), 4q35.1 (RP11-184A23 and RP11-51B8) and 8q24.21-q24.3 (RP11-195E4). Each BAC clone was hybridized to interphase and metaphase spread of normal controls to determine the hybridization efficiency and specificity. At least 200 hundred nuclei for each probe were counted and analysed by two independent observers. The RP11-504N9 probe for the 7q36.1 region spanning 169,515bp over the *PRKAG2* gene showed a high percentage (95.3%) of cells with two hybridization signals, while the RP11-104H2 probe for the same region spanning 149,873bp over the *RHEB* gene showed 90.75% of cells with two hybridization signals (figure 5-1). FISH was performed on metaphase and interphase cells obtained from the lymphoblastoid cell line GM17878B used as control.

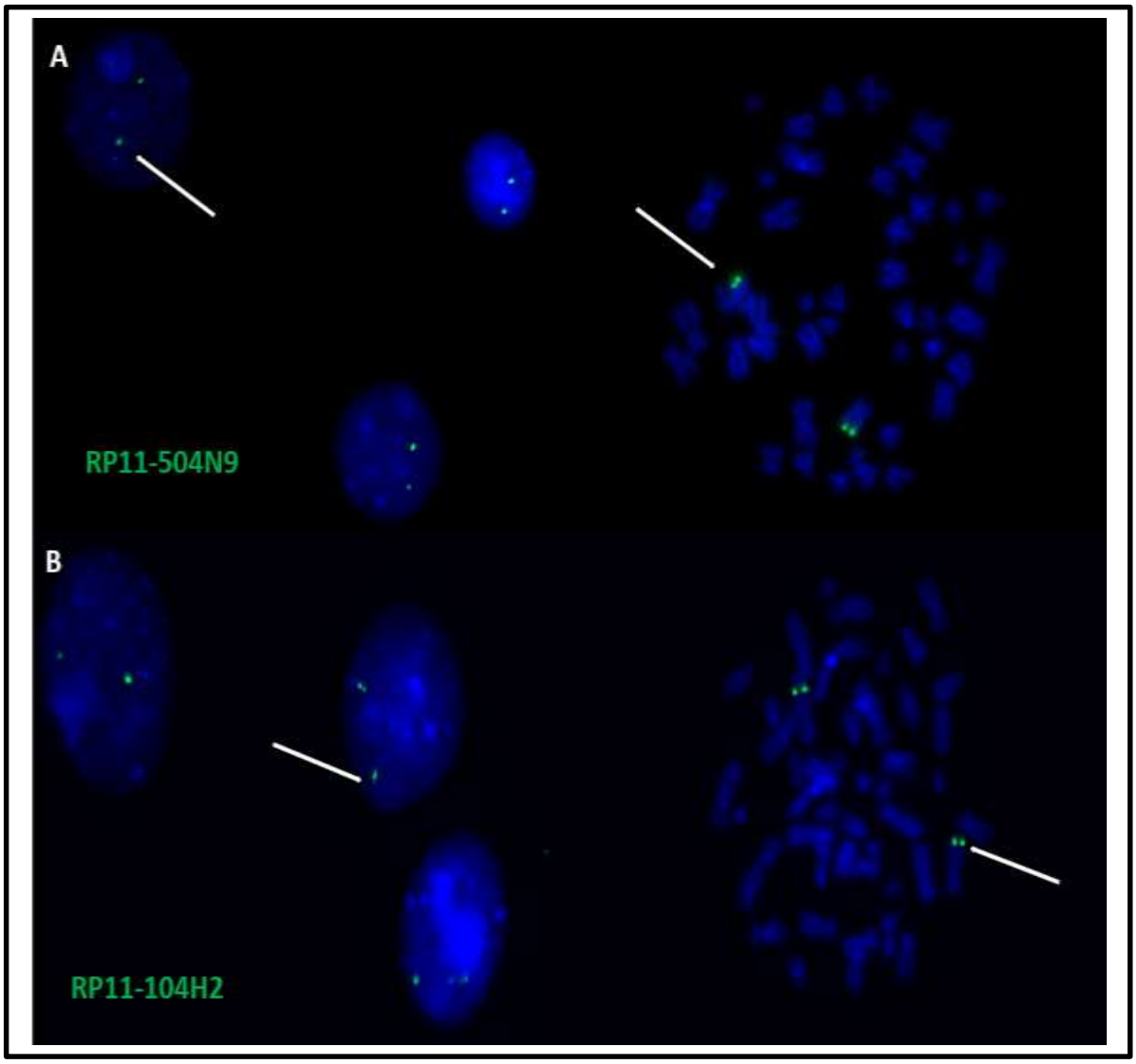

Figure 5-1: An example of FISH image using probes for the 7q36.1 region

(A) Interphase nuclei and a metaphase spread display two hybridization signals of RP11-504N9 probe to target *PRKAG2* gene on 7q36.1.

(B) Interphase nuclei and a metaphase spread show two hybridization signals of RP11-104H2 probe to target *RHEB* gene on 7q36.1. FISH signals are visible in green (FITC). Nuclei and chromosomes are counterstained in DAPI (in blue).

Furthermore, the RP11-184A23 and RP11-51B8 probes for the 4q35.1 region hybridized 166,003bp and 187,959bp over the RWDD4 gene showed 93% and 90.5% respectively of the cells with two hybridization signals (figure 5-2). FISH was performed on metaphase and interphase cells obtained from the lymphoblastoid cell line GM17878B used as control.

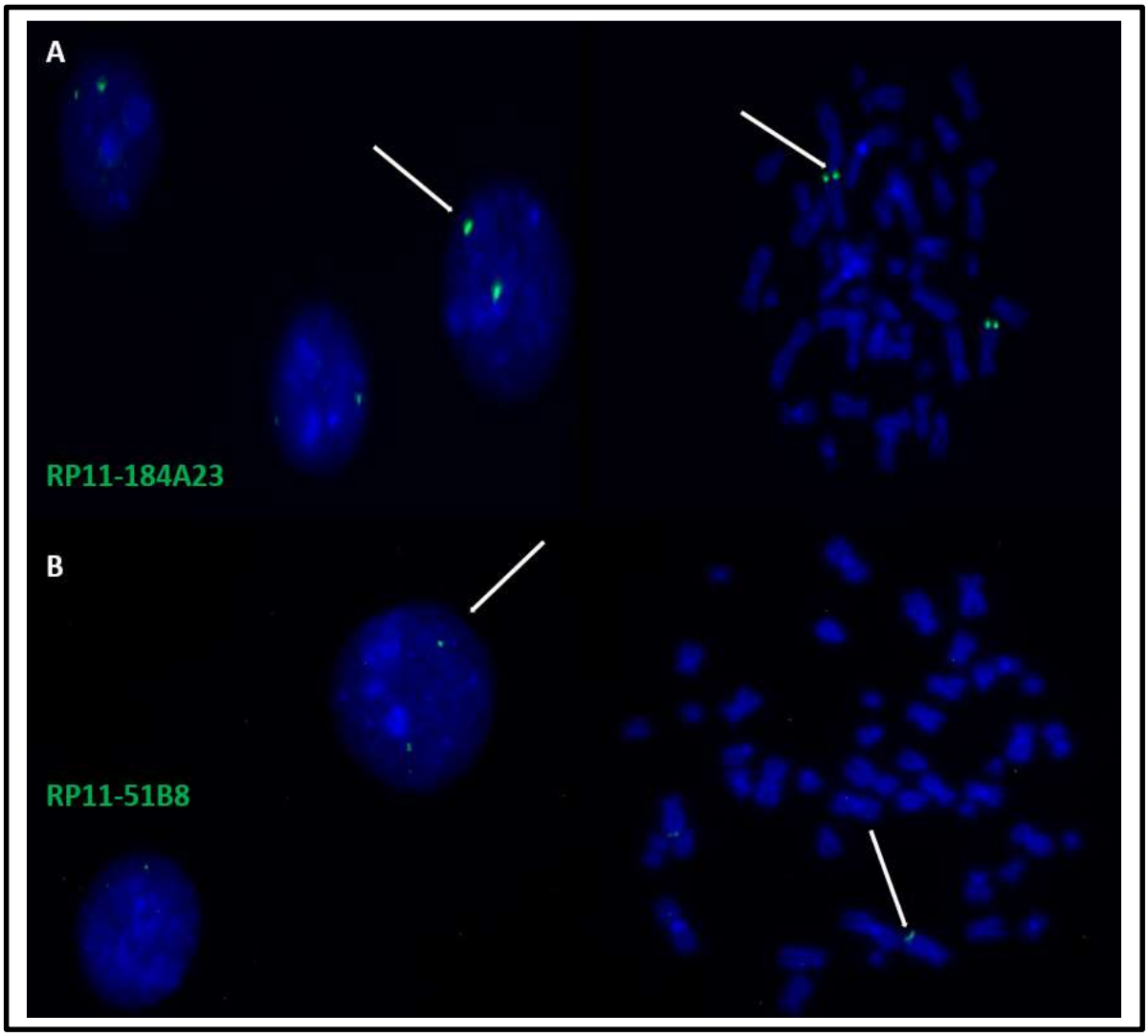

Figure 5-2: An example of FISH image using probes for the 4q35.1 region

(A) Interphase nuclei and a metaphase spread display two hybridization signals of RP11-184A23 probe to target *RWDD4* gene on 4q35.1.

(B) Interphase nuclei and a metaphase spread show two hybridization signals of RP11-51B8 probe to target *RWDD8* gene on 4q35.1. FISH signals are visible in green (FITC). Nuclei and Chromosomes are counterstained in DAPI (in blue).

For the RP11-195E4 which spans 177,174bp region over the CHRAC1 gene on 8q24.3, the percentage of cells with two hybridization signals was 94.1% (see figure 5-3). FISH was performed on metaphase and interphase cells obtained from the lymphoblastoid cell line GM17878B used as control.

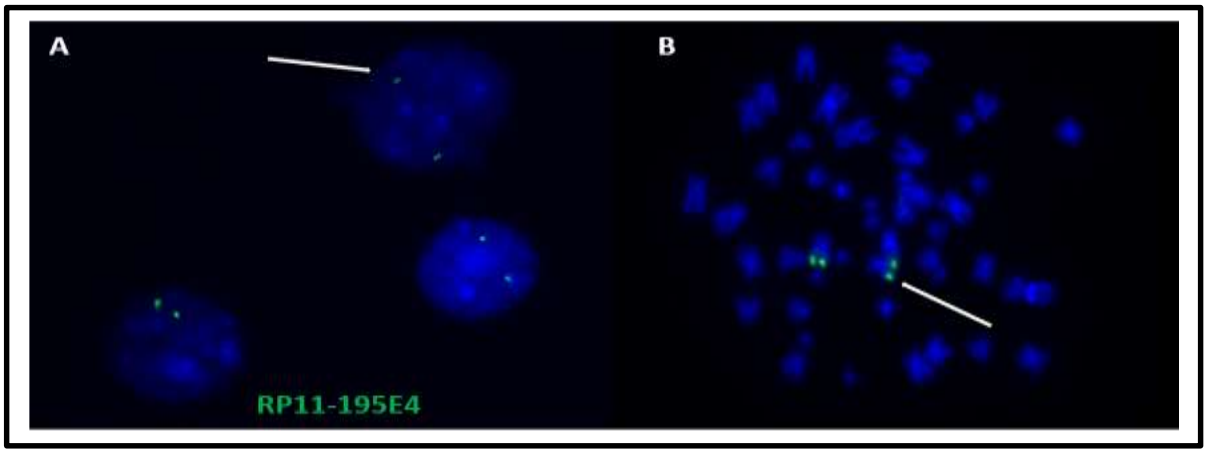

Figure 5-3: An example of FISH image using probes for the 8q24.21-q24.3 region

(A) Interphase nuclei display two hybridization signals of RP11-195E4 probe to target 8q24.1-q24.3 region.

(B) A metaphase spread shows two hybridization signals of RP11-195E4 probe to target 8q24.21-q24.3 region. FISH signals are visible in green (FITC). Nuclei and Chromosomes are counterstained in DAPI (in blue).

In addition, three BACs with high hybridization efficiency were selected and each of these BAC probes were combined individually with the inv(16) probe. Each of the three probe mixtures were hybridized to interphase and metaphase spreads of three different normal controls (CRL-2630, GM 17808B and GM 17878B). The hybridization signal pattern of at least 200 hundred nuclei from each cell line and patient samples were counted and analysed independently by three trained observers in order to establish cut-off levels.

5-4-3-1 Detection of homozygous copy loss of 7q36.1 region in patient no. 26

For the *PRKAG2* gene at 7q36.1 region, the RP11-504N9 probe in combination with inv(16) probe was hybridized to interphase and metaphase spread of CRL-2630, GM 17208B and GM 17878B and patient no. 26. The majority of cells (81.55%) from the three cell lines showed high percentage of two copies of the gene and normal chromosome 16 . Examples of FISH performed on the normal controls are shown in figure 5-4.

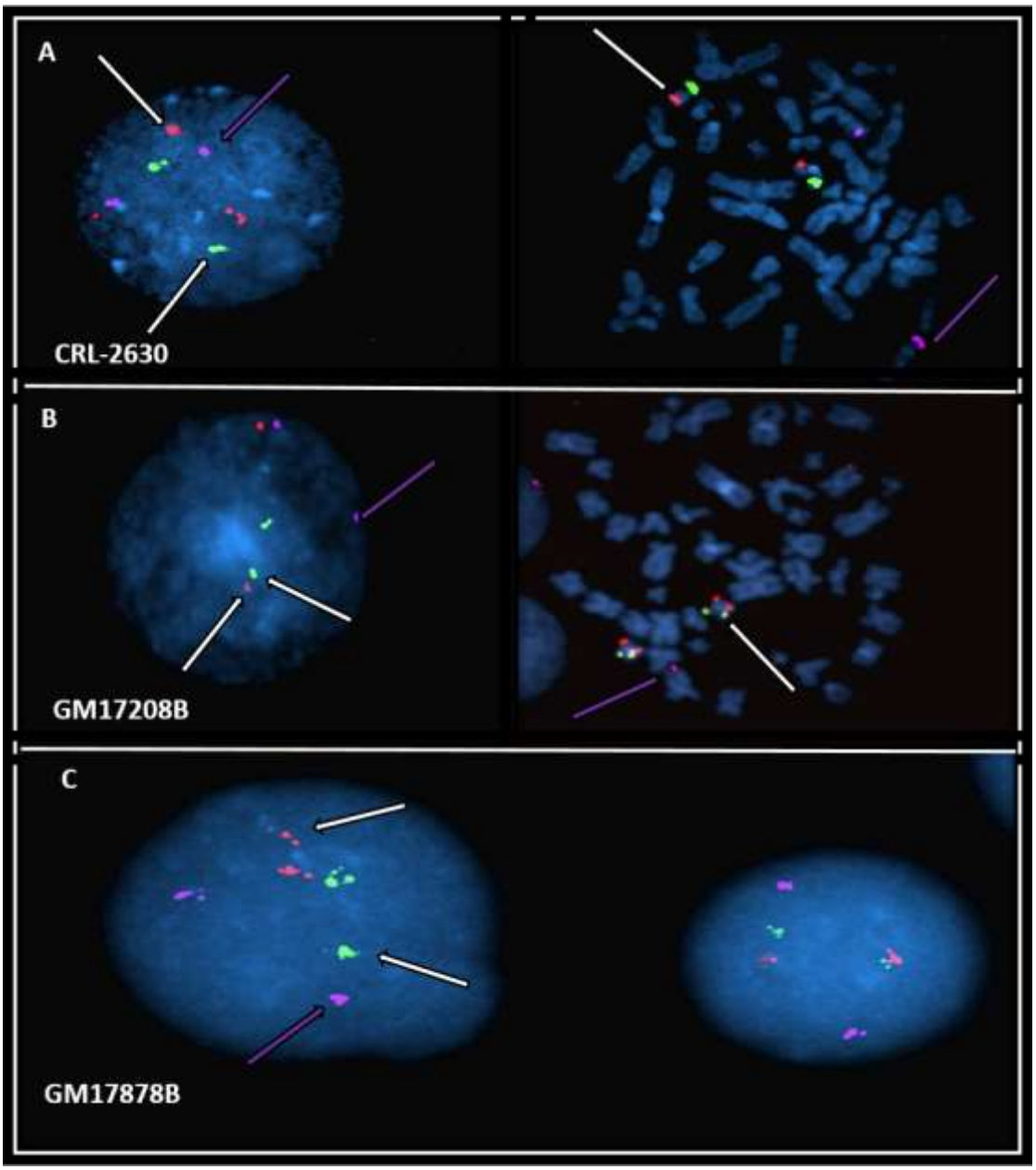

Figure 5-4: FISH performed on CRL-2630, GM17208B and GM17878B using a three colour FISH approach

Probes used were: a probe set for inv(16) (spectrumorange and FITC) in combination with RP11-504N9 probe specific for *PRKAG2* gene at 7q36.1 in each cell line in purple(Cy5). (A, B and C) Two signals for the *PRKAG2* gene at 7q36.1 in the presence of normal chromosome 16.

While the majority of cells without inv(16) rearrangements and cells harbouring inv(16) rearrangements from patient 26 were found to have complete loss of *PRKAG2* gene, a few cells without inv(16) rearrangements and cells with inv(16) rearrangements showed either one or two copies of the gene. No trisomy or tetrasomy were observed in both normal chr16 and inv(16) cells. Examples of FISH performed on patient no. 26 are shown in figure 5-5.

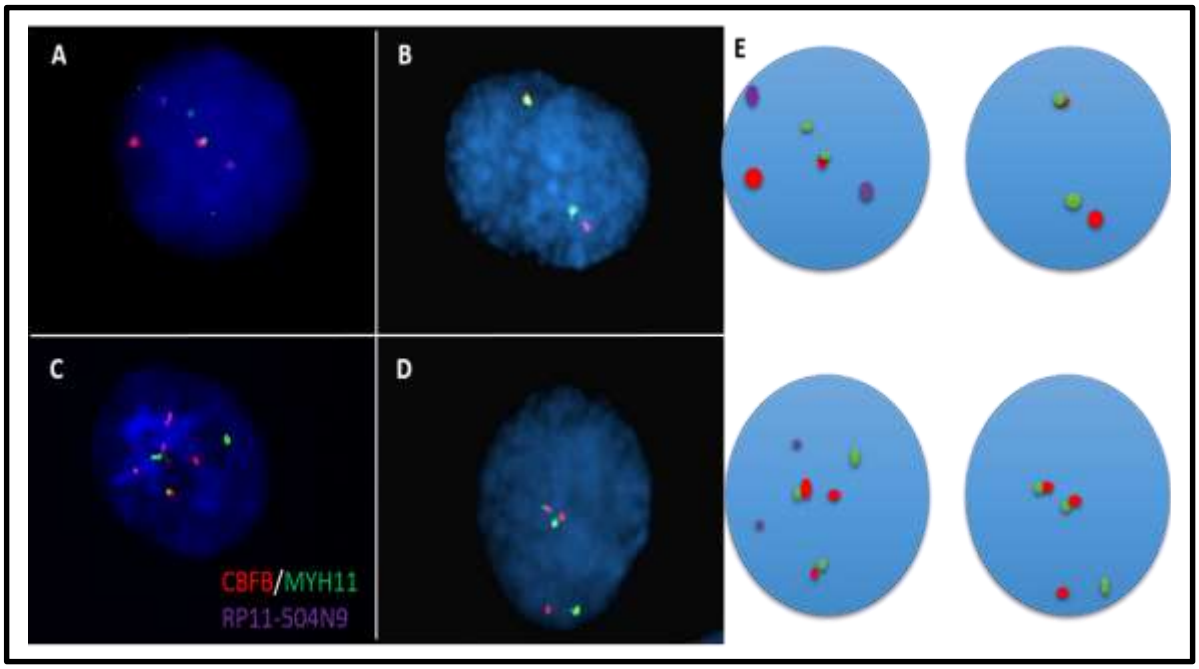

Figure 5-5: Images of interphase nuclei from patient no. 26 hybridized using a three colour FISH

Probes used were: a probe set for inv(16) (spectrumorange and FITC) in combination with RP11-504N9 probe specific for the *PRKAG2* gene at 7q36.1 in purple (Cy5).

(A) Two signals of *PRKAG2* gene in the presence of normal chromosome 16.

(B) No signals of *PRKAG2* gene shows loss of two copies in the presence of normal chromosome 16.

(C) Two signals of *PRKAG2* gene in the presence of inv(16).

(D) No signals of *PRKAG2* gene shows complete loss in the presence of inv(16).

(E) Schematic representation of the hybridization patterns observed in the nuclei to show the inv(16) and RP11-504N9 probes observed in this patient sample. Nuclei are counterstained in DAPI (in blue).

The average of cells carrying 0, 1, 2, 3, 4 copies of *PRKAG2* gene in the three cell lines counted by three observers was 3%, 12.11%, 81.55%, 2.5% and 0.84% respectively. In patient no. 26, the average of cells with 0, 1, 2, 3, and 4 copies of the gene was 92.17%, 5.66%, 2.17%, 0% and 0% respectively. The cell counts produced by the three observers are shown in appendix 1. The percentages of cells with number of hybridisation signals of the RP11-504N9 probe analysed by three observers is described in table 5-2.

Table 5-2: Percentages of cell with number of hybridisation signal of the RP11-504N9 probe for 7q36.1

No of hybridisation signals on NCs and pt26	0	1	2	3	4
AB- NC	2.5	11.5	83	2	1
VA-NC	3.33	12	81	2.33	1.33
AI-NC	3.17	12.83	80.66	3.17	0.17
Mean of NC	3	12.11	81.55	2.5	0.84
Cut off value (mean ± 3 × SD)	3 ± 3×0.44	12.11 ± 3 × 0.67	81.55 ± 3 × 1.265	2.5 ± 3 × 0.6	0.84 ± 3 × 0.96
Mean for patient 26	92.17	5.66	2.17	0	0

AB, VA and AI are the initials of the three observers; NC: normal control; 0, 1, 2, 3 and 4: percentages of cells with 0, 1, 2, 3 and 4 signals respectively.

The analysis reveals no significant difference between the three normal controls, and the majority of cells were found to have two signals. In the patient sample, the majority of cells showed complete loss of the gene (no signals of the probe). It is important to note that only 3% of control cells showed 0 signals of the probe. There was a large deviation of 75.33% between the cut off value and the percentage of patients' cells with two hybridisation signals. It is also clear that the percentage of cells with no hybridization signals in patient 26 was greater than the mean ± 3×SD of the control. There was a complete loss of *PRKAG2* gene at 7q36.1 in this patient in the majority of the cells (figure 5-6).

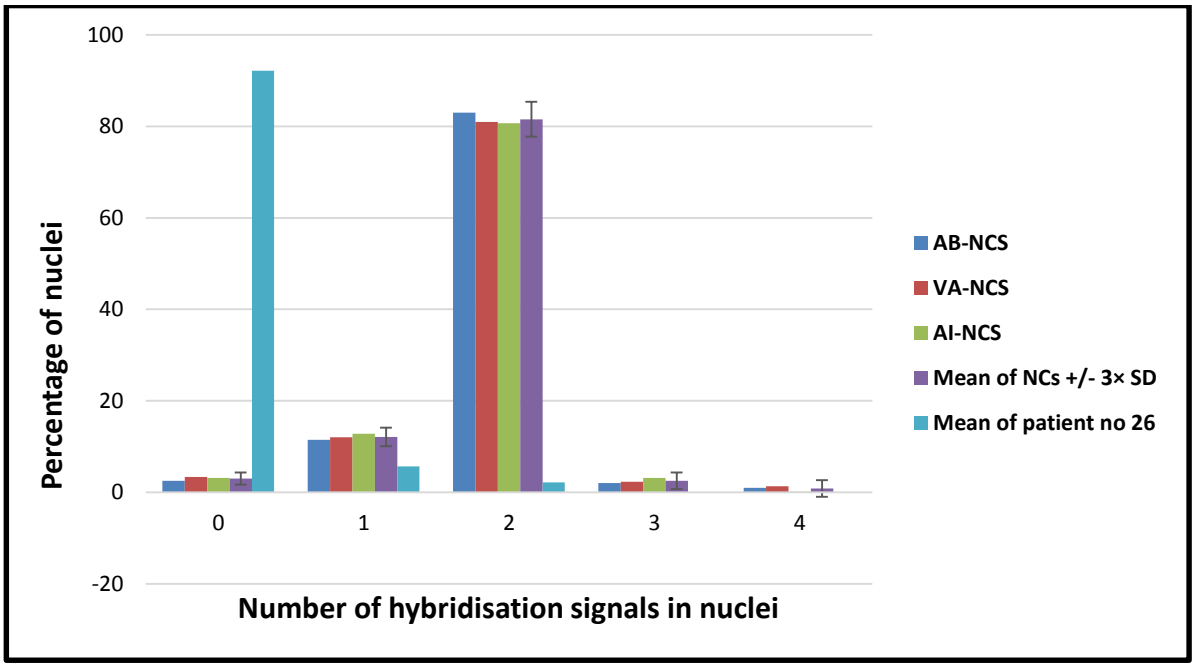

Figure 5-6: Bar graph showing percentage of hybridisation signals of RP11-504N9 probe from normal controls and patient 26 obtained from analysis of three observers

The X axis represents the average of hybridization signals of normal controls for each observer, the average of the three observers for the normal controls and the average of the three observers for the patient no. 26. The Y axis shows the percentage of nuclei. Error bars represent standard deviation.

5-4-3-2 Detection of mosaic loss of 4q35.1 region in patient 27

RP11-184A23 probe for 4q35.1 region containing the *RWDD4* gene was performed on both interphase and metaphase spread of CRL-2630, GM 17878B, GM 17208B cell lines and patient no. 27. All three cell lines were found to have high percentage of two copies of the *RWDD4* gene (two signals of probe). Examples of FISH performed on the normal controls are shown in figure 5-7.

However, the majority of patient's cells without inv(16) rearrangements and cells with inv(16) rearrangements had one copy of the *RWDD4* gene, whereas a few cells either without inv(16) rearrangements or inv(16) rearrangements showed two copies of the gene (two hybridization signals for the BAC probe). Examples of FISH performed on patient no. 27 are shown in figure 5-8.

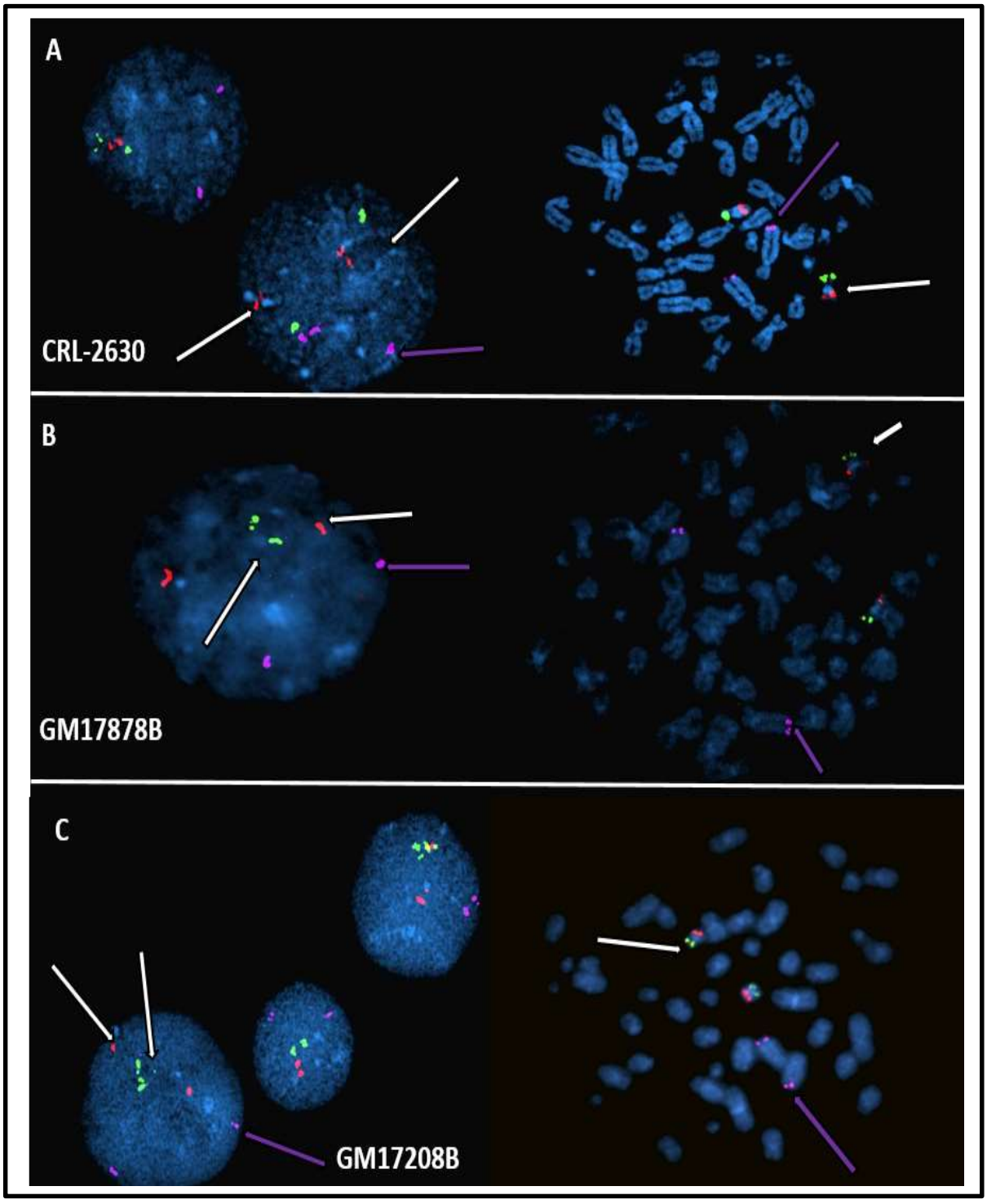

Figure 5-7: Images of interphase and metaphase cell of CRL-2630, GM17208B and GM17878B respectively using a three colour FISH approach

Probe used were: a probe set for inv(16) (spectrumorange and FITC) in combination with RP11-184A23 probe specific for *RWDD4* gene at 4q35.1 in each cell line in purple (Cy5). (A, B and C) Two signals for the *RWDD4* gene at 4q35.1 in the presence of normal chromosome 16.

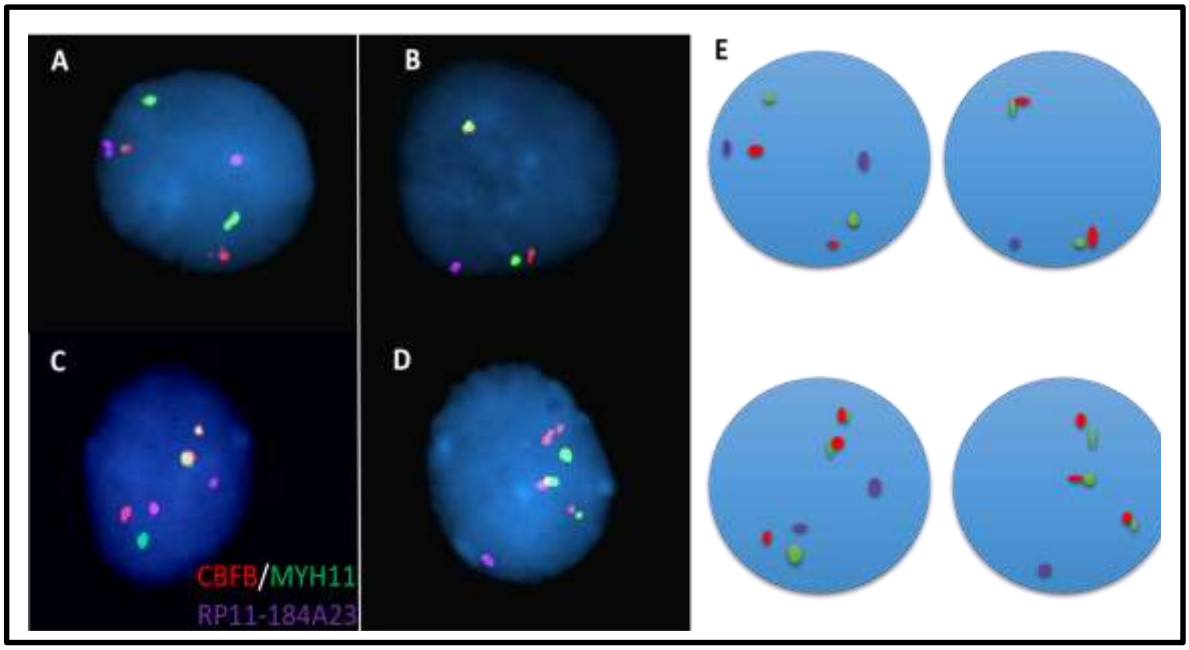

Figure 5-8: Images of interphase nuclei from patient no. 27 hybridized using a three colour FISH

Probes used were: a probe set for inv(16) (spectrumorange and FITC) in combination with RP11-184A23 probe specific for the *RWDD4* gene at 4q35.1 in purple(Cy5).

(A) Two signals of *RWDD4* gene in the presence of normal chromosome 16.

(B) One signal of *RWDD4* gene shows loss of one copy in the presence of normal chromosome 16.

(C) Two signals of *RWDD4* gene in the presence of inv(16).

(D) One signal of *RWDD4* gene shows loss of one copy in the presence of inv(16).

(E) Schematic representation of the hybridization patterns observed in the nuclei to show the inv(16) and RP11-184A23 probes observed in this patient sample. Nuclei are counterstained in DAPI (in blue)

In the three normal controls, the percentages of cells with 0, 1, 2, 3, 4 copies of the *RWDD4* gene which evaluated by the three observers were 2.346%, 8.28%, 80.63%, 7.63% and 0.94% respectively while the percentages of patient's cells having 0, 1, 2, 3, 4 copies of the gene were 9.15%, 64.9%, 25.7%, 0.25% and 0% respectively. The cell counts

produced by the three observers are in appendix 2. The percentages of cells with number of hybridisation signal of the RP11-184A23 probe for 4q35.1 region analysed by three observers is described in table 5-3.

Table 5-3: Percentages of cell with number of hybridisation signal of the RP11-184A23 probe for 4q35.1 region

No. of hybridisation signals on NCs and pt27	0	1	2	3	4
AB- NC	1.84	8	80.5	8.66	1
VA-NC	2	8.34	79.5	8.33	1.33
AI-NC	3.2	8.5	81.9	5.9	0.5
Mean of NC	2.346	8.28	80.63	7.63	0.94
Cut off Value (mean ± 3 × SD)	2.346 ± 3 × 0.741	8.28 ± 3 × 0.253	80.63 ± 3 × 1.206	7.63 ± 3 × 1.50	0.94 ± 3 × 0.416
Mean of Patient 27	9.15	64.9	25.7	0.25	0

AB, VA and AI are the initials of the three observers, NC: normal control, 0, 1, 2, 3 and 4: Percentages of cells with 0, 1, 2, 3 and 4 signals respectively.

There was no significant difference between the three normal controls, which were found to have high percentage of cells with two copies of the *RWDD4* gene (two signals of the probe). In comparison with patient sample, the percentage of cell with two copies of the gene was 25.7. Loss of one copy of the gene was found in 64.9% of the patient's cells, which was greater than the mean ± 3 × SD of the normal controls, where only 8.28% of normal controls cells had one copy of the gene. This confirms that the patient had loss of one copy of the gene at 4q35.1. Also 9.15% of the cells were found to have no copies of the gene while only 2.34% of control cells had no copies of the gene (figure 5-9).

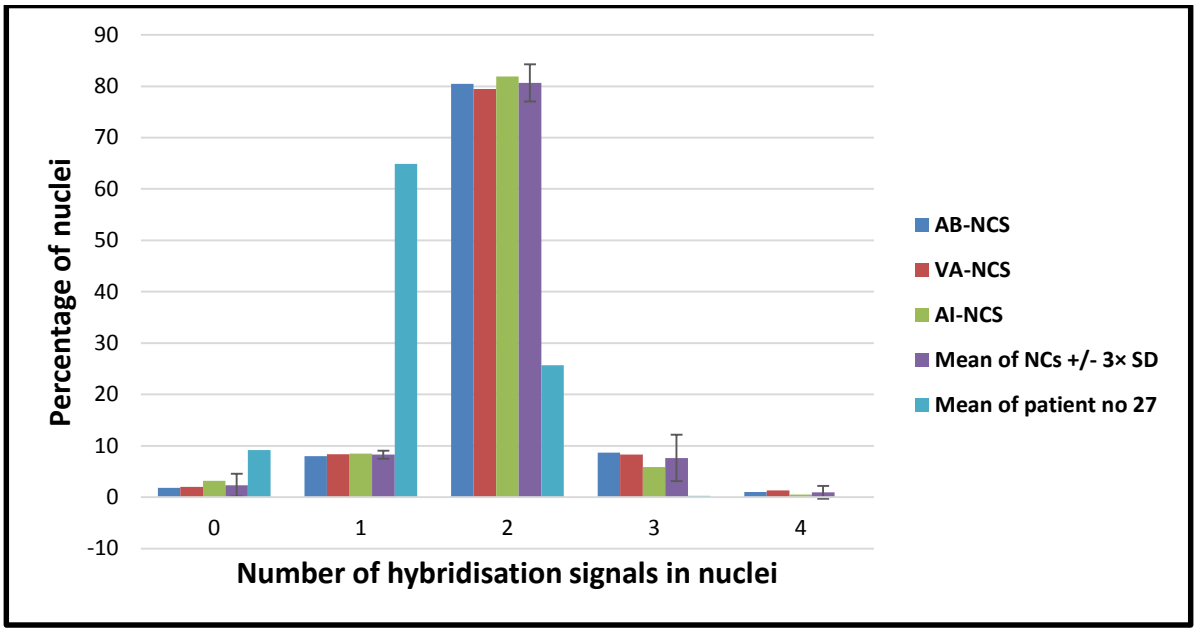

Figure 5-9: Bar graph showing percentage of hybridisation signals of RP11-184A23 probe from normal controls and patient 27 obtained from analysis of three observers

The X axis represents the average of hybridization signals of normal controls for each observer, the average of the three observers for the normal controls and the average of the three observers for the patient no. 27. The Y axis shows the percentage of nuclei. Error bars represent standard deviation.

5-4-3-3 Detection of loss of 16p13.11 region in patient no. 29

The inv(16) probe, which spans the at 16p13 region over the *MHY11* and *NDE1* genes and *CBFB* gene at 16q22 region, was hybridized to interphase of CRL-2630, GM 17208B, GM 17878B cell lines and patient no. 29. Approximately 100% of the normal controls' cells showed normal pattern of the probe, with two hybridization signals. None of the controls were found to have loss of 16p13 region. A total of 55.3% of the patient's cells were without inv(16). Of these, 5% showed loss of one copy of the 16p13 region. The cells without inv(16) and loss of 16p13 region showed three hybridisation signals of the probe (two red and one green signals). The inv(16) rearrangement was detected in 44.7% of the patient's cells, of these 7.5% of the cells were found to have one copy of the 16p13 region. The cells with inv(16) and loss of 16p13 region showed four hybridisation signals of the probe (3 red and one green signals). Examples of FISH performed on patient no. 29 are shown in figure 5-10. Probes used were: a probe set for inv(16) (spectrumorange and FITC), the

spectrumorange labelled probe hybridize *CBFB* gene on 16q22 and the FITC labelled probe targets the *MYH11* and *NDE1* genes on 16p13.11.

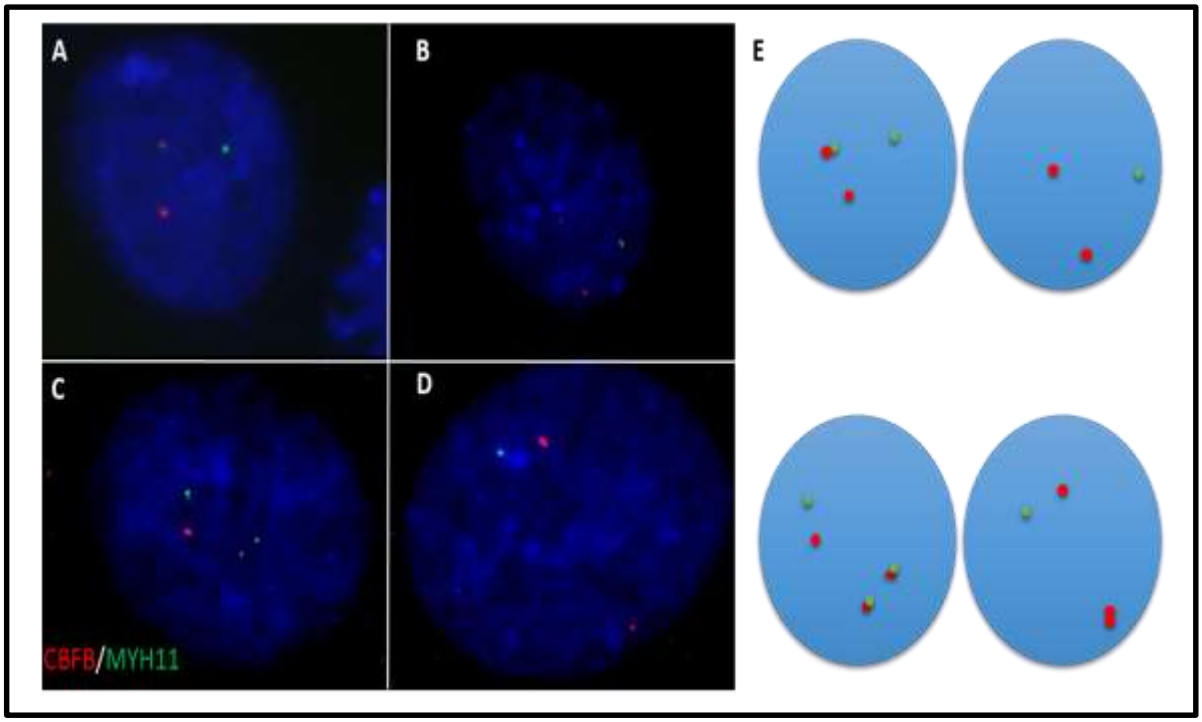

Figure 5-10: Images of interphase nuclei from patient no. 29 hybridized using dual colour FISH

(A) Two signals of *MYH11* gene in the presence of normal chromosome 16.

(B) One signal of *MYH11* gene shows loss of one copy in the presence of normal chromosome 16.

(C) Two signals of *MYH11* gene in the presence of inv(16).

(D) One signal of *MYH11* gene shows loss of one copy in the presence of inv(16).

(E) Schematic representation to show the inv(16) probe FISH patterns in this patient sample. Nuclei are counterstained in DAPI (in blue).

5-4-3-4 Detection of gain of 8q24.21-q24.3 regions in patient no. 30

The RP11-195E4 probe hybridized the *CHRAC1* gene at 8q24.3 was performed on interphase and metaphase cells of CRL-2630, GM17878, GM17208 lines and patient no. 30. The analysis of the three normal controls showed that the majority of cells had two copies of the gene (two identical signals of the probe). Examples of FISH performed on the normal controls are shown in figure 5-11.

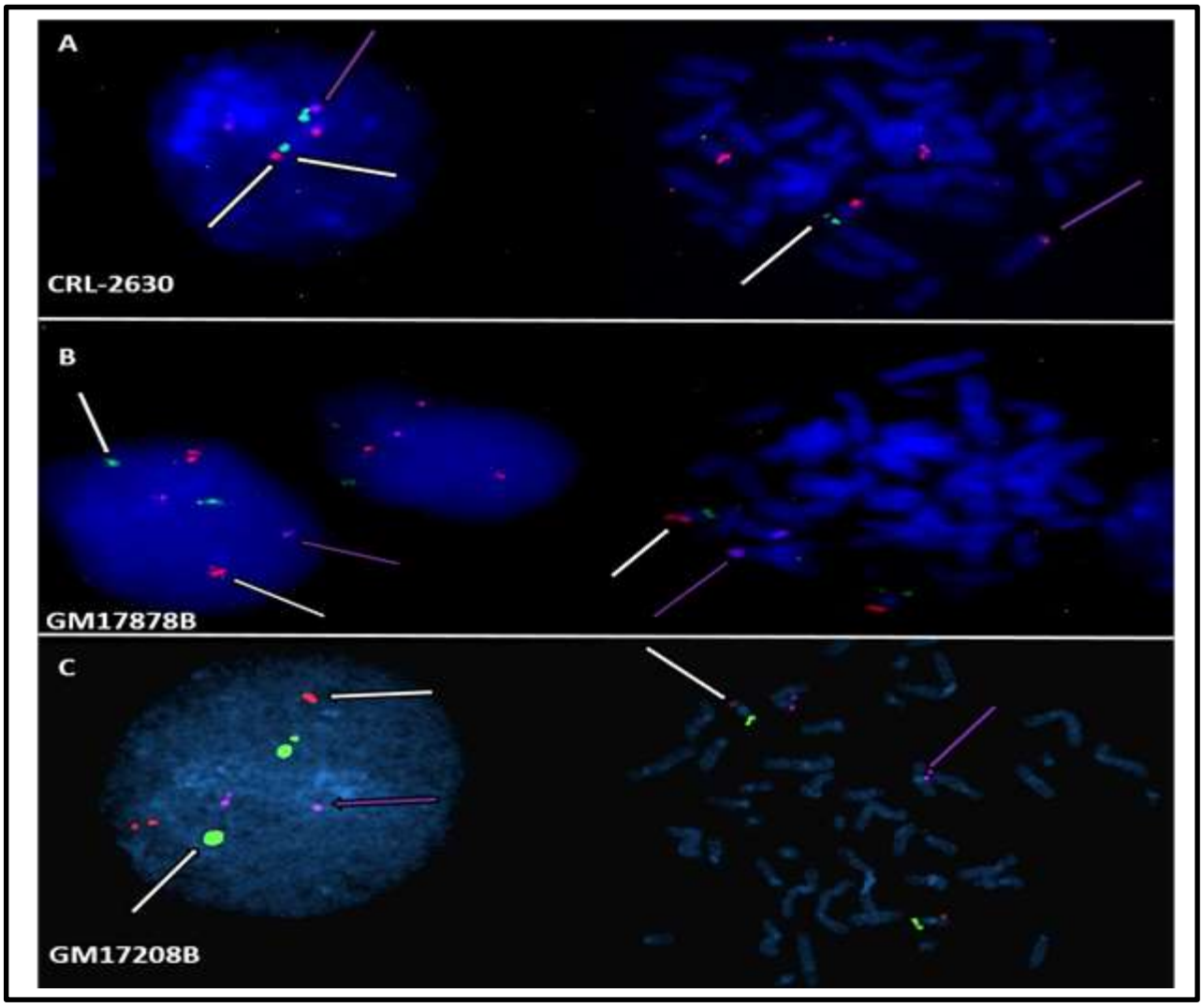

Figure 5-11: Images of interphase and metaphase cell of CRL-2630, GM17208B and GM17878B respectively using a three colour FISH approach

(A, B and C) Two signals for the *CHRAC1* gene at 8q24.3 in the presence of normal chromosome 16.

In the patient sample, the majority of cells without inv(16) rearrangements and cells with inv(16) rearrangements were also detected with two copies of the *CHRAC1* gene at 8q24.3 (two identical probe signals), while a few cells showed three copies of the gene (three signals of the probe). Examples of FISH performed on patient no. 30 are shown in figure 5-12. Probes used were: a probe set for inv(16) (spectrumorange and FITC) in combination with RP11-195E4 probe specific for the CHRAC1 gene at 8q24.3 in purple(Cy5).

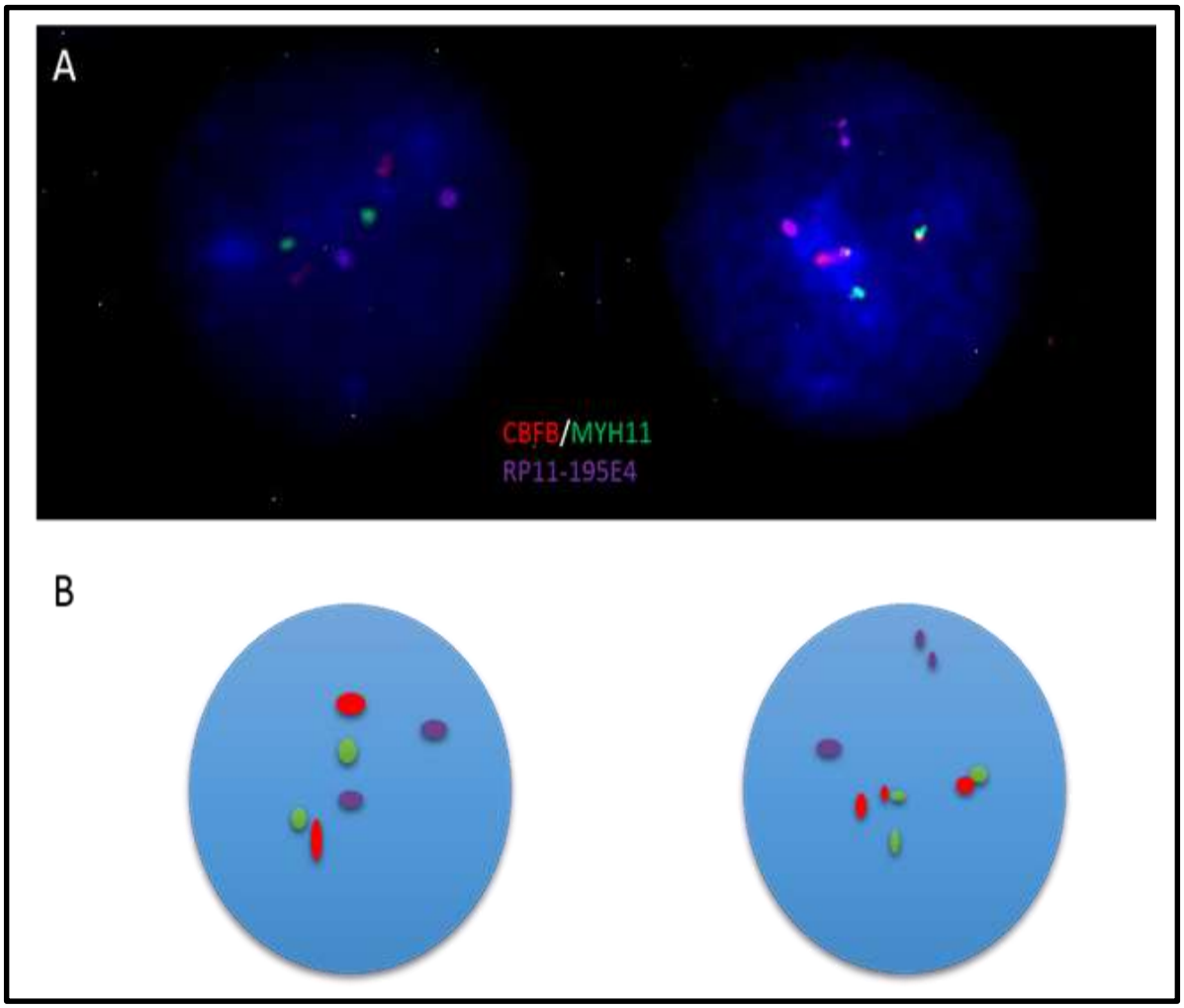

Figure 5-12: Images of interphase nuclei from patient no. 30 hybridized using a three colour FISH

(A) Shows two nuclei from the same patient. The left nucleus shows two signals of equal intensity for RP11-195E4 probe in the presence of normal chromosome 16, the right nucleus shows two signals of equal intensity for RP11-195E4 probe in the presence of two fusion signals to indicate the inv(16) rearrangement.

(B) Schematic representation of the hybridization patterns observed in the nuclei to show the inv(16) and RP11-195E4 probes observed in this patient sample. Nuclei are counterstained in DAPI (in blue).

The percentages of cells with 0, 1, 2, 3, 4 copies of the *CHRAC1* gene in the three cell lines evaluated by the three observers were 1.33%, 6.28%, 86.61%, 5.326% and 0.44% respectively, while the percentages of patients' cells having 0, 1, 2, 3, 4 copies of the gene were 2%, 3.33%, 85.5%, 9.17% and 0% respectively. The cell count produced by the three observers is in appendix 3. The percentages of cell with number of hybridisation signals of the RP11-195E4 probe for 8q24.3 region analysed by three observers are described in table 5-4.

Table 5-4: Percentages of cell with number of hybridisation signal of the RP11-195E4 probe for 8q24.3 region

No of hybridisation signals on NCs and pt30	0	1	2	3	4
AB- NC	1	6.36	89	3.3	0.34
VA-NC	1.16	6	88.33	3.85	0.66
AI-NC	1.83	6.5	82.5	8.83	0.34
Mean of NC	1.33	6.28	86.61	5.326	0.44
Cut off value (mean ± 3 × SD)	1.33 ± 3 × 0.44	6.28 ± 3 × 0.257	86.61 ± 3 × 3.756	5.326 ± 3 × 3.04	0.44 ± 3 × 0.184
Mean of patient 30	2	3.33	85.5	9.17	0

AB, VA and AI are the initials of the three observers, NC: normal control, 0, 1, 2, 3 and 4: Percentages of cells with 0, 1, 2, 3 and 4 signals respectively.

According to the analysis of RP11-195E4 probe, there was no significant difference between the normal controls cells carrying two copies of *CHRAC1* gene (two signals of the probe) and patients' cells with two copies of the gene (two signals of the probe); both had a similar level of two copies of the gene. Only a small proportion of cells in the normal controls and the patient showed one copy of the gene. The percentage of patients' cells with three copies of the gene (three signals of the probe) was within the three standard deviation interval around the normal controls mean. This indicates that the amplification of 8q24.21-q24.3 is not confirmed in this patient (figure 5-13).

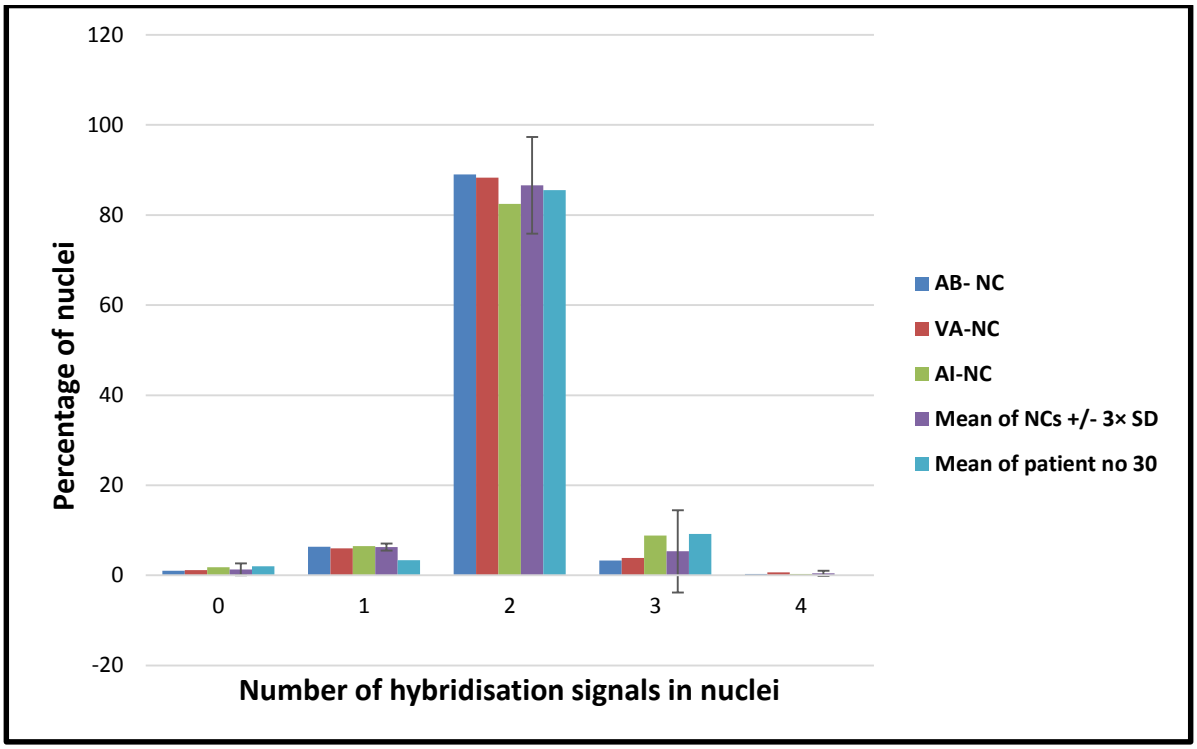

Figure 5-13: Bar graph showing percentage of hybridisation signals of RP11-195E4 probe from normal controls and patient 30 obtained from analysis of three observers

The X axis represents the average of hybridization signals of normal controls for each observer, the average of the three observers for the normal controls and the average of the three observers for the patient no. 30. The Y axis shows the percentage of nuclei. Error bars represent standard deviation.

5-4-4 Verification of CNAs in normal chromosome 16 cells and cell harbouring inv(16) rearrangement

As mentioned previously, a combination of BACs and inv(16) probes were performed on cells of four patient samples to confirm the Illumina array findings and to verify whether the CNAs can be found in cell with normal chromosome 16 or in cells carrying chromosome 16 inversion. Copy number loss was found both in normal chromosome 16 and inv(16) cells in the three patient samples. In patient no. 26, complete loss of *RPKGA2* gene at 7q36.1 was found in 92% of cells, of which 51.5% were carrying inv(16) rearrangement, while 43% of cells were without inv(16) rearrangements. In addition, there was a low percentage of cells without inv(16) rearrangements and cells inv(16) rearrangements had two copies of the gene (figure 5-14).

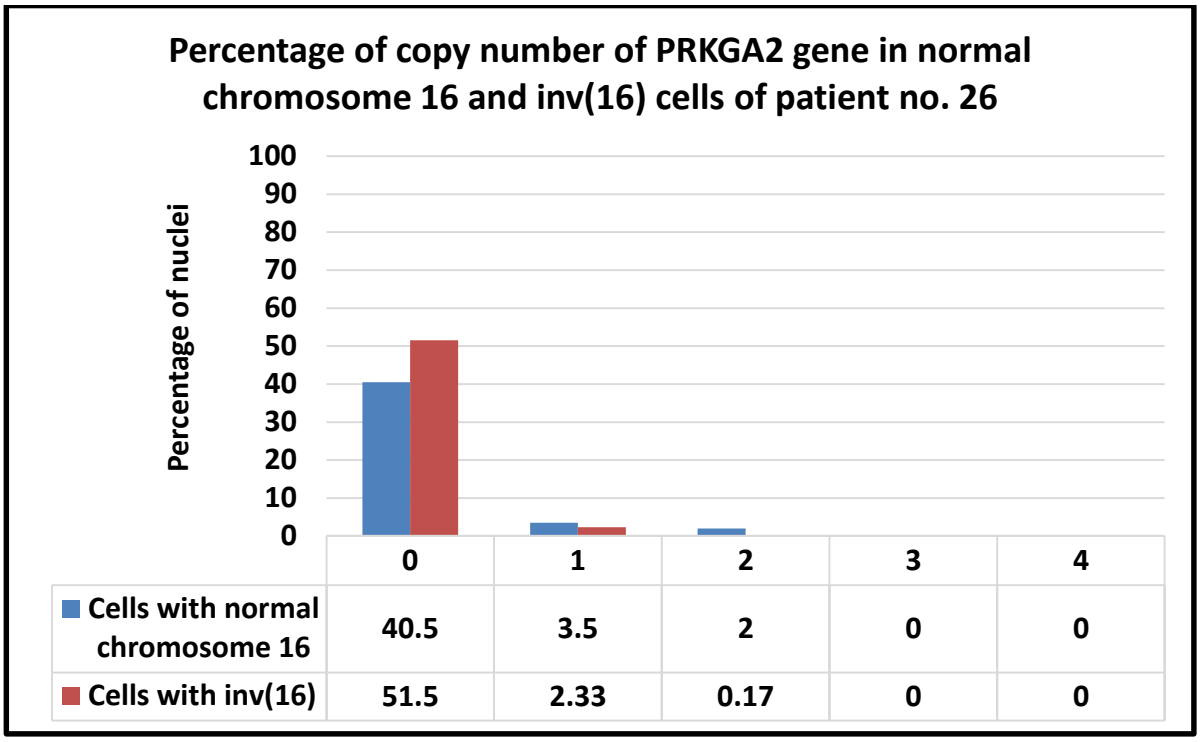

	0	1	2	3	4
Cells with normal chromosome 16	40.5	3.5	2	0	0
Cells with inv(16)	51.5	2.33	0.17	0	0

Figure 5-14: Bar chart illustrating the percentage of copy number of PRKAG2 gene at 7q36.1 region in cells without inv(16) and cells with inv(16) from patient no. 26

The X axis represents the percentage of copy number of the *PRKAG2* gene in cells with normal chromosome 16 and cells with inv(16) rearrangement. The Y axis shows the percentage of nuclei.

The loss of *RWDD4* gene at 4q35.1 was apparent in 64.9% of the cells in patient 27. 31% of cells carrying loss of the gene were harbouring inv(16) rearrangement, whereas 33.9% of cells with loss of the gene were found to have normal chromosome 16. Moreover, 11.2% of cells with two copies of the gene were without inv(16) rearrangements, while 14.5% of cells with two copies of the gene were with inv(16) rearrangement (figure 5-15).

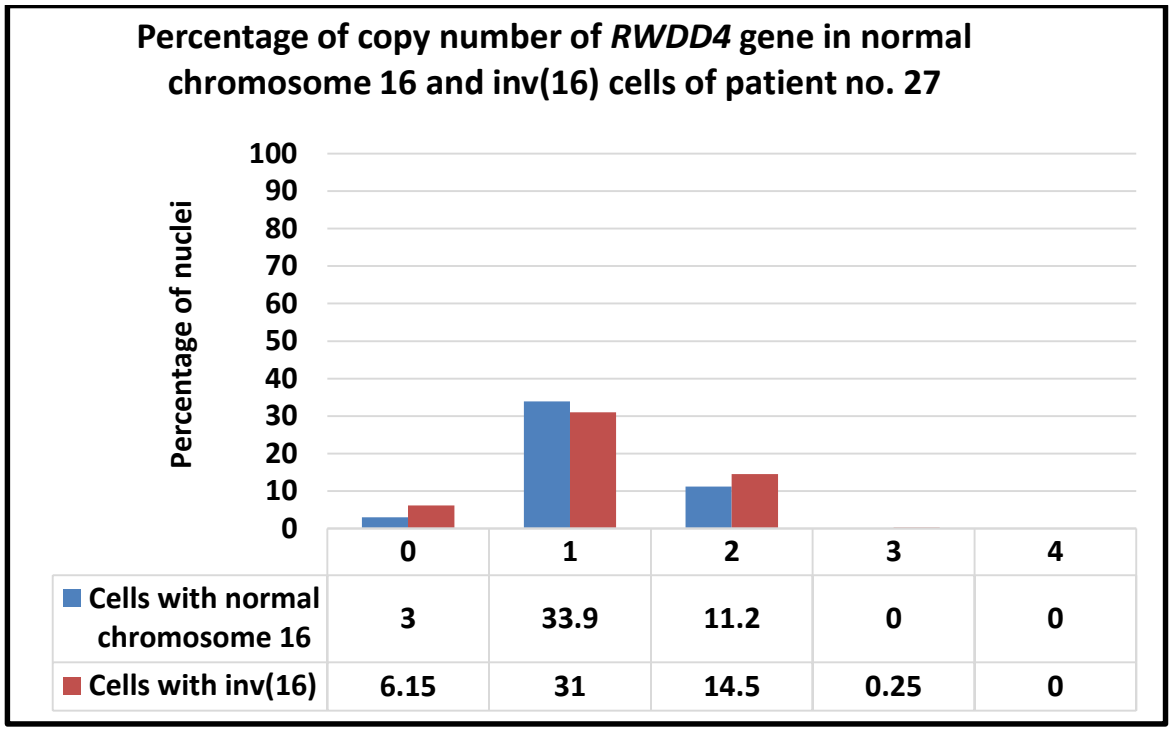

Figure 5-15: Bar chart illustrating the percentage of copy number of RWDD4 gene at 4q35.1 region in cells with normal chromosome 16 and cells with inv(16) from patient no. 27

The X axis represents the percentage of copy number of the *RWDD4* gene in cells without inv(16) and cells with inv(16) rearrangement. The Y axis shows the percentage of nuclei.

In patient 29, the copy number loss was also found both in cells with normal chromosome 16 and cells with inv(16) rearrangement. The percentage of cells with loss of *MHY11* gene was 12.5%, 5% of these cells were without inv(16) rearrangements, while 7.5% of cells were carrying inv(16) rearrangement. The percentage of both cells without inv(16) and with inv(16) with two copies of the *MYH11* gene was 87.5% (figure 5-16).

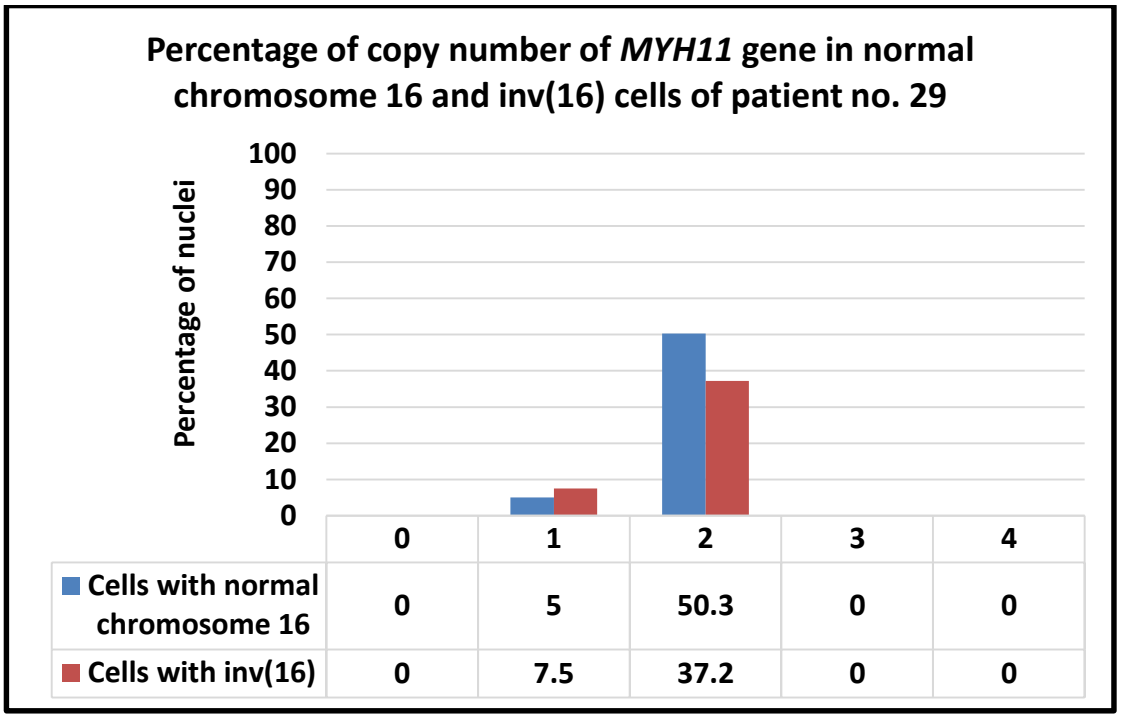

Figure 5-16: Bar chart illustrating the percentage of copy number of MHY11 gene at 16p13.11 region in cells with normal chromosome 16 and cells with inv(16) from patient no. 27

The X axis represents the percentage of copy number of the *MHY11* gene in cells with normal chromosome 16 and cells with inv(16) rearrangement. The Y axis shows the percentage of nuclei.

5-5 Discussion

To gain better insight in the genetic basis of leukaemia and its implication in the clinical practice, the Illumina beadarray approach was used to determine CNAs and CN-LOH regions in 22 AML patients samples with inv(16)(p13;q22) and t(8;21)(q22;q22).

Firstly, we identified low number of CNA losses and CN gains in 17 (77.27%) out of 22 cases. In total, 41 losses and gains events with an average of 1.86 CNAs per patient. Losses were more common than gains, with 27 loss regions (size range, 303.696-58356.271 kbp) and 14 gain regions (size range, 469.961- 63262.461 kbp). CN- LOH were also detected with an average of 6.7% per patient. Low recurrence of CNA regions was detected, including losses of 7q36.1 and 9q13-q33.1 and CN- LOH of 2p16.1, 2p21, 2q13, 6p12.3, 7q11.21, 7q11.22, 8q21.3, 8q23.3, 9q13, 12q24.11-q24.13 and 20q11.21. These results are in agreement with previous studies (Akagi et al., 2009; Barresi et al., 2010; Cosat et al., 2013; Kuhn et al., 2012; Redtke et la., 2009), which showed a low number of CNAs and low recurrent regions, including 7q36.1 and 9q13-q33.1 found in AML cases.

Secondly, chromosome banding analysis of four cases (no 26, 27, 29 and 30) showed additional gain of chromosome 22 materials (n=26), translocation between chromosome X and 1 (n=27), and in two cases (n=26 and n=30) the inv(16) rearrangement was the only abnormality observed. However, arrays identified deleted regions in 7q36.1, 4q35.1 and 16p13.11 in three cases were not observed by chromosome banding. Furthermore, a large amplified region >18 Mb was detected by array, while it was missed by G-banding. The trisomy 22 observed by G-banding in pt 26 was confirmed by array while the t(X;1) did not involve any deletion of amplification of genomic material.

Thirdly, to validate the CNAs in four cases showing a 7q36.1 deletion, 4q35.1 deletion, 16.13.11 deletion and 8q24.21-q24.3 gain, interphase FISH was performed using three BACS in a combination with inv(16) probe for the 7q36.1, 4q35.1 and 8q24.21-q24.3 regions and inv(16) (MHY11-CBFB) probe for 16p13.11 region. The homozygous copy loss of 7q36.1 was confirmed in 92% of the cells. In case 27 a mosaic Loss of 4q35.1 region was also confirmed in 64.9% of nuclei. In case 29 a copy number loss of 16p13.11 region was confirmed in 12.5% of cells. However, in case 30 a large gain of 8q24.21-q24.3 was not confirmed by FISH, as the results showed no significant difference between the normal controls and the patient's cells.

Ballabio et al. (2011) demonstrated that large CNAs identified in normal karyotype AML cases by aCGH analysis were confirmed by FISH and found in interphase but not in metaphase cells. Their hypothesis was that the abnormalities was confined to the non-dividing cells, therefore they could not be observed by chromosome banding analysis or by metaphase FISH. They demonstrated this by conducting immuno-FISH experiments using ki-67, a proliferation marker, and showing that the CNAs were detected only in ki-67 positive cells in the majority of cases. Based on this evidence, we decided to carry out further analyses of FISH data, to investigate whether CNAs are present in the same clone harbouring inv(16) or/and in the cells without inv(16); and to verify whether the CNAs were present in non-dividing population of cells.

Our results showed that the CNAs were found both in cells without inv(16) and cells harbouring the inv(16) rearrangement in all cases except case no. 30. In addition, a proportion of cells without inv(16) and with inv(16) were found to have a normal number of copies of 7q36.1 (no 26), 4q35.1 (no 27) and 16p13.11 (no 29). In cases no. 26, 27 and 29 the CNAs detected were invisible by G-banding and were too small to be seen by

chromosome banding methods. In two cases the CNAs occurred only in a proportion of cells, as shown in case 27 (64.9%) and case 29 (12.5%). This variance of the copy number loss of the gene detected in patient cells can be explained by somatic mosaicism of the patients, by which one copy of the gene was found in only 64.9% and 12.5% of the cells.

CHAPTER 6: PROLIFERATION STUDIES IN ACUTE MYELOID LEUKAEMIA

6-1 Introduction

Hematopoietic stem cells have the ability to self-renew and differentiate into different linages and mature blood cells. HSC is a very rare cell population in the bone marrow and generally arrested in G0 phase of cell cycle, but upon stimulation they can enter into cell cycle and proliferate (Bonnet, 2005). The developmental process of the stem cells is controlled by several transcriptional factors. Dysregulation of this program can therefore lead to initiate leukaemia proliferation (Lecuyer and Hoang, 2004).

Ki67 is a nuclear protein that is expressed in the proliferating cells during G1, S, G2 and M phases of the cell cycle (Bridger et al., 1998). Gerdes et al. (1983) reported that the ki67 antigen was produced by injecting of L428 cells derived from Hodgkin's disease to mice. The functions of ki67 remain unknown. The localization of ki67 antigen has been assessed in cells during interphase by immunofluorescence using normal human dermal fibroblasts (HDF) (Bridger et al., 1998). In this study, the ki67 antigen was localized or distributed in relation to the different phases of the cell cycle. The ki67 antigen was detected in nuclear foci in early G1 referred to it as pattern type I, whereas in late G1, S and G2 the ki67 antigen was located in the nucleolus showing a different patterns of ki67 staining referred to as pattern type II. The ki67 antigen was also seen surrounding metaphase chromosomes during mitosis, while it was not detected in the G0 phase of the cell cycle, when the cells exist in a quiescent state (Bridger et al., 1998; Kill, 1996).

Few studies have reported results for ki67 in normal blood cells. Gerdes et al. (1983) demonstrated that more than 80% of phytohaemagglutinin (PHA)-stimulated normal blood cells reacted with ki67 antibody, while unstimulated normal blood lymphocytes and monocytes did not. Moreover, ki67 was also found to react with the majority of cells from cancer cell lines, such as L428, Daudi, Raji, HL-60, U937 and k562. It has been shown that proliferating lymphoid cells have been identified in tonsils, adult bone marrow and thymus (Campana et al., 1988; Gerdes et al., 1986). Ki67 protein can be expressed by stimulating T lymphocytes in culture with PHA for 72 hours (Gerdes et al., 1983). Since 1983, Ki67 antibody has been widely used for the determination of the proliferative state

in different types of cancers including hematopoietic malignancies. The assessment of the proliferative state of the cancer cells before treatment may provide potential index for a better or worse prognosis and can assist the treatment strategy (Gerdes et al., 1986: Le Doussal et al., 1989; Querzoli et al., 1996; Trihia et al., 2003).

Nowicki et al. (2006) showed that a high percentage of ki67 positive cells among the leukaemic blasts, ranging from 88.4-99.8%, was detected in all samples taken from 46 patients with leukaemia on day 0 (baseline) of induction treatment; by day 15, 36 out of 46 patients responded to treatment and reached remission. In these patients, the level of blasts was 5% and linked to low risk, while the remaining 10 patients did not respond to the treatment and the number of blasts was higher than 5% (and associated with high risk). In four out of ten cases assigned to the high-risk group, the ki67 expression was found in 40% of blasts on day 15. However, the percentage of ki67 negative cells was identified in 60% of blasts among the remaining six patients. The authors concluded that patients found with a high percentage of ki67 negative blasts are associated with a poor prognosis. Lowenberg et al. (1993) treated 91 of 114 newly diagnosed AML patients with chemotherapy to determine the rate of cell proliferation. Of the 114 patients, 37, 39 and 38 had a low, intermediate and high level of cell proliferation (respectively). The prospect of three-year survival rate was for 36% of patients with low level of proliferation, and only 3% among patients with high level of growth fraction. Their data suggested that the higher proliferation level in leukaemic cells, the worse the outcome of patients.

Ballabio et al. (2011) showed that CNAs identified by FISH were found in interphase cells but were not seen in the metaphases of leukaemia patients within the same samples because they remain confined to non-proliferating cells. The authors explained that the majority of leukaemic cells (average 96.75%) carrying abnormalities were non-proliferating cells compared with an average of 72.25% of cells which did not carry abnormalities. Sun et al. (2003) investigated the growth fraction of samples obtained from 21 cases with AML type M4eo, 15 cases of other AML types and two normal cases. The authors reported that the growth fraction of cells with AML type M4eo (median 91%) was higher than the growth fraction of other AML types (median 80%).

6-2 Aims of this study

Little is known about the localization of ki67 antigen, staining patterns of ki67 and the proliferation status of normal peripheral blood cells and leukaemia cells and cell lines. The main of this study is to gain some knowledge on (i) the staining pattern of Ki67 (ii) to determine the localization of ki67 antigen (iii) to assess proliferation status of the above cells (iv) to determine the proportion of proliferative and non-proliferative of cells derived from patients with leukaemia. In order to achieve the above goal, the following objectives are outlined:

1. To use indirect immunofluorescence (IF) using anti-ki67 antibody in order to determine the localization of ki67 antigen and the proliferation satatus of stimulated and unstimulated peripheral blood cells and k562 cell line.
2. To use immuno-FISH using specific probes for regions of interest and Ki67 antibody to determine the proportion of proliferative and non-proliferative cells carrying specific chromosomal abnormalities.

6-3 Material and methods

6-3-1 Normal blood samples

Eight normal peripheral blood samples were used in this study, comprising two samples of untreated peripheral blood cells from healthy individuals (samples 2 and 5), and six samples of peripheral blood cells that have been stimulated to proliferate using PHA (samples AH, AN, GO, JS, PB and LU).

6-3-2 Patient samples

Five patient samples were selected for this study on the basis of: (i) presence of trisomy 8 in patients (L020944, H010340 and 0132108), deletion of 7q36.1 and inv(16) in one patient (no. 26) and deletion of 4q35.1 and inv(16) in another patient (no. 27); and (ii) availability of material in the form of fixed chromosomes and cell suspensions suitable for immune-FISH.

6-3-3 Cell lines

Three cell lines were used in this study:

1. Farage (CRL-2630) cell line was derived from patient who had DLCL.
2. K562 cell line was derived from a female patient with cryonic myeloid leukaemia.
3. Pfeiffer (CRL-2632) cell line was established from patient with lymphoma.

6-3-4 Probes

Probes used in this study were:

i. (D8Z2) for centromeric 8;
ii. RP5-1173K1 for *Nup98* at 11p15 region;
iii. inv(16) probe (MetaSystems….);
iv. RP11-504N9 For 7q36.1; and
v. RP11-184A23 For 4q35.1.

Probes iii-v were used as part of the experimental work described in chapter 5 of this thesis.

6-3-5 Antibodies

Antibodies used for IIF in this work were anti-ki67 monoclonal mouse primary antibody (Dako, Denmark) and anti-Mouse (FITC) secondary antibody (Vector Laboratories,UK), in addition to the reagents for detection of FISH probes described in previous chapters.

6-3-6 Indirect immunofluorescence

Indirect immunofluorescence (IIF) using ki67 antibody was performed on normal peripheral blood cells from 8 different healthy individuals and k562 cell line to assess the proliferation state in stimulated (treated with PHA for inducing T lymphocytes cells to proliferate) and unstimulated (untreated with PHA and most of cells are non-dividing cells) normal blood cells and one leukemic cell line. Of these, five samples (AH, AN, GO, JS, and LU) were already stimulated and two samples (2 and 5) were unstimulated, these samples were provided by Brunel University. PB sample was stimulated in the present study. The IIF procedure is described in detail in chapter 2.

6-3-7 Immuno-FISH

The immunoFISH procedure is described in detail in chapter 2, section 2-9.

6-3-8 Microscope analysis

The slides were viewed using Olympus BX41 Fluorescence microscope (Zeiss) and Zeiss axioplan epifluorescence microscope (Carl Zeiss). All slides were examined under 100X immersion oil objective. Metaphases and interphase cells were captured with a camera (Scion FW camera, image processor: Merge, and Version 1.0) and previewed on MAC computer using SmartCapture3 sofware and with a CCD camera (739 3 575, pixel size 11 3 11 mm) with metasystems Isis v. 5.3 software.

6-4 Results

6-4-1 Indirect immunofluorescence

IIF was performed on eight different stimulated and unstimulated normal peripheral blood samples and k562 cell line. The proliferation states of AH, AN, GO, JS, 2, 5, LU and k562 were observed and analysed by two independent observers, while the proliferation state of PB normal blood sample was analysed by one observer. Table 6-1 summarizes the number of stimulated and unstimulated samples, the total cell count, ki-67 positive and negative cells as assessed by first observer (i.e. the researcher).

Table 6-1: Number of stimulated and unstimulated samples, the total cell count, ki-67 positive and negative analysed by first observer

Samples ID	Fixation methods	Ki67 positive	Ki67 negative	Total cell count
Stimulated peripheral blood cells				
AH	M/ acetic acid	208 (74%)	73 (26%)	281
AN	M/ acetic acid	172 (81%)	41 (19%)	213
GO	M/ acetic acid	195 (84%)	38 (16%)	233
JS	M/ acetic acid	53 (24%)	167 (76%)	220
LU	M/ acetic acid	131 (74.5%)	45 (25.5%)	176
PB	M/ acetic acid	90 (79.7%)	23 (20.3%)	113
PB	4% PFA	134 (77.5%)	39 (22.5%)	173
Unstimulated peripheral blood cells				
2	M/ acetic acid	39 (11.7%)	295 (88.3%)	334
5	M/ acetic acid	51 (16.5%)	258 (83.5%)	309
PB	M/ acetic acid	10 (5.7%)	166 (94.3%)	176

Samples ID	Fixation methods	Ki67 positive	Ki67 negative	Total cell count
PB	4% PFA	14 (7.5%)	172 (92.5%)	186
Leukaemia cell line				
K562	4%PFA	200 (100%)	0 (0%)	200
K562	Methanol/acetone	135 (70%)	58 (30%)	193

6-4-1-1 Ki67 staining of unstimulated samples

From sample 2, 334 cells were counted; 88.3% of the cells were ki67 negative, while 11.7% were ki67 positive. For sample 5, the majority of cells were ki67 negative (83.5%) with 16.5% positive cells (see figure 6-1). Of 176 PB lymphocyte cells fixed with methanol/acetic acid analysed, 94.3% were ki67 negative and 5.7% were positive. Of 186 total PB lymphocyte cells fixed with 4% PFA, 170 (92.5%) were ki67 negative whereas 7.5% were positive (see figure 6-2).

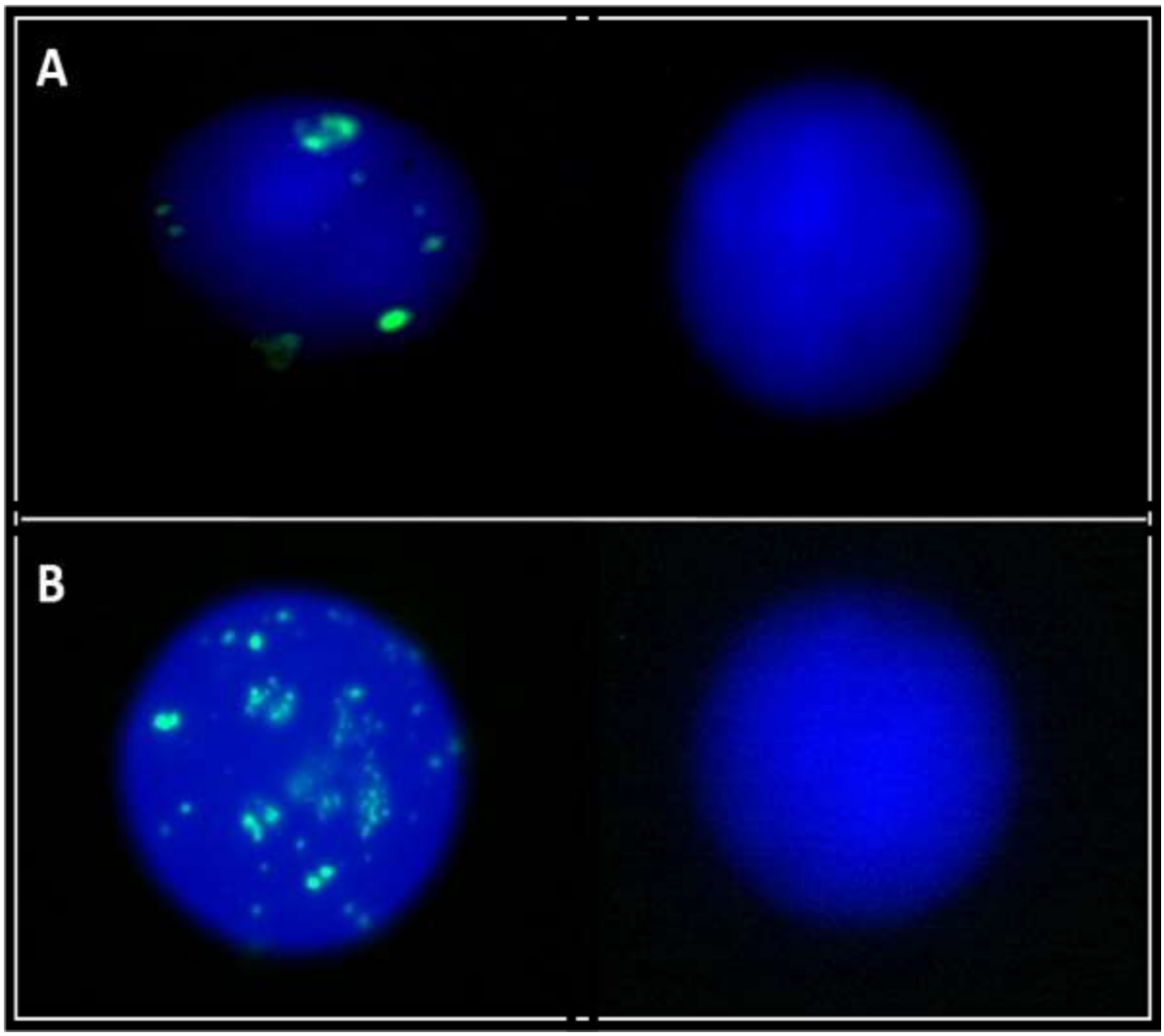

Figure 6-1: Examples of IIF images of unstimulated peripheral blood cells from normal individual samples

(A) Ki67 positive (left) and negative (right) staining of nuclei from sample 2.

(B) Ki67 positive (left) and negative (right) staining of nuclei from sample 5. Cells in both cases were prepared using standard methanol:acetic acid fixation used for the preparation of cell and chromosome suspensions. Nuclei are counterstained in DAPI (in blue).

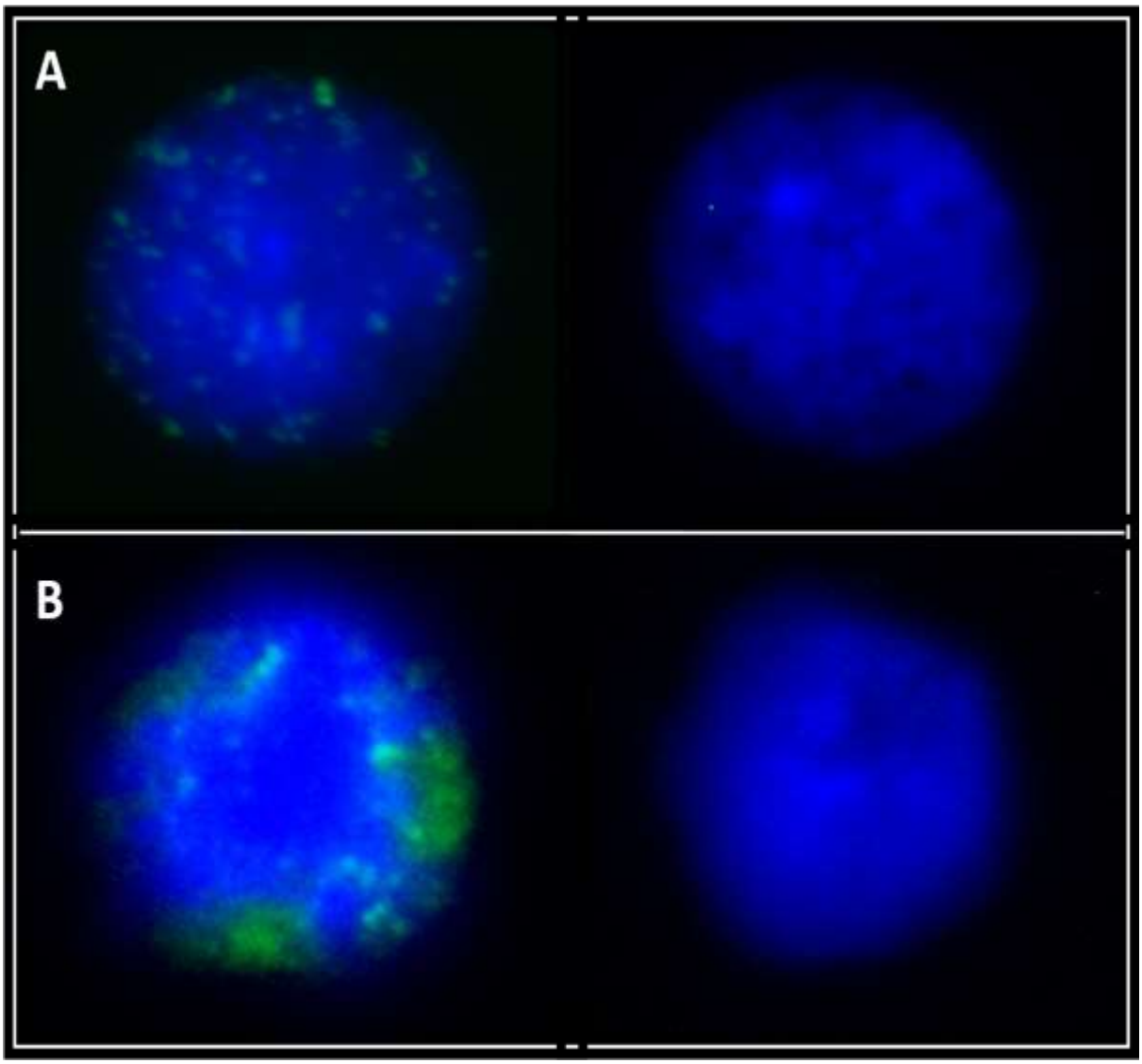

Figure 6-2: Examples of IIF images of unstimulated peripheral blood cells from normal individual samples using different fixation methods

(A) Ki67 positive (left) and negative (right) staining of nuclei of PB normal blood cells fixed with methanol/acetic acid.

(B) Ki67 positive (left) and negative (right) staining of nuclei of PB normal blood cells fixed with 4% PFA. Nuclei are counterstained in DAPI (in blue).

6-4-1-2 Ki67 staining of K562 cell line

Two-hundred k562 cells fixed with 4% paraformaldehyde were analysed, and 100% of them were found to be proliferating cells (i.e. ki67 positive). 193 k562 cells fixed with methanol/acetone were counted, and positive staining of ki67 was observed in 70% of them, while 30% showed negative staining (see figures 6-3 and 6-4).

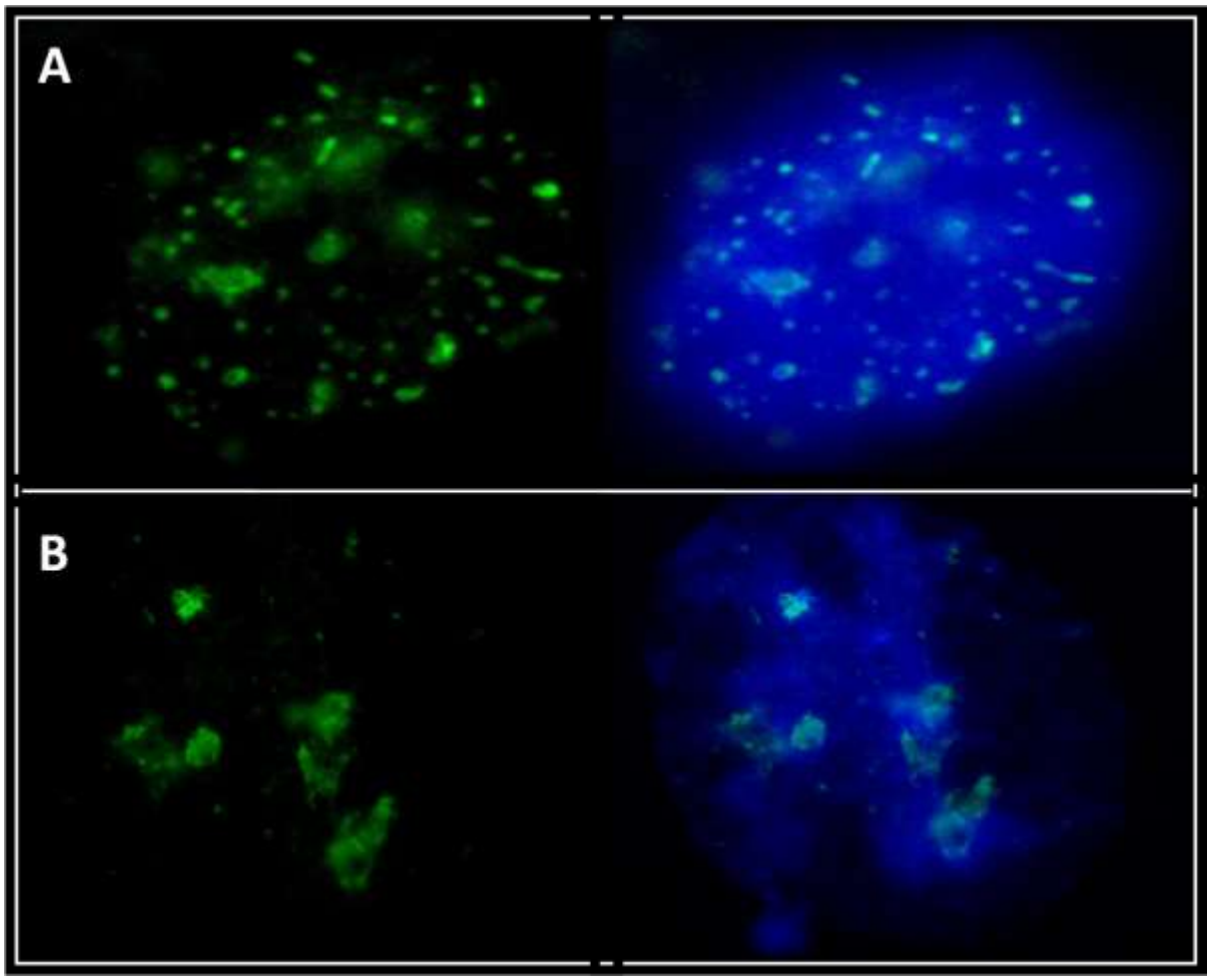

Figure 6-3: Examples of IIF performed on k562 cell line fixed with 4% PFA

(A) Shows positive staining of ki67 antibody in green (FITC) and also the localization of ki67 antigen during G1 (type I) phase of cell cycle.

(B) Shows positive staining of ki67 in green (FITC) and also the localization of ki67 antigen during late G1 (type II) phase of the cell cycle. Images on the left show antibody staining in green (FITC). Nuclei are counterstained with DAPI (in blue) and these are visible in the merge images on the right.

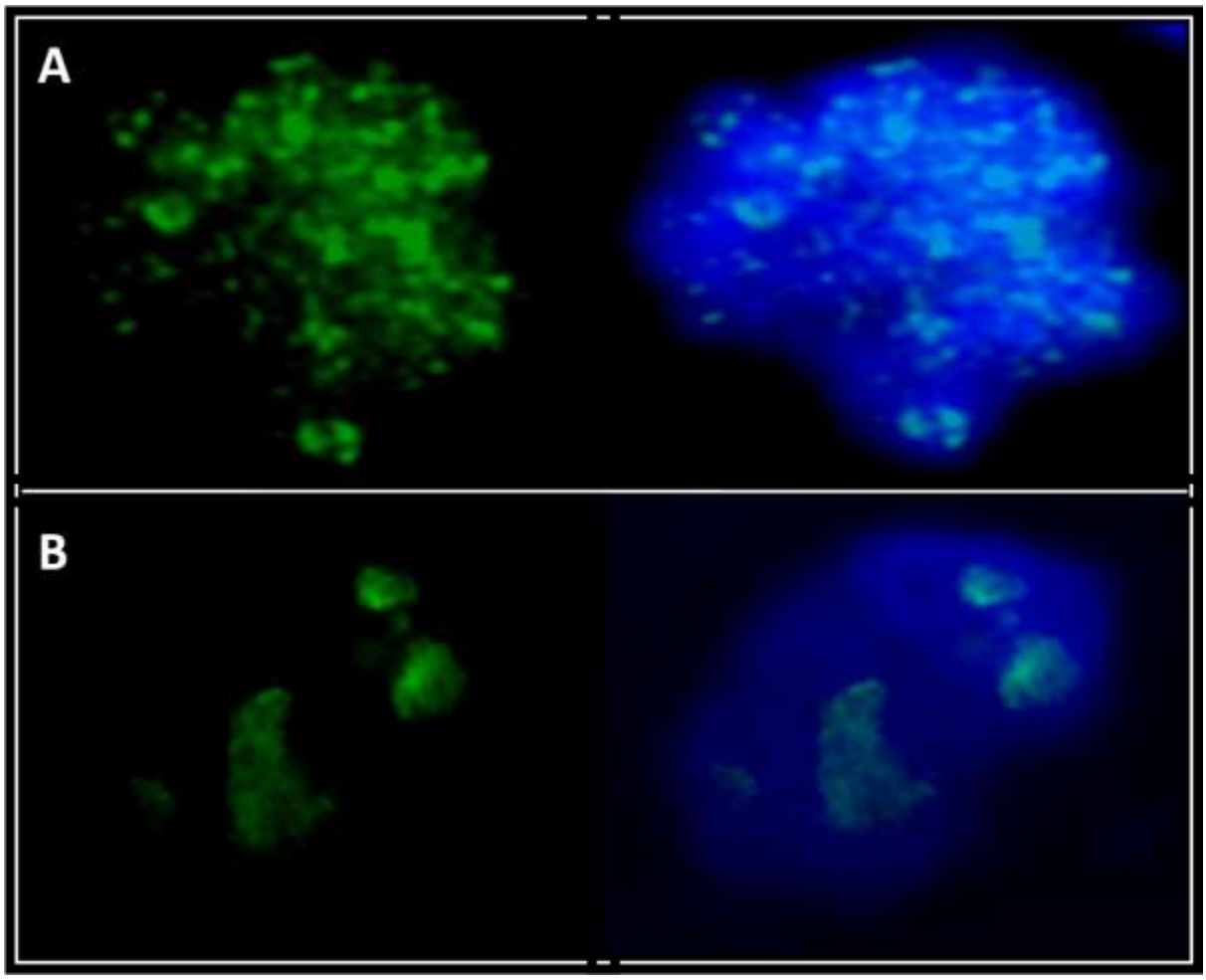

Figure 6-4: Examples of IIF performed on k562 cell line fixed with methanol/acetone

(A) Shows positive staining of ki67 antibody in green (FITC) and also the localization of ki67 antigen during G1 (type I) phase of cell cycle.

(B) Shows positive staining of ki67 in green (FITC) and the localization of ki67 during late G1 (type II) phase of the cell cycle. Images on the left show antibody staining in green (FITC). Nuclei are counterstained with DAPI (in blue) and these are visible in the merge images on the right.

6-4-1-3 Ki67 staining of stimulated samples

281 interphase cells were analysed for AH sample. The percentage of ki67 positive cells was 74%, while 26% were negative (see figure 6-5). 213 cells of AN sample were counted and analysed, and ki67 positive staining was observed in 81% of cells, with 19% negative (see figure 6-6). 233 interphase cells were counted from GO sample, of which 84% were ki67 positive and 16% negative (figure 6-7). Of 220 cells of JS samples, 24% were ki67 positive and 76% were negative (see figure 6-8). Of 176 cells from the LU sample 74.5% were proliferating cells (i.e. ki67 positive) while 25.5% were non-proliferating (i.e. ki67

negative) (see figure 6-9). 113 cells of PB sample fixed with methanol/acetic acid were analysed, and 79.7% of the cells were proliferating cells (ki67 positive) whereas 20.3% of cells were non-proliferating (ki67 negative) (see figure 6-10). The total cells counted for the PB sample fixed with 4% paraformaldehyde was 173; the percentage of cells with positive ki67 staining was 77.5% while 22.5% were negative (see figure 6.11). Various patterns of ki67 antigen were observed in the proliferating cells of all samples, including type I pattern typical of G1 phase of the cell cycle, type 2 typical of late G1 and S phase of the cell cycle and around chromosomes in M phase of the cell cycle.

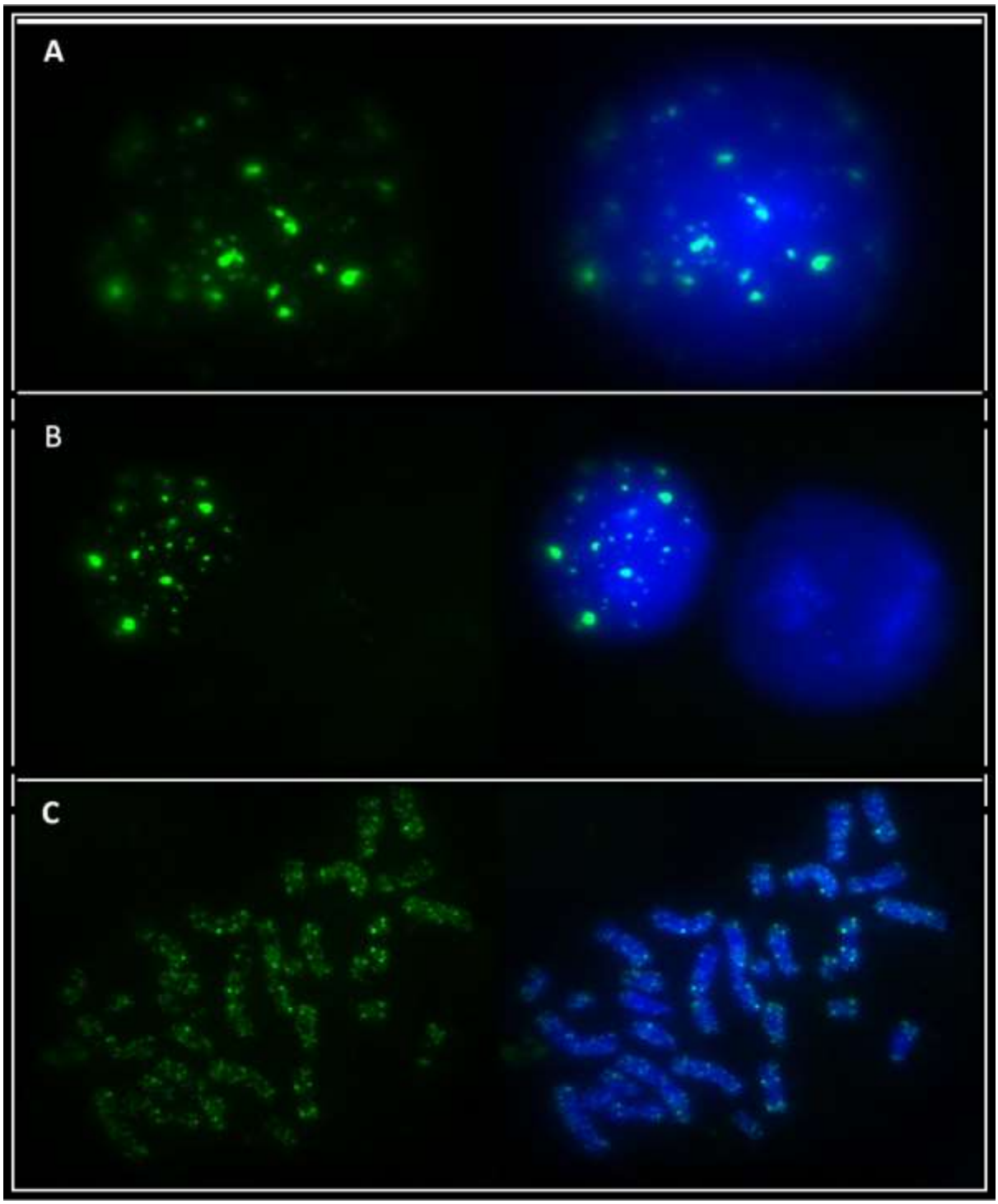

Figure 6-5: Examples of IIF performed on methanol/acetic acid fixed stimulated peripheral blood cells from normal individual (AH sample)

A and B show positive staining of ki67 antibody in green (FITC) and also the localization of ki67 antigen during G1 (type I) phase of cell cycle. (C) Shows positive staining of ki67 and the localization of ki67 during M phase of the cell cycle. Images on the left show antibody staining in green (FITC). Nuclei are counterstained with DAPI (in blue) and these are visible in the merge images on the right.

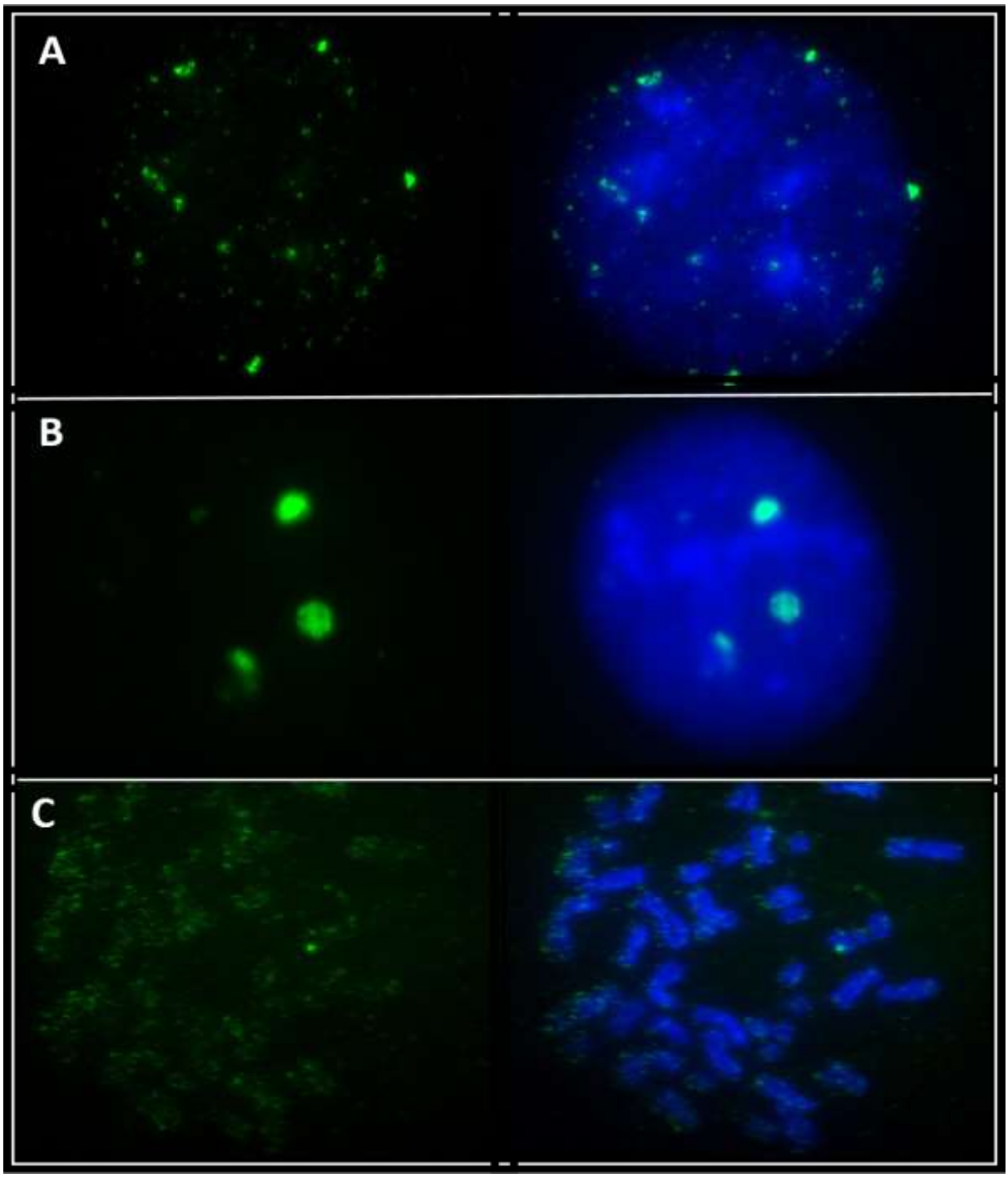

Figure 6-6: Examples of IIF performed on methanol/acetic acid fixed stimulated peripheral blood cells from normal individual (AN sample)

(A) Shows positive staining of ki67 antibody in green (FITC) and also the localization of ki67 antigen during G1 (type I) phase of cell cycle.

(B) Shows positive staining of ki67 antibody in green (FITC) and the localization of ki67 during late G1 (type II) phase of the cell cycle.

(C) Shows positive staining of ki67 and the localization of ki67 during M phase of the cell cycle. Images on the left show antibody staining in green

(FITC). Nuclei are counterstained with DAPI (in blue) and these are visible in the merge images on the right.

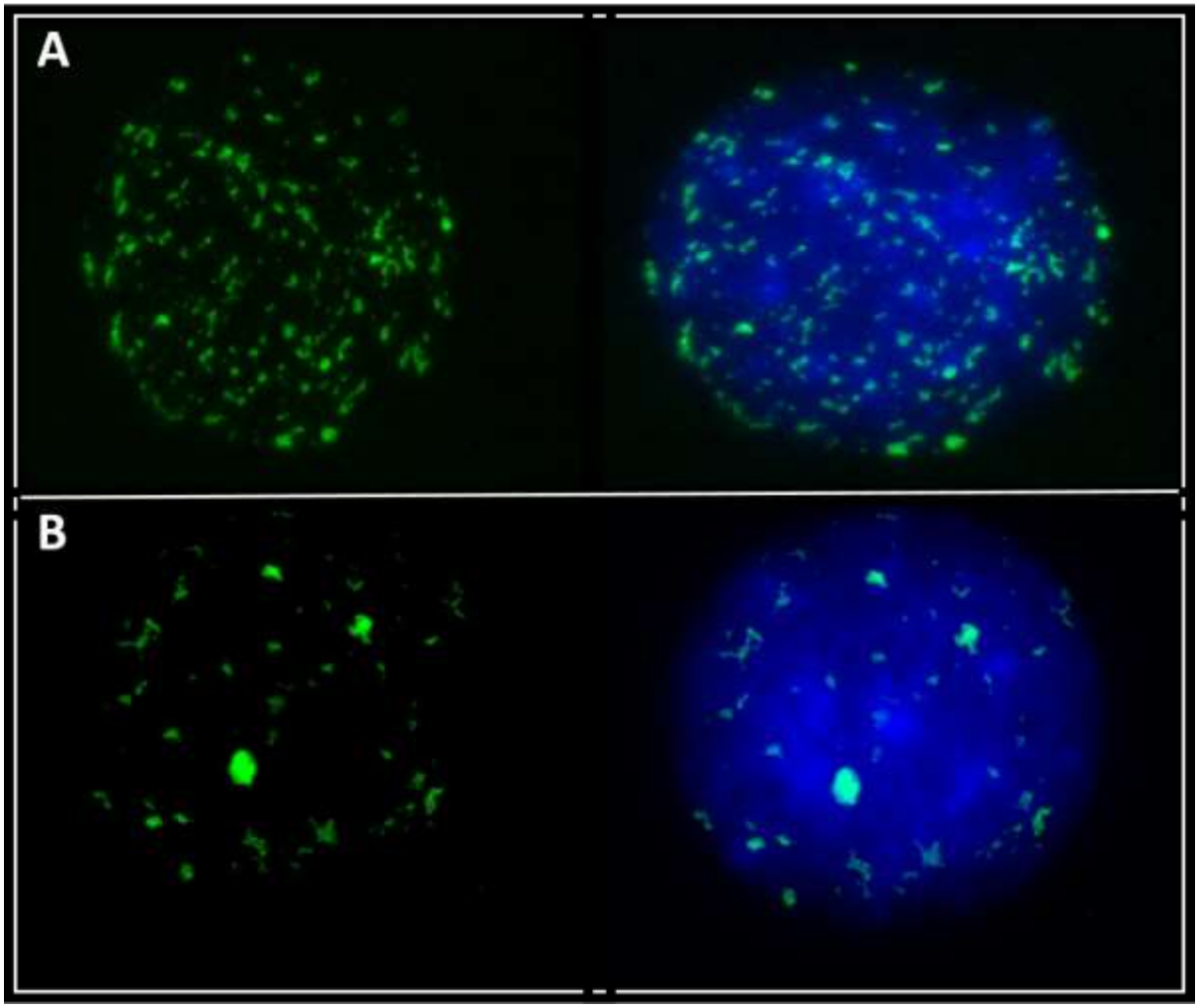

Figure 6-7: Examples of IIF performed on methanol/acetic acid fixed stimulated peripheral blood cells from normal individual (GO sample)

(A) Shows positive staining of ki67 antibody in green (FITC) and also the localization of ki67 antigen during G1 (type I) phase of cell cycle.

(B) Shows positive staining of ki67 antibody in green (FITC) and the localization of ki67 during late G1 (type II) phase of the cell cycle. Images on the left show antibody staining in green (FITC). Nuclei are counterstained with DAPI (in blue) and these are visible in the merge images on the right.

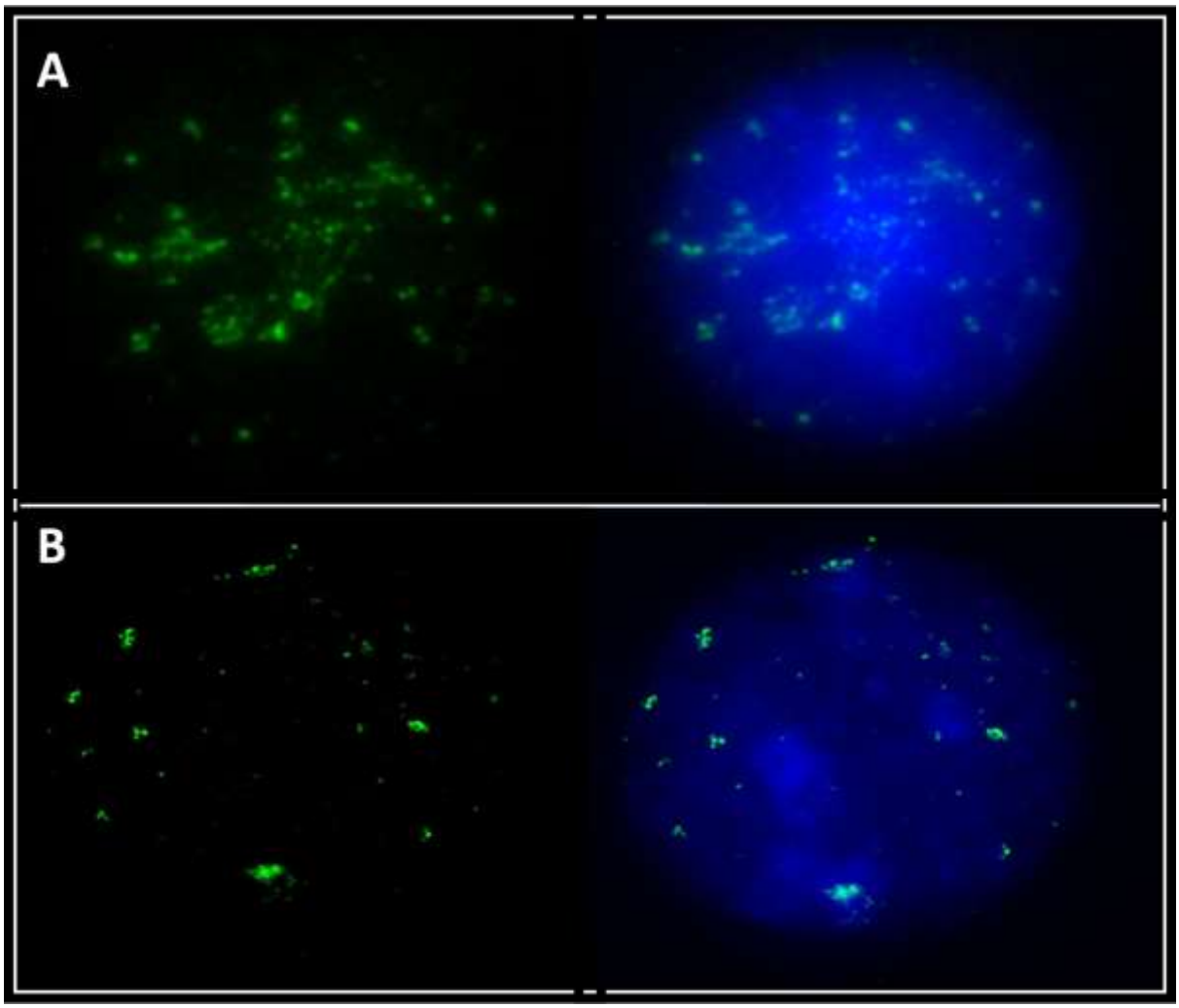

Figure 6-8: Examples of IIF performed on methanol/acetic acid fixed stimulated peripheral blood cells from normal individual (JS sample)

(A) Shows positive staining of ki67 antibody in green (FITC) and also the localization of ki67 antigen during G1 (type I) phase of cell cycle.

(B) Shows positive staining of ki67 antibody in green (FITC) and the localization of ki67 during late G1 (type II) phase of the cell cycle. Images on the left show antibody staining in green (FITC). Nuclei are counterstained with DAPI (in blue) and these are visible in the merge images on the right.

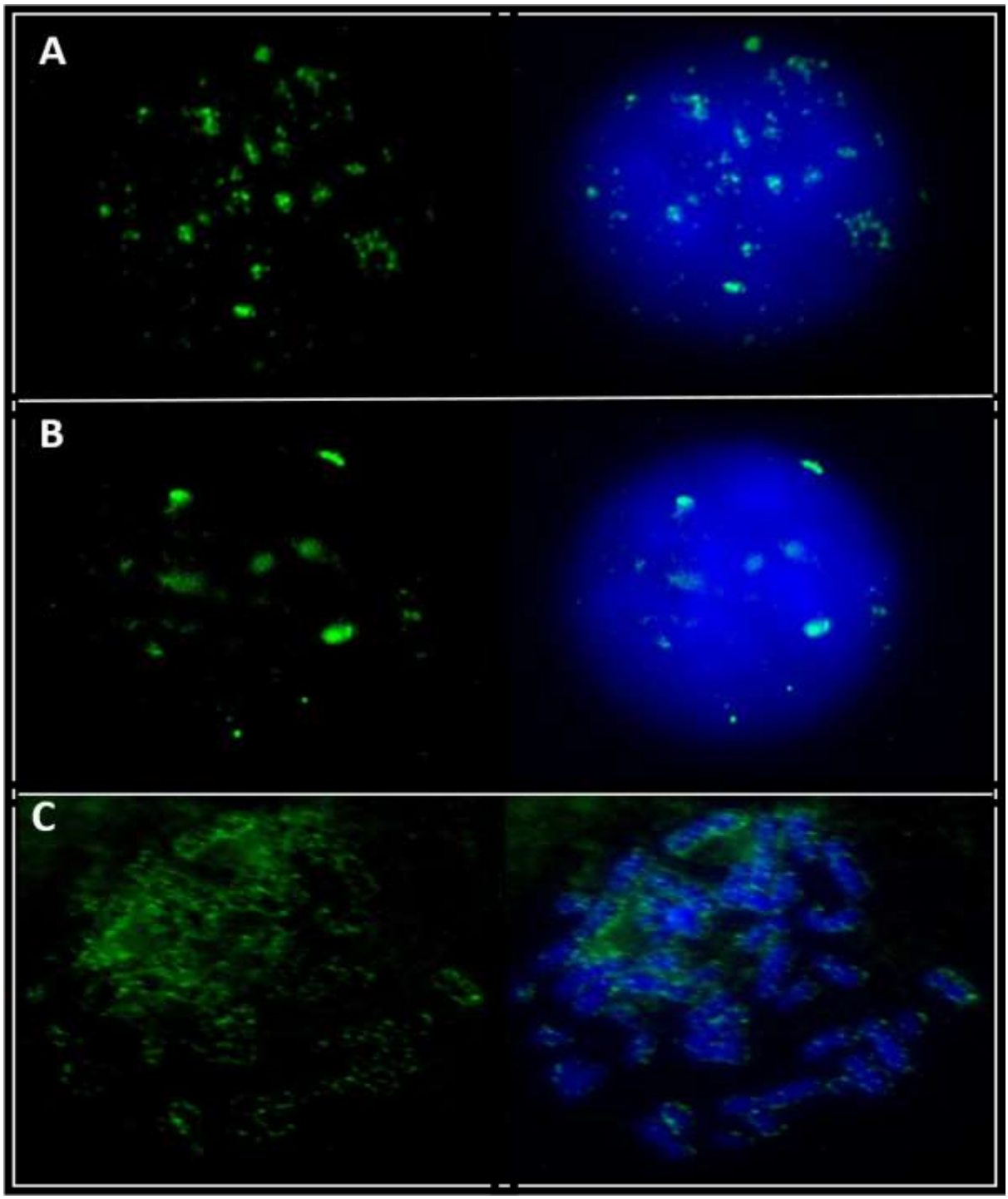

Figure 6-9: Examples of IIF performed on methanol/acetic acid fixed stimulated peripheral blood cells from normal individual (LU sample)

(A) Shows positive staining of ki67 antibody in green (FITC) and also the localization of ki67 antigen during G1 (type I) phase of cell cycle.

(B) Shows positive staining of ki67 antibody in green (FITC) and the localization of ki67 during late G1 (type II) phase of the cell cycle.

(C) Shows positive staining of ki67 and the localization of ki67 during M phase of the cell cycle. Images on the left show antibody staining in green

(FITC). Nuclei are counterstained with DAPI (in blue) and these are visible in the merge images on the right.

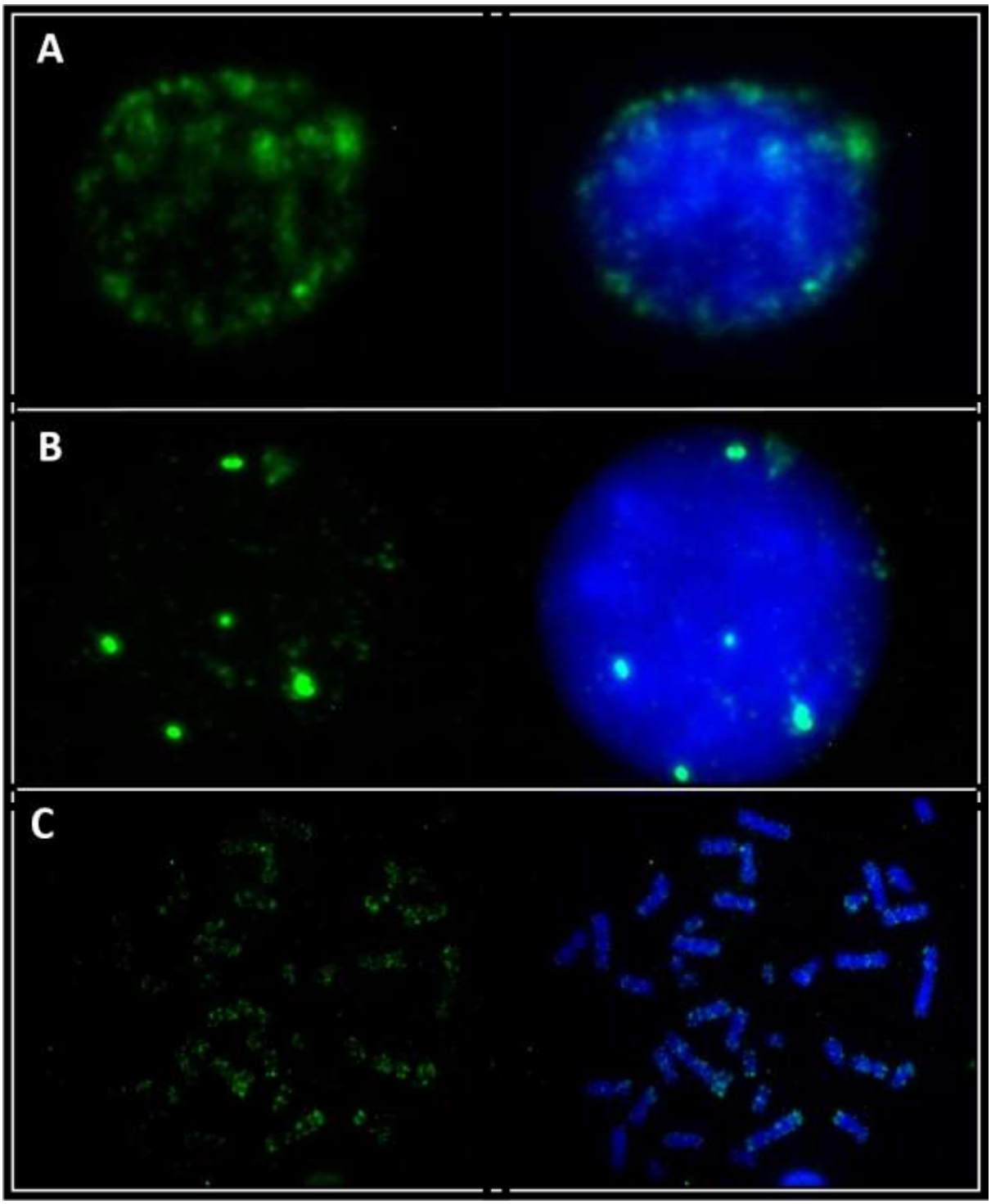

Figure 6-10: Examples of IIF performed on methanol/acetic acid fixed stimulated peripheral blood cells from normal individual (PB sample)

(A) Shows positive staining of ki67 antibody in green (FITC) and also the localization of ki67 antigen during G1 (type I) phase of cell cycle.

(B) Shows positive staining of ki67 antibody in green (FITC) and the localization of ki67 during late G1 (type II) phase of the cell cycle.

(C) Shows positive staining of ki67 and the localization of ki67 during M phase of the cell cycle. Images on the left show antibody staining in green (FITC). Nuclei are counterstained with DAPI (in blue) and these are visible in the merge images on the right.

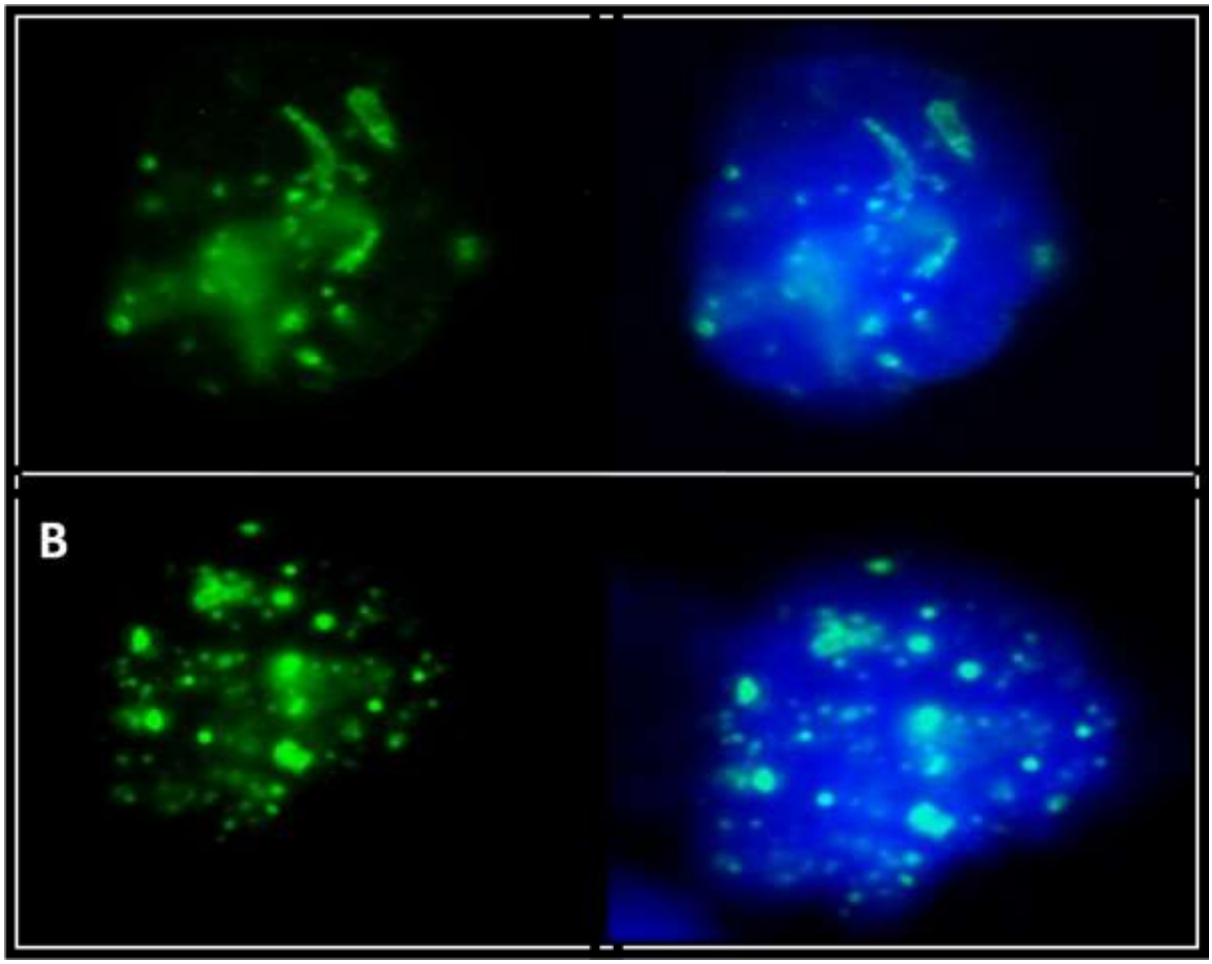

Figure 6-11: Examples of IIF performed on 4% PFA fixed stimulated peripheral blood cells from normal individual (PB sample

(A) Shows positive staining of ki67 antibody in green (FITC) and also the localization of ki67 antigen during G1 (type I) phase of cell cycle.

(B) Shows positive staining of ki67 in green (FITC) and the localization of ki67 during late G1 (type II) phase of the cell cycle. Images on the left show antibody staining in green (FITC). Nuclei are counterstained with DAPI (in blue) and these are visible in the merge images on the right.

6-4-1-4 Comparison of the evaluation of the two observers

A summary of number of samples and the results of ki67 analysed by second observer are shown in table 6-2. The percentage of ki67 positive of the stimulated normal blood cells analysed by the first observer was 74% (AH), 81% (AN), 84% (GO), 24% (JS) and 74.5%

(LU), whereas the percentage of ki67 positive observed by the second observer was 86% (AH), 77% (AN), 88% (GO), 20% (JS) and 81% (LU) (see figure 6-12). The number of proliferating cells in JS stimulated sample was lower than non-proliferating cells among the other stimulated samples (AH, AN, GO and LU) both in first and second observation. The percentages of unstimulated proliferating cells in samples 2 and 5 observed by the first observer were 11.7% and 16.5% respectively, while 18% and 15% of the unstimulated cells in samples 2 and 5 were proliferating cells investigated by the second observer. A hundred percent of k562 cells fixed with 4% paraformaldehyde were proliferating cells, as assessed by both the first and second observers. 70% of k562 cells fixed with methanol/acetone analysed by the first observer were proliferating cells, whereas 69% of proliferating cells were observed by the second observer.

Table 6-2: Proportion of ki67 positive and negative cells in unstimulated and stimulated samples analyzed by second observer

Cell sample	Total cell count	Ki67 positive	% of Ki67 positive	Ki67 negative	% of Ki67 negative
Unstimulated cells					
Sample 2	307	56	18%	251	82%
Sample 5	389	59	15%	330	85%
Stimulated cells					
AH	287	246	86%	41	14%
AN	268	206	77%	62	23%
GO	223	198	88%	25	12%
JS	223	45	20%	178	80%
LU	197	160	81%	37	19%
Leukemic cells					
K562+4%PFA	203	203	100%	0	0%
K562+Methanol/Acetone	202	140	69%	62	31%

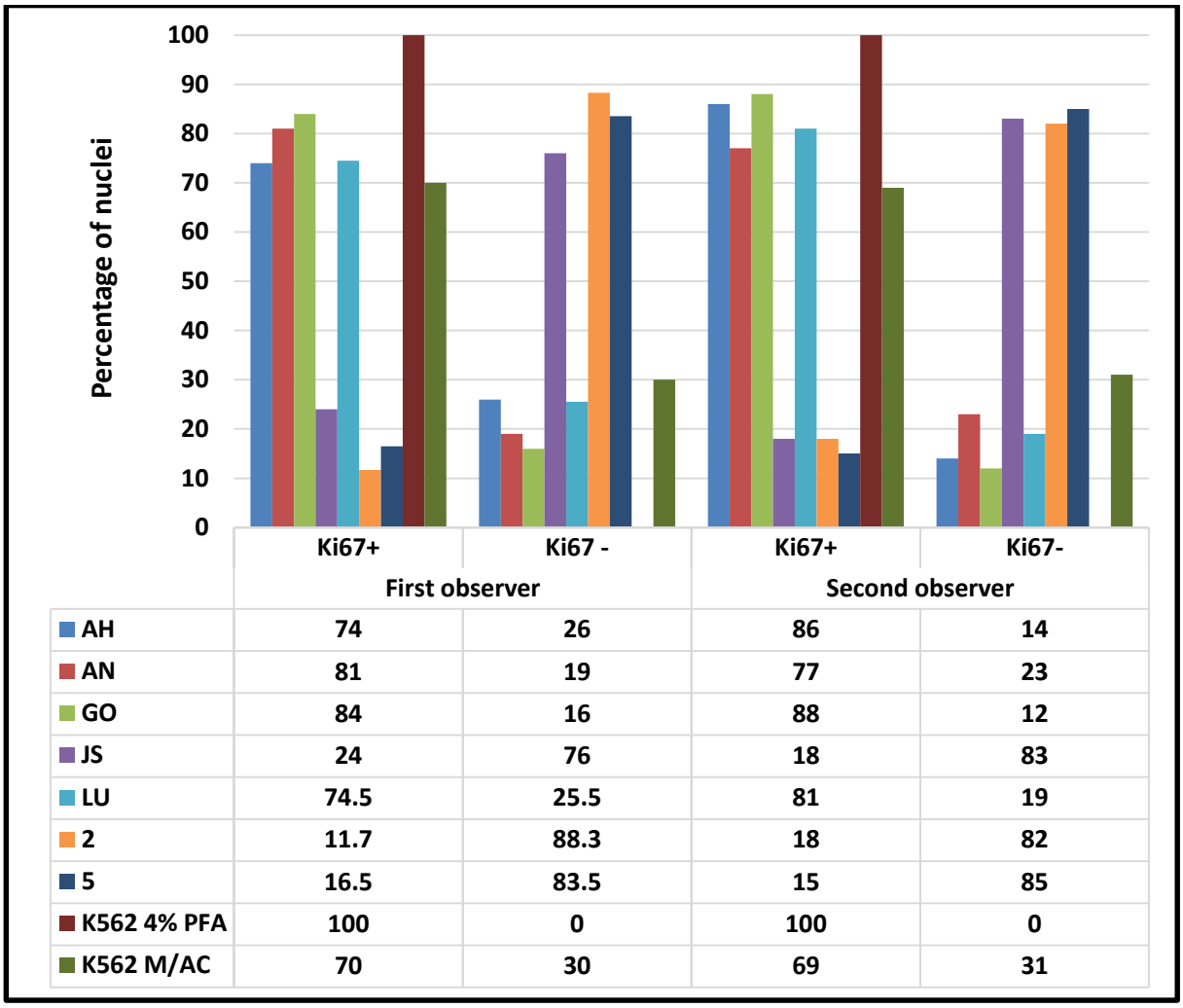

	First observer		Second observer	
	Ki67+	Ki67 -	Ki67+	Ki67-
AH	74	26	86	14
AN	81	19	77	23
GO	84	16	88	12
JS	24	76	18	83
LU	74.5	25.5	81	19
2	11.7	88.3	18	82
5	16.5	83.5	15	85
K562 4% PFA	100	0	100	0
K562 M/AC	70	30	69	31

Figure 6-12: Graph shows the percentage of ki67 positive versus ki67 negative in stimulated normal peripheral blood samples, unstimulated normal peripheral blood samples and K-562 cell line

The X axis represents the percentage of Ki-67 positive nuclei and the Ki-67 negative nuclei evaluated by two observers. The Y axis refers to the percentage of cells analysed.

6-4-2 Immuno-FISH results

Immuno-FISH was performed on archival cells and chromosome suspensions from five different patient samples and three cell lines (normal and leukaemia cell lines) using specific probes for regions of interest and ki67 proliferation marker to determine the proliferation status of cells. The proliferative state of cells in the cell lines CRL-2630, CRL2632 and K562, and patient samples 020944, 010340, 0132108, 26, and 27 was analysed and evaluated by two independent observers. Table 6-3 summarizes the percentage of major abnormalities detected in five patient samples and three cell lines and the percentage of ki67 positive and ki67 negative cells in both patient samples and cell lines analysed by first observers.

6-4-2-1 Immuno-FISH in lymphoma and leukaemia cell lines

Approximately 200 images were taken for each cell line, two copies of chromosome 8 were detected and cells were 100% proliferating in both CRL-2632 (Pfeiffer) and CRL-2630 (Farage) cell lines (see figures 6-13 and 6-14). In the K562 cell line, *Nup98* probe was used to detect the presence of chromosome 11; all cells were found to have two copies of *Nup98* gene, and 94.25% of cells were proliferating cells while 5.75% of the cells were non-proliferating cells (see figure 6-15). Moreover, two copies of 7q36.1 and/or 4q35.1 regions were observed in CRL-2630 cell line and the proportion of proliferating cells were 93% and 94.6% respectively (see figure 6-16). Different patterns of ki67 staining were observed in the cell lines including the typical patterns associated with G1, G2, S and M phase of the cell cycle.

6-4-2-2 Proliferation status of patient samples

Different cytogenetic abnormalities were found in the five different patient samples: nullisomy 7q36.1, monosomy 4q35.1, trisomy 8 and tetrasomy 8. 210 interphase cells were analysed in patient no. L020944; tetrasomy 8 was observed in 79% of the cells. Of these, 65.57% were non-proliferating while ki67 staining was positive in 34.43% of cells (see figure 6-17). In patient no. H010340, trisomy 8 was identified in 69.5% of the 200 interphase cells scored, 70% of which were positive for the ki67 proliferation marker, while 30% were negative for staining with ki67 antibody (see figure 6-18). 166 cells were also analysed for patient no. L0132108, and trisomy 8 was found in 35% of the cells, 79.3% of which were ki67 positive and the remaining 20.7% of which were negative (see figure 6-19). The proliferation status of patient no. 26 cells carrying nullisomy 7q36.1 and patient no. 27 harbouring monosomy 4q35.1 was determined; in the former, nullisomy 7q36.1 region was observed in 21% of cells without inv(16) and in 79% of cells with inv(16). The majority of cells (88%) including both clones was ki67 negative with only 12% of cells found to have positive staining of ki67 proliferation marker (see figure 6-20). Additionally, monosomy 4q35.1 region was detected in 89% of cells in patient 27. 7% of cells without inv(16) were found to have monosomy 4q35.1, whereas 93% of cells harbouring the inv(16) rearrangement were with monosomy of the 4q35.1 region. The percentage of ki67 negative cells with and without inv(16) was 87%, while 13% of cells were found to be negative for ki67 antibody (see figure 6-21).

Table 6-3: Type and percentage of major abnormalities detecting in five patient samples and three cell lines and the percentage of ki67 positive and ki67 negative analysed by first observer

Samples	Chromosome region	%Nullisomy	%Monosomy	% Disomy	% Trisomy	% Tetrasomy	% ki67 + in abnormal cells	% ki67 - in abnormal cells
CRL-2630	Chromosome 8 centromere	-	-	100	-	-	100	0
CRL-2630	7q36.1	-	-	100	-	-	93	7
CRL-2630	4q35.1	-	-	100	-	-	94.6	5.4
CRL-2632	Chromosome 8 centromere	-	-	100	-	-	100	0
K562	11p15	-	-	100	-	-	94.5	5.5
020944	Chromosome 8 centromere	-	-	9	-	79	34. 3	65. 7
010340	Chromosome 8 centromere	-	-	18.5	69.5	-	70	30
0132108	Chromosome 8 centromere	-	-	62	35	-	79.3	20.07
26	7q36.1	94.5	-	4.5	-	-	12	88
27	4q35.1	-	89	6.5	-	-	13	87

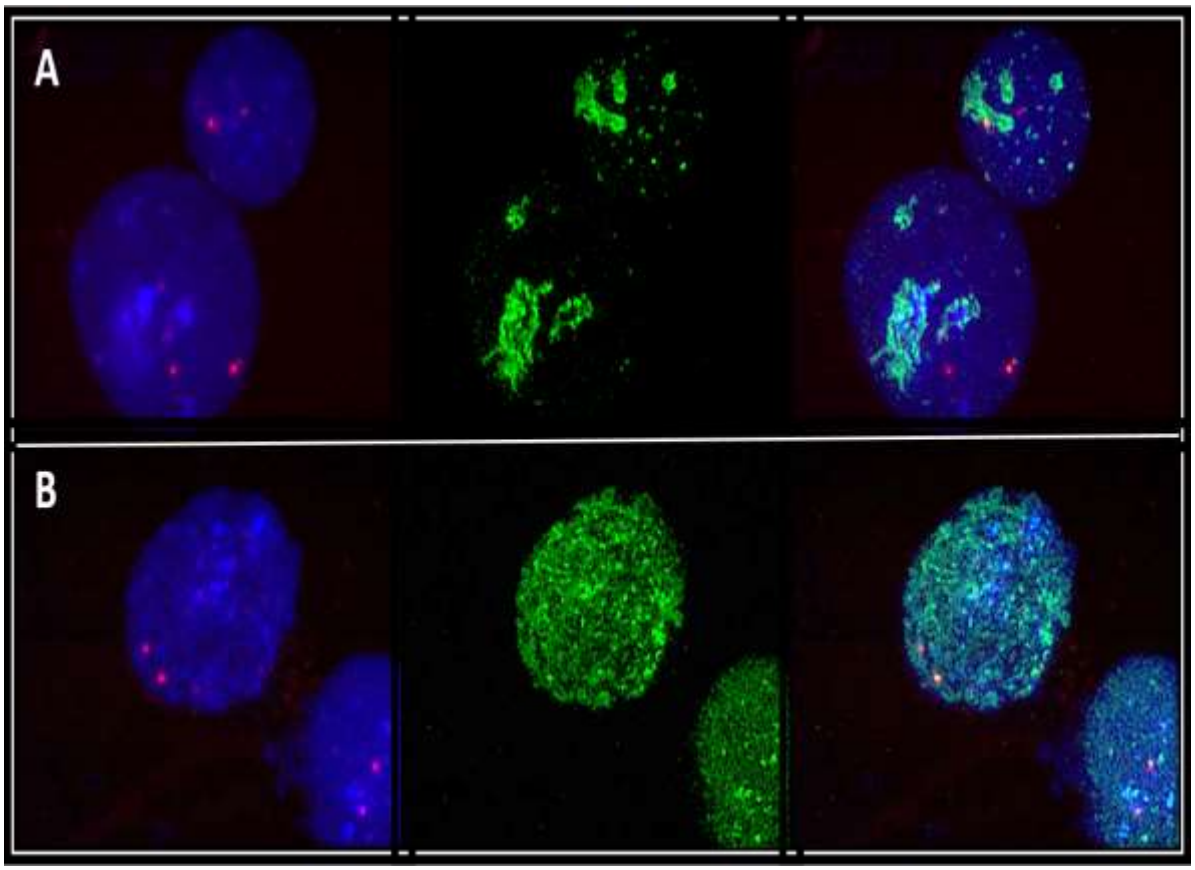

Figure 6-13: Examples of Immuno-FISH performed on cells from Pfeiffer cell line

(A) Shows two hybridisation signals of centromeric 8 in red (Cy3), ki67 positive staining for the both nuclei and the localization of ki67 antigen during late G1 (type II) phase of the cell cycle.

(B) Shows two hybridisation signals of centromeric in red (Cy3), ki67 positive staining for the both nuclei and the localization of ki67 antigen during G1 (type I) phase of the cell cycle. Nuclei are counterstained with DAPI (in blue).

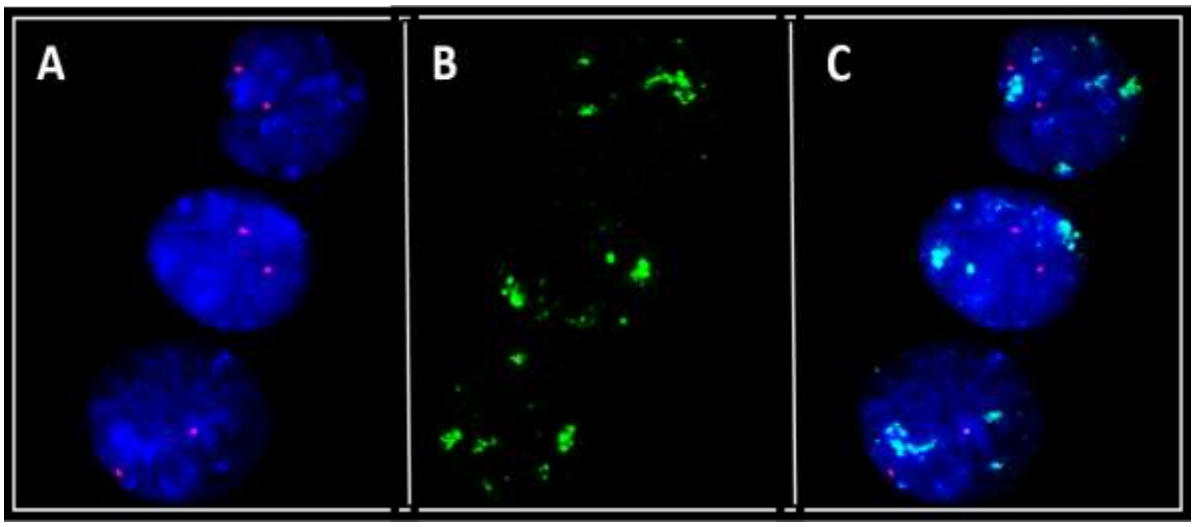

Figure 6-14: Example of Immuno-FISH performed on cells from CRL-2630 cell line

(A) Shows two hybridisation signals of centomoeric 8 in red (Cy3).

(B) Shows the ki67 positive staining visible in green (FITC) and the localization of ki67 antibody during late G1 (type II) phase of the cell cycle.

(C) Shows merge images. Nuclei are counterstained with DAPI (in blue).

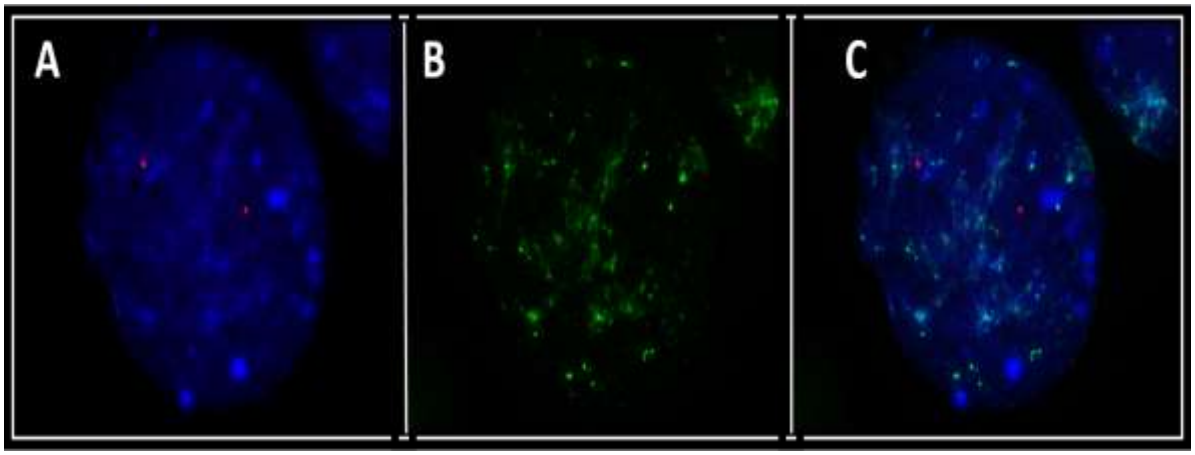

Figure 6-15: Example of Immuno-FISH performed on cells from k562 cell line

(A) Shows nucleus with two hybridisation signals of Nup98 probe in red (Cy3).

(B) pki67 positive staining visible in green (FITC).

(C) Shows merge image as it was taken under the fluorescence microscope. Nucleus is counterstained with DAPI (in blue).

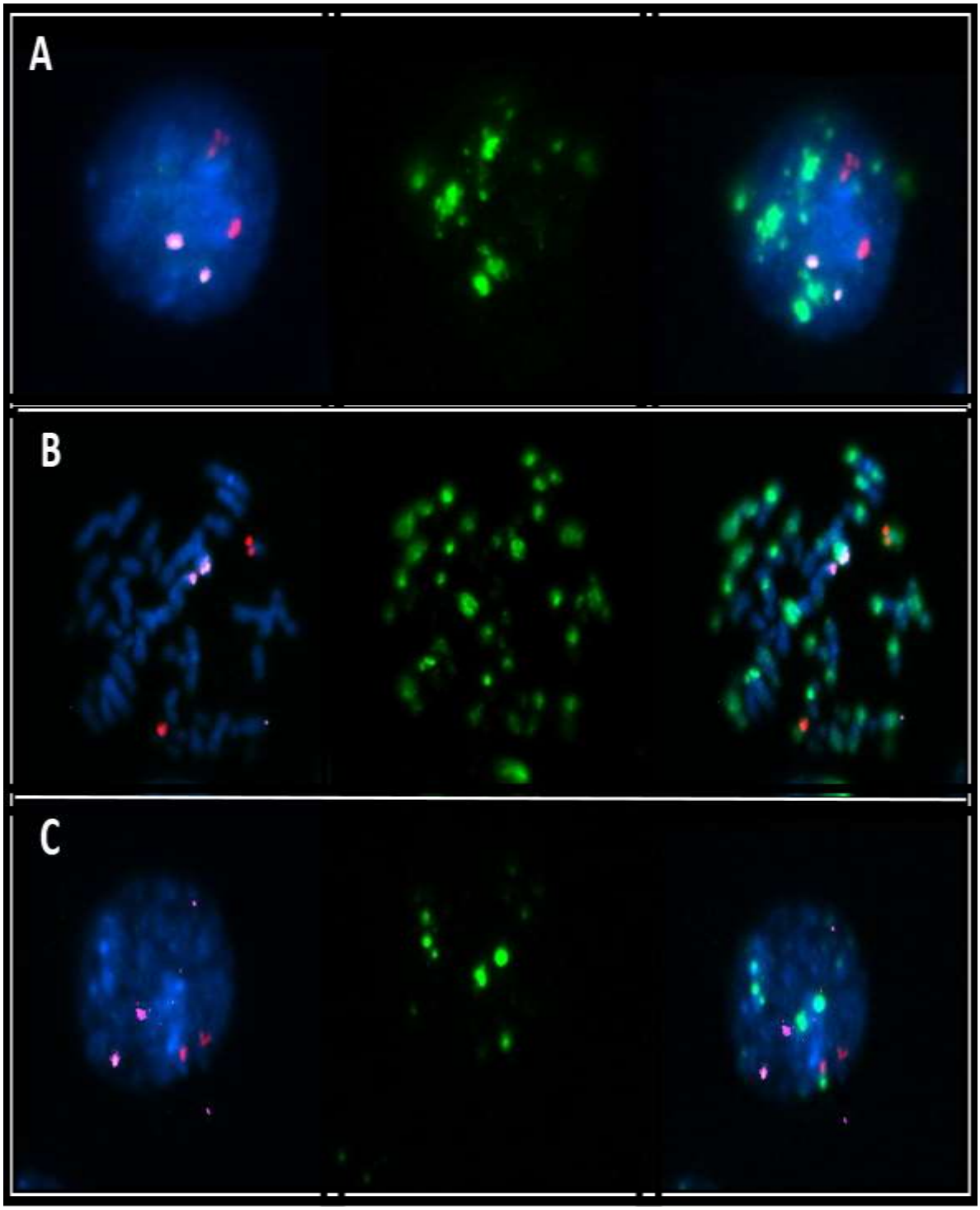

Figure 6-16: Examples of Immuno-FISH performed on cells from CRL-2630 cell line

(A) chromosome 16 hybridisation signals shown in red (Cy3), RP11-504N9 probe signals at 7q36.1 shown in pink (Cy5) and the localization of ki67 antigen in both nuclei during late G1 (type II) phase of the cell cycle (B and C) metaphase chromosome and interphase cell show chromosome 16 hybridisation signals in red (Cy3), RP11-184A23 probe signals at 4q35.1 shown in pink (Cy5) and the localization of ki67 antigen in both during late G1 (type II) and M phase of the cell cycle. The blue is the DAPI staining.

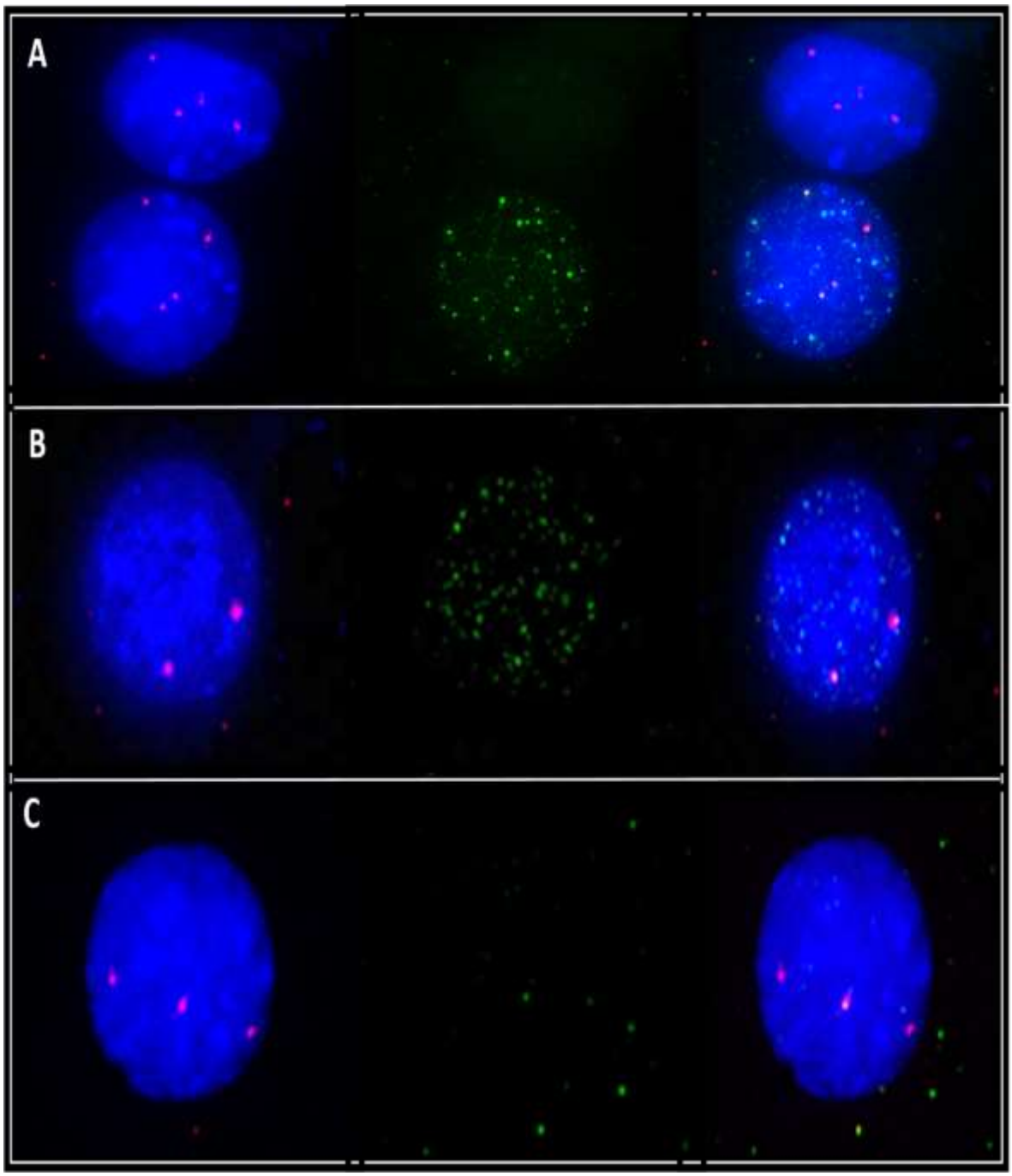

Figure 6-17: Examples of Immuno-FISH performed on cells from 020944 patient

(A) Anti-ki67 is shown in green (FITC), whereas the red signals correspond to the tetrasomy 8.

(B) The two FISH signals in the proliferating cell (ki67 positive) corresponding to the normal chromosome 8. Anti-Ki67 is shown in green (FITC).

(C) Shows non-proliferating nucleus with three FISH signals that corresponding to the trisomy 8. Anti-ki67 is shown in green (FITC). Nuclei are counterstained in DAPI (blue colour).

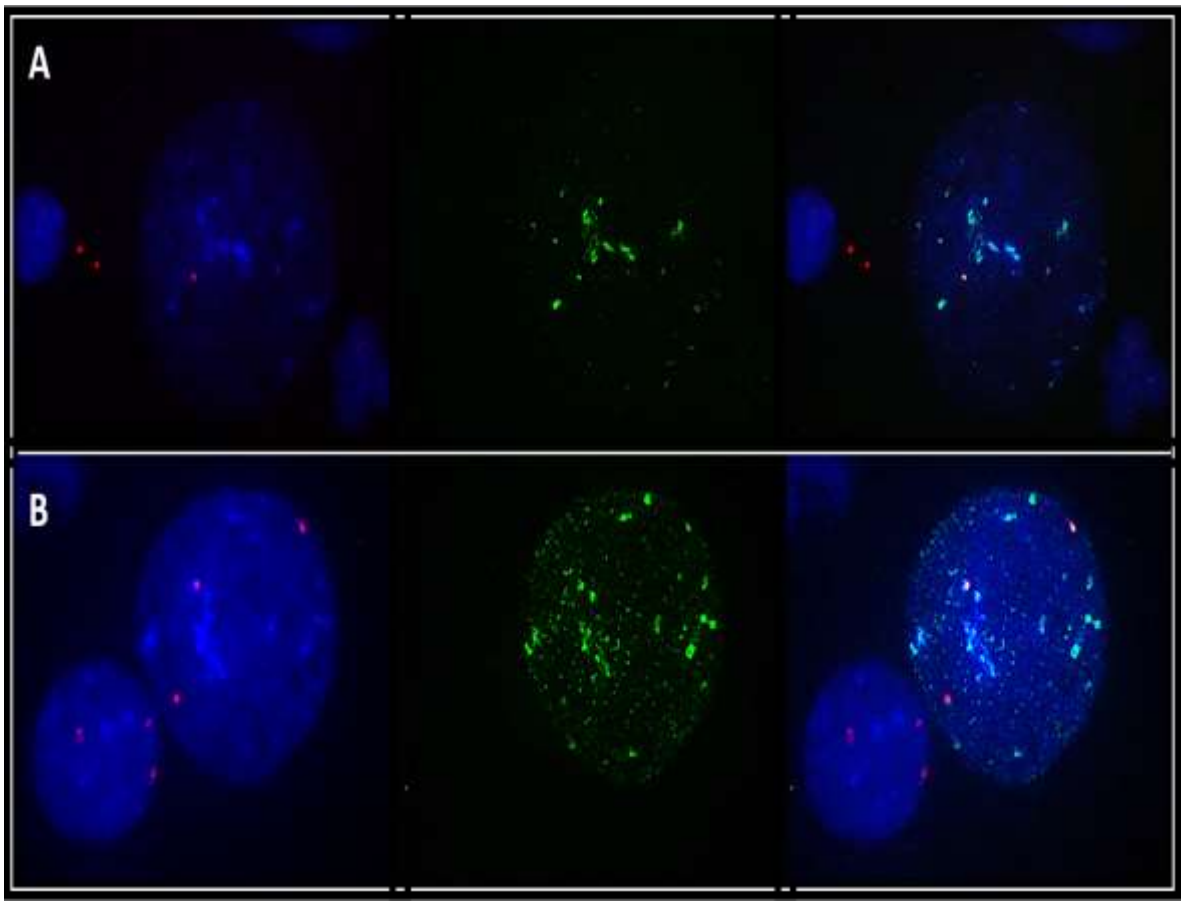

Figure 6-18: Examples of Immuno-FISH performed on cells from 010340 patient

(A) The hybridisation signals are shown in red (Cy3) corresponding to the normal chromosome 8 in proliferating cell, anti-ki67 is show in green (FITC).

(B) Shows two nuclei with trisomy 8, one is ki67 positive whereas, the another one is ki67 negative. Nuclei are counterstained in DAPI (blue colour).

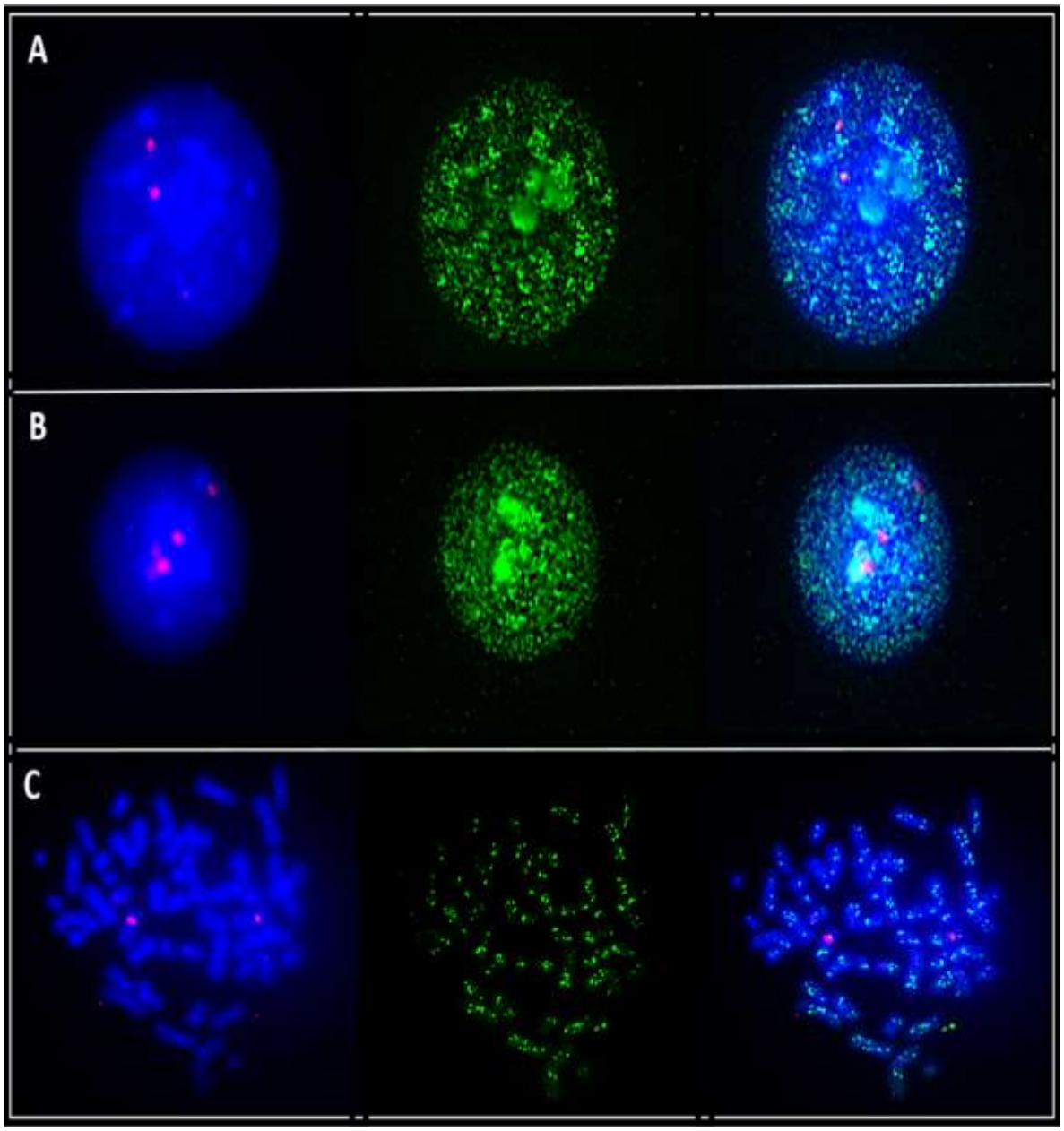

Figure 6-19: Examples of Immuno-FISH performed on cells from 032108 patient

(A) Hybridisation signals shown in red (Cy3) corresponding to normal chromosome 8 in proliferating nucleus.

(B) Trisomy 8 shown in the proliferating nucleus, the red (Cy3) signal corresponding to the centromeric 8 probe. Anti-pki67 is shown in green (FITC).

(C) Metaphase shows normal chromosome 8 with two red signals. The metaphase is ki67 positive. Nuclei are counterstained in DAPI (blue colour).

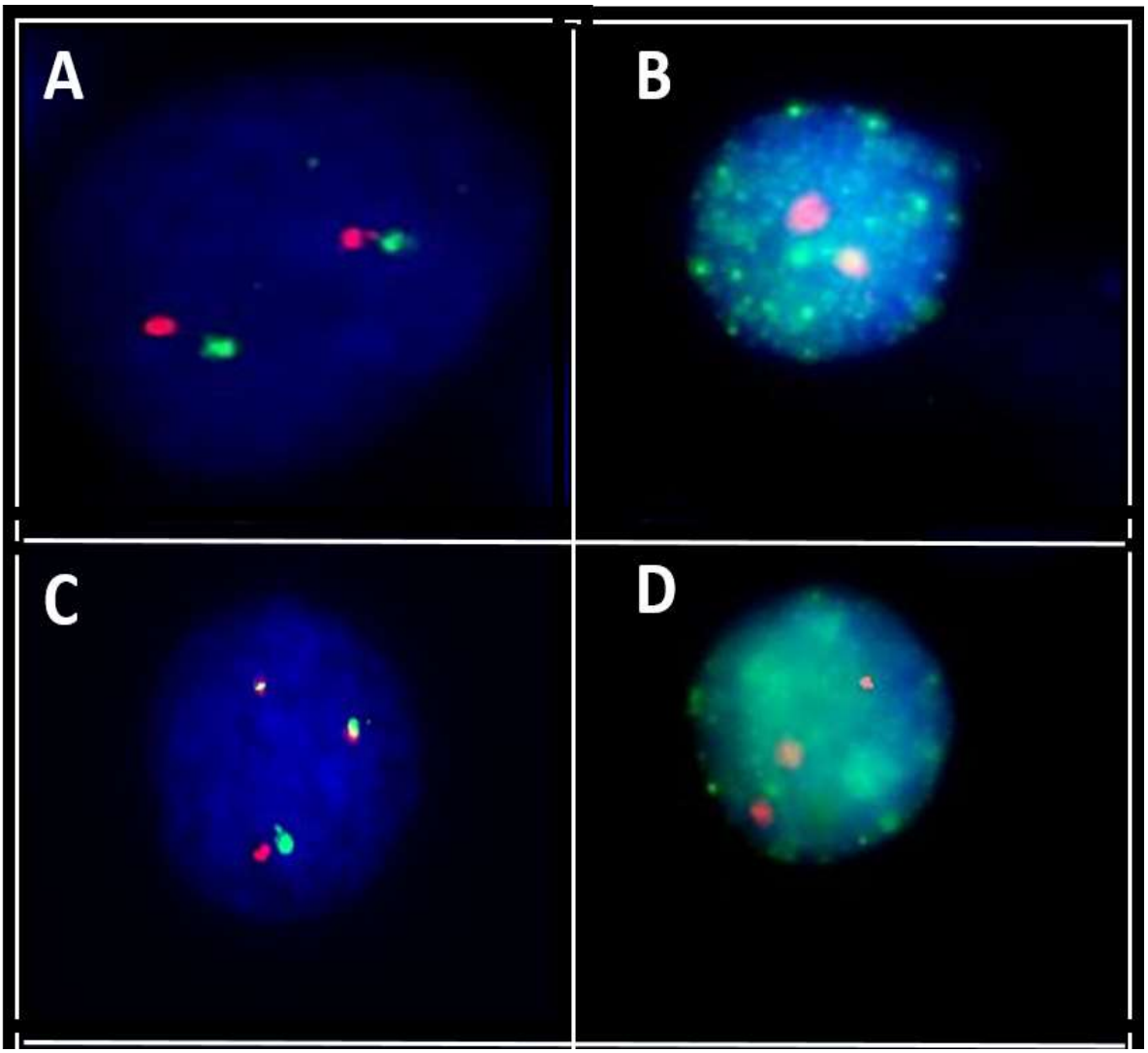

Figure 6-20: Examples of Immuno-FISH performed on cells from patient no. 26

(A) Shows non-proliferating nucleus with loss of 7q36.1 region, hybridisation signals shown in red (Cy3) and green (FITC) corresponding to normal chromosome 16.

(B) Proliferating nucleus with loss of 7q36.1 region, the red (Cy3) signal corresponding to the normal chromosome 16. Anti-pki67 is shown in green (FITC).

(C) non-proliferating nucleus with loss of 7q36.1 region, two fusion signals shown in red (Cy3) and green (FITC) corresponding to inversion chromosome 16 rearrangement.

(D) Shows proliferating nucleus with loss of 7q36.1, three red (Cy3) FISH signals that corresponding to the inv(16) rearrangement. Anti-ki67 is shown in green (FITC). Nuclei are counterstained in DAPI (blue colour).

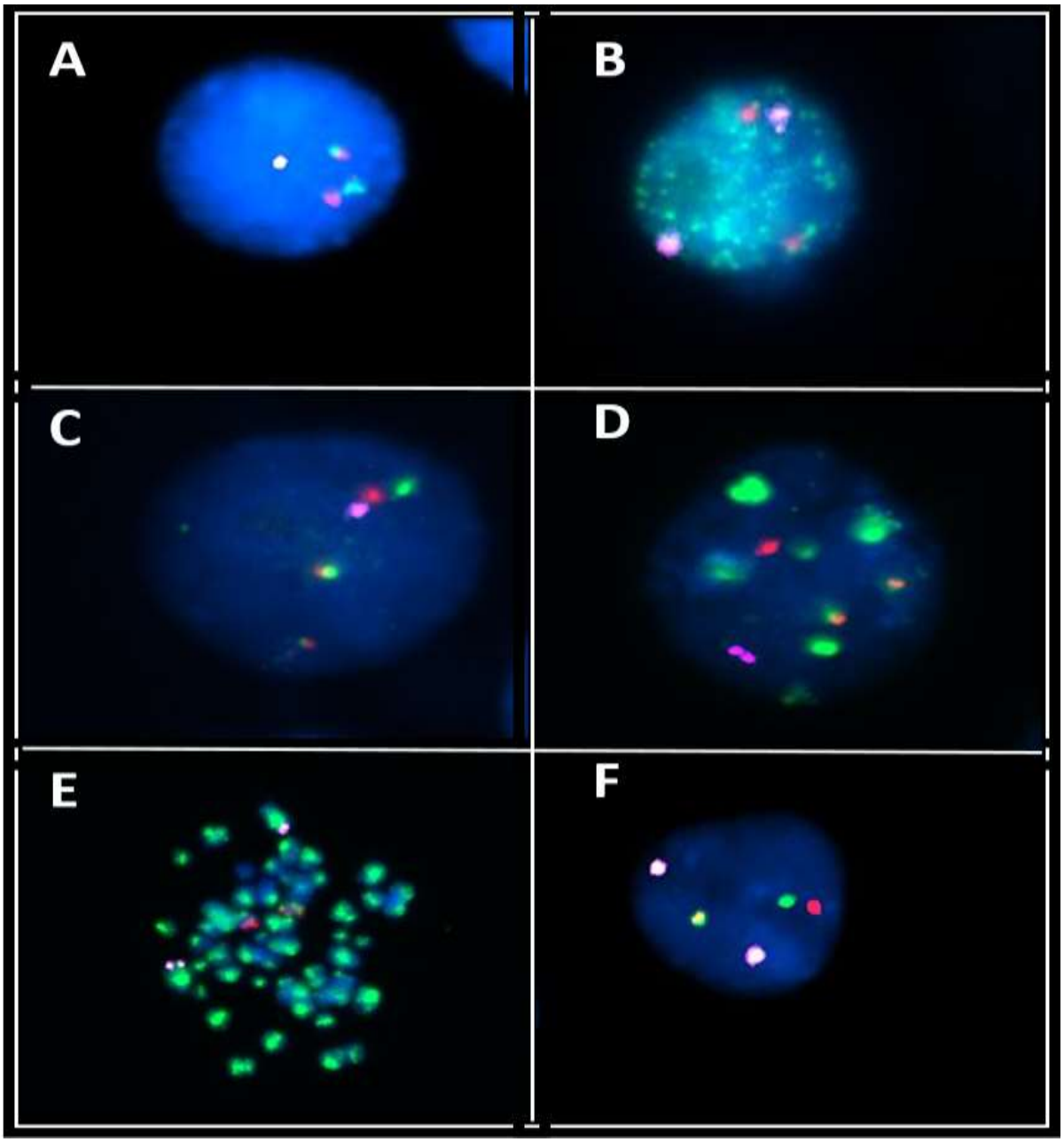

Figure 6-21: Examples of Immuno-FISH performed on cells from patient no. 27

(A) Shows non-proliferating nucleus with loss of one copy of 4q35.1 region in pink (Cy5) colour, hybridisation signals shown in red (Cy3) and green (FITC) corresponding to normal chromosome 16.

(B) Shows proliferating nucleus with two copies of 4q35.1 region in pink (Cy5) colour, the two red (Cy3) signals corresponding to the normal chromosome 16. Anti-pki67 is shown in green (FITC).

(C) Shows non-proliferating nucleus with loss of one copy of 4q35.1 region in pink (Cy5) colour, fusion signals shown in red (Cy3) and green (FITC) corresponding to inv(16) rearrangement.

(D) Shows proliferating nucleus with loss of one copy of 4q35.1 region in pink (Cy5) colour, three red (Cy3) FISH signals that corresponding to the inv(16) rearrangement. Anti-ki67 is shown in green (FITC).

(E) Metaphase shows normal chromosome 16 with two red (Cy3) signals and two copies of 4q35.1 region in pink (Cy5) colour. The metaphase is ki67 positive.

(F) non-proliferating nucleus with two copies of 4q35.1 region shown in pink (Cy5) and normal chromosome 16 shown in red (Cy3) and green (FITC) colour. Nuclei are counterstained in DAPI (blue colour).

6-4-2-3 Comparison of the evaluation of two observers

A summary of the number of samples and the results of ki67 analysed by the second observer are shown in table 6-4. The percentage of ki67 positive staining of cell lines analysed by the first observer was 100% (CRL-2630- chr8), 93% (CRL-2630- 7q36.1), 94.6% (CRL-2630- 4q35.1), 100% (CRL-2632- chr 8) and 94.5% (k562- 11p15), whereas the percentage of ki67 positive observed by the second observer was 99% (CRL-2630-), 91.5% (CRL-2630- 7q36.1), 94.5% (CRL-2630- 4q35.1), 100% (CRL-2632- chr 8) and 94.2% (k562- 11p15) (see figure 6-22). The percentage of proliferating cells was high in the three cell line. The results of proliferating cells analysed by two observers were very similar. The percentages of ki67 positive staining of patient cells carrying abnormalities observed by first observer was 34.3% (L020944), 70% (H010340), 79.3% (L0132108), 12% (26) and 13% (27), while the percentage of ki67 negative staining was 65.7%, 30%, 20.7% 88% and 87% respectively. However, when considering the cells carrying chromosomal abnormalities, the numbers of proliferating and non-proliferating cells in patient samples observed by second observer were very similar. The counts of ki67 negative cells were high in three patient samples, whereas in two patient samples the percentage of cells with ki67 negative staining was low (see figure 6-23).

Table 6-4: Type and percentage of major abnormalities detected in five patient samples and three cell lines and the percentage of ki67 positive and ki67 negative analysed by the second observer

Samples	Chromosome region	%Nullisomy	%Monosomy	% Disomy	% Trisomy	% Tetrasomy	% ki67 + in abnormal cells	%ki67 – in abnormal cells
CRL-2630	Chromosome 8 centromere	-	-	100	-	-	99	1
CRL-2630	7q36.1	-	-	100	-	-	91.5	8.5
CRL-2630	4q35.1	-	-	100	-	-	94.5	5.5
CRL-2632	Chromosome 8 centromere	-	-	100	-	-	100	0
K562	11p15	-	-	100	-	-	94.2	5. 8
L020944	Chromosome 8 centromere	-	-	5	-	79	34.5	65.5
H010340	Chromosome 8 centromere	-	-	15.7	69.5	-	70	30
L0132108	Chromosome 8 centromere	-	-	59	35.5	-	79.5	20.5
26	7q36.1	91.5	-	4.7	-	-	15	85
27	4q35.1	-	88	7.5	-	-	13	87

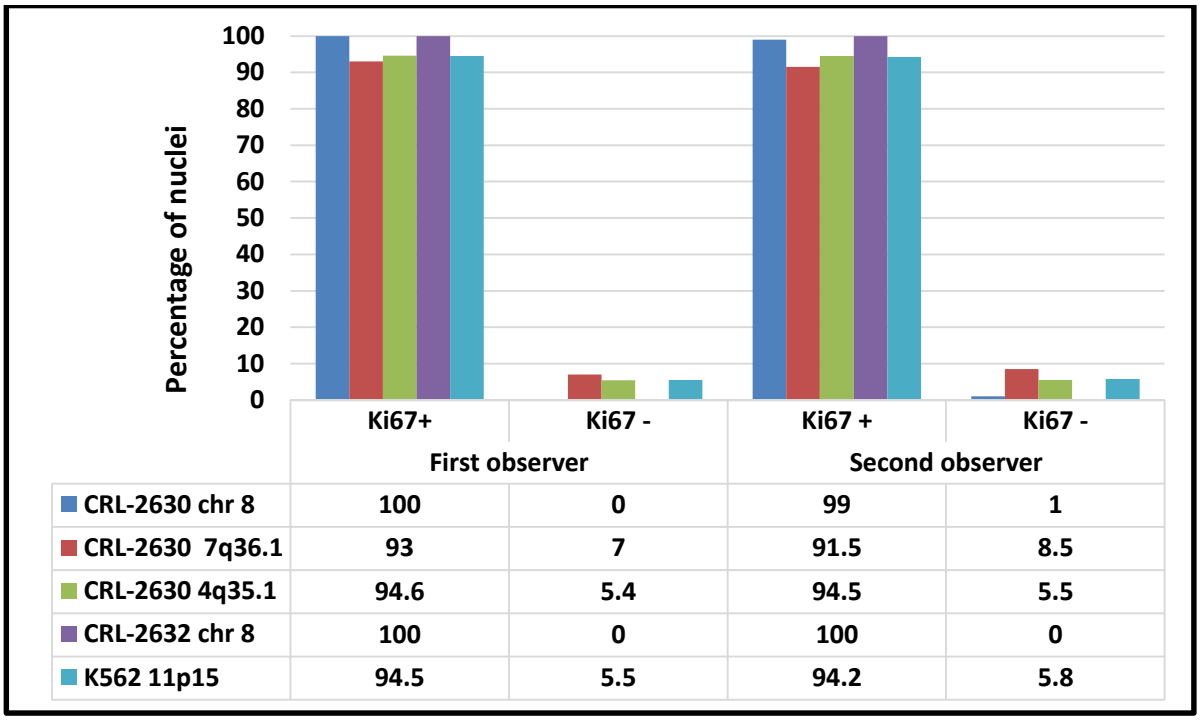

	First observer		Second observer	
CRL-2630 chr 8	100	0	99	1
CRL-2630 7q36.1	93	7	91.5	8.5
CRL-2630 4q35.1	94.6	5.4	94.5	5.5
CRL-2632 chr 8	100	0	100	0
K562 11p15	94.5	5.5	94.2	5.8

Figure 6-222: Graph showing the percentage of ki67 positive versus ki67 negative different cell lines

The X axis represents the percentage of Ki-67 positive nuclei and the Ki-67 negative nuclei evaluated by two observers. The Y axis refers to the percentage of cells analysed.

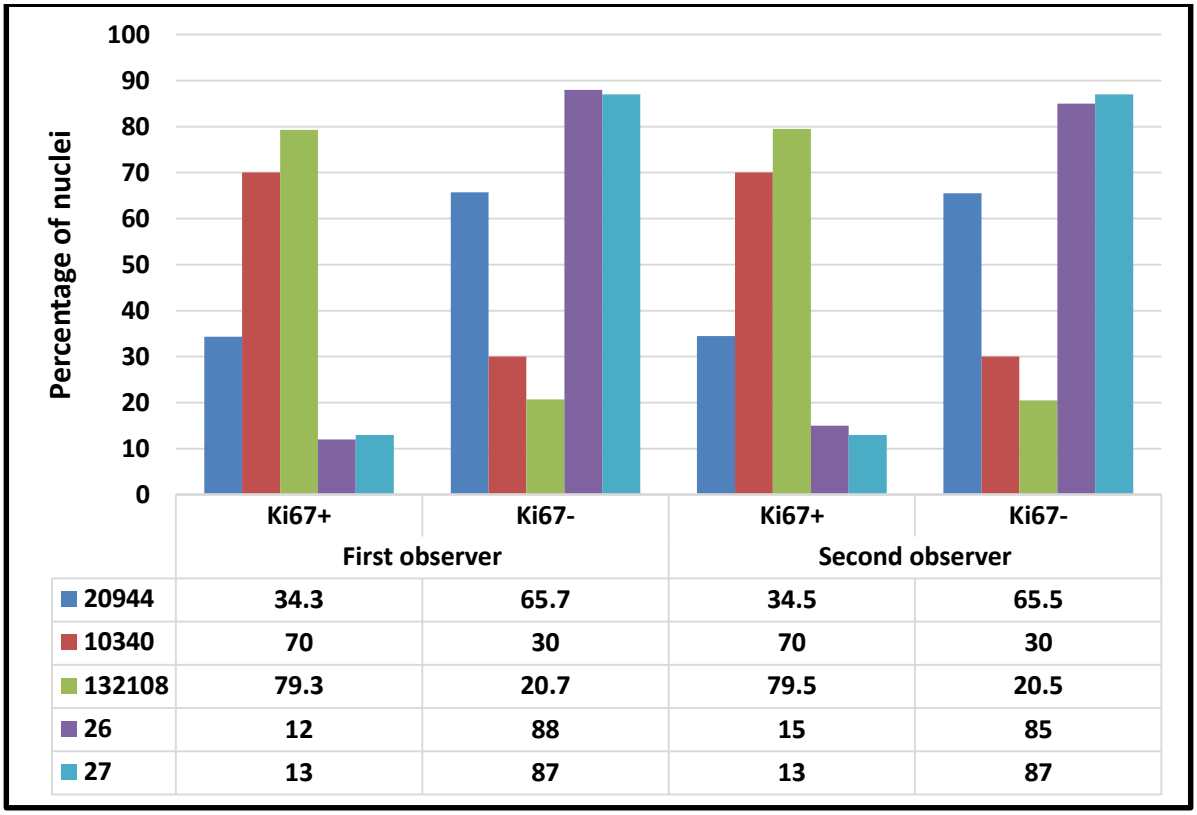

	Ki67+	Ki67-	Ki67+	Ki67-
	First observer		Second observer	
20944	34.3	65.7	34.5	65.5
10340	70	30	70	30
132108	79.3	20.7	79.5	20.5
26	12	88	15	85
27	13	87	13	87

Figure 6-23: Graph showing the percentage of ki67 positive versus ki67 negative in patient samples

The X axis represents the percentage of Ki-67 positive nuclei and the Ki-67 negative nuclei evaluated by two observers. The Y axis refers to the percentage of cells analysed.

6-5 Discussion

In the present study, IIF was performed on normal peripheral blood cells from eight different healthy individuals and k562 cell line to assess the proliferation state of ki-67 protein in stimulated and unstimulated normal blood cells and leukemic cell line using anti-ki67 antibody. Different fixation methods were used in these experiments to assess efficiency of antibody staining. Our ki67 staining results show a high percentage of ki67 positive staining (ranged 74%-84%) in five out of six stimulated samples when 4 fixed only with methanol/acetic acid (AH, AN, GO,LU) and one sample fixed with methanol/acetic acid and 4% PFA (PB) while a low percentage of ki67 positive was observed in the three unstimulated samples (sample 2 and sample 5 fixed with only methanol/acetic acid and sample PB fixed with both methanol/acetic acid and 4% PFA). Because the fixation methods were the same in the two groups of samples, the different proportion of Ki67

positive cells can be attributed to the fact that normal peripheral blood cells are non-proliferating, but they can be stimulated using phytohaemagglutinin in culture. Our results show high percentage of ki67 positive cells in four out of five stimulated samples, whereas one stimulated peripheral blood sample shows a low percentage of ki67 positive cells (24%). A high percentage of proliferating cells was detected in k562 cells fixed with methanol/acetone and 4% PFA (70%-100% respectively) our results of ki67 staining of normal peripheral blood cells and k562 cell line are in agreement with Gereds et al. (1983). Despite most of the k562 cells fixed with both fixation methods being ki67 positive, there was variation in the percentage of ki67 positive staining of cells (70% of cell fixed with methanol/acetone and 100% of cells fixed with 4% PFA). Our results showed that there was little difference between the percentages of ki67 positive cells in PB normal blood cells fixed with both methanol and 4% PFA fixation methods. Conversely, in k562 cells, there was a difference between the percentages of ki67 positive cells fixed in methanol compared to the ones fixed with 4% PFA. It is known that PFA acts as cross-linker, therefore the biological structures within the cells remain better preserved when other fixation methods are used.

Immuno-FISH was performed on five different patient samples using specific probes for the regions of interest to detect the chromosomal abnormalities, and ki67 antibody was used to assess the proliferation state of the cells. It was found that the proliferation state of the cells carrying chromosomal abnormalities in patients 010340 and 0132108 was higher than that of the cells carrying abnormalities in patient 020944, 26 and 27. In patients no 010340 and 0132108 the percentage of proliferating of cells carrying trisomy 8 was 70% and 79.3% respectively, while 30% and 20.7% of the same cells carrying trisomy 8 were non-proliferating cells. In patients no. 020944, 26 and 27 the percentage of non-proliferating cells carrying teatrosomy 8, loss of 7q36.1 region and loss of 4q35.1 region (65.57%, 88% and 87%) respectively was higher than the percentage of the proliferating cells (34.43%, 12% and 13%). Our data showed that there is a variation in the proliferation state of cells that carrying abnormalities. In other words, most of the cells carrying abnormalities were proliferating in two cases (010340 and 0132108) and non-proliferating in three cases (020944, 26 and 27).

The proportion of ki67 positive cells is particularly low for patients 26 and 27. As suggested by Ballabio et al. (2011), this might be the reason why the additional

abnormalities detected by array methods were not seen cytogenetically. As Ballabio demonstrated, in some cases the majority (94–100%) of nuclei carrying the abnormality were negative for the proliferation marker in all patients reported in their study. It should be noted that our selected cases were karyotypicllay abnormal, whereas all samples used by Ballabio et al. (2011) study were with normal or incomplete karyotype. Some of our data are similar to those presented by Nowicki et al. (2006), who showed that a high percentage of proliferating cells were identified in leukaemia blasts at day 0 (baseline) of diagnosis.

According to our data, it can be observed that chromosomal abnormalities can be found in both proliferating and non-proliferating cells. By way of explanation, our data do not fully support the hypothesis that the cells carrying abnormalities are largely confined to non-proliferating cells. However, the presence of a population of leukaemic blasts in non-proliferative state might be the reason why in a proportion of cases abnormalities are not detected by conventional chromosome banding analysis.

The majority of cells of human cell lines (k562, CRL-2630 and CRL-2632) used in this study were found to be stained with ki67 antibody, this ki67 results coincided well with data on reactivity of ki67 with various human cell lines (Gerdes et al., 1983).

Ki67 is a nuclear protein that is expressed in the proliferating cells during G1, S, G2 and M phases of the cell cycle. The ki67 antigen was detected in nuclear foci in early G1 referred to it as pattern type I whereas in late G1, S and G2 the ki67 antigen was located in the nucleolus showing different patterns of ki67 staining referred to it as pattern type II. The ki67 antigen was presented surrounding metaphase chromosomes during mitosis while it was not detected in G0 phase of cell cycle as the cells exist in the quiescent state (Bridger et al., 1998; Kill, 1996). Our data show different patterns of ki67 staining in stimulated normal peripheral blood cells, patient samples and human cancer cell lines. The patterns observed were similar to those previously described by other researchers (Bridger et al., 1998; Kill, 1996), and indicative of the presence of cells in all phases of the cell cycle. It was interesting to note that the proliferation rate in the human cancer cell lines was extremely high even compared to stimulated peripheral blood of healthy individuals, reaching 100% positive for ki67 staining in the K562 cell line in optimal fixation conditions.

CHAPTER 7: GENERAL DISCUSSION

7-1 A novel three-colour fluorescence *in situ* hybridization approach for the detection of t(7;12)

To validate a new three colour probe which enables the detection of the t(7;12)(q36;p13) rearrangement, FISH was performed on bone marrow form archival methanol/acetic acid fixed cell suspensions of seven patient samples. The results indicated that the new three-colour FISH approach used in this study has enabled the detection of a cryptic t(7;12) translocation as a part of a complex rearrangements in one patient that had previously been described as having t(7;16) and ETV6-HLXB9 fusion transcript at the molecular level (Wildenhain et al., 2010). To date, only two cases of a cryptic t(7;12) translocation have been reported in the literature (Park et al., 2009), neither of which involved chromosome 16 translocation. The possible mechanism for the formation of the t(7;12;16) complex rearrangement involves an insertion of chromosome 12 material into chromosome 7, a translocation between chromosome 7 and chromosome 16 and a subsequent inversion of chromosome 16. Further investigation of the mechanism of the formation of the t(7;12;16) complex rearrangement could be carried out in future studies using telomeric probe of chromosome 7 to verify whether this complex rearrangement involved a translocation between chromosome 7 and 12, or whether it is an inversion of chromosome 12 material into chromosome 7. Furthermore, the new three-colour FISH approach also enabled us to identify the t(7;12) in a new seven year-old patient with AML. This patient is the first case of childhood leukaemia with an onset after infancy positive for t(7;12). The results suggest that the use of the sensitive new three-colour probe approach might help to significantly improve the detection of t(7;12) rearrangement in AML cases. One-third of infant leukaemia cases were found to have t(7;12) rearrangement (Tosi et al., 2003; Von Bergh et al., 2006). The discovery of such a cryptic t(7;12) and the t(7;12) rearrangement in a seven year-old AML patient indicates that the incidence of t(7;12) rearrangement in AML might be higher than previously reported.

7-2 Three-colour probe sets for the detection of chromosome 7 abnormalities in myeloid malignancies

In this study, three-colour probe sets for del(7q22-q31) and del(7q22-q36) were validated on Farage (CRL-2630), GDM1, GF-D8 and K562 cell lines. The investigation of chromosome 7 rearrangements in GDM1 cell line shows normal localization of 7(q22-q31) and 7(q22-q36) regions. The GDM1 cell line known to have a t(6;7) (q23; q36) translocation with breakpoint proximal to HLXB9 gene at 7q36.3 (Nagel et al., 2005). Furthermore, the FISH results of GF-D8 cell line show trisomy 7, deletion of 7(q22-q31) with breakpoints within q22 and distal to q31 regions and an inv(7) as previously reported by Tosi et al. (1999a, 1999b).

However, the inv(7) breakpoints (distal to q22 and distal to q31) of GF-D8 observed in this study were different from Tosi et al. (1999a), who reported the proximal breakpoint of the inv(7) between 7q31.1 and 7q31.3 and the distal breakpoint between 7q35-q36 and 7q36. Nevertheless, the observation of the proximal breakpoint of inv(7) (distal to 7q22) is very much in agreement with Johnson et al. (1996), who found a constitutional inversion of 7q in two patients one with MDS and one had BM hypoplasia, the proximal breakpoint was mapped at 7q22.1. Moreover, the inv(7) breakpoints in GF-D8 cell lines were further confirmed by 7(q22-q36) probe, which shows normal position of 7q22 and 7q36. The 7q22-q36 probe also confirmed the deletion of 7q22-7q33 region and translocation or insertion of chromosome 7 q36 material onto the short arm of chromosome 12, as previously described by Tosi et al. (1999a). The 7(q22-q31) deletion was previously reported in MDS and AML cases (Dohner et al., 1998; Fischer et al., 1997). These studies proposed that this region might contain specific genes such as TSG that might contribute to MDS or AML development.

The structure of chromosome 7 in k562 cell line was previously investigated using M-FISH, CGH and Locus-Specific FISH (Gribble et al., 2000; Naumann et al., 2001); the rearrangements of chromosome 7 in both studies were described as tetrasomy 7, del 7q, inv(7)(p11-q). Interestingly, the three colour probe enabled the detection of a new rearrangement in k562 cell line, described as a duplication of 7q36 region followed by either an intrachromosomal insertion of long arm material into short arm of chromosome 7 or an intrachromosomal translocation between two ends of chromosome 7. This finding

was further confirmed using locus-specific probe for 7q36.1 in combination with WCP 7 and partial chromosome 7 p and 7q paint. The results showed that no pericentric inversion 7 was detected in this cell line, as previously described. It has been reported that the cytogenetic discrimination of the intrachromosomal insertion and peicentric inversion abnormalities can be difficult (Madan, 1995). Consequently, these results suggest that the intrachromosomal 7 insertion that identified in this cell line might be misdiagnosed as a pericentric inversion 7.

The intrachromosomal insertion identified in k562 cell line is uncommon form of chromosomal rearrangement; to date, there are only 41 cases reported in the literature, none of which had myeloid malignancy (Ardalan et al., 2005; Farrell and Chow, 1992; Kim et al., 2011; Lybaek et al., 2009; Madan and Menko, 1992). The other observation is the detection of a duplication of 7q36 region, which is known as a common deleted region in myeloid malignancy.

7-3 Study of copy number changes in inv(16) leukaemia

To identify CNAs and CN-LOH regions, Illumina beadarray approach was performed on 22 AML patient samples with inv(16)(p13;q22) and t(8;21)(q22;q22) rearrangements. The results showed a low number of copy number losses and copy number gains in 17 out of 22 cases (77.27%), with an average of 1.86 CNAs per case as well as copy neutral LOH with an average of 6.7% per patient. The results show that low recurrent CNAs regions were detected, including losses of 7q36.1 and 9q13-q33.1 and CN- LOH of 2p16.1, 2p21, 2q13, 6p12.3, 7q11.21, 7q11.22, 8q21.3, 8q23.3, 9q13, 12q24.11-q24.13 and 20q11.21. This results concur with previous literature (Akagi et al., 2009; Barresi et al., 2010; Cosat et al., 2013; Kuhn et al., 2012; Redtke et al., 2009), which identified a low number of CNAs and low recurrent regions, including 7q36.1 and 9q13-q33.1 in AML cases.

Furthermore, the array results were compared with chromosome banding analysis of four cases. The results show that three deleted regions in 7q36.1, 4q35.1 and 16p13.11 identified by array in three cases were not observed by chromosome banding. In addition to that, a large amplified region >18 Mb was detected by array in one case was missed by G-banding. Therefore, interphase FISH was carried out to validate the CNAs in four cases, showing a 7q36.1 deletion, 4q35.1 deletion, 16.13.11 deletion and 8q24.21-q24.3 gain. The FISH results confirmed homozygous copy loss of 7q36.1 in 92% of case 26 cells, a

mosaic loss of 4q35.1 region in 64.9% of case 27 nuclei and a copy number loss of 16p13.11 region in 12.5% of case 29 cells. However, in case 30 a large gain of 8q24.21-q24.3 was unconfirmed by FISH, as the results showed no significant difference between the normal controls and the patient's cells.

Ballabio et al. (2011) demonstrated that large CNAs identified in normal karyotype AML cases by aCGH analysis were confirmed by FISH, and found in interphase but not in metaphase cells. Their hypothesis was that the abnormalities were confined to the non-dividing cells and therefore could not be observed by chromosome banding analysis or metaphase FISH. They demonstrated this by conducting immuno-FISH experiments using ki-67, a proliferation marker, and showing that the CNAs were detected only in ki-67 positive cells in the majority of cases. Based on this evidence, further analysis of FISH data were carried out to investigate whether CNAs are present in the same clone harbouring inv(16) or/and in the cells without inv(16), and also to verify whether the CNAs were present in non-dividing population of cells. The results showed that the CNAs were found both in cells without inv(16) and cells harbouring the inv(16) rearrangement in all cases except case no. 30.

In addition, a proportion of cells without inv(16) and with inv(16) were found to have normal number of copies of 7q36.1 (no. 26), 4q35.1 (no. 27) and 16p13.11 (no. 29). In cases no. 26, 27 and 29 the CNAs detected in this study were invisible by G-banding because they were too small to be seen by chromosome banding methods. In two cases the CNAs occurred only in proportion of cells as shown in case 27 (64.9%) and case 29 (12.5%). This variance of the copy number loss of the gene detected in patient's cells can be explained by somatic mosaicism of the patients in which one copy of the gene found in only 64.9% and 12.5% of the cells. It has been shown that the CNAs have an impact on the clinical outcome of patients. Therefore, it would be of particular interest to understand whether the presence of CNAs together with the inv(16) has an impact on the prognosis of this specific subset of patients, who are generally characterized by a relatively good clinical outcome, in future studies.

7-4 Proliferation studies in leukaemia

Indirect immunofluorescence was used to determine the ki67 staining patterns in eight stimulated and unstimulated peripheral blood samples and k562 cell line. Different

fixation methods were used in these experiments to assess the efficiency of antibody staining. The results showed a high percentage of ki67 positive staining (74-84%) in five out of six stimulated samples, when 4 fixed only with methanol/acetic acid and one sample fixed with methanol/acetic acid and 4% PFA while low percentage of ki67 positive was observed in three unstimulated samples when two samples fixed with only methanol/acetic acid and sample one sample fixed with both methanol/acetic acid and 4% PFA). Because the fixation methods were the same in the two groups of samples, the different proportion of Ki67 positive cells can be attributed to the fact that normal peripheral blood cells are non-proliferating, but they can be stimulated using phytohaemagglutinin in culture. Moreover, a high percentage of proliferating cells was detected in k562 cells fixed with methanol/acetone and 4% PFA (70-100% respectively); our results of ki67 staining of normal peripheral blood cells and k562 cell line are in agreement with Gereds et al. (1983), who reported that more than 80% of PHA-stimulated normal blood cells reacted with ki67 antibody, while unstimulated normal blood lymphocytes and monocytes did not react with ki67 antibody, and ki67 was also found to react with a majority of cells in cancer cell lines.

Immuno-FISH was performed on five different patient samples and leukaemia cell lines using specific probes for the regions of interest to detect the chromosomal abnormalities and ki67 antibody was used to assess the proliferation state of the cells. The results showed that the proliferation state of the cells carrying chromosomal abnormalities in patients 010340 and 0132108 was higher than the proliferation state of the cells carrying abnormalities in patient 020944, 26 and 27. The results showed that there is a variation in the proliferation state of cells that carrying abnormalities. In other words, most of the cells carrying abnormalities were proliferating in two cases (010340 and 0132108) and non-proliferating in three cases (020944, 26 and 27). The proportion of ki67 positive cells is particularly low for patients 26 and 27. As suggested by Ballabio et al. (2011), this might be the reason why the additional abnormalities detected by array methods were not seen cytogenetically. As Ballabio et al. (2011) demonstrated, in some cases the majority (94–100%) of nuclei carrying the abnormality were negative for the proliferation marker in all patients reported in their study. Moreover, some of our data are similar to the findings presented by Nowicki et al. (2006), who showed that a high percentage of proliferating cells were identified in leukaemia blasts at day 0 (baseline) of diagnosis.

According to the results, our observation is that chromosomal abnormalities can be found in both proliferating and non-proliferating cells. Consequently, this study does not fully support the hypothesis that the cells carrying abnormalities are largely confined to non-proliferating cells. However, the presence of a population of leukaemic blasts in non-proliferative state might be the reason why in a proportion of cases abnormalities are not detected by conventional chromosome banding analysis. The majority of cells of human cell lines (k562, CRL-2630 and CRL-2632) used in this study were found to be stained with ki67 antibody, which coincides with data on the reactivity of ki67 with various human cell lines (Gerdes et al., 1983). The results have shown that different patterns of ki67 staining were observed in stimulated normal peripheral blood cells, patient samples and human cancer cell lines. The patterns observed were similar to those previously described by others (Bridger et al., 1998; Kill, 1996). It was interesting to note that the proliferation rate in the human cancer cell lines was extremely high even compared to stimulated peripheral blood of healthy individuals, reaching 100% of cells positive for ki67 staining in the K562 cell line in optimal fixation conditions.

7-5 Conclusion and future studies

The work carried out during my PhD focused on the study of leukaemia cases characterized by the presence of chromosomal translocations. I have analysed a number of samples mainly using molecular cytogenetics methods and immunofluorescence. In many cases, this study uncovered the presence of cryptic abnormalities in the form of three way translocation (chapter 3), intrachromosomal rearrangement (chapter 4), DNA copy number changes either of submicroscopic entity or confined to the non-dividing cell population (chapter 5 and 6). Altogether this work adds new information to the understanding of the growing complexity at the basis of cancer genetics. Some of this work has already been published during the course of my studies (chapter 3; Naiel et al., 2013), whereas some other aspects of my project are currently being organized for further manuscripts (chapters 4 and 5), that are planned to be submitted in the short term. My work has shown that a relatively simple and straightforward technique such as fluorescence in situ hybridization, has been able to unravel hidden chromosomal abnormalities in leukaemia that conventional methods of chromosome banding did not reveal. The same FISH technique has been able to confirm abnormalities detected by more modern molecular techniques involving arrays and further refine the proportion of

cells affected. Overall, my work has paved the basis for further functional studies aimed at understanding the biological meaning of these changes. The findings here reported concern loss and gain of genomic material that could harbour tumour suppressor genes or proto-oncogenes. Translocations might lead to the formation of fusion genes. More complex rearrangements might simply indicate clonal evolution and might be associated with worsening of the disease. Confirmation of the above will be topic for future studies.

BIBLIOGRAPHY

Abu-Duhier, F. M., Goodeve, A. C., Wilson, G. A., Care, R. S., Peake, I. R., & Reilly, J. T. (2001). Genomic structure of human FLT3: implications for mutational analysis. *British Journal of Haematology*, 113(4), 1076-1077.

Afonja,O., Smith,J.E., Jr., Cheng,D.M., Goldenberg,A.S., Amorosi,E., Shimamoto,T., Nakamura,S., Ohyashiki,K., Ohyashiki,J., Toyama,K., and Takeshita,K. (2000). MEIS1 and HOXA7 genes in human acute myeloid leukemia. Leuk. Res. 24, 849-855.

Akagi, T., Shih, L. Y., Ogawa, S., Gerss, J., Moore, S. R., Schreck, R., & Koeffler, H. P. (2009). Single nucleotide polymorphism genomic arrays analysis of t(8; 21) acute myeloid leukaemia cells. *Haematologica*, 94(9), 1301-1306.

Albertson, D., Collins, C., McCormick, F. and Gray, J. (2003). Chromosome aberrations in solid tumors. Nat Genet, 34(4), pp.369-376.

Alsabeh, R., Brynes, R. K., Slovak, M. L., Arber, D. A. (1997). Acute myeloid leukaemia with t(6;9) (p23;q34), association with myelodysplasia, basophilia, and initial CD34 negative immunophenotype. *Am J Clin Pathol*., 107(4), 430-7.

Andersen, C., Gruszka-Westwood, A., Ostergaard, M., Koch, J., Jacobsen, E., Kjeldsen, E., & Nielsen, B. (2004). A narrow deletion of 7q is common to HCL, and SMZL, but not CLL. *European Journal of Haematology*, 72(6), 390-402.

Andreasson, P., Hoglund, M., Bekassy, A., Garwicz, S., Heldrup, J., Mitelman, F., & Johansson, B. (2000). Cytogenetic and FISH studies of a single center consecutive series of 152 childhood acute lymphoblastic leukemias. *European Journal of Haematology*, 65(1), 40-51.

Antonchuk,J., Sauvageau,G., and Humphries,R.K. (2001). HOXB4 overexpression mediates very rapid stem cell regeneration and competitive hematopoietic repopulation. Exp. Hematol. 29, 1125-1134.

Antonchuk,J., Sauvageau,G., and Humphries,R.K. (2002). HOXB4-induced expansion of adult hematopoietic stem cells ex vivo. Cell 109, 39-45.

Ardalan, A., Prieur, M., Choiset, A., Turleau, C., Goutieres, F., & Girard-Orgeolet, S. (2005). Intrachromosomal insertion mimicking a pericentric inversion: molecular cytogenetic characterization of a three break rearrangement of chromosome 20. *American Journal of Medical Genetics Part, A*., 138(3), 288-293.

Arthur, D. C., Berger, ., R., Golomb, H. M., Swansburry, G. J., Reeves, B. R., Alimena, G., Van den Berghe, H., Bloomfield, C. D., De la Chapelle, A., Dewald, G. W., Garson, O. M., Hagemeijer, A., Kaneko, Y., Mitelman, F., Pierre, R. V., Ruutu, T., Sakurai, M., Lawler, S. D., Rowley, J. D. (1989). The clinical significance of karyotype in acute myelogenous leukemia. *Cancer Genet Cytogenet*, 40, 203-216.

Arthur, D. C., Bloomfield, C. D. (1983). Partial deletion of the long arm of chromosome 16 and bone marrow eosinophilia in acute nonlymphocytic leukemia: A new association. *Blood*, 61, 994-998.

Avigdor,A., Goichberg,P., Shivtiel,S., Dar,A., Peled,A., Samira,S., Kollet,O., Hershkoviz,R., Alon,R., Hardan,I., Ben Hur,H., Naor,D., Nagler,A., and Lapidot,T. (2004). CD44 and hyaluronic acid cooperate with SDF-1 in the trafficking of human CD34+ stem/progenitor cells to bone marrow. Blood 103, 2981-2989.

Bacher, U., Haferlach, C., Schnittger, S., Kohlmann, A., Kern, W., & Haferlach, T. (2010). Mutations of the TET2 and CBL genes: novel molecular markers in myeloid malignancies. *Annals of Hematology*, 89(7), 643-652.

Baer, M. and Bloomfield, C. (1992). Trisomy 13 in Acute Leukemia. Leukemia & Lymphoma, 7(1-2), pp.1-6.

Bailey, J. (2001). Segmental Duplications: Organization and Impact Within the Current Human Genome Project Assembly. Genome Research, 11(6), pp.1005-1017.

Bajaj, R., Xu, F., Xiang, B., Wilcox, K., DiAdamo, A., Kumar, R., Pietraszkiewicz, A., Halene, S., & Li, P. (2011). Evidence-based genomic diagnosis characterized chromosomal and cryptic imbalances in 30 elderly patients with myelodysplastic syndrome and acute myeloid leukemia. *Mol Cytogenet*, 4(3).

Baker, S., Fearon, E., Nigro, J., Hamilton, Preisinger, A., Jessup, J., vanTuinen, P., Ledbetter, D., Barker, D., Nakamura, Y., White, R. and Vogelstein, B. (1989). Chromosome 17 deletions and p53 gene mutations in colorectal carcinomas. Science, 244(4901), pp.217-221.

Baldwin, E. L., Lee, J. Y., Blake, D. M., Bunke, B. P., Alexander, C. R., Kogan, A. L., & Martin, C. L. (2008). Enhanced detection of clinically relevant genomic imbalances using a targeted plus whole genome oligonucleotide microarray. *Genetics in Medicine*, 10(6), 415-429.

Ballabio, E., Cantarella, C., Federico, C., Di Mare, P., Hall, G., Harbott, J., Hughes, J., Saccone, S. and Tosi, S. (2009). Ectopic expression of the HLXB9 gene is associated with an altered nuclear position in t (7; 12) leukaemias. *Leukemia,* 23(6), pp.1179--1182.

Ballabio, E., Regan, R., Garimberti, E., Harbott, J., Bradtke, J., Teigler, A., Biondi, A., Cazzaniga, G., Giudici, G., Wainscoat, J. S., Boultwood, J., Bridger, J. M., Knight, S. J. L., Tosi, S. (2011). Genomic imbalances are confined to non-proliferating cells in pediatric patients with acute myeloid leukemia and a normal or incomplete karyotype. *Plose One*, 6, 6, 20607.

Barresi, V., Romano, A., Musso, N., Capizzi, C., Consoli, C., Martelli, M. P., & Condorelli, D. F. (2010). Broad copy neutral-loss of heterozygosity regions and rare recurring copy number abnormalities in normal karyotype-acute myeloid leukemia genomes. *Genes, Chromosomes and Cancer*, 49(11), 1014-1023.

Bejjani, B. and Shaffer, L. (2006). Application of array-based comparative genomic hybridization to clinical diagnostics. The Journal of Molecular Diagnostics, 8(5), pp.528--533.

Bellantuono, I. (2004). Haemopoietic stem cells. *International Journal of Biochemistry & Cell Biology*, 36(4), 607-620.

Belloni, E., Trubia, M., Mancini, M., Derme, V., Nanni, M., Lahortiga, I., Riccioni, R., Confalonieri, S., Lo-Coco, F., & Di Fiore, P. (2004). A new complex rearrangement involving the ETV6, LOC115548, and MN1 genes in a case of acute myeloid leukemia. *Genes, Chromosomes and Cancer*, 41(3), 272-277.

Ben-Bassat, H., Korkesh, A., Voss, R., Leizerowitz, R., & Polliack, A. (1982). Establishment and characterization of a new permanent cell line (GDM-1) from a patient with myelomonoblastic leukaemia. *Leukemia Research*, 6(6), 743-752.

Bennett, J. M., Catovsky, D., Daniel, M. T., Flandrin, G., Galton, D. A., Gralnick, H. R., & Sultan, C. (1976). Proposals for the classification of the acute leukaemias. French-American-British (FAB) co-operative group. *British Journal of Haematology*; 33(4), 451-8.

Beran, M., Luthra, R., Kantarjian, H., & Estey, E. (2004). FLT3 mutation and response to intensive chemotherapy in young adult and elderly patients with normal karyotype. *Leukemia Research*, 28(6), 547-550.

Berger, R., Bernheim, A., Daniel, M. T., Valensi, F., Sigaux, F., & Flandrin, G. (1985). Cytogenetic studies on acute myelomonocytic leukaemia (M4) with eosinophilia. *Leukemia Research*, 9(2), 279-288.

Betts, D. R., ROHATINER, A., Evans, M. L., Rassam, S. M. B., Lister, T. A., & Gibbons, B. (1992). Abnormalities of chromosome 16q in myeloid malignancy: 14 new cases and a review of the literature. *Leukemia*, 6(12), 1250-1256.

Betz, B. L. and Hess, J. L. (2010). Acute myeloid leukemia diagnosis in the 21st century. *Archives of Pathology & Laboratory Medicine*, 134(10), 1427-1433.

Beverloo, H., Panagopoulos, I., Isaksson, M., van Wering, E., van Drunen, E., de Klein, A., Johansson, B., & Slater, R. (2001). Fusion of the homeobox gene HLXB9 and the ETV6 gene in infant acute myeloid leukemias with the t(7; 12)(q36; p13). *Cancer Research*, 61(14), 5374-5377.

Bloomfield, C. D., De la Chapelle, A. (1987). Chromosome abnormalities in acute nonlymphocytic leukemia: Clinical and biologic significance. *Semin Oncol*, 14, 372.

Bohl, and Er, S. (2001). Fusion genes in leukemia: an emerging network. *Cytogenetic and Genome Research*, 91(1-4), 52-56.

Bonnet, D. (2005). Normal and leukaemic stem cells. *British Journal of Haematology*, 130(4), 469-479.

Bridger, J. M., & Volpi, E. (2010). *Fluorescence In Situ Hybridization (FISH), Protocols and applications*. Vol. 659. New York: Springer.

Bridger, J. M., Kill, I. R., Lichter, P. (1998). Association of pKi-67 with satellite DNA of the human genome in early G1 cells. *Chromosome Research*, 6, 13-24.

Brozek, I., Babinska, M., Kardas, I., Wozniak, A., Balcerska, A., Hellmann, A., & Limon, J. (2003). Cytogenetic analysis and clinical significance of chromosome 7 aberrations in acute leukaemia. *Journal of Applied Genetics*, 44(3), 401-412.

Brun,A.C., Bjornsson,J.M., Magnusson,M., Larsson,N., Leveen,P., Ehinger,M., Nilsson,E., and Karlsson,S. (2004). Hoxb4-deficient mice undergo normal hematopoietic development but exhibit a mild proliferation defect in hematopoietic stem cells. Blood 103, 4126-4133.

Buske,C., Feuring-Buske,M., Abramovich,C., Spiekermann,K., Eaves,C.J., Coulombel,L., Sauvageau,G., Hogge,D.E., and Humphries,R.K. (2002). Deregulated expression of HOXB4 enhances the primitive growth activity of human hematopoietic cells. Blood 100, 862-868.

Byrd, J. C., Mrózek, K., Dodge, R. K., Carroll, A. J., Edwards, C. G., Arthur, D. C., & Bloomfield, C. D. (2002). Pretreatment cytogenetic abnormalities are predictive of induction success, cumulative incidence of relapse, and overall survival in adult patients with de novo acute myeloid leukemia: results from Cancer and Leukemia Group B (CALGB 8461). Presented in part at the 43rd annual meeting of the American Society of Hematology, Orlando, FL, December 10, 2001, and published in abstract form. 59. *Blood*, 100(13), 4325-4336.

Calvi,L.M., Adams,G.B., Weibrecht,K.W., Weber,J.M., Olson,D.P., Knight,M.C., Martin,R.P., Schipani,E., Divieti,P., Bringhurst,F.R., Milner,L.A., Kronenberg,H.M., and Scadden,D.T. (2003). Osteoblastic cells regulate the haematopoietic stem cell niche. Nature 425, 841-846.

Cameron, E. R., & Neil, J. C. (2004). The Runx genes lineage-specific oncogenes and tumor suppressors. *Oncogene*, 23, 4308-14.

Campana, D., & Janossy, G. (1988). Proliferation of normal and malignant human immature lymphoid cells. *Blood*, 71, 1201-10.

Campana, D., Coustant-Smith, E., & Janossy, G. (1988). Double and triple staining methods for studying the proliferation activity of human B and T lymphoid cells. *J Immunol Methods*, 107, 79-88.

Campbell, L. J. (2011). *Cancer Cytogenetics: Methods and Protocols.* 2nd edition. Sydney, Australia: Humana Press.

Care, R., Valk, P., Goodeve, A., Abu-Duhier, F., Geertsma-Kleinekoort, W., Wilson, G., Gari, M., Peake, I., Lowenberg, B. and Reilly, J. (2003). Incidence and prognosis of c-KIT and FLT3 mutations in core binding factor (CBF) acute myeloid leukaemias. British Journal of Haematology, 121(5), pp.775-777.

Care, R., Valk, P., Goodeve, A., Abu-Duhier, F., Geertsma-Kleinekoort, W., Wilson, G., Gari, M., Peake, I., L"owenberg, B. and Reilly, J. (2003). Incidence and prognosis of c-Kit and FLT3 mutations in core binding factor (CBF) acute myeloid leukaemias. British journal of haematology, 121(5), pp.775--777.

Castilla, L. H., Wijmenga, C., Wang, Q., Stacy, T., Speck, N. A., Eckhaus, M., Marin-Padilla, M., Collins, F. S., & Wynshaw-Boris, A. (1996). Failure of embryonic hematopoiesis and lethal hemorrhages in mouse embryos heterozygous for a knocked-in leukemia gene CBFB-MYH11. *Cell*, 87, 687–696.

Cho, S., Park, S., Kim, H., Park, I., Choi, J., Jung, H., & Park, J. (2011). Acute promyelocytic leukemia with complex translocation t(5; 17; 15)(q35; q21; q22), case report and review of the literature. *Journal of Pediatric Hematology/Oncology*, 33(7), 326-329.

Cools, J., Mentens, N., Odero, M. D., Peeters, P., Wlodarska, I., Delforge, M., Hagemeijer, A., & Marynen, P. (2002). Evidence for position effects as a variantETV6-mediated leukemogenic mechanism in myeloid leukemias with a t(4;12)(q11-q12;p13) or t(5;12)(q31;p13). *Blood*, 1,99(5), 1776-84.

Crescenzi, B., La Starza, R., Nozzoli, C., Ciolli, S., Matteucci, C., Romoli, S., Rigacci, L., Gorello, P., Bosi, A., & Martelli, M. (2007). Molecular cytogenetic findings in a four-way t(1; 12; 5; 12)(p36; p13; q33; q24) underlying the ETV6-PDGFRB fusion gene in chronic myelomonocytic leukaemia. *Cancer Genetics and Cytogenetics*, 176(1), 67-71.

Curtiss, N., Bonifas, J., Lauchle, J., Balkman, J., Kratz, C., Emerling, B., Green, E., Le Beau, M., & Shannon, K. (2005). Isolation and analysis of candidate myeloid tumor suppressor genes from a commonly deleted segment of 7q22. *Genomics*, 85(5), 600-607.

Da Silveira Costa, A. R., Vasudevan, A., Krepischi, A., Rosenberg, C., & Maria de Lourdes, L. F. (2013). Single-nucleotide polymorphism-array improves detection rate of genomic alterations in core-binding factor leukaemia. *Medical Oncology*, 30(2), 1-7.

Dash, A. and Gilliland, D. (2001). Molecular genetics of acute myeloid leukaemia. Best Practice & Research Clinical Haematology, 14(1), pp.49-64.

De Braekeleer, E., Douet-Guilbert, N., Morel, F., Le Bris, M., Basinko, A., & De Braekeleer, M. (2012). ETV6 fusion genes in hematological malignancies: a review. *Leukemia Research*, 36(8), 945-961.

Deininger, M. W. N., Goldman, J. M., & Melo, J. V. (1996). The molecular biology of chronic myeloid leukaemia. Blood, 96(10), 3343-3356.

Delaunay, J., Vey, N., Leblanc, T., Fenaux, P., Rigal-Huguet, F., Witz, F., Lamy, T., Auvrignonm A., Blaise, D., Pigneux, A., Mugneret, F., Bastard, C., Dastugue, N., Van den Akker, J., Fière, D., Reiffers, J., Castaigne, S., Leverger, G., Harousseau, J. L.,

Dombret, H. (2003). Prognosis of inv(16)/t (16; 16) acute myeloid leukaemia (AML), a survey of 110 cases from the French AML Intergroup. *Blood*, 15, 102(2), 462-9.

Delhommeau, F., Dupont, S., Della Valle, V., James, C., Trannoy, S., Massé, A., Kosmider, O., Le Couedic, J. P., Robert, F., Alberdi, A., Lécluse, Y., Plo, I., Dreyfus, F. J., Marzac, C., Casadevall, N., Lacombe, C., Romana, S. P., Dessen, P., Soulier, J., Viguié, F., Fontenay, M., Vainchenker, W., & Bernard, O. A. (2009). Mutation in TET2 in myeloid cancers. *New England Journal of Medicine.*, 28, 360(22), 2289-301.

Deng, C. (2003). Roles of BRCA1 in DNA damage repair: a link between development and cancer. Human Molecular Genetics, 12(90001), pp.113R-123.

Dicker, F., Haferlach, C., Kern, W., Haferlach, T. and Schnittger, S. (2007). Trisomy 13 is strongly associated with AML1/RUNX1 mutations and increased FLT3 expression in acute myeloid leukemia. Blood, 110(4), pp.1308-1316.

Dohner, K., Brown, J., Hehmann, U., Hetzel, C., Stewart, J., Lowther, G., Scholl, C., Frohling, S., Cuneo, A., & Tsui, L. (1998). Molecular cytogenetic characterization of a critical region in bands 7q35-q36 commonly deleted in malignant myeloid disorders. *Blood*, 92(11), 4031-4035.

Downward, J. (2003). Targeting RAS signalling pathways in cancer therapy. Nat Rev Cancer, 3(1), pp.11-22.

Drabkin,H.A., Parsy,C., Ferguson,K., Guilhot,F., Lacotte,L., Roy,L., Zeng,C., Baron,A., Hunger,S.P., Varella-Garcia,M., Gemmill,R., Brizard,F., Brizard,A., and Roche,J. (2002). Quantitative HOX expression in chromosomally defined subsets of acute myelogenous leukemia. Leukemia 16, 186-195.

Driessens, G., Beck, B., Caauwe, A., Simons, B. and Blanpain, C. (2012). Defining the mode of tumour growth by clonal analysis. Nature, 488(7412), pp.527-530.

Edelmann, L., Pandita, R. and Morrow, B. (1999). Low-Copy Repeats Mediate the Common 3-Mb Deletion in Patients with Velo-cardio-facial Syndrome. The American Journal of Human Genetics, 64(4), pp.1076-1086.

Egger, G., Liang, G., Aparicio, A. and Jones, P. (2004). Epigenetics in human disease and prospects for epigenetic therapy. Nature, 429(6990), pp.457-463.

Ernst,P., Fisher,J.K., Avery,W., Wade,S., Foy,D., and Korsmeyer,S.J. (2004a). Definitive hematopoiesis requires the mixed-lineage leukemia gene. Dev. Cell 6, 437-443.

Ernst,P., Mabon,M., Davidson,A.J., Zon,L.I., and Korsmeyer,S.J. (2004b). An Mll-dependent Hox program drives hematopoietic progenitor expansion. Curr. Biol. 14, 2063-2069.

Fan, J. B., Gunderson, K. L., Bibikova, M., Yeakley, J. M., Chen, J., Wickham Garcia, E., ... & Barker, D. (2006). [3] Illumina Universal Bead Arrays. Methods in enzymology, 410, 57-73.

Farag, S. S., Archer, K. J., Mrózek, K., Ruppert, A. S., Carroll, A. J., Vardiman, J. W. & Bloomfield, C. D. (2006). Pretreatment cytogenetics add to other prognostic factors predicting complete remission and long-term outcome in patients 60 years of age or older with acute myeloid leukaemia: Results from Cancer and Leukemia Group B 8461. *Blood*, 108(1), 63-73.

Farrell, S., & Chow, G. (1992). Intrachromosomal insertion of chromosome 7. *Clinical Genetics*, 41(6), 299-302.

Fenaux, P. (1993). Effect of all transretinoic acid in newly diagnosed acute promyelocytic leukaemia. Results of a multicenter randomized trial. *Blood*, 82, 3241–3249.

Feuk, L., Carson, A. R., & Scherer, S. W. (2006). Structural variation in the human genome. *Nature Reviews Genetics*, 7(2), 85-97.

Finlay, C., Hinds, P. and Levine, A. (1989). The p53 proto-oncogene can act as a suppressor of transformation. Cell, 57(7), pp.1083-1093.

Fischer, K., Frohling, S., Scherer, S., Brown, J., Scholl, C., Stilgenbauer, S., Tsui, L., Lichter, P., & Dohner, H. (1997). Molecular cytogenetic delineation of deletions and translocations involving chromosome band 7q22 in myeloid leukemias. *Blood*, 89(6), 2036-2041.

Freeman, J. L., Perry, G. H., Feuk, L., Redon, R., McCarroll, S. A., Altshuler, D. M., & Lee, C. (2006). Copy number variation: new insights in genome diversity. *Genome Research*, 16(8), 949-961.

Friend, S., Bernards, R., Rogelj, S., Weinberg, R., Rapaport, J., Albert, D. and Dryja, T. (1986). A human DNA segment with properties of the gene that predisposes to retinoblastoma and osteosarcoma. Nature, 323(6089), pp.643-646.

Frohling, S. (2005). Genetics of Myeloid Malignancies: Pathogenetic and Clinical Implications. Journal of Clinical Oncology, 23(26), pp.6285-6295.

Fröhling, S., Schlenk, R. F., Stolze, I., Bihlmayr, J., Benner, A., Kreitmeier, S., & Döhner, K. (2004). CEBPA mutations in younger adults with acute myeloid leukaemia and normal cytogenetics: prognostic relevance and analysis of cooperating mutations. *Journal of Clinical Oncology*, 22(4), 624-633.

Gaidzik, V., & Döhner, K. (2008). Prognostic implications of gene mutations in acute myeloid leukaemia with normal cytogenetics. *Seminars in Oncology*, 35(4), 346-355.

Gelsi-Boyer, V., Trouplin, V., Adélaïde, J., Bonansea, J., Cervera, N., Carbuccia, N., Lagarde, A., Prebet, T., Nezri, M., Sainty, D., Olschwang, S., Xerri, L., Chaffanet, M., Mozziconacci, M. J., Vey, N., & Birnbaum, D. (2009). Mutations of polycomb-

associated gene ASXL1 in myelodysplastic syndromes and chronic myelomonocytic leukaemia. *British Journal of Haematology*, 145(6), 788-800.

Gerdes, J., Schwab, U., Lemke, H., & Stein, H. (1983). Production of a mouse monoclonal antibody reactive with a human nuclear antigen associate with proliferation. *Int J Cancer*, 31, 13-20.

Gerdes, J., Schwarting, R., & Stein, H. (1986). High proliferative activity of Reed Sternberg associated antigen Ki-1 positive cells in normal lymphod tissue. *Journal of Clinical Pathology,* 39, 993-7.

Gilliland D. G. (2001). Hematologic malignancies. *Current Opinions in Hematology*, 8, 189-191.

Gilliland, D. G., & Griffin, J. D. (2002). The roles of FLT3 in hematopoiesis and leukaemia. *Blood*, 100(5), 1532-1542.

Gotlib, J., Cools, J., Malone, J. M., Schrier, S. L., Gilliland, D. G., & Coutré, S. E. (2004). The FIP1L1-PDGFRα fusion tyrosine kinase in hypereosinophilic syndrome and chronic eosinophilic leukaemia: implications for diagnosis, classification, and management. *Blood*, 103(8), 2879-2891.

Green, A., & Beer, P. (2010). Somatic mutations of IDH1 and IDH2 in the leukemic transformation of myeloproliferative neoplasms. *New England Journal of Medicine*, 362(4), 369-370.

Gribble, S., Roberts, I., Grace, C., Andrews, K., Green, A., & Nacheva, E. (2000). Cytogenetics of the chronic myeloid leukaemia-derived cell line K562: karyotype clarification by multicolor fluorescence in situ hybridization, comparative genomic hybridization, and locus-specific fluorescence in situ hybridization. *Cancer Genetics and Cytogenetics*, 118(1), 1-8.

Grimwade, D., & Hills, R. K. (2009). Independent prognostic factors for AML outcome. *ASH Education Program Book*, 1, 385-395.

Grimwade, D., Hills, R. K., Moorman, A. V., Walker, H., Chatters, S., Goldstone, A. H., & Burnett, A. K. (2010). Refinement of cytogenetic classification in acute myeloid leukaemia: determination of prognostic significance of rare recurring chromosomal abnormalities among 5876 younger adult patients treated in the United Kingdom Medical Research Council Trials. *Blood*, 116(3), 354-365.

Grimwade, D., Walker, H., Harrison, G., Oliver, F., Chatters, S., Harrison, C. J., & Goldstone, A. H. (2001). The predictive value of hierarchical cytogenetic classification in older adults with acute myeloid leukaemia (AML), analysis of 1065 patients entered into the United Kingdom Medical Research Council AML11 Trial. *Blood*, 98(5), 1312-1320.

Grimwade, D., Walker, H., Oliver, F., Wheatley, K., Harrison, C., Harrison, G., Rees, J., Hann, I., Stevens, R., & Burnett, A. (1998). The importance of diagnostic

cytogenetics on outcome in AML: analysis of 1,612 patients entered into the MRC AML 10 Trial. *Blood*, 92(7), 2322-2333.

Hagemeijer, A., Hahlen, K., & Abels, J. (1981). Cytogenetic follow-up of patients with nonlymphocytic leukaemia. II. Acute nonlymphocytic leukaemia. *Cancer Genetics and Cytogenetics*, 3(2), 109-124.

Hagemeijer, A., Van Zanen, G., Smit, E., & Hahlen, K. (1979). Bone marrow karyotypes of children with nonlymphocytic leukaemia. *Pediatric Research*, 13(11), 1247-1254.

Hahm, C., Mun, Y. C., Seong, C. M., Chung, W. S., & Huh, J. (2012). Additional genomic aberrations identified by single nucleotide polymorphism array-based karyotyping in an acute myeloid leukaemia case with isolated del (20q) abnormality. *Annals of Laboratory Medicine*, 32(6), 445-449.

Han, E., Wu, Y., McCarter, R., Nelson, J., Richardson, A. and Hilsenbeck, S. (2004). Reproducibility, Sources of Variability, Pooling, and Sample Size: Important Considerations for the Design of High-Density Oligonucleotide Array Experiments. The Journals of Gerontology Series A: Biological Sciences and Medical Sciences, 59(4), pp.B306-B315.

Hasle, H., Alonzo, T., Auvrignon, A., Behar, C., Chang, M., Creutzig, U., Fischer, A., Forestier, E., Fynn, A., Haas, O., Harbott, J., Harrison, C., Heerema, N., van den Heuvel-Eibrink, M., Kaspers, G., Locatelli, F., Noellke, P., Polychronopoulou, S., Ravindranath, Y., Razzouk, B., Reinhardt, D., Savva, N., Stark, B., Suciu, S., Tsukimoto, I., Webb, D., Wojcik, D., Woods, W., Zimmermann, M., Niemeyer, C. and Raimondi, S. (2007). Monosomy 7 and deletion 7q in children and adolescents with acute myeloid leukemia: an international retrospective study. Blood, 109(11), pp.4641-4647.

Hastings, P., Ira, G. and Lupski, J. (2009). A Microhomology-Mediated Break-Induced Replication Model for the Origin of Human Copy Number Variation. PLoS Genetics, 5(1), p.e1000327.

Hauer, J., Tosi, S., Schuster, F., Harbott, J., Kolb, H., & Borkhardt, A. (2008). Graft versus leukaemia effect after haploidentical HSCT in a MLL-negative infant AML with HLXB9/ETV6 rearrangement. *Pediatric Blood & Cancer*, 50(4), 921-923.

Heim, S., & Mitelman, F. (2009). *Cancer Cytogenetics, Chromosomal and Molecular Genetic Aberrations of Tumor Cells*. 3rd edition. Hoboken, NJ: John Wiley & Sons Inc.

Heinrichs, S., Li, C. and Look, A. (2010). SNP array analysis in hematologic malignancies: avoiding false discoveries. Blood, 115(21), pp.4157--4161.

Hoang, T. (2004). The origin of hematopoietic cell type diversity. *Oncogene*, 23(43), 7188-7198.

Hollington, P., Neufing, P., Kalionis, B., Waring, P., Bentel, J., Wattchow, D., & Tilley, W. (2004). Expression and localization of homeodomain proteins DLX4, HB9 and HB24

in malignant and benign human colorectal tissues. *Anticancer Research*, 24(2B), 955-962.

Holmes, R., Keating, M. J., Cork, A., Broach, Y., Trujillo, J., Dalton, W. T., McCredie, K. B., Freireich, E. J. (1985). A unique pattern of central nervous system leukaemia in acute myelomonocytic leukaemia associated with inv(l6)(pl3q22). *Blood*, 65, 1071.

Hu, L., Ru, K., Zhang, L., Huang, Y., Zhu, X., Liu, H., Zetterberg, A., Cheng, T. and Miao, W. (2014). Fluorescence in situ hybridization (FISH): an increasingly demanded tool for biomarker research and personalized medicine. Biomark Res, 2(1), p.3.

Ishkanian, A., Malloff, C., Watson, S., deLeeuw, R., Chi, B., Coe, B., Snijders, A., Albertson, D., Pinkel, D., Marra, M., Ling, V., MacAulay, C. and Lam, W. (2004). A tiling resolution DNA microarray with complete coverage of the human genome. Nat Genet, 36(3), pp.299-303.

Iwama,A., Oguro,H., Negishi,M., Kato,Y., Morita,Y., Tsukui,H., Ema,H., Kamijo,T., Katoh-Fukui,Y., Koseki,H., van Lohuizen,M., and Nakauchi,H. (2004). Enhanced self-renewal of hematopoietic stem cells mediated by the polycomb gene product Bmi-1. Immunity. 21, 843-851.

Jamieson, C., Ailles, L., Dylla, S., Muijtjens, M., Jones, C., Zehnder, J., Gotlib, J., Li, K., Manz, M., Keating, A., Sawyers, C. and Weissman, I. (2004). Granulocyte–Macrophage Progenitors as Candidate Leukemic Stem Cells in Blast-Crisis CML. New England Journal of Medicine, 351(7), pp.657-667.

Johansson, B., Fioretos, T., & Mitelman, F. (2002). Cytogenetic and molecular genetic evolution of chronic myeloid leukaemia. *Acta Haematologica*, 107(2), 76-94.

Johnson, E., Scherer, S., Osborne, L., Tsui, L., Oscier, D., Mould, S., & Cotter, F. (1996). Molecular definition of a narrow interval at 7q22. 1 associated with myelodysplasia. *Blood*, 87(9), 3579-3586.

Joos, S., Falk, M., Lichter, P., Haluska, F., Henglein, B., Lenoir, G. and Bornkamm, G. (1992). Variable breakpoints in Burkitt lymphoma cells with chromosomal t(8; 14) translocation separate c-myc and the IgH locus up to several hundred kb. Hum Mol Genet, 1(8), pp.625-632.

Kainz, B., Heintel, D., Marculescu, R., Schwarzinger, I., Sperr, W., Le, T., & Jaeger, U. (2002). Variable prognostic value of FLT3 internal tandem duplications in patients with de novo AML and a normal karyotype, t(15; 17), t(8; 21) or inv(16). *Hematology Journal*, 3(1), 283-289.

Kawankar, N., Korgaonkar, S., Kerketta, L., Madkaikar, M., Jijina, F., Ghosh, K., Vundinti, B. R. (2011). DNA copy number changes and immunophenotype pattern in karyotypically normal acute myeloid leukaemia patients from Indian population. *PMID*: 22106833.

Keen-Kim, D., Nooraie, F., & Rao, P. (2007). Cytogenetic biomarkers for human cancer. *Frontiers in Bioscience: A Journal and Virtual Library*, 13, 5928-5949.

Kelly, L. M., & Gilliland, D. G. (2002). Genetics of myeloid leukemias. *Annu Rev Genomics Hum Genet*, 3, 179–198.

Kill, I. R. (1996). Localisation of the Ki-67 antigen within the nucleolus: evidence for a fibrillarin-deficient region of the dense fibrillar component. *J Cell Sci.* 109(6), 1253-1263.

Kim, H. J., Ahn, H. K., Jung, C. W., Moon, J. H., Park, C. H., Lee, K. O., & Kim, D. H. D. (2013). KIT D816 mutation associates with adverse outcomes in core binding factor acute myeloid leukaemia, especially in the subgroup with RUNX1/RUNX1T1 rearrangement. *Annals of Hematology*, 92(2), 163-171.

Kim, J., Park, J., Oh, A., Choi, E., Ryu, H., Kang, I., Koong, M., & Park, S. (2011). Duplication of intrachromosomal insertion segments 4q32→ q35 confirmed by comparative genomic hybridization and fluorescent in situ hybridization. *Clinical and Experimental Reproductive Medicine*, 38(4), 238-241.

Kim, J., Park, T., Song, J., Lee, K., Lee, S., Cheong, J. and Choi, J. (2008). Tetrasomy 8 in a Patient with Acute Monoblastic Leukemia. Korean J Lab Med, 28(4), p.262.

Knudson, A. G. (2000). Chasing the cancer demon. *Annu Rev Genet*, 34, 1-19.

Kogan, S. C., Lagasse, E., Atwater, S., Bae, S. C., Weissman, I., Ito, Y. & Bishop, J. M. (1998). The PEBP2b–MYH11 fusion created by inv(16)(p13;q22) in myeloid leukaemia impairs neutrophil maturation and contributes to granulocytic dysplasia. *Proceedings of the National Academy of Sciences of the United States of America,* 95, 11863–11868.

Kosmider, O. and Moreau-Gachelin, F. (2006). From Mice to Human: The “Two-Hit Model” of Leukemogenesis. Cell Cycle, 5(6), pp.569-570.

Kottaridis, P. D., Gale, R. E., Frew, M. E., Harrison, G., Langabeer, S. E., Belton, A. A., & Linch, D. C. (2001). The presence of a FLT3 internal tandem duplication in patients with acute myeloid leukaemia (AML) adds important prognostic information to cytogenetic risk group and response to the first cycle of chemotherapy: analysis of 854 patients from the United Kingdom Medical Research Council AML 10 and 12 trials. *Blood*, 98(6), 1752-1759.

Kuhn, K., Baker, S., Chudin, E., Lieu, M., Oeser, S., Bennett, H., Rigault, P., Barker, D., McDaniel, T. and Chee, M. (2004). A novel, high-performance random array platform for quantitative gene expression profiling. Genome research, 14(11), pp.2347--2356.

Kühn, M. W., Radtke, I., Bullinger, L., Goorha, S., Cheng, J., Edelmann, J., & Downing, J. R. (2012). High-resolution genomic profiling of adult and pediatric core-binding factor acute myeloid leukaemia reveals new recurrent genomic alterations. *Blood*, 119(10), e67-e75.

Kundu, M., Chen, A., Anderson, S., Kirby, M., Xu, L., Castilla, L. H., & Liu, P. P. (2002). Role of Cbfb in hematopoiesis and perturbations resulting from expression of the leukemogenic fusion gene Cbfb-MYH11. *Blood*, 100(7), 2449-2456.

Kuroiwa, T. (1977). Studies on mitochondrial structure and function in Physarum polycephalum. V. Behaviour of mitochondrial nucleoids throughout mitochondrial division cycle. The Journal of Cell Biology, 72(3), pp.687-694.

Kuroiwa, T., Kawano, S. and Hizume, M. (1977). Studies on mitochondrial structure and function in Physarum polycephalum. V. Behaviour of mitochondrial nucleoids throughout mitochondrial division cycle. The Journal of cell biology, 72(3), pp.687--694.

LaFramboise, T. (2009). Single nucleotide polymorphism arrays: a decade of biological, computational and technological advances. Nucleic acids research, p.552.

Lawrence,H.J., Christensen,J., Fong,S., Hu,Y.L., Weissman,I., Sauvageau,G., Humphries,R.K., and Largman,C. (2005). Loss of expression of the HOXA-9 homeobox gene impairs the proliferation and repopulating ability of hematopoietic stem cells. Blood.

Le Beau, M. M., Larson, R. A., Bitter, M. A., Vardiman, J. W., Golomb, H. M., & Rowley, J. D. (1983). Association of an inversion of chromosome 16 with abnormal marrow eosinophils in acute myelomonocytic leukaemia: a unique cytogenetic–clinicopathological association. *New England Journal of Medicine*, 309(11), 630-636.

Le Caignec, C. (2005). Detection of genomic imbalances by array based comparative genomic hybridisation in fetuses with multiple malformations. Journal of Medical Genetics, 42(2), pp.121-128.

Le Doussal, V., Tubiana-Hulin, M., Friedman, S., Hacene, K., Spyratos, F., Brunet M. (1989). Prognostic value of histologic grade nuclear components of Scarff–Bloom–Richardson (SBR), an improved score modification based on a multivariate analysis of 1262 invasive ductal breast carcinomas. *Cancer*, 64, 1914–1921.

Le Scouarnec, S., & Gribble, S. M. (2012). Characterising chromosome rearrangements: recent technical advances in molecular cytogenetics. *Heredity*, 108(1), 75-85.

Lécuyer, E., & Hoang, T. (2004). SCL: from the origin of hematopoiesis to stem cells and leukaemia. *Experimental Hematology*, 32(1), 11-24.

Lessard,J. and Sauvageau,G. (2003). Bmi-1 determines the proliferative capacity of normal and leukaemic stem cells. Nature 423, 255-260.

Ley, T. J., Ding, L., Walter, M. J., McLellan, M. D., Lamprecht, T., Larson, D. E., Kandoth, C., Payton, J. E., Baty, J., & Welch, J. (2010). DNMT3A mutations in acute myeloid leukaemia. *New England Journal of Medicine*, 363, 2424-2433.

Liang, H., Castro, P., Ma, J., & Nagarajan, L. (2005). Finer delineation and transcript map of the 7q31 locus deleted in myeloid neoplasms. *Cancer Genetics and Cytogenetics*, 162(2), 151-159.

Liang, H., Fairman, J., Claxton, D., Nowell, P., Green, E., & Nagarajan, L. (1998). Molecular anatomy of chromosome 7q deletions in myeloid neoplasms: evidence for multiple critical loci. *Proceedings of the National Academy of Sciences*, 95(7), 3781-3785.

Licht, J. D. (2006). Reconstructing a disease: what essential features of the retinoic acid receptor fusion oncoproteins generate acute promyelocytic leukaemia? *Cancer Cell*, 9, 73-4.

Lin, C., Yang, L., & Rosenfeld, M. (2011). Molecular logic underlying chromosomal translocations, random or non-random? *Advances in Cancer Research*, 113, 241-279.

Liu, S., Li, Q., Pang, W., Bo, L., Qin, S., Liu, X., Teng, Q., Qian, L., & Wang, J. (2001). A new complex variant t(4; 15; 17) in acute promyelocytic leukaemia: fluorescence in situ hybridization confirmation and literature review. *Cancer Genetics and Cytogenetics*, 130(1), 33-37.

Lord, B. I., Testa, N. G. and Hendry, J. H. (1975). The relative spatial distributions of CFUs and CFUc in the normal mouse femur. Blood 46, 65-72.

Löwenberg., B., van Putten WL, Touw IP, Delwel., R., Santini V. (1993). Autonomous proliferation of leukemic cells in vitro as a determinant of prognosis in adult acute myeloid leukaemia. *New England Journal of Medicine*; 328, 614-619.

Lozzio, C. B., and Lozzio, B. B. 1975., Human Chronic Myelogenous Leukemia Cell-Line With Positive Philadelphia Chromosome. *Blood*, 45(3).

Lybaek, H., Prescott, T., Hovl, Breilid, H., Stansberg, C., Steen, V., & Houge, G. (2009). An 8.9 Mb 19p13 duplication associated with precocious puberty and a sporadic 3.9 Mb 2q23.3q24.1 deletion containing NR4A2 in mentally retarded members of a family with an intrachromosomal 19p-into-19q between-arm insertion. *European Journal of Human Genetics*, 17(7), 904-910.

Maciejewski, J. P., & Mufti, G. J. (2008). Whole genome scanning as a cytogenetic tool in hematologic malignancies. *Blood*, 112(4), 965-974.

Madan, K. (1995). Paracentric inversions: a review. *Human Genetics*, 96(5), 503-515.

Madan, K., & Menko, F. (1992). Intrachromosomal insertions: a case report and a review. *Human Genetics*, 89(1), 1-9.

Marchesi, F., Annibali, O., Cerchiara, E., Tirindelli, M., & Avvisati, G. (2011). Cytogenetic abnormalities in adult non-promyelocytic acute myeloid leukaemia: a concise review. *Critical Reviews in Oncology/Hematology*, 80(3), 331-346.

Mardis, E. R., Ding, L., Dooling, D. J., Larson, D. E., McLellan, M. D., Chen, K., Koboldt, D. C., Fulton, R. S., Delehaunty, K. D., & McGrath, S. D. (2009). Recurring mutations

found by sequencing an acute myeloid leukaemia genome. *New England Journal of Medicine*, 361, 1058-1066.

Marschalek, R. (2011). Mechanisms of leukemogenesis by MLL fusion proteins. *British Journal of Haematology*, 152(2), 141-154.

Mauritzson, N., Johansson, B., Albin, M., Billstrom, R., Ahlgren, T., Mikoczy, Z., Nilsson, P., Hagmar, L., & Mitelman, F. (1999). A single-center population-based consecutive series of 1500 cytogenetically investigated adult hematological malignancies: karyotypic features in relation to morphology, age and gender. *European Journal of Haematology*, 62(2), 95-102.

Mazzali,M., Kipari,T., Ophascharoensuk,V., Wesson,J.A., Johnson,R., and Hughes,J. (2002). Osteopontin--a molecule for all seasons. QJM. 95, 3-13.

McNerney, M., Brown, C., Wang, X., Bartom, E., Karmakar, S., B., Lamudi, C., Yu, S., Ko, J., Sandal, B. P., Stricker, T., Anastasi, J., Grossman, R. l., Cunningham, J. M., Le Beau, M. M., & White, K. P. (2013). CUX1 is a haploinsufficient tumor suppressor gene on chromosome 7 frequently inactivated in acute myeloid leukaemia. *Blood*, 121(6), 975-983.

Meani, N., & Alcalay, M. (2009). Role of nucleophosmin in acute myeloid leukaemia. *Expert Review of Anticancer Therapy*, 9(9), 1283-1294.

Mehta, Bain, Fitchett, Shah, and Secker-Walker, (1998). Trisomy 13 and myeloid malignancy - characteristic blast cell morphology: a United Kingdom Cancer Cytogenetics Group survey. British Journal of Haematology, 101(4), pp.749-752.

Mercher, T., Busson-Le Coniat, M., Nguyen Khac, F., Ballerini, P., Mauchauffé, M., Bui, H., Pellegrino, B., Radford, I., Valensi, F., Mugneret, F.,Dastugue, N., Bernard, O. A, & Berger, R. (2002). Recurrence of OTT-MAL fusion in t(1;22) of infant AML-M7. *Genes Chromosomes Cancer*, 33(1), 22-8.

Moe, W., Kazutaka, K., Yasushi, M., Tomoko, H., Masafumi, T., Shigeki, O., Hisashi, S., & Shuichi, M. (2008). Diagnosis of acute myeloid leukaemia according to the WHO classification in the Japan Adult Leukemia Study Group AML-97 protocol. *Int J Hematol*, 87, 144–151.

Moorman, A. V., Roman, E., Willett, E. V., Dovey, G. J., Cartwright, R. A., & Morgan, G. J. (2001). Karyotype and age in acute myeloid leukaemia: are they linked? *Cancer Genetics and Cytogenetics*, 126(2), 155-161.

Moreau-Gachelin F. (2006).Lessons from models of murine erythroleukemia to acute myeloid leukemia (AML): proof-of-principle of co-operativity in AML. Haematological, 91(12):1644-52.

Morris, C. M. (2011). Chronic myeloid leukaemia: cytogenetic methods and applications for diagnosis and treatment. *Methods Mol Biol.*, 730, 33-61.

Mrózek, K. (2008). Cytogenetic, molecular genetic, and clinical characteristics of acute myeloid leukaemia with a complex karyotype. *Seminars in Oncology*, 35(4), 365-377.

Mrózek, K., Heinonen, K., & Bloomfield, C. (2000). Prognostic value of cytogenetic findings in adults with acute myeloid leukaemia. *International Journal of Hematology*, 72, 261-271.

Mrózek, K., Heinonen, K., & Bloomfield, C. D. (2001). Clinical importance of cytogenetics in acute myeloid leukaemia. *Best Practice & Research Clinical Haematology*, 14(1), 19-47.

Mrózek, K., Marcucci, G., Paschka, P., & Bloomfield, C. D. (2008). Advances in molecular genetics and treatment of core-binding factor acute myeloid leukaemia. *Curr Opin Oncol*, 20(6), 711-718.

Mullighan, C. G., Su, X., Zhang, J., Radtke, I., Phillips, L. A., Miller, C. B., & Downing, J. R. (2009). Deletion of IKZF1 and prognosis in acute lymphoblastic leukaemia. *New England Journal of Medicine*, 360(5), 470-480.

Nagel, S., Kaufmann, M., Scherr, M., Drexler, H. G., & MacLeod, R. A. (2005). Activation of HLXB9 by juxtaposition with MYB via formation of t(6; 7)(q23; q36) in an AML-M4 cell line (GDM-1). *Genes, Chromosomes and Cancer*, 42(2), 170-178.

Naumann, S., Reutzel, D., Speicher, M., & Decker, H. (2001). Complete karyotype characterization of the K562 cell line by combined application of G-banding, multiplex-fluorescence in situ hybridization, fluorescence in situ hybridization, and comparative genomic hybridization. *Leukemia Research*, 25(4), 313-322.

Nawata, H., Kashino, G., Tano, K., Daino, K., Shimada, Y., Kugoh, H., Oshimura, M. and Watanabe, M. (2011). Dysregulation of Gene Expression in the Artificial Human Trisomy Cells of Chromosome 8 Associated with Transformed Cell Phenotypes. PLoS ONE, 6(9), p.e25319.

Nilsson,S.K., Johnston,H.M., and Coverdale,J.A. (2001). Spatial localization of transplanted hemopoietic stem cells: inferences for the localization of stem cell niches. Blood 97, 2293-2299.

Nilsson,S.K., Johnston,H.M., Whitty,G.A., Williams,B., Webb,R.J., Denhardt,D.T., Bertoncello,I., Bendall,L.J., Simmons,P.J., and Haylock,D.N. (2005). Osteopontin, a key component of the hematopoietic stem cell niche and regulator of primitive hematopoietic progenitor cells. Blood 106, 1232-1239.

Ohki, M, (1993). Molecular basis of the t(8; 21) translocation in acute myeloid leukaemia. *Semin Cancer Biol.*, 4(6), 369-75.

Owen, C., Fitzgibbon, J., & Paschka, P. (2010). The clinical relevance of Wilms Tumour 1 (WT1) gene mutations in acute leukaemia. *Hematol Oncol*, 28, 13-19.

Pabst, T., Mueller, B. U., Schnittger, S., Behre, G., Hiddemann, W., & Tenen, D. G. (1999). Dominant negative mutations of the tumor suppressor CCAAT/enhancer binding protein a (C/EBP a), role in acute myeloid leukaemia. *Blood*, 94(suppl. 1), 624a.

Park, J., Kim, M., Lim, J., Kim, Y., Han, K., Lee, J., Chung, N., Cho, B., & Kim, H. (2009). Three-way complex translocations in infant acute myeloid leukaemia with t(7; 12)(q36; p13): the incidence and correlation of a HLXB9 overexpression. *Cancer Genetics and Cytogenetics*, 191(2), 102-105.

Park, S., Chi, H., Min, S., Park, B., Jang, S. and Park, C. (2011). Prognostic impact of c-KIT mutations in core binding factor acute myeloid leukemia. Leukemia Research, 35(10), pp.1376-1383.

Paschka, P., Du, J., Schlenk, R. F., Gaidzik, V. I., Bullinger, L., Corbacioglu, A., & Döhner, K. (2013). Secondary genetic lesions in acute myeloid leukaemia with inv(16) or t(16; 16), a study of the German-Austrian AML Study Group (AMLSG). *Blood*, 121(1), 170-177.

Paschka, P., Marcucci, G., Ruppert, A. S., Mrózek, K., Chen, H., Kittles, R. A., Vukosavljevic, T., Perrotti, D., Vardiman, G. W., Carroll, J. A., Kolitz, J. E., Larson, R. A., & Bloomfield, C. D. (2006). Adverse prognostic significance of kit mutations in adult acute myeloid leukaemia with inv(16) and t(8;21), a cancer and Leukemia Group B Study. *J Clin Oncol*., 24(24), 3904-11.

Patel, P., Bakshi, S., Trivedi, P., Patel, D., Shukla, S., Brahmbhatt, M., Dalal, E., Purani, S. and Shah, P. (2012). Trisomy 8 in leukemia: A GCRI experience. Indian J Hum Genet, 18(1), p.106.

Pecorino, L., 2008. Molecular Biology of Cancer- Mechanisms, Targets and Therapeutics, Second Edition.

Peeters, J. and Van der Spek, P. (2005). Growing Applications and Advancements in Microarray Technology and Analysis Tools. CBB, 43(1), pp.149-166.

Perkins, D., Brennan, S., Carstairs, K., Bailey, D., Pantalony, D., Poon, A., Fern, Es, B., & Dube, I. (1997). Regional cancer cytogenetics: a report on 1,143 diagnostic cases. *Cancer Genetics and Cytogenetics*, 96(1), 64-80.

Pinkel, D., Segraves, R., Sudar, D., Clark, S., Poole, I., Kowbel, D., ... & Albertson, D. G. (1998). High resolution analysis of DNA copy number variation using comparative genomic hybridization to microarrays. Nature genetics, 20(2), 207-211.

Ponta,H., Sherman,L., and Herrlich,P.A. (2003). CD44: from adhesion molecules to signalling regulators. Nat. Rev. Mol. Cell Biol. 4, 33-45.

Preudhomme, C., Sagot, C., Boissel, N., Cayuela, J. M., Tigaud, I., de Botton, S., & Dombret, H. (2002). Favorable prognostic significance of CEBPA mutations in patients with de novo acute myeloid leukaemia: a study from the Acute Leukemia French Association (ALFA). *Blood*, 100(8), 2717-2723.

Querzoli, P., Albonico, G., Ferretti, S., Rinaldi, R., Magri, E., Indelli, M., Nenci I. (1996). MIB- 1 proliferative activity in invasive breast cancer measured by image analysis. *J Clin Pathol*. ; 49, 926-930.

Radtke, I., Mullighan, C. G., Ishii, M., Su, X., Cheng, J., Ma, J., & Downing, J. R. (2009). Genomic analysis reveals few genetic alterations in pediatric acute myeloid leukaemia. *Proceedings of the National Academy of Sciences*, 106(31), 12944-12949.

Raimondi, S., Chang, M., Ravindranath, Y., Behm, F., Gresik, M., Steuber, C., Weinstein, H., & Carroll, A. (1999). Chromosomal abnormalities in 478 children with acute myeloid leukaemia: clinical characteristics and treatment outcome in a cooperative pediatric oncology group study-POG 8821. *Blood*, 94(11), 3707-3716.

Rambaldi, A., Bettoni, S., Tosi, S., Giudici, G., Schirò, R., Borleri, G. M., Abbate, M., Chiaffarino, F., Colotta, F., Barbui, T., Biondi A. (1993). Establishment and characterization of a new granulocyte- macrophage colony-stimulating factor-dependent and interleukin-3-dependent human acute myeloid leukaemia cell line (GF-D8). *Blood*, 81(5), 1376-1383.

Reiter, A., Lengfelder, E., & Grimwade, D. (2004). Pathogenesis, diagnosis and monitoring of residual disease in acute promyelocytic leukaemia. *Acta Haematol*. ; 112(1-2), 55-67.

Reiter, E., Greinix, H., Rabitsch, W., Keil, F., Schwarzinger, I., Jaeger, U., Lechner, K., Worel, N., Streubel, B., Fonatsch, C., Mitterbauer, G., & Kalhs, P. (2000). Low curative potential of bone marrow transplantation for highly aggressive acute myelogenous leukaemia with inversioin inv(3)(q21q26) or homologous translocation t(3;3) (q21;q26). *Ann Hematol.*, 79(7), 374-7.

Reiter, L., Hastings, P., Nelis, E., De Jonghe, P., Van Broeckhoven, C. and Lupski, J. (1998). Human Meiotic Recombination Products Revealed by Sequencing a Hotspot for Homologous Strand Exchange in Multiple HNPP Deletion Patients. The American Journal of Human Genetics, 62(5), pp.1023-1033.

Renneville, A., Roumier, C., Biggio, V., Nibourel, O., Boissel, N., Fenaux, P. and Preudhomme, C. (2008). Cooperating gene mutations in acute myeloid leukemia: a review of the literature. Leukemia, 22(5), pp.915-931.

Roche-Lestienne, C., Richebourg, S., Laï, J., Andrieux, J., Soenen-Cornu, V. and Geffroy, S. (2006). Isolated tetrasomy 13: a fifth case report of a rare chromosome abnormality associated with poorly differentiated acute myeloid leukemia. Cancer Genetics and Cytogenetics, 168(2), pp.181-182.

Romana, S. P., Coniat, M. L., & Berger, R. (1994). t(12; 21), a new recurrent translocation in acute lymphoblastic leukaemia. *Genes, Chromosomes and Cancer*, 9(3), 186-191.

Rous, (1911). A Sarcoma of the Fowl Transmissible by an Agent Separable from the Tumor Cells. The American Journal of the Medical Sciences, 142(2), p.312.

Sahoo, T., Cheung, S., Ward, P., Darilek, S., Patel, A., del Gaudio, D., Kang, S., Lalani, S., Li, J., McAdoo, S., Burke, A., Shaw, C., Stankiewicz, P., Chinault, A., Van den Veyver, I., Roa, B., Beaudet, A. and Eng, C. (2006). Prenatal diagnosis of chromosomal abnormalities using array-based comparative genomic hybridization. Genet Med, 8(11), pp.719-727.

Sanganalmath, S. K., Abdel-Latif, A., Bolli, R., Xuan, Y. T., & Dawn, B. (2011). Hematopoietic cytokines for cardiac repair: mobilization of bone marrow cells and beyond. *Basic Research in Cardiology*, 106(5), 709-733.

Satake, N., Maseki, N., Nishiyama, M., Kobayashi, H., Sakurai, M., Inaba, H., Katano, N., Horikoshi, Y., Eguchi, H., Miyake, M., & others, (1999). Chromosome abnormalities and MLL rearrangements in acute myeloid leukaemia of infants. *Leukemia* (08876924), 13(7).

Sauvageau,G., Thorsteinsdottir,U., Eaves,C.J., Lawrence,H.J., Largman,C., Lansdorp,P.M., and Humphries,R.K. (1995). Overexpression of HOXB4 in hematopoietic cells causes the selective expansion of more primitive populations in vitro and in vivo. Genes Dev. 9, 1753-1765.

Schnittger, S. (2002). Analysis of FLT3 length mutations in 1003 patients with acute myeloid leukemia: correlation to cytogenetics, FAB subtype, and prognosis in the AMLCG study and usefulness as a marker for the detection of minimal residual disease. Blood, 100(1), pp.59-66.

Schnittger, S., Bacher, U., Haferlach, C., Kern, W., Alpermann, T. and Haferlach, T. (2011). Clinical impact of FLT3 mutation load in acute promyelocytic leukemia with t(15;17)/PML-RARA. Haematologica, 96(12), pp.1799-1807.

Schnittger, S., Schoch, C., Dugas, M., Kern, W., Staib, P., Wuchter, C., & Hiddemann, W. (2002). Analysis of FLT3 length mutations in 1003 patients with acute myeloid leukaemia: correlation to cytogenetics, FAB subtype, and prognosis in the AMLCG study and usefulness as a marker for the detection of minimal residual disease. *Blood*, 100(1), 59-66.

Schnittger, S., Schoch, C., Kern, W., Mecucci, C., Tschulik, C., Martelli, M. F., & Falini, B. (2005). Nucleophosmin gene mutations are predictors of favorable prognosis in acute myelogenous leukaemia with a normal karyotype. *Blood*, 106(12), 3733-3739.

Schoch, C., Kern, W., Schnittger, S., Hiddemann, W., & Haferlach, T. (2003). Karyotype is an independent prognostic parameter in therapy-related acute myeloid leukaemia (t-AML), an analysis of 93 patients with t-AML in comparison to 1091 patients with de novo AML. *Leukemia*, 18(1), 120-125.

Schoch, C., Kohlmann, A., Dugas, M., Kern, W., Schnittger, S. and Haferlach, T. (2006). Impact of trisomy 8 on expression of genes located on chromosome 8 in different AML subgroups. Genes, Chromosomes and Cancer, 45(12), pp.1164-1168.

Scholzen, T., and Gerdes, J. (2000). The Ki-67 protein: from the known and the unknown. *Journal of Cellular Physiology*, 182, 311-322.

Schoofs, T., Berdel, W. and Müller-Tidow, C. (2013). Origins of aberrant DNA methylation in acute myeloid leukemia. Leukemia, 28(1), pp.1-14.

Schwind, S., Edwards, C. G., Nicolet, D., Mrózek, K., Maharry, K., & Wu, Y. Z. (2013). inv(16)/ t(16;16) acute myeloid leukaemia with non-typeA CBFB–MYH11 fusions associated with distinct clinical and genetic features and lack KIT mutations. *Blood*, 121, 385-91.

Seltzer R, Richmond TA, Pofahl NJ, Green RD, Eis PS, Nair P et al. (2005). Analysis of chromosome breakpoints in neuroblastoma at sub-kilobase resolution using fine-tilling oligonucleotide array CGH. Genes Chromosomes Cancer 44: 305–319.

Shaffer, L., Kashork, C., Saleki, R., Rorem, E., Sundin, K., Ballif, B. and Bejjani, B. (2006). Targeted genomic microarray analysis for identification of chromosome abnormalities in 1500 consecutive clinical cases. The Journal of Pediatrics, 149(1), pp.98-102.e5.

Shaikh, T. (2007). Oligonucleotide arrays for high-resolution analysis of copy number alteration in mental retardation/multiple congenital anomalies. Genet Med, 9(9), pp.617-625.

Shin, S., Koo, S., Kwon, K., Park, J., Song, J., Ko, Y. and Jo, D. (2009). Chromosome 8 pentasomy with partial tandem duplication of 11q23 in a case of de novo acute myeloid leukemia. Cancer Genetics and Cytogenetics, 194(1), pp.44-47.

Silva, F., Lind, A., Brouwer-Mandema, G., Valk, P. and Giphart-Gassler, M. (2007). Trisomy 13 correlates with RUNX1 mutation and increased FLT3 expression in AML-M0 patients. Haematologica, 92(8), pp.1123-1126.

Simmons, H., Oseth, L., Nguyen, P., O'Leary, M., Conklin, K., & Hirsch, B. (2002). Cytogenetic and molecular heterogeneity of 7q36/12p13 rearrangements in childhood AML. *Leukemia* (08876924), 16(12).

Simmons,P.J., Zannettino,A., Gronthos,S., and Leavesley,D. (1994). Potential adhesion mechanisms for localisation of haemopoietic progenitors to bone marrow stroma. Leuk. Lymphoma 12, 353-363.

Slater, R., Kroes, W., Olde Weghuis, D., van den Berg, E., Smit, E., van Wering, E., Hahlen, K., Carroll, A., Raimondi, S., & Beverloo, H. (2001). t(7; 12)(q36; p13) and t(7; 12)(q32; p13)-translocations involving ETV6 in children 18 months of age or younger with myeloid disorders. *Leukemia* (08876924), 15(6).

Slovak, M. L., Kopecky, K. J., Cassileth, P. A., Harrington, D. H., Theil, K. S., Mohamed, A., & Appelbaum, F. R. (2000). Karyotypic analysis predicts outcome of preremission and postremission therapy in adult acute myeloid leukaemia: a Southwest Oncology Group/Eastern Cooperative Oncology Group Study. *Blood*, 96(13), 4075-4083.

Smith, M., Barnett, M., Bassan, R., Gatta, G., Tondini, C., Kern, W. (2004). Adult acute myeloid leukaemia. *Critical Reviews in Oncology/Hematology*, 50, 197-222.

Stankiewicz, P. and Lupski, J. (2002). Genome architecture, rearrangements and genomic disorders. Trends in Genetics, 18(2), pp.74-82.

STEHELIN, D., VARMUS, H., BISHOP, J. and VOGT, P. (1976). DNA related to the transforming gene(s) of avian sarcoma viruses is present in normal avian DNA. Nature, 260(5547), pp.170-173.

Sun, X., Medeiros, L., Lu, D., Rassidakis, G. and Bueso-Ramos, C. (2003). Dysplasia and high proliferation rate are common in acute myeloid leukaemia with inv (16)(p13q22). *American journal of clinical pathology,* 120(2), pp.236--245.

Takahashi, S. (2011). Current findings for recurring mutations in acute myeloid leukaemia. *J Hematol Oncol*, *4*, 36.

Takahashi, T., Harada, S., Oki, M., Yoshimoto, M., Tsujisaki, M., Maemori, M. and Sakai, H. (2006). Acute myelogenous leukemia with monosomy 7 in a Hiroshima survivor 60 years after the atomic bomb. Cancer Genetics and Cytogenetics, 170(2), pp.182-183.

Taketani, T., Taki, T., Sako, M., Ishii, T., Yamaguchi, S., & Hayashi, Y. (2008). MNX1-ETV6 fusion gene in an acute megakaryoblastic leukaemia and expression of the MNX1gene in leukaemia and normal B cell lines. *Cancer Genetics and Cytogenetics*, 186(2), 115-119.

Tang, J. L., Hou, H. A., Chen, C. Y., Liu, C. Y., Chou, W. C., Tseng, M. H., Huang, C. F., Lee, F. Y., Liu, M. C., Yao, M., Huang, S. Y., Ko, B. S., Hsu, S. C., Wu, S. J., Tsay, W., Chen, Y. C., Lin, L., & Tien, H. F. (2009). AML1/RUNX1 mutations in 470 adult patients with de novo acute myeloid leukaemia: prognostic implication and interaction with other gene alterations. *Blood*, 114(26), 5352-61.

Tetrasomy 13 as the sole cytogenetic abnormality in acute myeloid leukemia M1 without maturation. Cancer Genetics and Cytogenetics 135, pp. 192–195.

Thiede, C. (2002). Analysis of FLT3-activating mutations in 979 patients with acute myelogenous leukemia: association with FAB subtypes and identification of subgroups with poor prognosis. Blood, 99(12), pp.4326-4335.

Thiede, C., Steudel, C., Mohr, B., Schaich, M., kel US, Platzbecker, U., Wermke, M., User, M. B., Ritter, M., Neubauer, A., Ehninger, G., & Illmer, T. (2002). Analysis of FLT3-activating mutations in 979 patients with acute myelogenous leukaemia: association with FAB subtypes and identification of subgroups with poor prognosis. *Blood*, 99, 12.

Thorsteinsdottir,U., Mamo,A., Kroon,E., Jerome,L., Bijl,J., Lawrence,H.J., Humphries,K., and Sauvageau,G. (2002). Overexpression of the myeloid leukemia-associated Hoxa9 gene in bone marrow cells induces stem cell expansion. Blood 99, 121-129.

Thorsteinsdottir,U., Sauvageau,G., and Humphries,R.K. (1999). Enhanced in vivo regenerative potential of HOXB4-transduced hematopoietic stem cells with regulation of their pool size. Blood 94, 2605-2612.

Till, J. E., McCulloch, E. A., & Siminovitch, L. (1964). A STOCHASTIC MODEL OF STEM CELL PROLIFERATION, BASED ON THE GROWTH OF SPLEEN COLONY-FORMING CELLS. Proceedings of the National Academy of Sciences of the United States of America, 51(1), 29–36.

Toruner, G., Streck, D., Schwalb, M. and Dermody, J. (2007). An oligonucleotide based array-CGH system for detection of genome wide copy number changes including subtelomeric regions for genetic evaluation of mental retardation. American Journal of Medical Genetics Part A, 143A(8), pp.824-829.

Tosi, S., Cabot, G., Giudici, G., Attuati, V., Mor, I. P., Rambaldi, A., Dohner, H., & Biondi, A. (1996). Detection of the breakpoint cluster region-ABL fusion in chronic myeloid leukaemia with variant Philadelphia chromosome translocations by in situ hybridization. *Cancer Genetics and Cytogenetics*, 89(2), 153-156.

Tosi, S., Giudici, G., Mosna, G., Harbott, J., Specchia, G., Grosveld, G., Privitera, E., Kearney, L., Biondi, A., & Cazzaniga, G. (1998). Identification of new partner chromosomes involved in fusions with the ETV6 (TEL) gene in hematologic malignancies. *Genes, Chromosomes and Cancer*, 21(3), 223-229.

Tosi, S., Giudici, G., Rambaldi, A., Scherer, S., Bray-Ward, P., Dirscherl, L., Biondi, A., & Kearney, L. (1999). Characterization of the human myeloid leukaemia-derived cell line GF-D8 by multiplex fluorescence in situ hybridization, subtelomeric probes, and comparative genomic hybridization. *Genes, Chromosomes and Cancer*, 24(3), 213-221.

Tosi, S., Harbott, J., Teigler-Schlegel, A., Haas, O., Pirc-Danoewinata, H., Harrison, C., Biondi, A., Cazzaniga, G., Kempski, H., Scherer, S., & others, (2000). t(7; 12)(q36; p13), a new recurrent translocation involving ETV6 in infant leukaemia. *Genes, Chromosomes and Cancer*, 29(4), 325-332.

Tosi, S., Hughes, J., Scherer, S., Nakabayashi, K., Harbott, J., Haas, O., Cazzaniga, G., Biondi, A., Kempski, H., & Kearney, L. (2003). Heterogeneity of the 7q36 breakpoints in the t(7; 12) involving ETV6 in infant leukaemia. *Genes, Chromosomes and Cancer*, 38(2), 191-200.

Tosi, S., Scherer, S., Giudici, G., Czepulkowski, B., Biondi, A., & Kearney, L. (1999). Delineation of multiple deleted regions in 7q in myeloid disorders. *Genes, Chromosomes and Cancer*, 25(4), 384-392.

Trihia, H., Murray, S., Price, K., Gelber, R. D., Golouh, R., Goldhirsch, A., Coates, A. S., Collins, J., Castiglione-Gertsch, M., & Gusterson, B. A. (2003). Ki-67 Expression in breast carcinoma: its association with grading systems, clinical parameters, and other prognostic factors-a surrogate marker? *Cancer*, 97, 1321-1331.

Urban, A., Korbel, J., Selzer, R., Richmond, T., Hacker, A., Popescu, G., Cubells, J., Green, R., Emanuel, B., Gerstein, M., Weissman, S. and Snyder, M. (2006). High-resolution

mapping of DNA copy alterations in human chromosome 22 using high-density tiling oligonucleotide arrays. Proceedings of the National Academy of Sciences, 103(12), pp.4534-4539.

van Binsbergen, E. (2011). Origins and Breakpoint Analyses of Copy Number Variations: Up Close and Personal. *Cytogenetic and Genome Research*, 135(3-4), pp.271-276.

Van Handel, B., Prashad, S. L., Hassanzadeh-Kiabi, N., Huang, A., Magnusson, M., Atanassova, B., & Mikkola, H. K. (2010). The first trimester human placenta is a site for terminal maturation of primitive erythroid cells. *Blood*, 116(17), 3321-3330.

Vardiman, J. W., Harris, N. L., and Brunning, R. D. (2002). The World Health Organization (WHO) classification of the myeloid neoplasms. *Blood*, 100(7), 2292-302.

Vieira, L., Marques, B., Cavaleiro, C., Ambrosio, A., Jorge, M., Neto, A., Costa, J., Junior, E., & Boavida, M. (2005). Molecular cytogenetic characterization of rearrangements involving 12p in leukaemia. *Cancer Genetics and Cytogenetics*, 157(2), 134-139.

Von Bergh, A., van Drunen, E., van Wering, E., van Zutven, L., Hainmann, I., Lonnerholm, G., Meijerink, J., Pieters, R., & Beverloo, H. (2006). High incidence of t(7; 12)(q36; p13) in infant AML but not in infant ALL, with a dismal outcome and ectopic expression of HLXB9. *Genes, Chromosomes and Cancer*, 45(8), 731-739.

Von Neuhoff, C., Reinhardt, D., S., er, A., Zimmermann, M., Bradtke, J., Betts, D., Zemanova, Z., Stary, J., Bourquin, J., & Haas, O. (2010). Prognostic impact of specific chromosomal aberrations in a large group of pediatric patients with acute myeloid leukaemia treated uniformly according to trial AML-BFM 98. *Journal of Clinical Oncology*, 28(16), 2682-2689.

Walter, M. J., Payton, J. E., Ries, R. E., Shannon, W. D., Deshmukh, H., Zhao, Y., & Ley, T. J. (2009). Acquired copy number alterations in adult acute myeloid leukaemia genomes. *Proceedings of the National Academy of Sciences*, 106(31), 12950-12955.

Walter, M. J., Payton, J. E., Ries, R. E., Shannon, W. D., Deshmukh, H., Zhao, Y., Baty, J., Heath, S., Westervelt, P., Watson, M. A., Tomasson, M. H., Nanarajan, R., O'gara, B. P., Blomfield, C. D., Mrozek, K., Selzer, R. R., Richmond, T. A., Kitzman, J., Geoghegan, J., Eis, P. S., Maupin, R., Fulton, R. S., Mcelelan, M., Wilson, R. K., Mardis, E. R., Link, D. C., Graubert, T. A., Dipersio, J., F., & Ley, T. J. (2009). Acquired copy number alterations in adult acute myeloid leukaemia genomes. *Proceedings of the National Academy of Sciences*, 106, 12950-12955.

Wang, J. and Dick, J. (2005). Cancer stem cells: lessons from leukemia. Trends in cell biology, 15(9), pp.494--501.

Warner, J. K., Wang, J. C., Hope, K. J., Jin, L., & Dick, J. E. (2004). Concepts of human leukemic development. *Oncogene*, 23(43), 7164-7177.

Wildenhain, S., Ingenhag, D., Ruckert, C., Degistirici, Ö., Dugas, M., Meisel, R., Hauer, J., & Borkhardt, A. (2012). Homeobox protein HB9 binds to the prostaglandin E

receptor 2 promoter and inhibits intracellular cAMP mobilization in leukemic cells. *Journal of Biological Chemistry*, 287(48), 40703-40712.

Wildenhain, S., Ruckert, C., Rottgers, S., Harbott, J., Ludwig, W., Schuster, F., Beldjord, K., Binder, V., Slany, R., & Hauer, J. (2010). Expression of cell-cell interacting genes distinguishes HLXB9/TEL from MLL-positive childhood acute myeloid leukaemia. *Leukemia*, 24(9), 1657-1660.

Wilkens, L., Jaggi, R., Hammer, C., Inderbitzin, D., Giger, O., & von Neuhoff, N. (2011). The homeobox gene HLXB9 is upregulated in a morphological subset of poorly differentiated hepatocellular carcinoma. *Virchows Archiv*, 458(6), 697-708.

Williams, B. and Amon, A. (2009). Aneuploidy: Cancer's Fatal Flaw?. Cancer Research, 69(13), pp.5289-5291.

Wlodarska, I., La Starza, R., Baens, M., Dierlamm, J., Uyttebroeck, A., Selleslag, D., Francine, A., Mecucci, C., Hagemeijer, A., & Van den Berghe, H. (1998). Fluorescence in situ hybridization characterization of new translocations involving TEL (ETV6) in a wide spectrum of hematologic malignancies. *Blood*, 91(4), 1399-1406.

Wolman, S. (2002). Impact of trisomy 8 (+8) on clinical presentation, treatment response, and survival in acute myeloid leukemia: a Southwest Oncology Group study. Blood, 100(1), pp.29-35.

Wong, L., Dimmock, D., Geraghty, M., Quan, R., Lichter-Konecki, U., Wang, J., Brundage, E., Scaglia, F. and Chinault, A. (2008). Utility of Oligonucleotide Array-Based Comparative Genomic Hybridization for Detection of Target Gene Deletions. Clinical Chemistry, 54(7), pp.1141-1148.

Ylstra, B. (2006). BAC to the future! or oligonucleotides: a perspective for micro array comparative genomic hybridization (array CGH). Nucleic Acids Research, 34(2), pp.445-450.

Zhang,J., Niu,C., Ye,L., Huang,H., He,X., Tong,W.G., Ross,J., Haug,J., Johnson,T., Feng,J.Q., Harris,S., Wiedemann,L.M., Mishina,Y., and Li,L. (2003). Identification of the haematopoietic stem cell niche and control of the niche size. Nature 425, 836-841.

Zhu,J. and Emerson,S.G. (2002). Hematopoietic cytokines, transcription factors and lineage commitment. Oncogene 21, 3295-3313.

http://www.lgcstandards atcc.org/Home/tabid/477/Default.aspx

http://genome.ucsc.edu/cgi-bin/hgTracks?org=human

http://bacpac.chori.org/

Appendix 1: Cell counts of three observers of patient no. 26 and normal controls

No of hybridisation Signals	AB-patient 26	VA-patient 26	AI--atient 26	Mean from Pt 26
0	90 %	90 %	96.5 %	92.17
1	7 %	7 %	3 %	5.66
2	3 %	3 %	0.5 %	2.17
3	0 %	0 %	0 %	0
4	0 %	0 %	0%	0

AB, VA and AI are the initials of the three observers, 0, 1, 2, 3 and 4: Percentages of cells with 0, 1, 2, 3 and 4 signals respectively

No of hybridisation Signals	AB-NC	VA-NC	AI-NC	Mean from NCs
0	2.5 %	3.33 %	3.17 %	3
1	11.5 %	12 %	12.83 %	12.11
2	83 %	81 %	80.66 %	81.55
3	2 %	2.33 %	3.17 %	2.5
4	1 %	1.33 %	0.17 %	0.84

AB, VA and AI are the initials of the three observers, NCs: normal controls, 0, 1, 2, 3 and 4: Percentages of cells with 0, 1, 2, 3 and 4 signals respectively

Appendix 2: Cell counts of three observers of patient no. 27 and normal controls

No of hybridisation Signals	AB-patient 27	VA-patient 27	AI-patient 27
0	10.15 %	8.8 %	8.5 %
1	67.2 %	64 %	63.5 %
2	22.65 %	26.45 %	28 %
3	0 %	0.75 %	0 %
4	0 %	0 %	0%

AB, VA and AI are the initials of the three observers, 0, 1, 2, 3 and 4: Percentages of cells with 0, 1, 2, 3 and 4 signals respectively

No of hybridisation Signals	AB-NC	VA-NC	AI-NC	Mean of NCs
0	1.84%	2 %	3.2 %	2.4 %
1	8 %	8.34 %	8.5 %	8.3 %
2	80.5 %	79.5 %	81.9 %	80.66 %
3	8.66 %	8.83 %	5.9 %	7.64 %
4	1 %	1.33 %	0.5 %	1 %

AB, VA and AI are the initials of the three observers, NCs: normal controls, 0, 1, 2, 3 and 4: Percentages of cells with 0, 1, 2, 3 and 4 signals respectively

Appendix 3: Cell counts of three observers of patient no. 30 and normal controls

No of hybridisation Signals	AB-patient 30	VA-patient 30	AI-patient 30
0	2.5 %	2 %	1.5 %
1	3.5%	4 %	2.5 %
2	86.5 %	87.5 %	82.5 %
3	7.5 %	6.5 %	13.5 %
4	0 %	0 %	0%

AB, VA and AI are the initials of the three observers, 0, 1, 2, 3 and 4: Percentages of cells with 0, 1, 2, 3 and 4 signals respectively

No of hybridisation Signals	AB-NC	VA-NC	AI-NC	Mean of NCs
0	1 %	1.16 %	1.83 %	2.4 %
1	6.36 %	6 %	6.5 %	8.3 %
2	89 %	88.33 %	82.5 %	80.66 %
3	3.3 %	3.85 %	8.83 %	7.64 %
4	0.34 %	0.66 %	0.34 %	1 %

AB, VA and AI are the initials of the three observers, NCs: normal controls, 0, 1, 2, 3 and 4: Percentages of cells with 0, 1, 2, 3 and 4 signals respectively